Non-alcoholic fatty liver disease in type-2 diabetes mellitus: population analysis, metabolic profile and referral management pathway

Roberta Forlano

Imperial College London

Division of Digestive Diseases

Department of Metabolism, Digestion and Reproduction

2022

Thesis submitted for the degree of Doctor of Philosophy

Declaration of originality

This thesis is submitted to Imperial College London in support of my application for the degree of Doctor of Philosophy. I, Roberta Forlano, declare that this thesis has been written by myself and that this is work of my own.

All clinical and laboratory work was carried out by myself, except for the MiSeq Illumina Sequencing which was carried out by Mr Jesus Miguens Blanco, Imperial College London. Al statistical analyses were conducted by myself using SPSS version 22 and GraphPad Prim 9, except for complex modelling on metabonomic which was carried out by Dr Laura Martinez Gili, Imperial College London.

Copyright declaration

Dedication

This thesis is dedicated to my precious family and to the love of my life, my husband Marco. During these years, they have encouraged me with the biggest love and enthusiasm, and for that I will always be grateful.

Acknowledgements

First and foremost, I am extremely grateful to my supervisors, Professor Mark Thursz and Dr Pinelopi Manousou for their invaluable advice and continuous support during my PhD. Their immense knowledge and plentiful experience have encouraged me in all the time of my academic research and clinical practice. I am also genuinely grateful for this project, which I have been passioned about from the very beginning of the PhD.

Also, I have been lucky for having met such incredible people over these years. One of these is Ben, who has been a wonderful colleague and a great friend throughout the time of the PhD and beyond; his support has been unconditional and essential in many difficult times. Celia and Gary have also been an incredible asset to me. Not only they have shared good times and bad times with me like true friends, but they have also treated all the patients with the best care and professionalism. I have also been very lucky to meet a great travel companion for this journey, Jesus. I will always treasure the wonderful time spent together and our existential conversations in early mornings or late evenings. Also, I want to thank Cathrin for her friendship and for the nice time spent together, which have made the office (and London) much more enjoyable. I also want to say thank you to other very good friends I have made on my way: Suj, Rooshi, Sebastiana, Tong and Evangelos. I also would like to thank Charlie for her invaluable help in setting up the in-vitro model of gut permeability.

Finally, I would also like to thank Dr Laura Martinez Gili, Dr Pantelis Takis and the National Phenome Centre for their technical support and immense help in generating the data on metabolomics and gut microbiome. Mrs Claire Parsonage has been also a real asset to this project

and has supported me all the way through. Dr Emmanouil Tsochatzis and Dr Salvatore Petta should also be thanked as they kindly provided me with external cohorts to validate the findings from current study.

Funding

This thesis is an independent research arising from a PhD fellowship funded by the European Association for the Study of the Liver (EASL) through the Juan Rodes PhD fellowship program 2018-2021.

Abstract

Introduction: Non-alcoholic fatty liver disease is strongly associated with type-2 diabetes mellitus, with diabetic patients being at higher risk for adverse outcomes. The aim of this thesis was to explore in detail the clinical and metabolic phenotype of diabetics screened for NAFLD in primary care and to develop a referral management pathway for this population. Moreover, this thesis investigated the impact of alterations of the gut-liver axis on the severity of liver disease in such cohort.

Methods: In this cross-sectional study, consecutive diabetic patients from primary care were screened for liver disease and NAFLD. Nuclear magnetic resonance and liquid chromatography-mass spectrometry were used to explore the metabolic profile of the patients against severity of liver disease. Stool meta-taxagenomics allowed for the analysis of the composition of the microbiome, while gut permeability was investigated using an in-vitro model and an ex-vivo measurement of faecal protease activity. Inflammatory cytokines profile was also analysed in serum as well as in faecal samples.

Results: Clinically significant NAFLD was highly prevalent in the diabetic population in primary care. According to the results of this study, applying FIB-4 with a cut-off of 1.3 in this population would miss up to 38% of the patients with significant liver disease. The BIMAST score, which was derived based on simple clinical parameters, was validated both internally and externally, outperformed conventional screening methods and optimised risk-stratification in primary care. Among the metabolites, only lysine deficiency was associated with increased hepatic collagen content. Moreover, specific changes in gut microbiome were associated with more severe liver disease, while intestinal permeability tended to increase with liver disease severity. A combination of host and microbiota-related factors were associated with a leakier gut in this population.

Conclusions: Current risk-stratification for NAFLD among diabetics in primary care can be improved. Exploring the gut-liver axis may offer diagnostic as well as therapeutical insights in this population.

Publications arising from this work

R. Forlano, B. H. Mullish, L. A. Roberts, M. Thursz, P. Manousou. The intestinal barrier and its dysfunction in patients with metabolic diseases and Non-alcoholic fatty liver disease. *International Journal of Molecular Sciences. DOI: 10.3390/ijms23020662*

R. Forlano, B. H. Mullish, A. Dhar, R. D. Goldin, M. R. Thursz, P. Manousou. Liver function tests and MAFLD: Changes in Upper Normal Limits, Does It Really Matter? *World Journal of Hepatology, in press. DOI: 10.4254/wjh.v13.i12.2104*

R. Forlano, C. Harlow, B. H. Mullish, M. R. Thursz, P. Manousou. Binge-eating disorder is associated with an unfavourable body mass composition in patients with non-alcoholic fatty liver disease. *International Journal of Eating Disorders. DOI: 10.1002/eat.23584*

R. Forlano, B. H. Mullish, J. B Maurice, M. R. Thursz, R. D. Goldin, P. Manousou. NAFLD: time to apply quantitation in liver biopsies as endpoints in clinical trials. *Journal of Hepatology. DOI: 10.1016/j.jhep.2020.08.025*

R. Forlano, B. H. Mullish, S. K. Mukherjee, R. Nathwani, C. Harlow, P. Crook, R. Judge, A. Soubieres, P. Middleton, A. Daunt, P. Perez-Guzman, N. Selvapatt, M. Lemoine, A. Dhar, M. R. Thursz, S. Nayagam, P. Manousou. In-hospital mortality is associated with inflammatory response in NAFLD patients admitted for COVID-19. *PLOS ONE. DOI: 10.1371/journal.pone.0240400*

P. N Perez-Guzman, A. Daunt, S. Mukherjee, P. Crook, **R. Forlano**, M. Kont, A. Løchen, M. Vollmer, P. Middleton, R. Judge, C. Harlow, A. Soubieres, G. Cooke, P. J. White, T. B. Hallett, P. Aylin, N. Ferguson, K. Hauck, Mark R. Thursz, Shevanthi Nayagam. Clinical characteristics and predictors of outcomes of hospitalized patients with COVID-19 in a multi-ethnic London NHS Trust: a retrospective cohort study. *Clinical Infectious Diseases. DOI: 10.1093/cid/ciaa1091*

R. Nathwani, S. Mukherjee, **R. Forlano**, B. H. Mullish, N. Vergis, N. Selvapatt, P. Manousou, S. Nayagam, M. Lemoine, A. Dhar. Letter: liver disease and COVID-19—not the perfect storm. *Alimentary Pharmacology and Therapeutics. DOI: 10.1111/apt.15813*

R. Forlano, B. H. Mullish, A. Dhar, M.R. Thursz, P. Manousou. NAFLD and Vascular Disease. Special Issue – Emerging risk factors for Vascular Disease. *Current Vascular Pharmacology. DOI: 10.2174/1570161118666200318103001*

R. Forlano*, B. H. Mullish*, N. Giannakeas*, J. B. Maurice, N. Angkathunyakul, J. Lloyd, A. T. Tzallas, M. Tsipouras, M. Yee, M. R. Thursz, R. D. Goldin, P. Manousou. *joint first authors. High-Throughput, Machine Learning-based Quantification of Steatosis, Inflammation, Ballooning, and Fibrosis in Biopsies From Patients with Nonalcoholic Fatty Liver Disease. *Clinical Gastroenterology and Hepatology. DOI: 10.1016/j.cgh.2019.12.025*

B. H. Mullish*, **R. Forlano***, R. D. Abeles, M. R. Thursz, P. Manousou. Letter: role of mean platelet volume levels in the prediction of major acute cardiovascular events in patients with non-alcoholic fatty liver disease-authors' reply. *Alimentary Pharmacology and Therapeutics. DOI:* 10.1111/apt.15531. *joint first authors.

B. H. Mullish*, **R. Forlano***, M. R. Thursz, R. D. Abeles, P. Manousou. Editorial: importance of an elevated mean platelet volume for prediction of major adverse cardiovascular events in non-alcoholic liver disease – authors' reply. *joint first authors. *Alimentary Pharmacology and Therapeutics. DOI:10.111/apt.15215*.

R. D. Abeles*, B. H. Mullish*, **R. Forlano***, T. Kimhofer, M. Adler, A. Tzallas, N. Giannakeas, M. Yee, J. Mayet, R. D. Goldin, M. R. Thursz, P. Manousou. Derivation and validation of a cardiovascular risk score for prediction of major acute cardiovascular events in non-alcoholic fatty liver disease; the importance of an elevated mean platelet volume. *Alimentary Pharmacology and Therapeutics. DOI:10.1111/apt.15192*. *joint first authors.

A. Arjmand, **R. Forlano**, M. G. Tsipouras, A. Tzallas, P. Manousou, N. Giannakeas. Quantification of liver fibrosis - A comparative study. *Applied sciences. DOI: 10.3390/app10020447*

A. Arjmand, C. T. Angelis, V. Christou, A. T. Tzallas, M. G. Tsipouras, E. Glavas, **R. Forlano**, P. Manousou, N. Giannakeas. Training of Deep Convolutional Neural Networks to Identify Critical Liver Alterations in Histopathology Image Samples. *Applied Sciences. DOI:10.3390/app1001004.*

R. Nathwani, B. H Mullish, D. Kockerling, **R. Forlano**, P. Manousou, A. Dhar. A review of Liver fibrosis and emerging therapies. *European Medical Journal. EMJ. 2019;4[4]:105-116.*

D. Kockerling, R. Nathwani, **R. Forlano**, P. Manousou, B. H Mullish, A. Dhar. Current and future pharmacological therapies for managing cirrhosis and its complications. *World Journal of Gastroenterology. DOI: 10.3748/wjg.v25.i8.888*

B. Mullish, **R. Forlano**, P. Manousou, D. Mikhailidis. Non-Alcoholic Fatty Liver Disease and cardiovascular risk: an update. *Expert Review of Gastroenterology and Hepatology. https://doi.org/10.1080/17474124.2018.1533117*

Abstracts presented

R. Forlano, B. H. Mullish, T. Liu, E. Triantafyllou, C. Skinner, M. R. Thursz, J. R. Marchesi, P. Manousou. Increased gut permeability may be associated with bacterial protease activity, not intestinal inflammation in patients with significant liver disease due to NAFLD. *E-poster - EASL NAFLD Summit 2021*

R. Forlano, B. H. Mullish, M. Yee, M. R. Thursz, P. Manousou. The BAST score performs predicts the presence of liver disease better than FIB-4 and NAFLD fibrosis score in a cohort of patients with type-2 diabetes mellitus in primary care. *E-poster - EASL NAFLD Summit 2021*

R. Forlano, B. H. Mullish, C. Izzi-Engbeaya, M. Yee, W. S. Dhillo, M. R. Thursz, P. Manousou. Menopausal women with NAFLD show impaired metabolism of branched chain aminoacids. *E-poster - EASL NAFLD Summit 2021*

L. D. Tyson, **R. Forlano**, E. Ulucay, N. Vergis, N. Giannakeas, A. Tzallas, M. R. Thursz, R. D. Goldin, S. Atkinson, P. Manousou. Automated quantitation of histological features could predict mortality in patients with severe alcoholic hepatitis. *E-poster - EASL International Liver Congress 2021*

R. Forlano, B. H. Mullish, M. Yee, R. D. Goldin, M. R. Thursz, P. Manousou. A prospective cohort study for the prevalence and screening policy of NAFLD in patients with T2DM in primary care. *E-poster - EASL International Liver Congress 2021*

R. Forlano, C. Harlow, B. H. Mullish, M. R. Thursz, P. Manousou, M. Yee. Binge Eating Disorder is associated with an unfavourable body mass composition in patients with Non-Alcoholic fatty liver disease. *E-poster - EASL International Liver Congress 2021*

R. Forlano, B. H. Mullish, J. Miguens Blanco, N. Danckert, M. R. Thursz, P. Manousou. A serum metabolic fingerprint may predict advanced fibrosis due to NAFLD in a cohort of diabetic patients. *E-poster and oral presentation - EASL International Liver Congress 2021*

R. Forlano, B. H. Mullish, N. Giannakeas, M. Tsipouras, A. Tzallas, M. Yee, J. Lloyd, R. D. Goldin, M. Thursz, P. Manousou. Impact of BMI and Ethnicity on histology as assessed by automated quantitation in liver biopsies of patients with NAFLD. *E-poster – AASLD – The Liver Meeting 2019 and EASL NAFLD Summit 2019*

C. Tiantos, C. Tsolias, **R. Forlano**, K. Karaivazoglou, S. Manolakopoulos, I. Aggeletopoulou, G. Theocharis, M. Melachrinou, R. Goldin, K. Thomopoulos, P. Manousou. The role of sub-mucosal collagen deposition in patients with inflammatory bowel diseases. *Poster - Digestive Disease Week 2019*

R. D. Abeles, B. H. Mullish, **R. Forlano**, M. Adler, N. Giannakeas, A. Tzallas, M. Yee, J. Mayet, R. D. Goldin, M. R. Thursz, P. Manousou. Derivation and validation of a cardiovascular risk score for prediction of major acute cardiovascular events in Non-Alcoholic Fatty Liver Disease; the importance of an elevated mean platelet volume. *E-poster - EASL International Liver Congress 2019*

R. Forlano, B. H. Mullish, M. Yee, A. Dhar, M. R. Thursz, P. Manousou. Liver function tests in NAFLD: Changes in upper normal limits, does it really matter? *E-poster - EASL International Liver Congress 2019*

R. Nathwani, D. Kockerling, S. Balarajah, **R. Forlano**, N. Selvapatt, P. Manousou, A. Dhar. Evaluating the impact of non-selective beta-blocker use in decompensated cirrhosis based on setting of patient care*. E-poster - EASL International Liver Congress 2019*

R. Forlano, N. Giannakeas, B. H. Mullish, M. Tsipouras, A. Tzallas, M. Yee, J. Lloyd, R. D. Goldin, M. R. Thursz, P. Manousou. Automated quantitation of steatosis, fibrosis and ballooning using machine learning in routine histological images of liver biopsies of patients with NAFLD. *E-poster – AASLD – The Liver Meeting 2018 - HEPATOLOGY 2018; volume 68, number 1 (suppl)*

R. Forlano, N. Giannakeas, B. H. Mullish, M. Tsipouras, A. Tzallas, M. Yee, Rita M. Luìs, J. Lloyd, R. D. Goldin, M. R. Thursz, P. Manousou. Automated quantitation of ballooning, inflammation, steatosis and fibrosis using machine learning in routine histological images of liver biopsies of patients with NAFLD. *E-poster –EASL NAFLD Summit 2018 and EASL International Liver Congress 2019*

R. Forlano, B. H. Mullish, N. Katertsidis, N. Giannakeas, A. Tzallas, M. Tsipouras, M. Yee, S. Taylor-Robinson, M. R. Thursz, P. Manousou. A Mobile Application For Lifestyle Modifications In Patients With Non-Alcoholic Fatty Liver Disease. Poster – *Io T Sm 2018: International Conference on Industrial Internet of Things and Smart Manufacturing - Imperial College London – 2018*

R. Forlano, D. Kockerling, R. Nathwani, J. Clancy, H. Marcinkowski, M. Yee, M. R. Thursz, H. Antoniades, A. Dhar, P. Manousou. Prediction of decompensation events in NASH cirrhosis patients. *Poster - EASL International Liver Congress 2018 - Journal of Hepatology 2018 vol. 68: S605-S842*

R. Morrison, **R. Forlano**, N. Giannakeas, A. Tzallas, M. Tsipouras, J. Lloyd, M. Yee, M. R. Thursz, P. Manousou, R. D. Goldin. Lipofuscin is detected in early stages of the disease in liver biopsies of patients with Non-Alcoholic Fatty Liver Disease. *Poster and Oral e-poster - EASL International Liver Congress 2018 - Journal of Hepatology 2018 vol. 68: S605-S842*

R. Forlano, B. H. Mullish, N. Katertsidis, N. Giannakeas, A. Tzallas, M. Tsipouras, M. Yee, S. Taylor-Robinson, M. R. Thursz, P. Manousou. A mobile application for the management and follow-up of

patients with Non-Alcoholic Fatty Liver Disease. *Poster and Oral e-poster - EASL International Liver Congress 2018 - Journal of Hepatology 2018 vol. 68: S605-S842*

Table of Contents

List of Tables

List of Figures

List of Abbreviations

CLD: chronic liver disease

UK: United Kingdom

AIH: Autoimmune hepatitis

PBC: primary sclerosing cholangitis

WD: Wilson's disease

ALD: alcoholic liver disease

NAFLD: non-alcoholic fatty liver disease

CHB: chronic hepatitis B

CHC: chronic hepatitis C

LFT: liver function test

NAFL: non-alcoholic fatty liver

NASH: non-alcoholic steato-hepatitis

T2DM: type-2 diabetes mellitus

BMI: body mass index

IR: insulin resistance

ECM: extra cellular matrix

CVD: cardiovascular disease

PNPLA3: phospholipase domain containing protein 3

TM6SF2: transmembrane 6 superfamily member 2

HCC: hepato-carcinoma

NASH CRN: NASH clinical research network

NIT: non-invasive test

HSC: hepatic stellate cell

PLT: platelet

FIB-4: fibrosis score 4

ELF: enhanced liver fibrosis

TE: transient elastography

ARFI: acoustic radiation force imaging

MRE: magnetic resonance elastography

kPa: kilopascal

CAP score: controlled attenuation parameter

PPV: positive predictive value

GP: general practitioner

US: ultrasound

ALT: alanine aminotransferase

EASL: european association for the study of the liver

QALY: quality-adjusted life years

CV: cardiovascular

NAS: NASH activity score

GLP-1R: glucagone-like peptide-1 receptor agonist

DPP-4i: dipeptyl-dipeptidase-4 inhibitor

FXR: farnesoid-X receptor

SCFA: short chain fatty acid

GPCR: G-protein couple receptor

FIAF: fasting-induced adipocyte factor

LPL: lipoprotein lipase

AA: aminoacids

BCAA: branched chain aminoacid

AAA: aromatic aminoacid

BA: bile acid

FFA: free fatty acid

TNF-α: tumour necrosis factor-alpha

HOMA-IR: homeostatic model assessment for insulin resistance

LPS: lipopolysaccharide

FMT: fecal microbiota transplantation

GI: gastrointestinal

TJ: tight junction

TEER: transepithelial electric resistance

EVOM: epithelial voltohmeter

FABP: fatty acid binding protein

FABP-2: fatty acid binding protein-2

MLC: myosin light chain

GLP-2: glucagone-like peptide 2

PAMP: pathogen-associated molecular pattern

TLR: toll-like receptor 4

ATM: adipose tissue macrophage

IL-1β: interleukin-1 beta

IL-6: interleukin-6

DAMP: damage-associated molecular pattern

TGF-β: transforming growth factor-beta

IL-10: interleukin-10

BAFLD: both alcoholic and non-alcoholic fatty liver disease

IMD: index of multiple deprivation

LSM: liver stiffness measurement

IQR/M: interquartile range/median ratio

IQR: interquartile

OR: odd ratio

ROC: receiver operating characteristic

AUROC: areas under ROC curve

NPV: negative predictive value

NMR: nuclear magnetic resonance

MS: mass spectrometry

rRNA: ribosomial ribonucleic acid

UPLC-MS: ultra performance liquid chromatography – mass spectrometry

SOP: standard operating procedures

FW: fecal water

RT: room temperature

PBS: phosphate-buffered saline

SMolESY: small molecule enhancement spectroscopy

QC: quality control

DNA: deoxyribonucleic acid

dsDNA: double-stranded DNA

PCA: principal component analysis

OPLS-DA: orthogonal projections to latent structures discriminant analysis

CV-ANOVA: cross-validated ANOVA

H&E: haematoxylin and eosin

CPA: collagen proportionate area

BCA: Bicinchoninic acid assay

BSA: bovine serum albumin

WR: working reagent

MDCK: Madin-Darby Canine cocker spaniel kidney

DMEM: Dulbecco's modified eagle medium

HBSS: Hanks' balanced salt solution

IFN-γ: interferon gamma

IL-2: interleukin-2

IL-4: interleukin-4

IL-8: interleukin-8

IL-12p70: interleukin-12p70

IL-13: interleukin-13

MSD: meso scale discovery

ELISA: enzyme-linked immune-absorbent assay

GGT: gamma-glutamyl transferase

95%CI: 95% confidence interval

LCA: lithocholic acid

GDCA-3S: glycoursodeoxycholic acid-3 sulfate

PAI-1: plasminogen activator inhibitor

1. INTRODUCTION

1.1 Non-Alcoholic Fatty Liver Disease: definition, diagnosis, screening and management

1.1.1 Definition and epidemiology of NAFLD

Chronic liver disease (CLD) is the only major cause of death still rising in the United Kingdom (UK), reporting 500% increase in mortality rates for patients younger than 65 years (Williams et al., 2014). It has been estimated that one in five young people has steatosis and one in 40 has significant fibrosis around the age of 24 years already (Abeysekera et al., 2020). Only 7% of overall CLD is attributable to autoimmune (autoimmune hepatitis-AIH), cholestatic (primary biliary cholangitis-PBC, primary sclerosing cholangitis-PSC) and to genetic disorders (haemochromatosis, Wilson's disease, WD). The most common contributors of CLD are: alcoholic liver disease (ALD), non-alcoholic fatty liver disease (NAFLD) and viral hepatitis (chronic hepatitis B-CHB, chronic hepatitis C-CHC) (Williams et al., 2014). Histologically, NAFLD encompasses a spectrum of pathological disorders characterised by macro-vescicular fat accumulation (steatosis, Non-alcoholic fatty liver, NAFL) with or without hepatocellular injury and/or inflammation (Non-Alcoholic Steato-Hepatitis, NASH) and a variable degree of fibrosis through to cirrhosis (Kleiner et al., 2005, Brunt et al., 2021).

NAFLD is the most common cause of abnormal liver function tests (LFTs) worldwide, with an estimated prevalence ranging between 19–46% (Younossi et al., 2019d). Overall, the NAFLD prevalence is particularly higher in those with metabolic syndrome, i.e. a combination of central obesity, insulin resistance, type 2 diabetes mellitus (T2DM), hypertension and dyslipidaemia (Glen et al., 2016). Mirroring the epidemic of metabolic syndrome, the prevalence of NAFLD is constantly increasing, going from 15% in 2005 to 25% in 2010 and, in similar fashion, the prevalence of NASH from 33% to 59.1% (Younossi et al., 2019b). Furthermore, NASH has become the fastest growing indication for liver transplantation in the USA, and it is still raising (Younossi et al., 2019a). Notably, the NAFLD prevalence is even higher among high-risk groups. According to tertiary care studies, more than 50% of the patients with T2DM will have NAFLD (Glen et al., 2016). As one would expect, the prevalence of NAFLD is as high as 45% among those with increased Body mass index (BMI>30 kg/m^2) and up to 90% among those undergoing bariatric surgery (Tanajewski et al., 2017). As large

part of the epidemiological data derives from tertiary care centres, there is not much evidence on the prevalence of NAFLD in the general population.

In the UK, NAFLD also represents a major cause of abnormal liver functions tests, accounting for 26.4% of the cases (Armstrong et al., 2012). In 2018, the number of patients diagnosed with NAFLD in the UK was estimated to be almost 11 million people, while the number of those with NASH almost 1,75 million (Statistics, Mid-2018). Interestingly, autopsy data suggests that 4-9% of people with BMI between 27.5 and 35 kg/m^2 have histological evidence of NASH, a figure which rises up to 19% in those with a BMI greater than 30 kg/m^2 (Wanless and Lentz, 1990). Given the current prevalence of obesity at 25% in the UK, this translates into about 1 in 20 in the general population having NASH. Moreover, considering the estimated trend in obesity prevalence, 50-60% of the population will have a BMI greater than 30 kg/m^2 and, therefore, one in ten people will have NASH (Office, April, 2014, Morgan et al., 2021). Even more concerning is the data on future generations, as a steep increase in childhood obesity has been reported during the last decade. According to Public Health England, the prevalence of obesity is now 9.3% among 4-5 years old, and up to 18.9% in age 10-11 years. Of note, such estimates have already doubled in the last few years (Health and Social Care Information Centre (HSCIC), April 2014).

1.1.2 Natural history of NAFLD

Far from the old concept of being a dichotomic disease, NAFLD is now considered to be a dynamic disease with a wide spectrum of disease activity within different cases of simple steatosis or NASH (Kleiner and Makhlouf, 2016). Insulin resistance (IR) plays a crucial role in the development and progression of liver disease, as this stimulates de novo lipogenesis and is associated with impaired lipolysis, resulting into an increase flux of fatty acid to the liver (Bugianesi et al., 2010). Of note, hepatic triglyceride storage is not harmful *per se*. Nevertheless, when the hepatic capacity of using, storing and exporting free fatty acids becomes saturated, lipotoxicity may occur within the liver. Overall, lipotoxicity is thought to be the crucial driver for the development and progression of hepatocellular injury, inflammation, hepatic stellate cell activation and extracellular matrix (ECM)

deposition (Neuschwander-Tetri, 2010). Overall, a status of IR also drives a dysfunctional adipose tissue, which produces metabolically active cytokines (Guilherme et al., 2008) **Figure 1.1**.

The development and progression of liver disease in NAFLD is now being explained with a multi-hit hypothesis, where a plethora of dietary, environmental and genetic factors contribute to the disease along with the worsening of IR (**Figure 1.1)**. Along with hyperinsulinaemia, hyperglucagonaemia can also be observed in patients with NAFLD. Hepatic glucacon resistance may result into impaired aminoacids metabolism beta-oxidation and lipolysis (Galsgaard, 2020). Dietary elements, both in terms of overall calories intake and specific dietary patterns, may contribute to the development of NAFLD. Specifically, high-fat diets, increased fructose and red meat intake have been associated to worsening hepatic steatosis and to inducing a pro-inflammatory status (Bergheim et al., 2008, Ma et al., 2015, Zelber-Sagi et al., 2018). Moreover, there has been a large body of work showing that gut microbiome plays an essential role in disease activity in patients with NAFLD (Hu et al., 2020). The interactions between the liver and the gut, the so called “gut-liver axis”, result from a complex interplay between the gut and the immune system, which ranges from immune tolerance to immune activation. Changes in gut microbiome composition, gut permeability and the translocation of pro-inflammatory bacterial by-products are now included among the factors involved in the progression of liver disease in this population (Kirpich et al., 2015). Genetic factors also represent an important contribution to NAFLD progression. Few genes have been identified as conferring different levels of susceptibility to fat accumulation, hepatic inflammation and lipotoxicity, such as patatin-like phospholipase domain containing protein 3 (PNPLA3), Transmembrane 6 superfamily member 2 (TM6SF2) and membrane-bound O-acyltransferase domain containing 7 (MBOAT7) (Buzzetti et al., 2016).

Clinical data from paired liver biopsies and placebo arms of clinical trials have demonstrated that up to 25% of patients with NAFL, a condition which was previously considered “benign”, may also progress to advanced fibrosis. Among those with NASH, up to 35% present fibrosis progression, while 40% remain relatively stable over time. Overall, NAFLD is considered a slow-progressive disease, with a 1-stage fibrosis progression over 14 years for those with fibrosis stage 1 and over 7 years in patients with advanced fibrosis (Pais et al., 2013). However, those with NASH seem to

progress more rapidly than those with NAFL (Chalasani et al., 2012), with up to 20% of patients with NASH and fibrosis stage 3 progressing to cirrhosis (Torres et al., 2012, Ascha et al., 2010). Baseline inflammation status and worsening of metabolic risk factors have been suggested as the main contributors to disease progression in these patients (Pais et al., 2013). Overall, the yearly cumulative incidence of NASH-related hepato-carcinoma (HCC) is low (1.5-2%) compared to 4% of HCC from chronic viral hepatitis (Ascha et al., 2010, Estes et al., 2018). Moreover, recent evidence also suggests that pre-cirrhotic NAFLD may confer an increased risk for HCC, independent of cirrhosis (Estes et al., 2018) (**Figure 1.2**). Specifically, NAFLD-associated NAFLD in the absence of cirrhosis accounts for up to 25-46% of all NAFLD-associated HCC cases (Dyson et al., 2014, Piscaglia et al., 2016).

The main cause of death among NAFLD patients is cardiovascular disease (CVD) (33% of deaths), followed by non-gastrointestinal cancer (19% of deaths) and then liver related complications (19% of deaths) (Adams et al., 2010). In terms of absolute risk, patients with NAFLD have been shown to have significantly increased risk of all overall-causes mortality (Hazard ratio 2.2, 95%CI 1.2-44), mainly driven by malignancy (Adams et al., 2010). However, CVD is still highly prevalent and represents an important cause of mortality and morbidity in these patients (Abeles et al., 2019, Targher et al., 2016). Previously published studies have explored clinical, biochemical and histological variables that could predict mortality in patients with NAFLD, concluding that age and T2M are strong predictors for adverse events (Adams et al., 2020). However, it is now established that fibrosis stage represents the main prognostic factor in this population (Ekstedt et al., 2015).

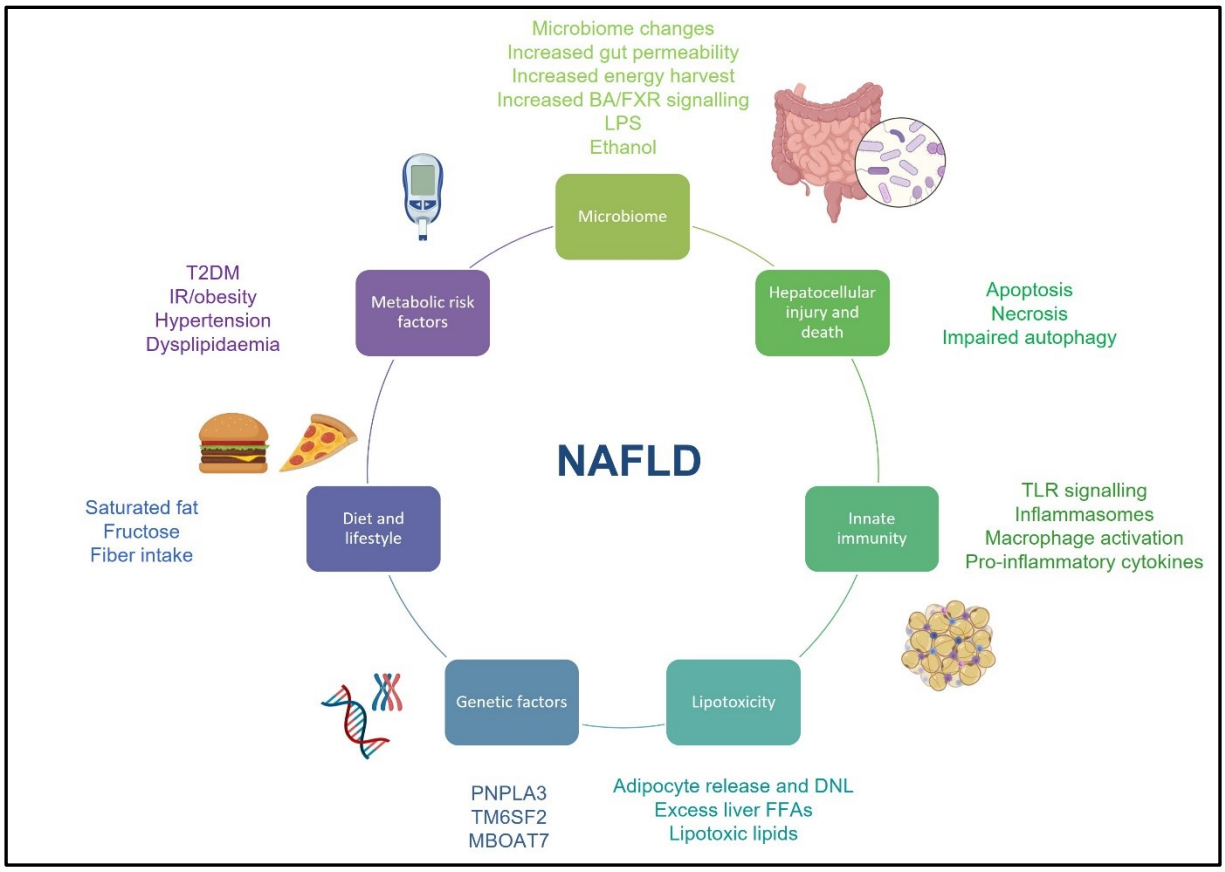

Figure 1.1 Risk factors for development and progression of NAFLD. NAFLD illustrates the most common risk factors associated with the development and progression of NAFLD.
Abbreviations: NAFLD: non-alcoholic fatty liver disease, BA: bile acid, FXR: farnesoid-x-receptor, LPS: lipopolysaccharide, TLR: toll-like receptor, DNL: de-novo lipogenesis, T2DM: type 2 diabetes mellitus, IR: insulin resistance, patatin-like phospholipase domain containing protein 3 (PNPLA3), Transmembrane 6 superfamily member 2 (TM6SF2) and membrane-bound O-acyltransferase domain containing 7 (MBOAT7).

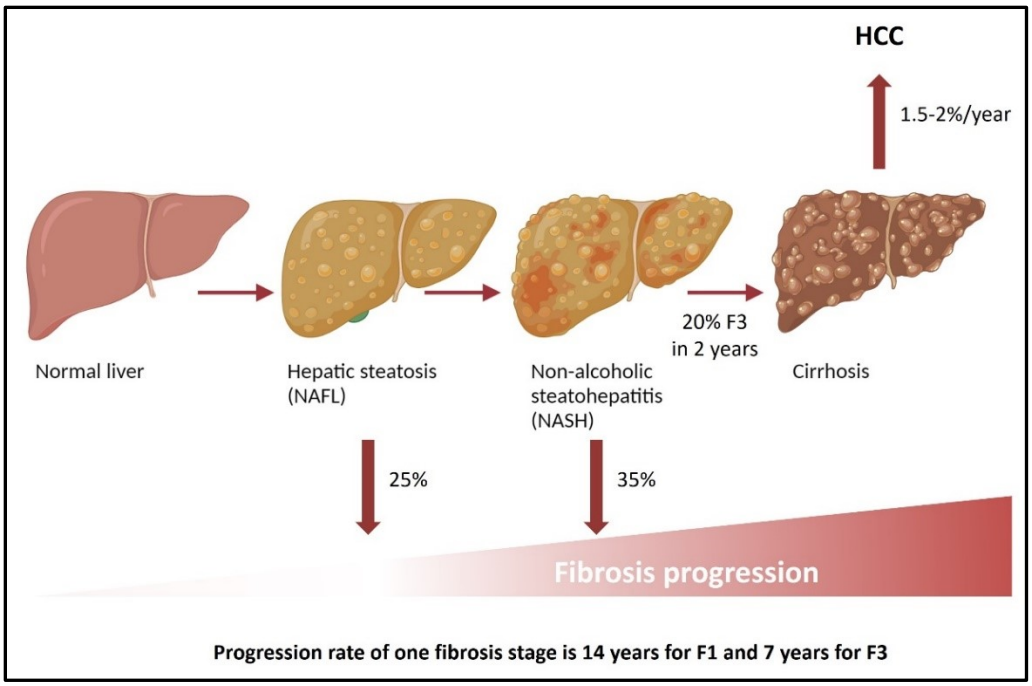

Figure 1.2. Natural history of NAFLD. NAFLD affects almost 25% of the population worldwide. Up to 25% of patients with simple steatosis and up to 35% of patients with NASH may develop cirrhosis. Overall, progression rate for one fibrosis stage is 14 years for F1 and 7 years for F3. However, a subgroup (20%) of patients with NASH and F3 may be fast progressors and develop cirrhosis in 2 years. The overall yearly incidence of HCC in those with NASH cirrhosis is 1.5-2%.
Abbreviations: NAFLD: non-alcoholic fatty liver disease, NASH: non-alcoholic steatohepatitis, F3: fibrosis stage 3, F1: fibrosis stage 1.

1.1.3 Diagnosis and non-invasive assessment of NAFLD

The vast majority of patients with NAFLD are asymptomatic. Hepatomegaly is the most common clinical finding on physical examination. As patients progress to advanced liver disease, signs and symptoms related to portal hypertension become evident. A diagnosis of NAFLD should be suspected in all patients with at least one component of the metabolic syndrome, presenting with evidence of hepatic steatosis on imaging. Of note, NAFLD represents still a diagnosis of exclusion of other common causes of liver disease, especially chronic alcohol consumption (European Association for the Study of the Liver. Electronic address et al., 2021, Glen et al., 2016).

Histopathological assessment of the liver biopsy remains the gold standard for diagnosing NASH and staging liver disease in NAFLD (Bugianesi et al., 2010, European Association for the Study of the Liver. Electronic address et al., 2021, Glen et al., 2016). Currently, the interpretation of liver biopsy relies on the use of semi-quantitative scores, such as the NASH clinical research network (NASH CRN) scoring system. When using such scores, disease activity is defined based on the

assessment of steatosis, hepatocyte ballooning and lobular inflammation, while staging is based on the assessment of fibrosis (Kleiner et al., 2005). However, obtaining a liver biopsy is expensive, invasive and associated with potential complications. More importantly, considering the high prevalence of the disease, histology cannot be considered in all the patients but should be limited to selected sub-groups, such as those at high risk for progressive disease, and/or in the setting of clinical trials (Kleiner and Makhlouf, 2016, Nalbantoglu and Brunt, 2014).

Given the drawbacks of performing a liver biopsy, there has been an explosive development and use of non-invasive tests (NIT), with significant (fibrosis stage F≥2) and advanced (fibrosis stage F≥3) fibrosis being the main clinical endpoints(European Association for Study of and Asociacion Latinoamericana para el Estudio del, 2015). Overall, blood-based NIT are mainly divided into direct (or class 1) and indirect (or class 2) biomarkers. The direct NIT correlate directly with or are parts of the liver matrix produced by the hepatic stellate cells (HSC) during fibrogenesis. Conversely, indirect NIT consist of a combination of routine biochemical tests, such as LFTs, platelet (PLT) count and albumin, and patient demographics, such as age, BMI or the presence of T2DM. Patented NIT are usually a combination of both class 1 and class 2 NIT. The majority of the indirect NITs have been validated against histology and provide dual cut-offs: a low cut-off with high sensitivity (to *rule out* the disease) and a high cut-off with high specificity (to *rule in* the disease). The use of each cut-off is mainly dictated by the clinical setting and/or on the disease prevalence. If these cut-offs are combined, then the number of false positive and false negative are usually reduced. However, when applying such system, a significant sub-group of patients would inevitably fall in the indeterminate-risk group and, therefore, will require further investigations as per those in the high-risk category. Main NITs used in NAFLD are displayed in **Table 1.1**. Overall, the Fibrosis-4 score (FIB-4) (Vallet-Pichard et al., 2007), NAFLD fibrosis score (Angulo et al., 2007) and Enhanced liver fibrosis (ELF) (Rosenberg et al., 2004) are the most frequently used NIT in clinical practice.

New imaging modalities based on ultrasound elastography have offered better sensitivity and specificity for predicting liver fibrosis than conventional imaging techniques. This is the case of transient elastography (TE) (Fibroscan, Echosens, Paris), followed by acoustic radiation force imaging (ARFI), shear wave elastography and magnetic resonance elastography (MRE) (Cassinotto

et al., 2016, European Association for Study of and Asociacion Latinoamericana para el Estudio del, 2015). Briefly, TE employs vibrations of mild amplitude and low frequency, which propagate within the liver. The subsequent pulse-echo ultrasonic acquisitions are reflective of the hepatic elastic properties, i.e. stiffness, and are expressed in kilopascals (kPa). On a patient perspective, TE is painless and rapid (<5 minutes) and thus highly acceptable. On a clinical perspective, TE provides high accuracy and reproducibility for detecting advanced liver fibrosis (European Association for Study of and Asociacion Latinoamericana para el Estudio del, 2015). In addition, the Controlled attenuation parameter (CAP) score, which has been recently applied to TE, can estimate the presence of steatosis, based on the physical impact of fat on shear-wave propagation (Pu et al., 2019). Using this non-invasive technique, it is now possible to measure fat content and to predict disease severity in a large number of patients.

The choice of NIT used in clinical practice is usually based upon different factors, such as the availability and cost of the test/technique, as well as the "context of use". For instance, class 2 biomarkers, which require inexpensive and widely available parameters, can be easily used to predict liver fibrosis in large populations (i.e primary care). Conversely, sophisticated, time-consuming and expensive techniques like MRE are acceptable in selected groups of patients and for research purposes (i.e tertiary care) (Crossan et al., 2015, Han et al., 2017) .

Notably, most of the NITs were developed and validated in secondary or tertiary care settings and, therefore, their performance in primary care is largely unknown. Due to the *spectrum effect*, NITs will have lower sensitivity and higher specificity in populations with lower disease prevalence. On the other hand, in secondary/tertiary care settings (higher disease prevalence) the positive predictive value (PPV) will be higher, as it is higher *a priori* the probability of observing true positive cases. As such, when selecting patients from a low prevalence population, a first NIT with high PPV should be used to rule out (or screen) the disease, followed by a highly accurate non-invasive tool which should rule in (or diagnose) significant liver disease (2-tiers system) (Crossan et al., 2015, Usher-Smith et al., 2016).

Direct serum markers	Indirect serum markers	Patented serum markers
Hyaluronate	AST/ALT ratio	Fibrotest
Laminin	PGA	Fibroindex
YKL-40	APRI	Hepascore
Procollagen type I carboxy-terminal peptide (PICP)	Forns index	Fibrospect
Procollagen type III amino-terminal peptide (PIIINP)	FIB-4	ELF
Metalloproteinases (MMP)-1 and MMP-2	Lok index	Fibrometers
Tissue inhibitors of the metalloproteinases (TIMPs)	Fibrosis probability index (FPI)	
Transforming growth factor β1 (TGF-β1)	NAFLD fibrosis score	
MP3	BARD	
Microfibril-associated glycoprotein 4 (MFAP-4)	GGT to PLT ratio	

Table 1.1 Overview of the main non-invasive tests based on blood tests and clinical parameters.

1.1.4 The relationship between NAFLD and T2DM

Overall, patients with NAFLD tend to have components of metabolic syndrome such as obesity, T2DM, hyperlipidaemia and hypertension. Among these comorbidities, NAFLD and T2DM display a bidirectional association, due to their common pathogenic mechanism of IR. Not only NAFLD is a frequent finding in patients with T2DM, but also a diagnosis of NAFLD confers a 2 to 5-fold risk of developing T2DM (Lonardo et al., 2018, Tilg, 2017). This risk parallels the severity of liver disease and improves with the resolution of NAFLD over time. Nevertheless, the exact prevalence of NAFLD in T2DM is unknown, previously pooled at 55.5% (95%CI: 47.3-63.7%) with variability according to different diagnostic techniques and selection criteria of a screened population (Dai et al., 2017). However, most of the data comes from observational studies carried out mainly in tertiary care centres (Kim et al., 2021, Poynard et al., 2021), while evidence derived from primary care is small (Williamson et al., 2011). Interestingly, a recent study has suggested that the prevalence of NAFLD among diabetics in primary care was 78.72%, with steatosis being diagnosed based on CAP score greater than 248 dB/m (Chen et al., 2020b).

On a clinical perspective, the impact of T2DM on NAFLD seems to occur both early (with greater lipid accumulation) and later (with liver inflammation and fibrosis) within the spectrum of liver disease in NAFLD (Targher et al., 2021). In terms of natural history, T2DM is also an important prognostic factor for adverse clinical outcomes, such as the occurrence of advanced fibrosis and HCC (Adams et al., 2010, Harrison et al., 2021). According to Public health England, the obesity pandemic could result in the number of people with T2DM increasing further up to 6.2 million by 2034. Given the expected increases in the incidence of T2DM, it is expected a subsequent tremendous rise in the disease burden from NASH and its complications in the United States as well as in the other Western countries (Younossi and Henry, 2021).

1.1.5 Screening for NAFLD in primary care

Primary care clinicians play an essential role in identifying patients with NAFLD who are at risk of significant liver disease (European Association for the Study of the Liver. Electronic address et al., 2021). In this sense, the Lancet commission on liver disease identified the need for diagnostic pathways for screening people with NAFLD as a priority area to defeat liver disease (Williams et al., 2014). Interestingly, a recent UK-based study has demonstrated that the diagnosis and management of NAFLD is perceived as a great challenge by the General practitioners (GPs). Moreover, another recent study has shown that up to two-thirds of the new referral to Hepatology clinics are discharged once received their first assessment, confirming that current risk-stratification from primary care needs optimisation (Elangovan et al., 2020). As many promising drugs are in the pipeline, identifying those with advanced fibrosis or at risk of developing advanced fibrosis in the community will become a clinical priority in the next future.

Given the high prevalence and severity of NAFLD in the diabetic population, there is an expected large burden of undiagnosed NAFLD with advanced fibrosis in the community, and – as such - a major interest in early detection of the disease among diabetics in primary care (European Association for the Study of the Liver. Electronic address et al., 2021). Nevertheless, there is a substantial lack of awareness among clinicians and policy makers. For instance, current diabetes management guidelines do not advise for NAFLD screening in the general population (Davies et al.,

2018). Conversely, the latest NICE guidelines recommend screening for NAFLD subjects with T2DM and metabolic syndrome, performing LFTs and/or ultrasound (US). However, LFTs assessment is not sufficient alone for screening NAFLD, since it is well established that NASH and significant fibrosis can occur in patients with normal range LFTs (Ma et al., 2020). Specifically, more than 12% of diabetic men and 7% of diabetic women have been found to have advanced fibrosis with normal alanine aminotransferase (ALT) (Wong et al., 2009). Furthermore, US has low reproducibility and was not designed to stage disease severity (European Association for the Study of the Liver. Electronic address et al., 2021).

The latest European guidelines recommend screening NAFLD in high-risk populations (i.e. patients with metabolic syndrome) following a 2-tiers system. Specifically, it is recommended that patients should be stratified using FIB-4 and/or ELF in primary care, followed by TE in a specialist setting (European Association for the Study of the Liver. Electronic address et al., 2021). However, it should be noted that FIB-4 was derived from a tertiary care setting, and its performance in primary care has not been fully evaluated (Vallet-Pichard et al., 2007).

Although screening for NAFLD in high-risk populations has been supported by European association for the study of the liver (EASL) guidelines, a consensus on cost-effectiveness of screening hasn't been reached yet. Corey and colleagues performed a simulation to compare quality-adjusted life years (QALYs) between screening with liver biopsy vs non screening and including pioglitazone as therapeutical option. The authors reported that NASH screening could have been cost-effective, if superior treatment had been made available at the time of the model (Corey et al., 2016). Interestingly, a UK-based study comparing risk stratification using TE vs standard of care proved to be cost-effective in the general population (Tanajewski et al., 2017). Moreover, a recent cost-utility analysis also demonstrated that screening patients with T2DM with US and LFTs, followed by non-invasive tests was more effective than not screening (Noureddin et al., 2020). Based on this evidence, a recent position paper from the American Gastroenterological Association strongly recommends screening for NAFLD in patients within primary care (Ando and Jou, 2021) (Noureddin, Gastroenterology 2021).

Another important limitation to screening pathways of NAFLD is an overall low awareness among primary care clinicians, possibly as the result of gaps in knowledge as well as lack of awareness of relevant practice guidelines. In a survey study, over 40% of GPs were not familiar with clinical published guidelines for NAFLD management (Said et al., 2013). Moreover, such GPs were more likely to screen low-risk patients while neglecting patients at high-risk for liver fibrosis. Again, this phenomenon has been attributed to the misconception that LFTs may reflect disease severity. Along with developing cost-effective screening for NAFLD in primary care, future work should also focus on academic teaching regarding the burden of NAFLD and high-risk stratification as well as building awareness among GPs.

1.1.6 Management and treatment of patients with NAFLD

Patient with NAFLD or NASH without fibrosis are generally considered to be at low risk of developing liver-related complications within 10-15 years of follow-up. Nevertheless, such patients carry major metabolic comorbidities and, therefore, have an increased risk of mortality resulting from both cardiovascular disease and extra-hepatic malignancies (Adams et al., 2020). It is advisable that their cardiovascular (CV) risk should be optimised and that they should be screened for malignancy following up-to-date guidelines. Of note, recommendations on CV risk and cancer screening should be applied to all patients with NAFLD, regardless of the severity of liver disease. Patients with NASH and fibrosis stage 1 or 2 have a good prognosis but are known to have higher risk of progression to cirrhosis (Pais et al., 2013, Pais et al., 2011, Dyson et al., 2015) compared to patients with no fibrosis. Furthermore, patients with NASH and advanced fibrosis stage (F>3) should be considered for pharmacological treatment wherever possible, in addition to aggressive lifestyle modification (Rinella and Charlton, 2016). Finally, patients with evidence of cirrhosis should be followed-up for surveillance of complications, such as HCC and portal hypertension.

Lifestyle modifications and weight loss represent the cornerstone of treatment for all patients with NAFLD (Rinella and Charlton, 2016). Several studies have supported weight loss as effective treatment for reducing steatosis and disease activity (expressed as NASH activity score (NAS)) on histology. Specifically, modest weight loss (5% weight loss) may reduce ALT levels and steatosis,

whereas more marked weight loss (>10% weight loss) can favour NASH resolution and fibrosis regression, although this was achieved by a small group of patients (Vilar-Gomez et al., 2015, Wong et al., 2013a, Promrat et al., 2010). Moreover, several studies have investigated whether specific macronutrients and/or dietary patterns may have an independent impact on treating NAFLD. Overall, carbohydrate-restricted diets have been linked to greater reduction in hepatic fat content compared to low-calories diet alone, as high sugar intake was associated with greater inflammation (Browning et al., 2012, Browning et al., 2008, Oarada et al., 2015). Diets with limited cholesterol content may be beneficial in patients with NAFLD not only because they reduce their de novo lipogenesis but also as they lower the CV risk (Yasutake et al., 2009). Among others, the Mediterranean diet, which is naturally enriched with fibre and polyunsaturated fatty acids, is considered the best approach and has been able to reduce hepatic steatosis effectively over a period of 6 weeks with benefits being independent from weight loss achieved (Ryan et al., 2013, Stewart, 2018, Properzi et al., 2018). Nevertheless, the advantage of short-term changes in diet remains limited in a clinical perspective.

A previous prospective study including 293 patients demonstrated the effect and sustainability of weight loss after 52 weeks of monitored diet and exercise. Interestingly, the overall rate of NASH resolution was proportional with the amount of weight lost. However, only 30% of the patients managed to lose 5% weight and even less subjects achieved a 10% weight loss (Vilar-Gomez et al., 2015). These results raise important question on how sustainable these changes may be in the long term. An exercise plan should also be evaluated and tailored on patients' medical condition. Ideally, a combination of aerobic and resistance training should be favoured (Rinella and Charlton, 2016). When feasible, also a behavioural assessment for eating disorders should be offered to those patients who require support (Stewart et al., 2015, Forlano et al., 2021). Bariatric surgery represents also another option in a selected population of patients, as this improved liver histology as well as other obesity-related comorbidities (Jan et al., 2015). However, as complications may occur according to the procedure chosen, a careful risk-benefit analysis should be carried out on single cases.

Currently, there is no pharmacological treatment for NAFLD. However, as NAFLD is strictly intertwined with T2DM, several antidiabetic drugs have been previously considered and/or are

currently under evaluation to treat the condition. Specifically, metformin, although effective in ameliorating IR, has not shown any beneficial effect on liver histology (European Association for the Study of the et al., 2016, Polyzos and Mantzoros, 2016). Other antidiabetic medications, such as thiazolidinediones, showed a positive effect on disease severity but carry an unfavourable safety profile (Glen et al., 2016). Two classes of incretin-based therapies, the glucagon-like peptide-1 receptor agonists (GLP-1RA) and the dipeptyl peptidase-4 inhibitors (DPP-4i) represent promising new medications for treating NASH. Specifically, preliminary results from phase-2 studies with liraglutide (Keating et al., 2012) and semaglutide (Da and Satapathy, 2021) have shown encouraging results on weight loss and NASH resolution but not clear results on fibrosis regression. In another study, liralutide treatment reduced ALT in dose-dependent manner, especially in patients who had higher LFTs levels at baseline (Vilsboll et al., 2012). Liraglutide was also able to alter the fat distribution by decreasing waist circumference, wait/hip ration and the amount of visceral fat content (Suzuki et al., 2013). Moreover, a combination of exenatide with pioglitazone (Sathyanarayana et al., 2011) or with dapagliflozin (Gastaldelli et al., 2020) seem to further potentiate the effect in reduction of hepatic steatosis. Morerover, obethicolic acid, a synthetic bile acid acting as an farnesoid-X receptor (FXR) is also considered another promising agent for the treatment of NASH, as it has proved effective in improving histology in pre-clinical and human studies (Chitturi et al., 2018, Younossi et al., 2019c). There is a multitude of other medications in development for treating NAFLD/NASH (Albhaisi and Sanyal, 2021). Finally, manipulation of gut microbiome as potential treatment for NAFLD will be discussed in **Paragraph 1.2.5**.

To conclude, since established and licensed pharmacotherapies for NASH are on their way, it is of great importance to identify high risk patients. A correct risk-stratification will also allow for the development of a NAFLD referral/management strategy pathway. As a result, there will be a reduction in progression rates to end-stage liver disease, the number of non-liver and liver-related events as well as requirement for liver transplantation.

1.2 Gut microbiota and metabolic profile in NAFLD

1.2.1 Definition of gut microbiota and metabolomics

The term “gut microbiota” refers to the microorganism community residing in the intestinal lumen. Adult gut microbiota includes on average 10^{13} bacterial cells, resulting from more than 250 different species of bacteria, fungi, viruses and archaea (Sender et al., 2016). The human intestinal microbiota is mainly composed of bacteria from the *Firmicutes* (60 to 80%), the *Bacteroidetes* (20 to 40%), the *Proteobacteria* and the *Acinetobacteria* phylum, with high variability among individuals (Ley et al., 2006, Rinninella et al., 2019). Overall, the intestinal flora is susceptible to a wide range of factors, such as environmental, immunological or host factors as well as alteration in bile flow, gastric pH or intestinal dysmotility. However, although gut microbiota composition can be modulated by such factors, this is relatively stable in the long term (Wilson et al., 2020). Of note, the relationship between the host and the gut microbiota is symbiotic and plays a crucial role in modulating the health status. Specifically, the term “dysbiosis” refers to the disruption of the normal composition of the gut microbiota and conditions of dysbiosis have been associated with specific disease status in humans.

The term “metabolomics” includes a wide range of techniques which investigate the presence of small molecules (i.e. metabolites) which result from the interaction between the host and the gut microbiota. Therefore, the metabolome analysis aims to elucidate the biological implications that such metabolites have in the host-gut system.

1.2.2 The role of gut microbiota in the pathogenesis of NAFLD

Over the last decade, there has been a growing body of evidence linking the presence of intestinal dysbiosis to the pathogenesis of human liver disease, with a primary focus on metabolic disease and, specifically, NAFLD. Preliminary studies had associated NASH with small intestinal bacterial overgrowth in human subjects (Wigg et al., 2001). Further animal experiments involving the manipulation of the gut microbiome offered then the strongest evidence supporting the role of dysbiosis in NAFLD. Specific intestinal microbiome profile was associated with increased intestinal energy harvest from diet in obese mice. Interestingly, this trait was shown to be transmissible to lean,

germ-free mice via microbiome transfer (Turnbaugh et al., 2006). Furthermore, IR *per se* could be ameliorated after the administration of antibiotics (Membrez et al., 2008). In human studies, when obese men with metabolic syndrome received FMT from lean donors, they showed a significant improvement in IR and in butyrate-producing intestinal microbiota (Vrieze et al., 2012).

Over the last years, there has been an explosion of studies exploring changes in microbiome and their association with liver disease in NAFLD. A summary of the main changes described in NAFLD is summarised in **Table 1.2**. Overall, an increased abundance of *Proteobacteria* and *Firmicutes* as well as a reduction in *Bacteroidetes* and *Prevotellaceae* has been noted in patients with NAFLD compared to healthy controls (Hoyles et al., 2018, Aron-Wisnewsky et al., 2020, Lanthier et al., 2021, Astbury et al., 2020). Notably, the majority of the studies have focused on comparing healthy controls vs patients with NASH or with simple steatosis, as well as comparing different grades of steatosis. It should also be noted that studies comparing the bacterial taxonomic composition of patients with NAFLD vs those with NASH produced variable and even contradictory findings, as a result of differences in the cohorts analysed and in the methods used to assess liver disease (Schnabl, 2021). Unfortunately, there is only small evidence exploring specific changes in gut microbiota with regards to fibrosis stage in NAFLD, despite this being the main predictor factor in these patients.

Short chain fatty acid (SCFA), such as acetic, propionic, and butyric acid, play a crucial role in modulating the interaction between the host and the gut microbiota. Specifically, SCFA are the major products of carbohydrate fermentation and are mainly produced by gut microorganism up to a daily production of 50-100 mmol/l (Duncan et al., 2009). The SCFA influence the energetic metabolism, the immune response and the expansion of the adipose tissue (Arslan, 2014). Many of the effects of the SCFA are mediated via G-protein coupled receptors (GPCRs), which are mainly expressed on the immune system cells, the adipocytes and the intestinal endocrine cells. Within the intestine, SCFA act on GPCRs, slowing gastric emptying, intestinal transit and nutrient absorption (Musso et al., 2010). Moreover, specific SCFA, such as butyrate, might also suppress inflammation directly as a result of their interaction with T regulatory cells in the mucosa (Bollrath and Powrie, 2013, Furusawa et al., 2013).

Interestingly, SCFA were able to reduce the amount of hepatic steatosis, via modulating fatty acid synthetase activity and hepatic lipid synthesis in mice fed with high fat diet. In the same model, there was also a two-fold increase in hepatic lipid oxidation in the SCFA-fed mice, mainly due to an enhanced lipid oxidative state (den Besten et al., 2015). Despite clear results arising from animal models, the role of SCFA in altering the energy harvest has been less elucidated in humans. An early study reported a lower faecal energy excretion in those with obesity when compared with lean individuals (Wostmann et al., 1983). Among others, *Bacteroidetes* are the main contributors to the production of SCFA, with changes in their abundance impacting on the level of SCFA. Specifically, it has been demonstrated that a 20% decrease in faecal Bacteroidetes and a correspondent increase in Firmicutes translates into 150 kcal increase in energy harvest from the diet (Turnbaugh et al., 2006) (Jumpertz et al., 2011). Of note, such functional change in the microbiota composition can occur after few days of overeating, hinting at the presence of a very dynamic response with caloric intake. On a similar note, another study including adults with NAFLD showed an association between the presence of NASH and increased percentage of *Firmicutes* vs a reduced percentage of *Bacteroides*, after adjusting for BMI and dietary fat intake (Mouzaki et al., 2013). Not only microbiota but also diet composition have an influence on SCFA production and they can influence each other. Specifically, it is well known that dietary fibres represent an important source of SCFA. Moreover, high-fibre diets may promote the Bacteroidetes phylum, *Prevotella*, whereas high-fat diet reduce diversity and promote Firmicute growth (de Wit et al., 2012).

Another postulated mechanism linking the microbiome to NAFLD is its effects on the stimulation of adipose tissue. Specifically, disturbances of the microbiota can result in changes in the production of the intestinal form of fasting-induced adipocyte factor (FIAF). FIAF is a secreted protein which inhibits lipoprotein lipase (LPL) in several extra-intestinal sites, such as white adipose tissue, brown adipose tissue, muscles and hepatocytes (Backhed et al., 2004). Inhibiting intestinal FIAF has been linked to increased lipolysis in the adipose tissue and to reduced fatty acid oxidation in the muscles (Backhed et al., 2004). In the liver, FIAF inhibition results into activation of lipogenic enzymes and increased fat accumulation (Cani et al., 2007) (Mao et al., 2015).

Finally, several studies have also demonstrated that gut microbiota may influence host metabolism in NASH as a result of an augmented production of dietary ethanol. An early study linked dysbiosis with increased production of ethanol from the intestine; for example, 1 gr of Escherichia coli was able to produce 0.8 gr of ethanol per hour in anaerobic conditions (Dawes and Foster, 1956). Additionally, *Protebacteria*, which are well known alcohol-producing bacteria, were found to be substantially increased in patients with NASH (Zhu et al., 2013). Interestingly, ethanol per se may contribute to liver injury by increasing intestinal permeability and portal LPS levels, ultimately triggering inflammation (Parlesak et al., 2000). Furthermore, the gut microbiome may elicit the inflammatory response in the hepatocytes and macrophages directly via increased flux of tryptophan metabolites through the portal system (Krishnan et al., 2018).

DISEASE SEVERITY	BACTERIAL MICROBIOTA CHANGES	
NAFLD vs healthy controls	**Phylum**	↑ *Proteobacteria*
	Family	↑ *Enterobacteriaceae* ↓ *Rikenellaceae, Rhuminococcaceae*
	Genera	↑ *Escherichia coli, Dorea, Peptoniphilus* ↓ *Anaerosporobacter, Coprococcus* *Eubacterium, Faecalibacterium, Prevotella*
Severe steatosis or NASH vs controls or mild steatosis	**Phylum**	↑ *Fusobacteria*
	Family	↑ *Enterobacteriaceae* ↓ *Prevotellaceae, Clostridiaceae*
	Genera	↑ *Bacteroides, Ruminococcus, Shigella,* *Escherichia coli* ↓ *Clostridium*

Table 1.2. Summary of the main alterations of the intestinal microbiota previously described in patients with NAFLD and NASH. The table summarises the main finding from recent studies exploring the association between changes in microbiome in patients with NAFLD (Hoyles et al., 2018, Aron-Wisnewsky et al., 2020, Lanthier et al., 2021, Astbury et al., 2020).
Abbreviations: NAFLD: non-alcoholic fatty liver disease, NASH: non-alcoholic steatohepatitis.

1.2.3 Disturbances in metabolic profile in patients with NAFLD

Metabolomic techniques have been employed widely to explore the role of small molecules and metabolic products, such as amino acids (AA), fatty acids, and carbohydrates, in the field of NAFLD research (Dumas et al., 2014). It is well known that the metabolism of AA modulates oxidative stress, insulin resistance and inflammation in the liver tissue. Specific disturbances in the level of circulating AA have been described in patients with NAFLD, such as an increase in branched chain aminoacids (BCAAs; leucine, isoleucine, valine) and in aromatic aminoacids (AAAs; tryptophan, tyrosin, phenylalanine), with a reduction in AA related to the metabolism of glutathione (glutamine, glycine, serine) (Yamakado et al., 2017, Newgard et al., 2009). Furthermore, plasma levels of BCAAs are also augmented in patients with other metabolic comorbidities such as patients with obesity and/or T2DM (Newgard et al., 2009, Laferrere et al., 2011), while higher levels of BCAAs have been described in men compared to women, suggesting gender discrepancy in terms of metabolic profile and risk for NAFLD (Krumsiek et al., 2015).

There has been an increasing body of evidence hinting at a possible role of circulating aromatic aminoacids as non-invasive markers for NAFLD severity. In a recent study, hepatocellular ballooning and inflammation, as assessed by NASH CRN scoring system, were associated with increased branched chain aminoacids and aromatic aminoacids, while fibrosis stages could be predicted using a combination of glutamate, serine and glycine (Gaggini et al., 2018). Moreover, plasma branched chain aminoacids correlated with NAFLD severity, more pronouncedly in women compared to men (Grzych et al., 2020). Another study by Masarone et al (Masarone et al., 2021) attempted to differentiate a cohort of biopsy-proven NAFLD patients into NAFL, NASH and NASH with cirrhosis, based on an untargeted plasma metabolomics profile and an algorithm with machine learning. A combination of glycocholic acid, taurocholic acid, phenylalanine and branched chain aminoacids could predict the NAFLD severity with an accuracy >80%.

In large scale clinical studies, increased fasting plasma levels of branched chain aminoacids have been positively associated with peripheral IR and developing T2DM (Newgard et al., 2009, Wang et al., 2011). Specifically, in obese non-diabetics, higher baseline concentrations of the branched chain and aromatic aminoacids were significantly associated with the risk of developing

diabetes in 12 years follow-up. Moreover, normoglycemic patients showed normal levels of those AA and their increase was associated with an up to a 4-fold increased risk of developing diabetes in the future (Wang et al., 2011). However, an opposite trend in aminoacids is usually reported when liver disease progresses, as elevated aromatic aminoacids and lowered branched chain aminoacids, especially in those with cirrhosis, mainly due to their impaired hepatic metabolism (Morgan et al., 1978, Fischer et al., 1976). As such, a reduced branched chain aminoacids to aromatic aminoacids ratio (known as Fischer's ratio) has been suggested to identify patients with more severe liver disease (Michitaka et al., 2010). Interestingly, branched chain aminoacids are mainly catabolized in peripheral organs such as muscle and adipose tissue (Newgard et al., 2009), while aromatic aminoacids are mainly metabolised in the liver (Matthews, 2007). Moreover, the majority of such aminoacids have been associated with hepatic IR, while only glutamate, glycine and tyrosine levels result from peripheral IR (Gaggini et al., 2018, Haufe et al., 2016).

Finally, the metabolism of aminoacids seems to be associated with oxidative stress, via modulating the metabolism of glutathione in NAFLD. Specifically, Zhou et al demonstrated that alterations of key aminoacids of the metabolism of glutathione may be clinically relevant. Specifically, patients with NASH showed increased levels of glutamate and isoleucine, and decreased levels of glycine and serine. A scoring system based on glutamate, isoleucine, glycine, two lipids and a combination of clinical features was able to predict the presence of NASH which high accuracy (Zhou et al., 2016).

1.2.4 The role of bile acids in the pathogenesis of NAFLD

Bile acids (BA) are potent "digestive surfactants" that promote the absorption of lipids, including fat-soluble vitamins. Moreover, BA are involved in the primary pathway for the metabolism of cholesterol catabolism and account for ~50% of its daily turnover (Abadie et al., 1994). BA are mainly synthetised in the liver, resulting from the conversion of cholesterol into more water-soluble compounds (Acalovschi et al., 2009); BAs are then secreted into the hepatic canaliculi and stored in the gallbladder. After excretion and digestive process, about 95% of the BAs are re-absorbed from the terminal ileum, while only 5% reach the colon. In the colon, the remaining fraction of BAs is

passively reabsorbed after modifications, i.e. deconjugation and oxidation. The intestinal microbiota is actively involved in modulating the pool circulating and extracted BAs, as they participate actively to hydrolysis and dehydrogenation reactions (Cai and Chen, 2014). Overall, BAs display several functions as they are involved not only in the digestion and absorption of lipids, but they also act as signalling molecules modulating the metabolism of glucose and lipids through the FXR and the C protein-coupled bile acid receptor TGR5 (Masoodi et al., 2021). In the liver, FXR activation results in the downregulation of free fatty acid (FFA) synthesis and de novo lipogenesis (Chiang, 2017). FXR are also involved in carbohydrate metabolism, as this regulates hepatic gluconeogenesis, and prevents hepatic inflammation (Khalid, 2015).

An increased level of BAs has been widely demonstrated in liver tissue (Dasarathy et al., 2011), plasma (Dasarathy et al., 2011, Aranha et al., 2008) and faeces (Aranha et al., 2008) of patient with NASH. There is unanimous consensus that higher levels of serum BAs in patients with NASH and NAFL is mainly driven by increased levels of conjugated Bas, while evidence on secondary BAs is still conflicting (Noureddin et al., 2020). A large body of work has demonstrated a dysregulation of BA metabolism in patients with NASH, including elevated primary conjugated BA, decreased levels of specific secondary BA and alteration of excreted BA (Newgard et al., 2009, Dasarathy et al., 2011, Aranha et al., 2008). Moreover, the expression of BA transporters also seems to be impacted in patients with NASH or simple steatosis (Puri et al., 2018, Legry et al., 2017). Specifically, the concentrations of cholic, chenodeoxycholic and deoxycholic acids were significantly increased in the liver in patients with NASH compared to controls (Aranha et al., 2008). Moreover, cholic acid has been strongly associated with inflammatory markers, with deoxycholic acid showing an opposite trend (Aranha et al., 2008). Interestingly, a recent study suggested that there might be specific trend in taurine-conjugated vs glycine-conjugated BAs, with the first being elevated and the latter suppressed in patients with NASH (Lake et al., 2013). Nevertheless, it should be noted that many studies have not accounted for confounding factors such as obesity and IR, which have an independent influence on BA metabolism.

1.2.5 Manipulation of microbiota as therapeutic option in NAFLD

Given the recent exploration of the role of the microbiota in NAFLD, there has been an increasing interest in evaluating the manipulation of the intestinal flora as potential treatment option for patients with NAFLD. In this sense, different strategies have been investigated, including the use of nondigestible prebiotics, probiotics and symbiotics (Patel and DuPont, 2015). Probiotics display important beneficial effects that could be useful in patients with NAFLD, such as antimicrobial properties, support of the integrity of the intestinal barrier and immune modulation (Patel and DuPont, 2015). The administration of VSL#3, a mixture of eight probiotic strains, for 4 months in children with obesity improved NAFLD and BMI, possibly as a result of increased levels of GLP-1 (Lee et al., 2012, Campbell and Drucker, 2013). In adults with NAFLD, treatment with *Bifidobacterium longum* was able to lower the levels of inflammatory markers (Tumour necrosis factor (TNF-α), c reactive protein, lipopolysaccharide (LPS)), insulin resistance (as expressed as homeostatic model assessment for insulin resistance, HOMA-IR), AST and steatosis after 24 weeks compared with lifestyle alone (Malaguarnera et al., 2012). In another study, the administration of a probiotic formula could reduce intra-hepatic triglyceride content and improve ALT levels in patients with biopsy-proven NASH (Wong et al., 2013c). In a further analysis by the same group, a decrease in *Bacteroidetes* was considered the main driver of the therapeutical effect, with the overall biodiversity being equal (Wong et al., 2013b). Similarly, symbiotic supplementation has shown to reduce fasting insulin and triglyceride levels in patients with T2DM (Beserra et al., 2015). Although it has been proved that probiotics are able to modify the microbiota, there are important limitations to the studies previously published in the field, such as variable dosing, small numbers of participants and techniques used to assess liver disease (Ferolla et al., 2015).

Faecal microbiota transplantation (FMT) involves transferring functional microbiomes from healthy individuals to the gastrointestinal (GI) tract of patients with intestinal dysbiosis. FMT is an effective therapeutic option for recurrent *Clostridium difficile* infection, as well as for metabolic diseases associated with intestinal microbiota dysbiosis. Previous results from animal models demonstrated that transplanting the gut microbiota from lean or obese mice may induce similar phenotypes to that of the host (Ridaura et al., 2013, Walker and Parkhill, 2013). Similarly, overweight

patients with metabolic syndrome showed a significant improvement in hepatic and peripheral IR 6 weeks after receiving FMT (Vrieze et al., 2012). Other studies have also demonstrated that FMT may have a therapeutical role in improving T2DM (Anderson et al., 2012). Nevertheless, other studies have suggested that the effect of FMT in these patients is limited (Craven et al., 2020). However, evidence from human studies is limited and yet in development, with a large number of studies still in the recruitment phase (Chen et al., 2020a, Odenwald and Turner, 2013).

To conclude, the interaction between the intestinal microbiota and the host plays an important role in the development and progression of liver disease in patients with NAFLD. Such effect is mediated by an intricated combination of SCFA, small metabolites and circulating BA on the host metabolic status. So far, large number of studies have focused on NASH and simple steatosis. It would be clinically important to explore the presence of specific gut microbiota changes and metabolic profiles with regards to liver fibrosis, as this represents the main prognostic factor in these patients.

1.3 Gut barrier in NAFLD

1.3.1 Definition of gut barrier and gut permeability

The intestinal barrier function is defined as the ability of the mucosa and of the components of the extracellular barrier to prevent the exchange between the intestinal lumen and the tissues (Odenwald and Turner, 2013). Conversely, intestinal permeability refers to the property that allows such exchange. The GI mucosa is a semi-permeable barrier with multiple properties, such as the absorption of nutrients and immune sensing. The gut barrier plays an important role in limiting the passage of potentially pathological molecules and microorganisms into the systemic circulation. Moving from the luminal to the basolateral layer, the intestinal barrier includes the gut microbiota, the mucus layer, the monolayer of epithelial cells and then the immune cells located in the lamina propria. The mucus layer represents a physical barrier which separates the microbiota and large molecules from contacting the epithelial cells, but also acts as a facilitator for the passage of small molecules. Ultimately, the mucus layer defends the epithelium from acid and digestive enzymes. In

such distribution, the bacteria from the intestinal flora are mainly restrained within the outer part of the film of mucus (Johansson et al., 2008) (**Figure 1.3**).

The intestinal epithelium represents the crucial component of the intestinal mucosal barrier. The epithelial layer is composed of different cell populations, of which the enterocytes are the most abundant. Enterocytes display several essential properties, such as protective function and uptake of nutrients and other substances from the intestinal lumen. Goblet cells also populate the intestinal barrier, being actively involved in the secretion of mucus, while the enteroendocrine cells produce GI hormones, peptides and neurotransmitters. Moreover, the Paneth cells, which are mainly located at the intestinal crypts, as well as the T-cells, mainly located in the lamina propria, participate to the immune response as they secrete anti-microbial compounds (Crosnier et al., 2006).

The tight junctions (TJ) are the main structures forming the complex for cell-to-cell adhesion that polarizes the intestinal epithelium, as they regulate the passage of ions and, therefore, create a potential difference at either side of the tissue. Among other structures, the hemi-desmosomes are also important for the adhesion of the epithelial cells to the lamina propria (Farquhar and Palade, 1963). Of note, products may cross the epithelium from the lumen using different pathways, which depend mainly on chemical properties, such as size and hydrophobicity. Small, hydrophilic and lipophilic compounds can use the transcellular route to cross the plasma membrane on the enterocytes. Ions, water and larger hydrophilic compounds between 400 Da and 10-20 kDa are transported using the paracellular route between enterocytes, which is principally regulated by TJs. Several other macro-nutrients, such as amino acids, vitamins and carbohydrates may cross the enterocytes actively, using specific transporters. Even larger peptides, proteins and bacteria may move to systemic blood stream, via a combination of endocytosis, transcytosis, and subsequent exocytosis.

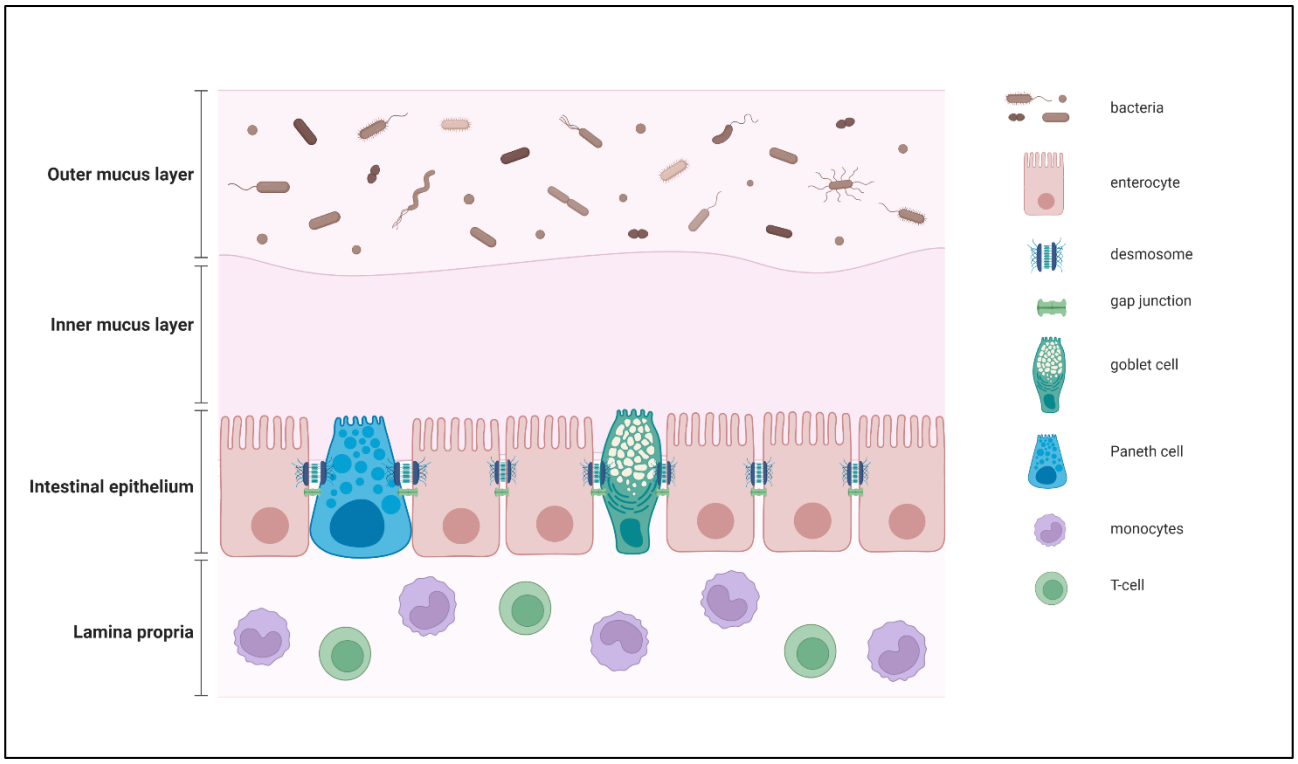

Figure 1.3 Intestinal mucosal barrier. Epithelial cells, together with Paneth cells and goblet cells, form a layer that works as a mechanical barrier which is sealed by a complex combination of desmosomes and gap junctions. The layer of mucus acts as a chemical barrier that limits the direct contact between the gut microbiome and the intestinal epithelium. Immune cells reside mainly in the lamina propria.

1.3.2 Methods for assessing the gut permeability

Several techniques have been employed to measure the intestinal permeability both *in-vitro* and *in-vivo*. Commonly, permeability has been assessed as Transepithelial electric resistance (TEER) measured across monolayers of specific cell lines or biopsies of the GI mucosa. The TEER is usually measured in Ohms and it is a quantitative measure of the integrity of the gut barrier. The classic set-up used for the measurement of TEER consists of a cellular monolayer cultured on a semipermeable insert which compartmentalises the model into an apical (upper) and basolateral (or lower) space. Two electrodes are placed in the upper and lower compartment and therefore, are physically separated by the cellular monolayer. Hypothetically, the ohmic resistance can be calculated by applying a direct current voltage to the electrodes and measuring the actual current between them. The ohmic resistance is calculated based on Ohm's law as the ratio of the voltage and current. These experiments are usually carried out with the use of an epithelial volt/ohm meter (EVOM) employing an alternating current, which reduces the possibility of direct electric damage to

the monolayer. Moreover, EVOM works on a frequency of 12.5 Hz which is designed to avoid any charging effect on the cell layer (Srinivasan et al., 2015). Other techniques for measuring the permeability across cell monolayer in vivo have used probe molecules, such as dextran 4 or 40, exploiting a similar concept (Schoultz and Keita, 2020).

Interestingly, the intestinal permeability may also be measured *in vivo* as the urinary excretion of indigested probes (mainly saccharides) that cross the intestinal epithelium by the paracellular pathway, are filtered by the glomerulus and excreted in the urine without active reabsorption. The majority of the saccharides used in these techniques are absorbed in the small bowel and colon, with different timing of urinary excretion reflecting different regional absorption throughout the GI tract (Camilleri and Vella, 2021).

Recent studies have also suggested that the assessment of serum levels of Fatty acid binding proteins (FABP) and zonulin may be of use as an estimation of gut permeability in humans. Specifically, FABP-2 are small cytosolic proteins which transport fatty acids and include several isotypes which are expressed in different tissues, such as heart, liver, intestine, muscle and adipocyte (Niewold et al., 2004). Intestinal FABP (i-FABP or FABP-2) is uniquely located in mature small-intestinal enterocytes. Moreover, the peculiar position within the intestinal villi facilitates its leakage into the circulation when damage to the intestinal mucosa occur (Kanda et al., 1992). Early studies confirmed that FABP-2 could be detected in plasma or urine as a result of intestinal ischemia in both animals (Gollin et al., 1993) and in humans (Kanda et al., 1996). In the field of liver disease, individuals with CHB and CHC have shown higher plasma levels of FABP-2 compared to controls, suggesting some degree of enterocytes death (Sandler et al., 2011). Finally, there is also recent evidence suggesting the use of zonulin and calprotectin as ex-vivo serum markers of increased gut permeability (Fasano, 2012, Schoepfer et al., 2010, Konikoff and Denson, 2006).

1.3.3 Intestinal bacterial products translocation

The term intestinal bacterial translocation refers to the passage of viable micro-organism from the gut lumen toward the mesenteric lymphatic system, and, subsequently, towards the system

bloodstream to extraintestinal sites, such as the spleen and liver (Berg and Owens, 1979). Notably, a certain degree of bacteria and bacterial products may translocate even under physiological conditions. LPS is a dominant molecule which is located on the surface of Gram-negative bacteria. Elevated levels are found in the plasma of patients with GI and non-GI inflammatory diseases (Dlugosz et al., 2015, Du Plessis et al., 2013). The translocation of molecules between 200 Da and 4 kDa implies some degree of increased intestinal permeability via the paracellular route.

Under physiological conditions, the paracellular pathway is limited to molecules up to 20 kDa. As such, bacteria or large particles cannot translocate across the epithelium using this pathway. Specifically, the uptake of bacteria occurs mainly via the Peyer's patches M-cells, and to a lesser extent via the enterocytes (Keita and Soderholm, 2010). Of note, the M-cells present a poorly organised border with short and irregular microvilli, which facilitate the internalization of bacteria, viruses and large molecules from the intestinal lumen to the lymphoid system. In enterocytes, the uptake of enteric bacteria relies on the phosphorylation of the myosin light chain (MLC). Notably, the IFN-γ regulated the MLC and therefore its disturbances may enhance the paracellular permeability to molecules up to 10 kDa, but not to small molecules of 200 Da (Watson et al., 2005).

1.3.4 Gut permeability in T2DM

The presence of T2DM is known to be associated with low-grade systemic inflammation as well as with alterations of the intestinal barrier function. Specifically, gut permeability has been studies extensively in vivo using the Dextran FITC assay in animal models and was described as increased in diabetic obese mice (Cani et al., 2008) (Cani et al., 2009). Interestingly, such changes were modifiable to some extent when the gut microbiome was manipulated, ie with the administration of prebiotics (Cani et al., 2008) or antibiotics (Cani et al., 2009).

There is also a growing evidence supporting the presence of increased gut permeability in patients with T2DM, expressed as increased serum levels of LPS (Harte et al., 2012, Pussinen et al., 2011). When compared to non-diabetics, patients with T2DM show significantly higher levels of LPS (Gomes et al., 2017). Moreover, LPS levels were also predictive of developing T2DM in 10

years follow-up, in the FINRISK97 cohort (Pussinen et al., 2011). Furthermore, patients with T2DM not only have higher absolute concentration of LPS, but also higher post-prandial excursions of LPS following a high fat diet meal (Harte et al., 2012). These results suggest a chronic increase in LPS and also a higher susceptibility to further increase of LPS as a response to diet in patients with T2DM.

Changes in the composition of the gut microbiota have also been described as contributing to an impaired mucosal barrier (Dabke et al., 2019). Specifically, microbial perturbations have been associated with elevated levels of LPS in the systemic circulation of patients with T2DM (Dabke et al., 2019). Systemically, the LPS interacts with TLR-4 receptors and activates a pro-inflammatory cascade, mediated by the release of cytokines, adhesion molecules and reactive oxygen species (Kim and Sears, 2010). Moreover, in patient with T2DM, decreased levels of glucagon-like peptide 2 (GLP-2) have also been associated with disruption of zonulin-1, occluding and claudin-1, resulting in abnormalities in the TJ barrier (Yu et al., 2016).

Patients with T2DM may also present other peculiar mechanism by which intestinal permeability may be impaired. For instance, in vitro experiments have shown that leptin may modulate the expression of TJ proteins directly (Ahmad et al., 2017). Of note, leptin is a hormone which regulates the appetite sensation; its dysfunction has been described among patients with T2DM (Gruzdeva et al., 2019). A previous study involving animal models demonstrated that consumption of high sugar diet facilitates the degradation of the mucus barrier via the selection of mucus-degrading bacteria (Desai et al., 2016). Furthermore, hyperglycaemia has been shown to damage the intestinal epithelial cells directly by altering TJ integrity, with a mechanism which depends on glucose transporter-2 (GLUT2) (Thaiss et al., 2018). In the same study, when hyperglycaemia was corrected, the deletion of inhibition of GLUT-2 was able to restore barrier function (Thaiss et al., 2018). Finally, an inadequate glycaemic control has been associated with increased translocation of microbial products in the systemic circulation (Thaiss et al., 2018).

1.3.5 Gut permeability in NAFLD

There is evidence suggesting that plasma endotoxin concentrations are increased in the early stages of liver disease from NAFLD in a paediatric population, suggesting the presence of some degree of increased gut permeability already in the initial phases of the disease (Nier et al., 2017). Moreover, children diagnosed with NASH show higher levels of LPS concentrations compared to control subjects, hinting at a relationship between bacterial translocation and triggering the immune system in NAFLD (Giorgio et al., 2014).

Not only excessive food intake but also specific dietary patterns have proved to be strongly associated with alterations in the intestinal barrier (Alvarez-Mercado et al., 2019). A previous study reported an improvement in visceral adiposity, weight and serum LFTs in patients with NAFLD who were following a Mediterranean dietary regime or low-calorie diet for 16 weeks (Biolato et al., 2019). However, there was no specific change in intestinal permeability (Sanchez-Rodriguez et al., 2020). Conversely, when obese patients with steatosis underwent a weight-reduction regime and lifestyle modifications for 52 weeks, there was an improvement in the gut permeability up to within normal values (Damms-Machado et al., 2017). Moreover, increasing the dietary fibre intake translated into a reduction in serum zonulin levels, LFTs levels and hepatic steatosis in patients with NAFLD, possibly by altering intestinal permeability (Krawczyk et al., 2018).

Intestinal dysbiosis may also impact upon the expression of TJ, increasing gut permeability and translocation of bacterial products (Nicoletti et al., 2019). Among others, bacteria from the *Bacteroides* spp have been shown to increase the expression of zonulin and improve epithelial barrier function (Yoshida et al., 2018). Specifically, a recent study suggested that the improvement seen in the intestinal permeability reported after chronic physical exercise is mainly driven by an increase of the *Firmicutes* to *Bacteroides* ratio, as well as to an improvement in microbial diversity (Keirns et al., 2020). The composition of gut microbiota may also modulate the abundance of SCFA, which in turn may have protective effect on the intestinal epithelium, as they promote epithelial cell proliferation and adhesion (Mailing et al., 2019). Specifically, elevated levels of butyrate induce the release of anti-inflammatory cytokines and promote the integrity of the intestinal barrier (Keirns et

al., 2020). In this sense, the intestinal inflammatory milieu could increase the permeability per se and be contributing to decompensation events in patients with more advanced liver disease (Riva et al., 2020).

A recent metanalysis including studies that investigated the increased permeability in paediatric and adult NAFLD, concluded that small intestinal permeability increased with the degree of hepatic steatosis, while no association was found with hepatic inflammation, ballooning or fibrosis (De Munck et al., 2020, Miele et al., 2009). Moreover, the number of patients included in those studies was relatively small (De Munck et al., 2020). On a biological point of view, it is expected that an augmented translocation of bacterial products leads to inflammation and fibrogenesis in the liver, via the stimulation of TLR-4. As such, an association between the degree of increased gut permeability and severity of NAFLD is somehow predicted.

To conclude, there is evidence suggesting that patients, mainly paediatrics, with NAFLD may have increased gut permeability. A combination of diet, changes in gut microbiota, hyperglycaemia, hormonal status may be responsible of such changes in the intestinal epithelium in diabetic patients with NAFLD. However, a clear association between gut permeability and severity of liver disease in NAFLD has not been demonstrated so far.

1.4 Inflammatory status in NAFLD

1.4.1 Definition of metabolic inflammation

The term “metabolic inflammation” (or meta-inflammation) identifies the activation of pro-inflammatory signalling pathways and cytokine production in metabolic tissues, i.e. adipose tissue, in presence of IR and obesity. Interestingly, metabolic inflammation shows a different course compared to the classic acute inflammatory response noted in bacterial infections, where a strong immune response leads to the elimination of the pathogen and to a rapid resolution to baseline conditions. Metabolic inflammation is characterised by a chronic, low-grade inflammation. Moreover, inflammatory mediators behave as true metabolic hormones which regulate insulin signalling and sensitivity (Hotamisligil, 2017).

1.4.2 The role of the gut-liver axis towards meta-inflammation in NAFLD

The gut-liver axis is one of the main contributors to the meta-inflammation in NAFLD. Not only a gut dysbiosis is associated with intestinal inflammation, but also with systemic inflammatory response via the translocation of bacterial products(Grabherr et al., 2019). A large number of gut metabolites have been proved to elicit a chronic inflammatory status, including ethanol production, changes in short chain fatty acids, secondary bile acids, branched chain aminoacids and many more. Among others, pathogen-associated molecular patterns (PAMPs) are also considered to play a major role in the development and progression of NAFLD. Such intestinal metabolites may all modulate the immune response in many target organs, such as adipose tissue, muscle and liver (Zmora et al., 2017).

The contribution of PAPMs to liver damage has been shown in preclinical studies, where steatosis, inflammation and fibrosis are reduced in TLR-4 deficient mice under HFD (Rivera et al., 2007, Saberi et al., 2009). Furthermore, inflammasome deficiency-associated changes in gut microbiota result in hepatic steatosis and inflammation with the influx of TLR-4 and TLR-9 agonists, leading to enhanced TNF-alpha expression and inflammation in mice (Henao-Mejia et al., 2012).

1.4.3 The role of the adipose tissue-liver axis for meta-inflammation in NAFLD

Adipose tissue plays an important role in the development of IR and NAFLD. Specifically, the presence of obesity has been associated with an enhanced lipolysis and with the secretion of inflammatory and pro-fibrogenic molecules, whose main target organ is the liver (Luci et al., 2020). Notably, the rapid expansion of the adipose tissue leads to relative hypoxia and, therefore, adipocyte cell death, as the cellular expansion rate tends to exceed the local oxygen availability, even though in presence on an enhanced angiogenesis (Lefere et al., 2016). Typically, such necrotic/apoptotic cells release a wide range of inflammatory cytokines, which perpetuate the inflammation and activate adipose tissue macrophages (ATMs), which cluster in a characteristic “crown-line” structure surrounding dying adipocytes (Choe et al., 2016). In addition to an increase in the numbers of ATM, obesity is also associated with a change in their phenotype towards a pro-inflammatory M1 state, characterised by the expression of TNF-α, IL-6 and IL-12 (Lumeng et al., 2008). These various

mediators then converge on inflammatory signalling pathways such as the activation of c-jun N-terminal kinase and IκB kinaseβ, which in turn may alter insulin sensitivity and energy homeostasis (Gao et al., 2002). Interestingly, it has been shown that the severity of ATM correlated with the degree of hepatic steatosis, inflammation and fibrosis within the liver (Kolak et al., 2007, Tordjman et al., 2009).

With regards to meta-inflammation, there might as well be space for an adipose tissue-gut axis, as obesity *per se* has been linked to intestinal inflammation and the up-regulation of TNF-α, resulting in a further increase in the gut permeability (Henao-Mejia et al., 2012). Furthermore, Interleukin-1 beta (IL-1β), which is mainly produced by the liver, may also contribute to an increased gut permeability, as such molecule can alter the expression of MLCK (Al-Sadi et al., 2013). Similarly, Interleukin-6 (IL-6) may also be able to modulate the permeability of the intestinal epithelium through the regulation of claudin-2 up-regulation (Suzuki et al., 2011).

1.4.4 Hepatic inflammation in NAFLD

A large amount of innate and adaptive immune cells is involved in the onset of inflammation in the liver in patients with NAFLD. Overall, hepatic inflammation results from the complex interaction of monocytes, resident macrophages (Kupffer cells), neutrophils as well as parenchymal hepatocytes and liver sinusoidal cells (Luci et al., 2020, Cai et al., 2019). The hepatocytes and the Kupffer cells interact with portal and systemic metabolites, such as PAMPs and damage-associated molecular patterns (DAMPs) and translate them into a cascade of inflammatory events and metabolic dysfunction in the liver (Cai et al., 2019, Hammoutene and Rautou, 2019). Subsequently, the liver transits from an immune-tolerant to an immune-active state, with a further production of inflammatory cytokines, such as transforming growth factor-beta (TGF-β), interleukin-10 (IL-10), IL-1, IL-6 and TNF-α.

Liver macrophages are important drivers of hepatic inflammation. At early stages of NAFLD, the enhanced pro-inflammatory polarization of liver-resident Kupffer cells could contribute to hepatic steatosis and initiate inflammation (Stienstra et al., 2010, Huang et al., 2010) and facilitate the

recruitment of other immune cells into the liver. In animal models, the depletion of Kupffer cells improves hepatic steatosis and hepatic IR in rats on high-fat diet (Huang et al., 2010). Moreover, it has been demonstrated that a state of macrophage activation towards a classically “M1” phenotype is able to promote hepatic steatosis and inflammation in mice (Navarro et al., 2015). As such, it has been argued that the balance between a pro-inflammatory versus anti-inflammatory state in macrophages may be crucial for the development and progression of NAFLD, even in the early stages of the disease (Wan et al., 2014). In this sense, bacterial products, toxic lipids and adipokines may shift the balance towards a pro-inflammatory polarization and the recruitment of further immune cells, which is the hallmark characteristic of NASH and fibrogenesis (Krenkel et al., 2018).

To conclude, NAFLD is characterised by a systemic low-grade inflammatory status which translates into disease progression. Both the gut and the adipose tissue contribute to the maintenance of such pro-inflammatory status, and therefore to liver injury. However, the complex interplay between gut, adipose tissue and liver has not been fully elucidated.

1.5 HYPOTHESES OF THE STUDY

Hypothesis 1. Clinically significant NAFLD is highly prevalent among patients with T2DM in the community and the risk-stratification for NAFLD can be improved

Aims:

1. To assess the prevalence of clinically significant NAFLD among patients with T2DM in the community

2. To assess the prevalence of other undiagnosed chronic liver disease among patients with T2DM in the community

3. To perform a risk-stratification for the development of a NAFLD referral/management strategy pathway from primary care

Hypothesis 2. Metabolic profile and gut microbiota composition are associated to more severe liver disease in diabetic patients screened for NAFLD

Aims:

1. To compare the metabolic profile and gut microbiome between diabetics with normal liver vs diabetics with NAFLD and different liver disease severity, all confounders included

2. To compare the metabolic profile and gut microbiome between diabetics with normal liver vs diabetics with NAFLD and different liver disease severity, correcting for metabolic risk factors

3. To compare the metabolic profile and gut microbiome between diabetics with and without NAFLD, correcting for metabolic risk factors

Hypothesis 3. Increased gut permeability is associated with more severe liver disease in diabetic patients screened for NAFLD

Aims:

1. To explore gut permeability in diabetic patients with and without NAFLD and with different stages of liver disease severity using an in-vitro model

2. To explore the factors associated with increased gut permeability in diabetic patients screened for NAFLD

Hypothesis 4. A pro-inflammatory status is associated with more severe liver disease in diabetic patients screened for NAFLD

Aims:

1. To analyse the inflammatory status of diabetic patients screened for NAFLD

2. To explore the clinical and metabolic factors associated with the inflammatory status in diabetic patients screened for NAFLD

2. MATERIALS AND METHODS

2.1 Study cohort

2.1.1 Enrolment of the patients

This single-centre, cross-sectional study included all consecutive patients with T2DM being followed up in primary care. Specifically, patients were recruited from diabetes primary care (Tier 1) and community (Tier 2) clinics from the North-West London GP network (England, June 2018). Patients were invited to take part to the study by their routine care team, such as GPs, dieticians, podiatrists and diabetic nurses. Inclusion criteria were ability to give informed consent, age >18 years and presence of T2DM as defined by medical history, and specifically on fasting plasma glucose ≥7 mmol/L or on the 2 h post-challenge plasma glucose ≥11.1 mmol/L. Exclusion criteria were inability to give informed consent, age <18 years and use of anti-diabetic drugs for conditions not including T2DM (i.e. the use of metformin for polycystic ovary syndrome alone).

Sample size was calculated using a sample size calculator under the following assumptions: the prevalence of NAFLD in patients with T2-DM expected to be 60%, derived from tertiary care studies, the level of confidence 95% and the proposed power of the study 80%. The sample size was then adjusted for the percentage of patients expected to decline screening (10%), the percentage of patients with other causes of CLD (3%) and the dropout rate expected for the liver biopsy (a proportional 10%) resulting in 410 patients. Overall, the enrolment rate was significantly impacted by the COVID-19 pandemic and associated restrictions and closed earlier at 300 patients.

2.1.2 Clinical assessment and screening process

All consecutive patients were screened for liver disease and NAFLD using blood tests (LFTs, lipid and metabolic profile, fasting insulin, HbA1c, ferritin), full liver screen (anti-HCV antibodies, HBV serologic panel, auto-antibodies, ferritin, caeruloplasmin, alpha-1 antitrypsin), transient elastography and ultrasound. Based on blood tests, non-invasive markers of fibrosis (such as NAFLD fibrosis score and FIB-4) were also calculated as per published formula (Angulo et al., 2007, Vallet-Pichard et al., 2007). Moreover, medical history, alcohol consumption, dietary intake assessment and

anthropometric parameters (BMI, waist and hip circumference) were recorded for each patient. Patients' ethnic background was clustered into six groups: White Caucasian, White Hispanic, South Asian, East Asian, Black African and Afro-Caribbean, Arab. A diagnosis of both alcoholic and non-alcoholic fatty liver disease (BAFLD) was defined as having NAFLD and reporting chronic alcohol consumption greater than 14 UI of alcohol per week, regardless of gender (guidelines, 2010).

As an estimation of socio-economic status, patients' postcodes were used to assign a deprivation rank according to the English Index of Multiple Deprivation (IMD). Briefly, in England, the IMD scores identify areas of poverty, inequality and decreased opportunity based on income, employment, education attainment and other attributes. IMD divides England into 32,844 small areas, ranging from 1 (most deprived) to 32,844 (least deprived). IMD and related single domains were analysed as continuous variable (median of IMD and single domains) as well as categorical variable (percentage of patients into terciles of IMD and single domains).

TE and US were performed by a single operator, myself, after fasting for 4 hours. Liver stiffness measurement (LSM) and controlled attenuation parameters score were therefore recorded. Only LSM meeting the following criteria were included in the analysis: ≥ 10 valid measurements, ≥ 60% success rate, and interquartile range/median ratio (IQR/M) ≤0.3 (Boursier et al., 2013). Presence of hepatic steatosis on US was defined as per previously published criteria (Hernaez et al., 2011). A clinical diagnosis of cirrhosis was based on biochemical, ultrasonographic (irregular hepatic profile, caudate lobe hypertrophy and splenomegaly) and elastographic (LSM) features (LSM≥12 kPa).

Based on the results of TE performed on the day of the enrolment, the patients were therefore stratified according to LSM ≥ 8.1 kPa (European Association for the Study of the Liver. Electronic address et al., 2021). A further cut-off of TE, LSM≥12.1 kPa, was applied for further stratification of the patients for severity of liver disease. The subgroup of patients with elevated LSM were considered for further investigations (such as a liver biopsy) and referred to specialist care as per guidelines' recommendation and standard of care.

2.1.3 External validation cohorts

Two external centres provided a retrospective cohort of patients with T2DM diagnosed with NAFLD as external validation cohorts: the Royal Free Hospital (London, UK) and the Palermo University Hospital (Palermo, Italy). The diagnosis of NAFLD was based on either US or histology, in absence of other causes of liver disease, use of steatogenic drugs and chronic alcohol consumption above14 UI per week (Browning et al., 2008). Anthropometric parameters, blood tests and TE measurements were recorded for all the patients. FIB-4 was also calculated based on available blood tests.

Specifically, the cohort from the Royal Free Hospital included consecutive patients with T2DM who were firstly referred from primary care through the Camden and Islington pathway (Srivastava et al., 2019). As such, this group included patients selected from primary care based on FIB-4>1.3 and/or ELF>9.5 (selected primary care population). The cohort from the Palermo Hospital included consecutive patients with T2DM who were followed-up in the specialist NAFLD clinic (tertiary care population).

2.1.4 Liver histology

Liver biopsies were performed using the True-cut technique. Only liver biopsies performed within 3 months from the clinical assessment and TE measurements were included in the study. Specimens were formalin-fixed and paraffin-embedded and stained as per standard of care. Histology was assessed by expert pathologists in liver disease referring to the NASH CRN scoring system (Kleiner et al., 2005). Significant fibrosis was defined as F≥2, while advanced fibrosis as F≥F3. In terms of NAS score, “possible NASH” was defined as 3≤NAS<5, while “definite NASH” as NAS≥5.

2.1.5 Statistical analysis

The distribution of variables was explored using the Shapiro-Wilk test. Continuous variables were reported as medians and interquartile range (IQR), while categorical variables were expressed as relative frequencies and percentages. Univariate analysis was carried out using Mann-Whitney

for continuous, and chi-square test for categorical variables respectively. Kruskal-Wallis or ANOVA with post-hoc corrections was used for comparison between multiple groups. In terms of clinical characteristics, significant variables were carried forward to multivariate regression analysis to identify the odd ratios (OR) of the variables independently associated with clinical outcome (LSM≥ 8.1 kPa). Binary logistic regression was then used to generate a formula for the prediction of the presence of liver disease secondary to NAFLD in the derivation cohort. Furthermore, calibration and goodness-of-fit were estimated computing the Brier score, with values ranging from 0 (accurate) to 1 (not accurate), and the Hosmer-Lemeshow test, with values ranging from 0 (lowest fit) to 1 (best fit).

ROC (receiver operating characteristic) curves were used to assess the diagnostic performance of the derived formula compared to traditional screening methods for liver disease. Areas under ROC curve (AUROC) with 95% confidence intervals were calculated under nonparametric (distribution free) assumption. Optimal cut-off values were calculated to maximise sensitivity and specificity, according to the Youden index. For each cut-off, sensitivity, specificity, PPV and negative predictive value (NPV) were reported based upon the observed prevalence of liver disease within the population. Finally, pairwise statistical comparison of AUROCs was performed using the DeLong method between the derived score and traditional screening methods.

All tests were two-sided and a *P* value 0.05 was considered significant. Statistical analysis was performed using SPSS© (version 24.0; SPSS Inc Chicago, IL).

2.1.6 Regulatory Approval

All patients' recruitment was conducted in line with Good Clinical Practice and sample handling according to Human Tissue Act regulations. The main cross-sectional study (derivation cohort) obtained full ethical approval from the Research Ethics Committee (REC approval 18/LO/1742, IRAS 251274), sponsorship from Imperial College London and adoption from Clinical Research Network Portfolio.

The validation cohorts of patients provided by the Royal Free Hospital and the Palermo University Hospital were retrospective collection of routinely performed investigation and anonymised patients' data. As such, ethical approval was not required as stated under the UK policy framework for health and social care. All activities were performed in accordance with the guidelines of the Helsinki Declaration.

2.2 Metabolomics and gut microbiome analysis

2.2.1 Overview

Metabolomics aims at the comprehensive and quantitative analysis of the wide arrays of metabolites in biological samples. The currently available techniques providing multiparametric metabolic profiling are mainly centred on Nuclear Magnetic Resonance (NMR) spectroscopy and mass spectrometry (MS), as both techniques provide in-depth information on the structure and the conformation of the multiple classes of metabolites in a single analysis. NMR technology provides a fast, quantitative and highly reproducible method for analysing metabolites and does not require extensive sample preparation. Furthermore, NMR may come with both a targeted and an untargeted approach. Targeted approaches require a priori knowledge of metabolites of interests, while non-targeted approaches provide a global, unbiased profiling of the metabolome. Interestingly, MS allows for the quantification of compounds at a very low molecular concentration. However, MS shows low reproducibility and requires a time-consuming process for the preparation of the samples. If combined, the two techniques provide a comprehensive metabolic profiling of biological samples. In terms of gut microbiome profiling, metagenomic approaches have become popular techniques as these are simple and cost-effective.

Among others, the 16s ribosomial RNA (rRNA) gene amplicons sequencing allows to target a specific RNA domain which is restricted to bacteria and archae. Taken together the metabolomics and the gut microbiome profiling provide a comprehensive snapshot of the bacteria-host interactions.

In this study, targeted and untargeted metabolic profile was carried out in serum, urine and faecal extracts using NMR, while bile acid profile was obtained from serum and faecal extracts using

Ultra performance liquid chromatography – mass spectrometry (UPLC-MS). Gut microbiome was analysed in stool samples by 16s rRNA gene sequencing.

2.2.2 Metabolic profiling

2.2.2.1 Biological samples collection and storage

Serum, urine and stool samples were collected, processed and stored as per the Hepatology and Gastroenterology divisional standard operating procedure (SOP). Briefly, bloods and urines were collected on the same day of the clinical assessment and screening procedures. Blood samples were collected in a whole blood bottle, left 30 mins to allow the blood to clot, then centrifuged at 1600g for 15 mins at 4 °C and finally aliquoted in 3 Eppendorf tubes. Urine samples were collected in a sterile container. A volume of 1 mL of urine were transferred into Eppendorf tubes and centrifuged at 13.000g for 10 minutes at 4°C. Using a syringe filter, aliquots of 600 µL of the supernatant were transferred into Eppendorf tubes.

Stool samples were collected within one week from the baseline clinical assessment and were delivered within 3 hours from being produced. For this purpose, on the day of the clinical assessment and screening procedures, patients were provided with a Fecotainer, a disposable cool bag and detailed, illustrated instructions for use. Samples were transported by the patient to the Liver and anti-viral unit, based at St Mary's Hospital and then aliquoted as neat samples in 1.5 ml Eppendorf. There was no specific dietary restriction or recommendation before collecting the faecal samples, while stool from patients who had received antibiotic treatment for the previous 2 weeks were excluded from the analysis.

All samples were stored at -80°C in the Hepatology Clinical research facility based at Imperial college London, St Mary's Hospital. All samples were kept frozen until processing for analysis consistently with standard protocols (Sarafian et al., 2015, Gratton et al., 2016, Mullish et al., 2018).

2.2.2.2 Nuclear Magnetic Resonance

Overall, NMR is an established technique used to quantify the most abundant compounds present in a biological fluid. Main advantages of the NMR are the reproducibility of the results and the simple pre-analytical preparation of the samples. The main disadvantage of the NMR are the cost and the low sensitivity.

In this study, targeted and untargeted metabolic profiles were obtained from serum, urine and faecal extracts (faecal water, FW) using NMR, which was carried out at the MRC-NHR National Phenome centre, Imperial College London, UK, adhering to standard operating procedures and established protocols (Dona et al., 2014, Beckonert et al., 2007). Briefly, 600 µL of each serum sample was centrifuged at 1200g at 4°C for 5 min. Afterwards, 350 µL of the centrifuged serum sample was transferred to a 96-well plate and mixed with 300 µL of serum buffer into a SampleJet NMR tube (Dona et al., 2014). Serum samples were analysed with a rate of 72 samples within 24 hours (~19 min per sample). In terms of urines, 600 µL of each sample was centrifuged at 12000g for 5 min at 4°C, and 540 µL of the supernatant was then moved into a SampleJet NMR tube together with 60 µL of urine Buffer. Urine samples were analysed with a rate of 96 samples withing 24 hours (~15 min per sample). Faecal samples were thawed at room temperature (RT) before undergoing protein extraction. Glass beads were added to the 150-00 mg neat sample in a safe-lock Eppendorf tube, where also double the volume of phosphate-buffered saline (PBS) was previously pipetted. Samples were then vortexed and then centrifuged at 20,000 x g for 10 min at 4°C. The resulting supernatant was accurately filtered and aliquoted for NMR analysis. Reagents, equipment, NMR calibration, optimal parameters settings are described in (Dona et al., 2014). Spectra from serum, urine and FW were obtained for all the samples and were adjusted for the small molecule enhancement spectroscopy (SMolESY) technique. Briefly, the SMolESY is a computational technique which increases the resolution of the spectra directly from H1D-NMR spectrum without any modulation of the intensity of the peaks. This allows for a better characterisation and quantification of the metabolites captured in the spectra (Takis et al., 2020).

Overall, the targeted metabolic profile provided the concentration for 41 metabolites in the serum samples, 49 in the urine samples and 19 metabolites in FW. With the untargeted metabolic profile, thousands of buckets of signals were generated for each sample. The Statistical total correlation spectroscopy analysis was applied to identify metabolites of interests within the samples based on their most discriminatory features.

2.2.2.3 UPLC-MS for bile acid profiling and tryptophane assay

Overall, UPLC-MS represents an innovative bioanalytical technique that integrates the resolving power of Liquid Chromatography with the detection specificity of Mass Spectrometry. In this study, UPLC-MS was used to characterize the bile acid profile in the serum (Sarafian et al., 2015), and bile acid and tryptophane profile in stool samples collected from the study population (Mullish et al., 2018). UPLC-MS was carried out at the MRC-NHR National Phenome centre, Imperial College London, UK.

Briefly, stool samples where thawed, lyophilized for 24 hours with a VirTis Benchtop 78 BTP 8ZL freeze dryer (BPS, UK) and then weighed. A mixture of 2:1:1 water, acetronitrile and 2-pronanolol was used to extract bile acids in a Biospec bead beater with 1.0 mm Zirconia beads. Diluted samples were then centrifuged at 16.000g for 2 minutes, while the supernatant was collected and filtered with nylon membranes (Costar, Corning). Serum samples were thawed and a 75 µL volume of the thawed serum was added to 225 µL of cold methanol, followed by incubation at -20oC for >2 hours. Tubes were centrifuged (9500 x g, 20 minutes) and 120 µL of supernatant loaded into vials.

After being allocated randomly in the machine, faecal extracts were analysed for bile acid using ACQUITY UPLC (Waters Ltd, Elstree, UK) coupled to a Xevo G2 Q-ToF mass spectrometer equipped with an electrospray ionization source operating in negative ion mode (ESI-) (Sarafian et al., 2015). Quality control (QC) samples were prepared using equal parts of the faecal filtrates and used to monitor the performance of the assay (Sangster et al., 2006). QC samples were also spiked

with mixtures of bile acid standards (55 bile acid standards including 36 non-conjugated, 12 conjugated with taurine, seven conjugated with glycine (Steraloids, Newport, RI, USA)) and were run with the stool samples to determine the chromatographic retention times of bile acids and to allow for a better identification of the metabolites. As per protocol, QCs were injected 10 times at the beginning of the run, then every 10 injections and finally at the end of the analysis to assess the stability and reproducibility f MS. Waters raw data files were converted to NetCDF format and XCMS (v1.50) package with R (v3.1.1) software was used to extract the data. XCMS is open-access software which allows for the pre-processing of LC-MS software that can be customised for specifications by the user, such as peak width, peak intensity, etc (Smith et al., 2013). Correction of dilution effects was performed using a probabilistic quotient normalisation (Veselkov et al., 2011), while chromatographic features with coefficient variation larger than 30% in the QC samples were excluded from further analysis. Chromatographic features were expressed as relative intensities and corrected for the dry weight of the original stool samples. The bile acids were then identified from the final database, comparing expected m/z ratios of 79 standards comparing with appropriate databases (particularly the Human Metabolome Database). Results were normalised for the statistical analysis.

2.2.3 Analysis of the gut microbiome

2.2.3.1 DNA extraction and quantification

Deoxyribonucleic acid (DNA) was extracted from approximately 100 mg neat faecal using the PowerLyzer PowerSoil DNA Isolation kit and following manufacturer's instructions. The faecal water (FW) was added to a 2 ml microcentrifuge tube containing 0.1 mm glass beads. Sixty µL of C1 and 750 µL of bead solution were added and then vortexed. Briefly, solution C1 is a cell lysis solution including sodium dodecyl sulphate which lyses cell membrane fatty acids and lipids. Bead beating was carried out using the Bullet Blender Storm instrument for 3 min, while tubes were therefore centrifuged at 13,000 x g for 1 min. A 400-500 µL volume of the supernatant was transferred to a sterile tube where 250 µL of solution C2 was added. Tubes were vortexed, incubated

for 5 min at 4˚C and centrifuged for 13,000 x g for 1 min. This step leads to the physical separation of the liquid phase (containing the DNA) from the solid phase (pellet). Six hundred µL of supernatant was transferred to a sterile collection tube and 200 µL of solution C3 was added. At this stage, tubes were vortexed again, incubated for 5 min at 4˚C and centrifuged for 1 minute at 13,000 x g. Adding the C3 causes the additional cellular debris to be broken down and proteins to precipitate. Similarly, a volume of 750 µL supernatant was transferred to a sterile tube and added to a 1.2 mL of C4 solution. Six hundred and fifty µL of the supernatant mix was transferred onto a spin filter and centrifuged at 10,000 x g for 1 minute with the remaining flow through discarded. This process was repeated for several passages until all the supernatants had fully been filtered, so that DNA was bound to the membrane. To clean the DNA bound to the filter, 500 µL of solution C5 was added to the spin filter and centrifuged for 1 min at 10,000 x g. The flow through was discarded and the spin filter centrifuged again for 1 min at 10,000 x g to remove all remaining ethanol. The spin filter was transferred to a sterile collection tube and 100 µL of solution C6 was added to elute the DNA, followed by centrifuging for 1 min at 10,000 x g. The so-obtained DNA was aliquoted into Eppendorf-tube and stored at -80 ˚C, while the spin filter was discarded.

2.2.3.2 DNA concentration

The Qubit dsDNA BS assay kit was used to analyse the DNA concentration in the research samples. This assay is highly selective for double-stranded DNA (dsDNA) and accurate for detecting DNA for sample concentrations ranging from 10 pg/µL to 100 ng/µL. Briefly, the Qubit working solution was made up by diluting the Qubit dsDNA BS Reagent (1:200) in Qubit dsDNA BS buffer. Both the standards and samples were prepared in Qubit working solution to a final volume of 200 µL and vortexed for 2-3 sec. All tubes were incubated at RT for 2 mins. The Qubit 2.0 Fluorometer was employed to measure the standards and samples, providing with a final reading in ng/µL.

2.2.3.3 Meta-taxonomic analysis

16s RNA gene sequencing is commonly used for identification, classification and quantitation of microbes with complex biological mixtures, such as the gust microbiome (Cox 2013. Sequencing

the human microbiome in health and disease). The 16s rRNA gene is a highly conserved component of the transcriptional machine of all DNA-based life forms and thus highly suited as a target gene for sequencing DNA in samples containing up to thousands of different species. Universal PCR primers can be designed to target the conserved regions of 16S rRNA. Also, sequencing the variable regions allows discrimination between specific different microorganism. Sample libraries were prepared based on the amplification of the V1-V2 region of the 16S rRNA gene employing the primers listed in **Table 2.3** (previously reported in (Mullish et al., 2018)). Sample libraries were quantified using the NEBNext Library Quant Kit for Illumina (New England Biolabs, Hitchin, UK) and as per the 16S Metagenomic Sequencing Library Preparation Protocol from Illumina's.

Sequencing was carried out on an Illumina MiSeq platform (Illumina Inc., Saffron Walden, UK) using the MiSeq Reagent Kit v3 (Illumina) and paired-end 300bp chemistry. The data which derive from the sequencing were processed using RStudio, version 1.3.1056 (R Studio Team (2020). RStudio: Integrated Development for R. RStudio, PBC, Boston, MA) and according to the DADA2 v.1.18.0 pipeline as previously described (Callahan et al., 2016). The SILVA Taxonomy Database v.132 (https://www.arb-silva.de/) was used to align the sequences. Subsequently, decontam package (Davis et al., 2018) was used to identify and remove the possible contaminants present in the samples.

The software STAMP was used to discriminate differences in relative and absolute abundance between different groups at all taxonomic levels, from genus to phylum (Xia and Wishart, 2010). Specifically, differences between two groups were tested using a two-sided White's non-parametric t test with post-hoc correction (Benjamini-Hochberg correction). Only results where the difference in the mean proportion of sequences was greater than 1% were retained.

A neighbor-joining phylogenetic tree was built based om the R packages DECIPHER (ES Wright (2016) "Using DECIPHER v2.0 to Analyze Big Biological Sequence Data in R." The R Journal, 8(1), 352-359.) and phangorn (Schliep, 2017). The Vegan library was used to calculate the alpha diversity indexes (https://cran.r-project.org/web/packages/vegan/index.html) within the R studio.

Primer name	Primer sequence
28F-YM (forward primer)	**TCGTCGGCAGCGTCAGATGTGTATAAGAGACAG**GAGTTTGATYMTGGCTCAG
28F-Borrelia (forward primer)	**TCGTCGGCAGCGTCAGATGTGTATAAGAGACAG**GAGTTTGATCCTGGCTTAG
28FChloroflex (forward primer)	**TCGTCGGCAGCGTCAGATGTGTATAAGAGACAG**GAATTTGATCTTGGTTCAG
28F-Bifido (forward primer)	**TCGTCGGCAGCGTCAGATGTGTATAAGAGACAG**GGGTTCGATTCTGGCTCAG
388R (reverse primer)	**GTCTCGTGGGCTCGGAGATGTGTATAAGAGACAG**TGCTGCCTCCCGTAGGAGT

Table 2.3. Primers used for 16s rRNA gene sequencing on the Illumina MiSeq. The forward primer mix was composed of four different forward primers, mixed at a ratio of 4:1:1:1 (28F-YM:28F-Borrelia:28F-Chloroflex:28F-Bifido). The MiSeq adapter sequences are highlighted in bold.

2.2.4 Image analysis for the quantitation of steatosis, inflammation, ballooning and fibrosis in images of liver biopsies

Metabolic profile was then compared against liver histology. As liver biopsies from the present study were limited in number, a group of serum samples matched with liver biopsies were included from the cohort of patients followed-up in the specialist NAFLD liver clinic, based at St Mary's Hospital, Imperial college NHS Trust, London, UK. Metabolic profile was analysed in serum samples from this population using NMR, following the same procedures as the main metabolic profiling.

Liver biopsies were stained in haematoxylin & eosin (H&E) and Sirius Red, scored by histopathologist as per NASH CRN scoring system. Liver biopsies were also digitalised and analysed for automated quantitation of histological features. Specifically, our group has developed and validated a fast-operating, high-throughput automated image analysis method to quantitate steatosis, ballooning, inflammation and fibrosis in routine histological images of patients with NAFLD (Forlano et al., 2020). Such methodology does not require sophisticated equipment and has shown

reliable and reproducible results when compared to semi-quantitative scores (NASH CRN scoring system). The software computes the percentages of fat, inflammation and ballooning analysing images of liver biopsies stained in H&E (**Figure 2.1**). Fibrosis is analysed as collagen proportionate area (CPA) using images of liver biopsies stained in Sirius Red (**Figure 2.2**). All percentages are expressed as relative percentages against the whole tissue area.

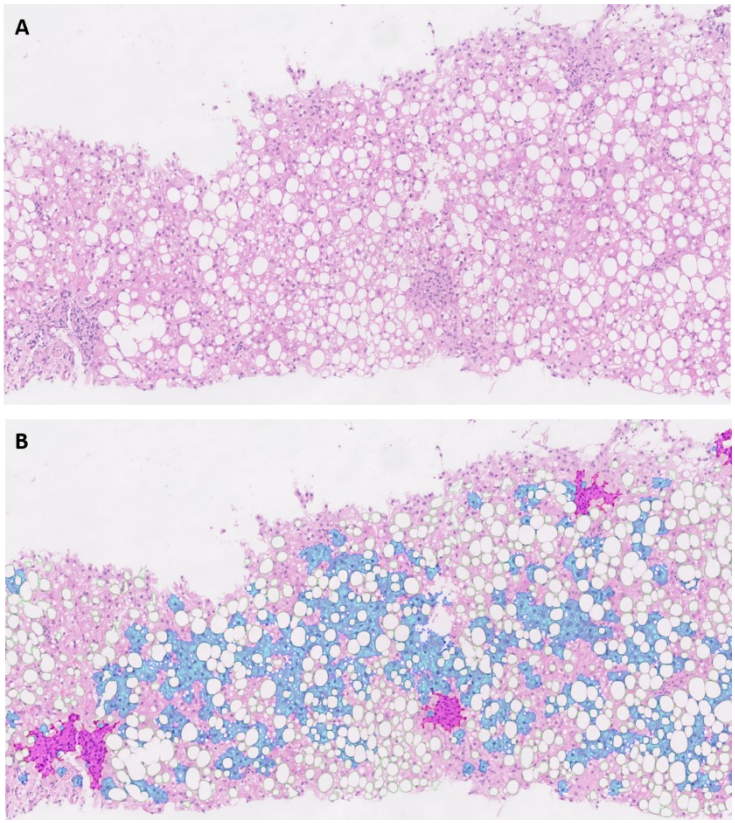

Figure 2.1. Image analysis for quantitation of steatosis, inflammation and ballooning. Figure 2.1A illustrated a magnified image of a liver biopsy stained in H&E and scored as Steatosis Grade 3 (moderate, ≥66%), Lobular Inflammation score 1 (≤2 foci) and Ballooning score 1 (Few ballooned cells) as per NASH CRN scoring system. Figure 2.1B illustrates the results of image analysis were Fat% 30.9% (in green), Inflammation% 3.4% (in purple) and Ballooning% 10.8% (in blue).
Abbreviations: NASH CRN scoring system: Non-alcoholic steatohepatitis clinical research network scoring system; H&E: haematoxylin and eosin

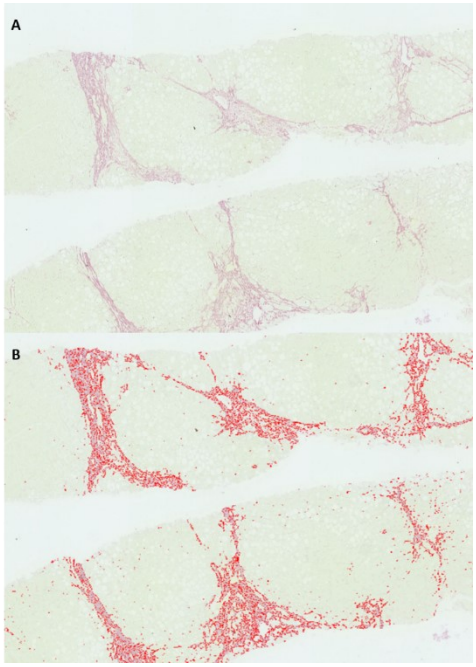

Figure 2.2. Image analysis for quantitation of fibrosis. Figure 2.2A illustrates the image of a liver biopsy stained in Sirius Red and scored as Fibrosis stage 4 as per NASH CRN Scoring System. Figure 2.2B illustrates the result of image analysis showing a CPA 22.5%.
Abbreviations: NASH CRN scoring system: Non-alcoholic steatohepatitis clinical research network scoring system; CPA: collagen proportionate area.

2.2.5 Statistical analysis

Pre-processing of the data and meta-identification of the untargeted metabolic profile obtained by NMR was performed by Dr Takis Panteleimon (Imperial College London, UK). The pre-processing of the data on the spectra obtained by LC-MS was performed by NPC, Imperial college London, UK. The results obtained from the 16s rRNA sequencing were kindly pre-processed by Mr Jesus Miguens Blanco (Imperial college London, UK).

The data table obtained as output from NMR and UPLCMS were introduced to SIMCA v 14.1 (MKS Umetrics AB), with UPLCMS data were pareto-scaled. A principal component analysis (PCA) was performed so that clustering of the samples could be visualised in a unsupervised fashion. Afterwards, a supervised analysis, called orthogonal projections to latent structures discriminant analysis (OPLS-DA), was carried out to demonstrate the features responsible for the discrimination between two groups. OPLS-DA models were validated using cross-validated residuals ANOVA (CV-ANOVA) (Eriksson et al., 2000), while S-plots were used to visualise the most-influential features

discriminating the groups which are typically located at the far ends of the plot (Wiklund et al., 2008). Heatmap were produced based on R Pearson coefficient of bile acids against microbial abundances and reporting with a false discovery rate 10% threshold. Part of the initial statistical analysis was performed by myself with the help of Dr Benjamin H. Mullish (Imperial college London, UK). The data table obtained as output from NMR and UPLCMS was also analysed more in depth by Dr Laura Martinez Gili (Imperial College London, UK). Such more complex modelling was performed on Software R, using linear regression analysis with mixed effect model. Differences between groups were adjusted with post-hoc Benjamini test and values were reported with a 10% significance threshold.

2.2.6 Regulatory Approval

Blood samples from healthy controls and from patients of the NAFLD clinic (and related clinical information) were collected under the Imperial Hepatology and Gastroenterology Biobank which is fully REC approved by the Oxford Research Ethics Committee under the REC reference 16/SC/0021.

2.3 Assessment of the gut permeability

2.3.1 Biological samples collection and storage

Serum and stool samples were collected, processed and stored as per the Hepatology and Gastroenterology divisional SOP. Samples were handled and stored as described in **paragraph 2.2.2.1**.

2.3.2 Preparation of faecal water

Faecal samples were thawed at RT before undergoing protein extraction. Glass beads were added to the 150-00 mg neat sample in a safe-lock Eppendorf tube, where also double the volume of PBS was previously pipetted. Samples were then vortexed to ensure homogeneity and then

centrifuged at 20,000 x g for 10 min at 4°C. The resulting supernatant was accurately filtered and then exported for the protein extraction.

2.3.3 Protein extraction and quantitation

The Bicinchoninic acid assay (BCA) was used to extract the protein content from the sample as per the manufacturer's instructions. Bovine serum albumin (BSA) was used as a reference standard. As part of the protocol, diluted BSA standards from 0 µg/mL to 2000 µg/mL were prepared from the 2 mg/mL albumin stock provided in the kit. The BCA working reagent (WR) was prepared from a 50:1 Reagent A:B mixing. Twenty-five µL of each study sample and 25 µL of each standard were pipetted into a 96 well plate and then incubated at 37°C for 30 min. Afterwards, the 96 well plate was cooled at RT before being read at 562 nm on a Thermoscientific Multiskan go machine.

2.3.4 Assessment of protease activity

A Pierce Fluorescent Protease assay kit (Thermo Scientific, UK) was used to measure total protease activity. Briefly, this assay employs fluorescein-labelled casein for use as a substrate to assess the activity of proteases present in a sample. Fluorescence properties of this protein substrate change significantly upon digestion by proteases, resulting into a measurable indication of proteolysis. TPCK Trypsin, a modified trypsin, is provided in the kit as a general protease calibrator so that the results can be compared to a reference protease.

As per manufacturer's instructions, lyophilized TPCK trypsin was dissolved in 1 mL of ultrapure water to make a 50 mg/mL stock solution. Fresh aliquots of trypsin stock were thawed to prepare standards before any protease measurement. PBS was plated as a control. A preliminary 96 well plate was preliminarily run so that an appropriate inhibition dilution of FW was established. Dilutions of 25 ng/µL and 10 ng/µL were made from 1 mg/mL total protein samples, using TBS as the diluent. Equal volumes (100 µL) of each sample dilution and standards (prepared in duplicate) were added to a black 96-well plate. One hundred µL of fluorescein thiocyanate (FTC)-casein WR was added and then mixed thoroughly. At RT, the plate was left to incubate for 60 min and then was measured at 485 – 520 nm on a BMG Labtech FLUOstar OPTIMA. The blank reading was subtracted

from each sample and standard measurement to determine the protease activity levels. The change in relative fluorescence units of the standards vs. protease concentration were plotted as standard curve. Before protease activity assay was run, FW samples were normalised to 1 mg/mL total protein using PBS as the diluent. After total protease activity had been measured in the samples, a second black 96-well plate was run with the addition of inhibitors. A volume of 100 µL of FTC-casein WR was added again to each well and left to incubate at RT for 60 min. The plate was measured at 485 – 520 nm on a BMG Labtech FLUOstar OPTIMA. Measurements were replicated adding a commercial bacterial protease inhibitor cocktail (Protease inhibitor cocktail powder for use with bacterial cells extracts, lyophilized powder, Merck Life Science UK Limited, UK) to calculate the protease activity in inhibited FW.

2.3.5 In-vitro model of gut-permeability with MDCK cell culture

2.3.5.1 Thawing of frozen cells

Frozen vials of the Madin-Darby Canine cocker spaniel kidney (MDCK, Sigma-Aldrich) were purchased and stored in liquid nitrogen. On the day of the experiment, MDCK were thawed in the water bath for approximately 2 mins, keeping the cap out of the water so that the risk of contamination could be minimised. Once thawed, the vial was removed from the bath, sterilised with 70% ethanol and transferred to an aseptic flow hood. The vial was then spun at 125 G for 6 minutes. Subsequently, supernatant was discarded, and the pellet resuspended in 1 ml complete media. Complete media was previously prepared based on modified Dulbecco's Modified Eagle Medium (DMEM) 500 ml + 1ml Plasmocin + 50ml Fetal bovine serum + 5ml 200mM L-glutamine. One ml of resuspension was then added to a T-25 flask and incubated at 37.5°C, 5% CO2 until this reached confluence.

2.3.5.2 Cell line maintenance, splitting and seeding procedure

The following steps were conducted under an aseptic flow hood which had been sprayed with ethanol so that the risk of contamination could be minimised. Prior to passaging cells, complete media, PBS and 0.25% (w/v) Trypsin 0.53 mM EDTA were warmed for 30 min. Typically after 48-72

hours, MDCK cells had reached confluence. Cell media was removed from the culture flask and cells were washed with 5 mL of PBS x 2 times. Five mL 0.25% (w/v) Trypsin 0.53 mM EDTA was pipetted into the flask and incubated at 37°C for 15 min until the cells had detached. Once cells had trypsinised, the flask was gently pipetted to break up cell clumps. A volume of 1 mL of trypsinised cells was then transferred to a new T-25 cm^2 flask with 5 mL of fresh complete media and incubated at 37°C, 5% CO_2. Media was changed every 2 or 3 days. Cells were then split upon reaching confluence.

The density of the cells was assessed using a haemocytometer and Trypan blue staining. Briefly, the Trypan blue colours dead cells as blue and highlights those that are still living. The following calculation was used:

$$(n/4) \times \text{dilution factor} \times 10^4 = X \text{ cells in 1 mL}$$

where n = the number of cells counted within the 4 grids in the haemocytometer.

Based on this calculation, aliquots of 1-2 x 10^5 MDCK cells were cultured in on Millicell 0.4 µm PTFE Transwell inserts (0.3 cm^2 surface area, Merck KGaA, Darmstadt, Germany) in a 24 well plate. Cultured cells were maintained at 37°C, 5% CO_2, for 72-96 hours to allow for monolayer formation, while culture media was changed every day. As some level of variability from different passages was previously described (Furuse and Tsukita, 2006), only passages between 17 and 22 were used for this study.

2.3.5.3 Measurement of Trans-epithelial electric resistance

The integrity of individual monolayers was assessed by measuring TEER using a EVOM (**Figure 2.3**). Cell culture plate was left at RT for 1 hour, while FW were prepared and diluted in PBS to get a standard protein concentration of 300 ug per 200 µL of PBS+FW solution. Culture media was replaced with 1 mL of the Hanks' Balanced Salt Solution (HBSS) in the basolateral and 200 µL in the apical compartment, and cells were allowed to equilibrate in medium for at least 30 min at 37°C. Monolayers were considered intact when TEER measurements were stable after at least 2

days from seeding. Monolayers with TEER values < 150 Ωcm^2 after 72 hours were not considered intact and were excluded from use.

At time zero, HBSS from the apical compartment of each well was removed and replaced by equal volume of either PBS (as negative control), *Enterococcus faecalis* (*E. faecalis*) spent medium (as positive control) or FW derived from the faecal samples of patients enrolled in the study. Specifically, *E.faecalis* was chosen as positive control, given its peculiar proteolytic activity through the production of specific gelatinases and serine proteases (Nesuta et al., 2017). To prepare *E. faecalis* supernatant, this was grown on an anaerobe plat and left to incubate overnight. After 24 hours, a sterile loop of colonies was added to a flask of a standard culture broth and then left for further 24 hours. FW samples were prepared as per **paragraph 2.3.2**. Once PBS, *E. faecalis* spent meium and FW were added to the wells (time zero), TEER was then measured at a sequence of 5, 30, 90, 120 mins and 24 hours. Experiments with FW were repeated in triplicates, i.e. each FW sample was incubated in 3 adjacent wells. Moreover, in each well, TEER was measured in triplicates at all time points.

Experiments were replicated with the addition of a commercial bacterial protease inhibitor cocktail to differentiate the contribution from host and microbial proteases (Protease inhibitor cocktail powder for use with bacterial cells extracts, lyophilized powder, Merck Life Science UK Limited, UK). At the end of the experiments, cells from each well were resuspended and stained with Tryptan blue to check for cell viability

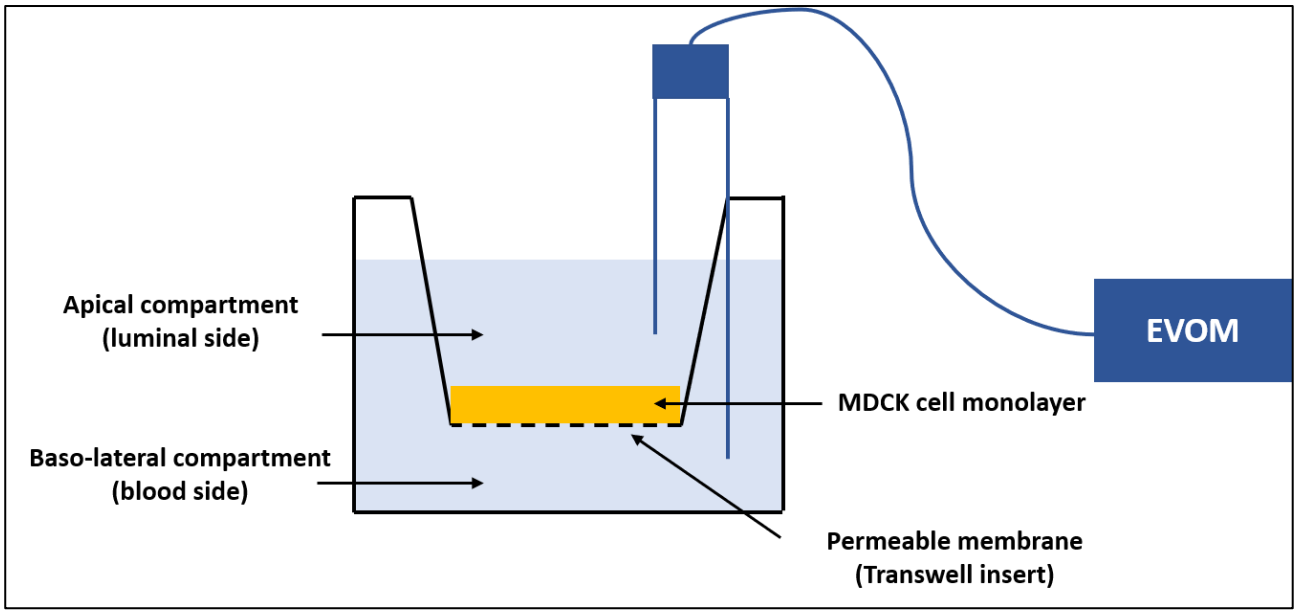

Figure 2.3. Measurement of Trans-epithelial electric resistance. The picture illustrates the in-vitro model of gut permeability. Briefly, MDCK were cultured on Transwell insert positioned in each well. The model created therefore two separated compartments: the apical (luminal side) and baso-lateral (blood side) compartment. FW, E, faecalis spent medium or PBS were added to the apical side of the model (luminal side). The integrity of the MDCK monolayer was assessed by TEER from an EVOM.
Abbreviations: TEER: trans-epithelial electric resistance, EVOM: epithelial volt/ohm meter, MDCK: Madin-Darby Canine Kidney cells, E. faecalis: Enterococcus Faecalis, PBS: phosphate-buffered saline, FW: faecal water.

2.3.6 Measurement of serum FABP-2

The level of FABP-2 was measured in serum samples from the patients enrolled in the study, using a Human FABP2/I-FABP Quantikine Enzyme-Linked immunosorbent Assay (ELISA, R&D, USA) Kit, which is essentially a sandwich ELISA. All reagents were brought to RT as per manufacturer's instructions. The wash buffer, substrate solution and Human FABP-2 standard were constituted as per protocol.

Firstly, 50 µL of Assay diluent RD1-63 were added to each well. Secondly, another 50 µL of standard, control or serum sample were added to each well. Sera were prepared using a 5-fold dilution and were added to the plate in duplicates, i.e. each sample was aliquot to two consecutive wells. The plate was covered with the adhesive strip provided and incubates at RT on a horizontal orbital microplate shaker set at 500 ± 50 rpm. After two hours of incubation, each well was washed with 400 µL of wash buffer for three times. After the last wash, wash buffer was completely aspirated, and the plate was inverted and blotted against clean paper towel so that any remaining of buffer

could be removed. At the following step, 200 µL of Human FABP-2 Conjugate was transferred to each well. The plate was then covered with a new adhesive strip and incubated at RT on the shaker. After 2 hours, another sequence of aspiration and wash was performed. A 200 µL of the Substrate solution was aliquoted in each well, while the plate was left for incubation for 30 minutes at RT on the benchtop, carefully protected from light. Afterwards, 50 µL of the Stop Solution was also added to each well and a change of colour from blue to yellow was noted in the wells. Finally, the 96 well plate was read at 570 nm on a Thermoscientific Multiskan go machine.

2.3.7 Measurement of faecal cytokines

The faecal levels of interferon-gamma (IFN-γ), IL-1β, interleukin-2 (IL-2), interleukin-4 (IL-4), IL-6, interleukin-8 (IL-8), IL-10, interleukin-12p70 (IL-12p70), interleukin-13 (IL-13), and TNF-α were measured in the FW obtained from samples of the patients enrolled in the study, using the V-plex Proinflammatory Panel 1 (Meso scale discovery, MSD) - essentially a sandwich immunoassay. As per manufacturer's instructions, all reagents were left at RT. Calibrator dilutions, controls, detection antibody solution, wash buffer and read buffer T were constituted as per protocol. The MSD plate was washed 3 times with 150 µL of wash buffer to provide greater uniformity of the results of the assay. Fifty µL of samples, calibrators and controls were added in each well. Filtered FW samples were loaded on the MSD after a 2-fold dilution with Diluent 2. Serial 4-fold dilutions of the standards were run to generate a 7-standard concentration set, and the diluent alone was used as a blank. The plate was then sealed with an adhesive plate seal and incubated at RT on a shaker for 2 hours. Afterwards, the plate was washed again for three times with 150 µL of wash buffer. A volume of 25 µL of detection antibody solution was transferred to each well. The plate was sealed with an adhesive seal and incubates at RO with shaking for 2 hours. Another sequence of three washes with 150 µL of wash buffer was done with the MSD plate. As final step, 150 µL of 2 X read buffer T was added to each well. The plate was then analysed on an MSD reader (Faculty of Medicine, Imperial College London) within 30 minutes. The standard curves for each cytokine were generated using the premixed lyophilized standards provided in the kits.

2.3.8 Statistical analysis

The distribution of variables was explored using the Shapiro-Wilk test. Continuous variables were reported as medians and IQR, while categorical variables were expressed as relative frequencies and percentages. Univariate analysis was carried out using Mann-Whitney for continuous, and chi-square test for categorical variables respectively. Kruskal-Wallis or ANOVA with post-hoc corrections was used for comparison between multiple groups. Spearman correlation and logistic regression carried out to explore the relationship between variables.

All tests were two-sided and a *P* value 0.05 was considered significant. Statistical analysis was performed using GraphPad Prism (version 9.1) and SPSS (version 24.0; SPSS Inc Chicago, IL).

2.3.9 Regulatory approval

Blood samples from healthy controls were collected under the Imperial Hepatology and Gastroenterology Biobank which is fully REC approved by the Oxford C Research Ethics Committee under the REC reference 16/SC/0021.

2.4 Systemic inflammatory status

2.4.1 Biological samples collection and storage

Serum samples were collected, processed and stored as per the Hepatology and Gastroenterology divisional standard operating procedure. Samples were handled and stored as described in **paragraph 2.2.2.1**.

2.4.2 Measurement of serum cytokines level

The serum levels of IFN-γ, IL-1β, IL-2, IL-4, IL-6, IL-8 (CXCL8), IL-10, IL-12p70, IL-13, and TNF-α were measured using the V-plex Proinflammatory Panel 1 (MSD), which is essentially a sandwich immunoassay. Preparation and reading of the assay were identical to the protocol used for the measurement of faecal cytokines (**paragraph 2.3.7**). Values of cytokines which were at or lower than the lower limit of detection (LLOD) were reported as LLOD for these analytes. Median

LLOD were derived from the assay protocol (**Table 2.4**). Percentage detected was also derived from the assay protocol and reported the percentage blood samples from healthy patients with concentrations at or above the LLOQ.

	Median LLOD (pg/ml)	% Detected serum (N=27)
IFN-gamma	0.37	96
IL-1β	0.05	22
IL-2	0.09	33
IL-4	0.02	30
IL-6	0.06	37
IL-8	0.07	100
IL-10	0.04	52
IL-12p70	0.11	11
IL-13	0.24	11
TNF-alpha	0.04	70

Table 2.4. Lower limit of detection and percentage of detected cytokines in healthy serum samples.

2.4.3 Measurement of serum PAI-1

The serum level of PAI-1 was measured using a Human Serpin E1/PAI-1 Quantikine ELISA Assay (R&D systems, USA) Kit, which is essentially a sandwich ELISA. All reagents were brought to RT as per manufacturer's instructions. The wash buffer, substrate solution and Human Serpin E1/PAI-1 standard were constituted as per protocol.

Firstly, 50 µL of Assay diluent RD1-57 were added to each well. Secondly, another 50 µL of standard, control or serum sample were added to each well and completed within 15 minutes. Sera were prepared using a 5-fold dilution and were added to the plate in duplicates, i.e. each sample was aliquot to two consecutive wells. The plate was covered with the adhesive strip provided and incubates at RT. After two hours of incubation, each well was washed with 400 µL of wash buffer for three times. After the last wash, wash buffer was completely aspirated, and the plate was inverted

and blotted against clean paper towel so that any remaining of buffer could be removed. At the following step, 200 µL of Human Serpin E1/PAI-1 Conjugate was transferred to each well. The plate was then covered with a new adhesive strip and incubated at RT. After 2 hours, another sequence of aspiration and wash was performed. A 200 µL of the Substrate solution was aliquoted in each well, while the plate was left for incubation for 30 minutes at RT on the benchtop, carefully protected from light. Afterwards, 50 µL of the Stop Solution was also added to each well and a change of colour from blue to yellow was noted in the wells. Finally, the 96 well plate was read at 570 nm on a Thermoscientific Multiskan go machine.

2.4.4 Statistical analysis

The distribution of variables was explored using the Shapiro-Wilk test. Continuous variables were reported as medians and IQR, while categorical variables were expressed as relative frequencies and percentages. Univariate analysis was carried out using Mann-Whitney for continuous, and chi-square test for categorical variables respectively. Kruskal-Wallis or ANOVA with post-hoc corrections was used for comparison between multiple groups. Spearman correlation and logistic regression carried out to explore the relationship between variables.

All tests were two-sided and a *P* value 0.05 was considered significant. Statistical analysis was performed using GraphPad Prism (version 9.1) and SPSS (version 24.0; SPSS Inc Chicago, IL).

3. POPULATION ANALYSIS AND REFERRAL MANAGEMENT PATHWAY

3.1 Introduction

NAFLD is the most common cause of abnormal LFTs worldwide, with an estimated prevalence ranging between 19–46% (Younossi et al., 2019b). Of note, NAFLD is also expected to become a leading cause of end-stage liver disease in the next decades(Younossi et al., 2019d). Histologically, NAFLD encompasses a spectrum of disorders from steatosis with or without hepatocellular injury and/or inflammation (NASH) and a variable degree of fibrosis through to cirrhosis(Kleiner and Makhlouf, 2016). In terms of clinical outcomes, fibrosis stage represents the strongest clinical predictor in these patients (Ekstedt et al., 2015).

Liver biopsy is still considered the gold standard for diagnosing and staging NAFLD (Kleiner et al., 2005) but it is invasive, expensive and it is associated with potential complications. As such, during the last few years, there has been an explosive development and use of non-invasive markers of fibrosis worldwide, as it is unfeasible for each patient with NAFLD to undergo a liver biopsy. Overall, FIB-4 (Vallet-Pichard et al., 2007) and NAFLD fibrosis score (Angulo et al., 2007), among the non-invasive markers based on blood tests, and TE, among the imaging techniques, have become the commonest non-invasive markers of fibrosis used in clinical practice. Specifically, FIB-4 and NAFLD fibrosis score can be calculated on a large scale, while TE is easy to perform, patient-friendly and has high accuracy in detecting advanced fibrosis (Boursier et al., 2013).

NAFLD and T2DM display a bidirectional association due to their common pathogenic mechanism of IR (Tilg, 2017). Nevertheless, the exact prevalence of NAFLD in T2DM is unknown, ranging broadly between 43% and 94% based on different diagnostic techniques and selection criteria of the screened population (Younossi et al., 2019d). Moreover, the majority of the data focusing on NAFLD and T2DM derive from tertiary care populations, whilst evidence from primary care is scarce. On a clinical perspective, the presence of T2DM is an independent predictor of advanced fibrosis in NAFLD, with a greater prevalence of NASH and cirrhosis in diabetic compared to non-diabetic patients, especially in younger patients (Hossain et al., 2009, Pais et al., 2011, Harrison et al., 2021). Furthermore, T2DM is highly prevalent among those patients with NAFLD who progress from simple steatosis to significant fibrosis (Pais et al., 2011).

Given the high prevalence and severity of NAFLD in the diabetic population, there is a major interest in early detection of the disease especially in primary care (European Association for the Study of the Liver. Electronic address et al., 2021, Noureddin et al., 2020). On a GP perspective, diagnosing NAFLD is perceived as a clinical challenge, with specific concerns on performing a risk-stratification among patients (Sheridan et al., 2017). Notably, current diabetes management guidelines do not advise for NAFLD screening in the general population. The EASL guidelines recommend screening NAFLD in high risk-populations (i.e. patients with metabolic syndrome) following a 2-tier system. Specifically, patients should be stratified using FIB-4 and/or ELF in primary care, followed by TE in a specialist setting (European Association for the Study of the Liver. Electronic address et al., 2021). However, such strategy relies heavily of FIB-4, which was derived from a tertiary care setting, and whose performance in primary care is still under investigation.

Recent evidence suggests that screening in primary care may be cost-effective but only in high-risk groups while using optimised algorithms for diagnosing (Noureddin et al., 2020). Nevertheless, substantial uncertainties still surround the development of a screening policy for NAFLD, such as scarce knowledge on disease progression and long-term outcomes, as well as the absence of a licensed treatment). However, as pharmacotherapies for NAFLD not yet available, it is of great importance to identify patients with high risk of progressive disease. As a result, there might be a subsequent reduction in progression rates to end-stage liver disease and associated healthcare burden.

Therefore, the main objectives of this part of the project were:

1. To assess the prevalence of clinically significant NAFLD among patients with T2DM in the community

2. To assess the prevalence of other undiagnosed chronic liver disease among patients with T2DM in the community

3. To perform a risk-stratification for the development of a NAFLD referral/management strategy pathway from primary care

3.2 Materials and methods

3.2.1 Study cohort and screening process

This single-centre, cross-sectional study included all consecutive patients with T2DM being followed up in primary care. Specifically, all patients were recruited from primary care (Tier 1) and community (Tier 2) clinics from the North-West London GP network. Patients were invited to take part to the study by their routine care team, such as GPs, dieticians, podiatrists and diabetic nurses. All consecutive patients were screened for liver disease and NAFLD using blood tests, full liver screen, TE and US.

Based on the results of TE performed on the day of the enrolment, the patients were therefore stratified according to LSM ≥ 8.1 kPa. The subgroup of patients with elevated LSM were considered for further investigations (such as a liver biopsy) and referred to specialist care as for guidelines' recommendation and standard of care. Only liver biopsies performed within 3 months from the clinical assessment and TE measurements were included in the study.

3.2.2 External validation

Two external centres provided retrospective cohorts of patients with T2DM diagnosed with NAFLD as external validation cohorts for clinical findings: the Royal Free Hospital (London, United Kingdom) and the Palermo University Hospital (Palermo, Italy). Specifically, the cohort from the Royal Free Hospital included consecutive patients with T2DM who were firstly referred from primary care through the Camden and Islington pathway. As such, this group included patients selected from primary care based on FIB-4>1.3 and/or ELF>9.5 (selected primary care population). The cohort from the Palermo Hospital included consecutive patients with T2DM who were followed-up in the specialist NAFLD clinic (tertiary care population).

3.2.3 Statistical analysis and regulatory approval

Statistical analysis was performed using SPSS© (version 24.0; SPSS Inc Chicago, IL). All patients' recruitment was conducted in line with Good Clinical Practice and sample handling

according to Human Tissue Act regulations. The main cross-sectional study (derivation cohort) obtained full ethical approval from the Research Ethics Committee (REC approval 18/LO/1742, IRAS 251274), sponsorship from Imperial College London and adoption from Clinical Research Network (CRN) Portfolio. The validation cohorts of patients provided by the Royal Free and Palermo were retrospective collection of routinely performed investigation and anonymised patient data. As such, ethical approval was not required as stated under the UK policy framework for health and social care. All activities were performed in accordance with the guidelines of the Helsinki Declaration.

3.3 Results

3.3.1 Study population

Between April 2019 and January 2021, a total of 300 patients with T2DM were enrolled from the North-West London GP network. Overall, 287 patients underwent the whole screening procedure, while 13 did not complete the screening and were excluded (**Figure 3.1**).

In the study population (n=287), median age was 61 (54-66) years, median BMI 30.4 (26.9-34.4) kg/m^2 and 53% (160/287) were men. In terms of ethnic background, 32% (102/287) of the patients are White Caucasian, 28% (74/287) Arab, 17% (47/287) South Asian, 12% (33/287) Black African or Caribbean, 8% (24/287) East Asian and 2% (6/287) White Hispanic (**Table 3.1**). In terms of socio-economic status, 51% (149/287) of the patients lived in the most deprived neighbourhoods (1st tertile) for income rank, 47% (136/287) for employment rank and 83% (239/287) for living environment rank. However, 49% (142/287) lived in the least deprived areas (3rd tertile) for education rank and 43% (143/287) for health and disability rank (**Table 3.2**).

As per comorbidities, 67% (191/287) had hypertension, 52% (148/187) dyslipidaemia and 15% (41/287) a psychiatric disorder. Moreover, 10% (28/287) reported history of acute cardiovascular event, while 75% (214/287) were on statin treatment for either primary or secondary CV prophylaxis (**Table 3.1**). In terms of diabetes control, median HbA1c was 60 (49-70) mmol/mol, insulin level 24 (8.1-26.5) μU/ml and HOMA index 8 (1.9-8.9). Furthermore, the median time from diagnosis of T2DM was 11 (4-16) years, with 16% (45/287) of the patients being diagnosed with at

least one known diabetic complication (i.e. diabetic retinopathy, nephropathy, neuropathy). In terms of anti-diabetic treatment, 13% (39/287) of the patients were on diet only, 79% (227/287) on oral agents. 13% (37/287) on GLP-1RA and 25% (74/287) on insulin treatment (**Table 3.1**).

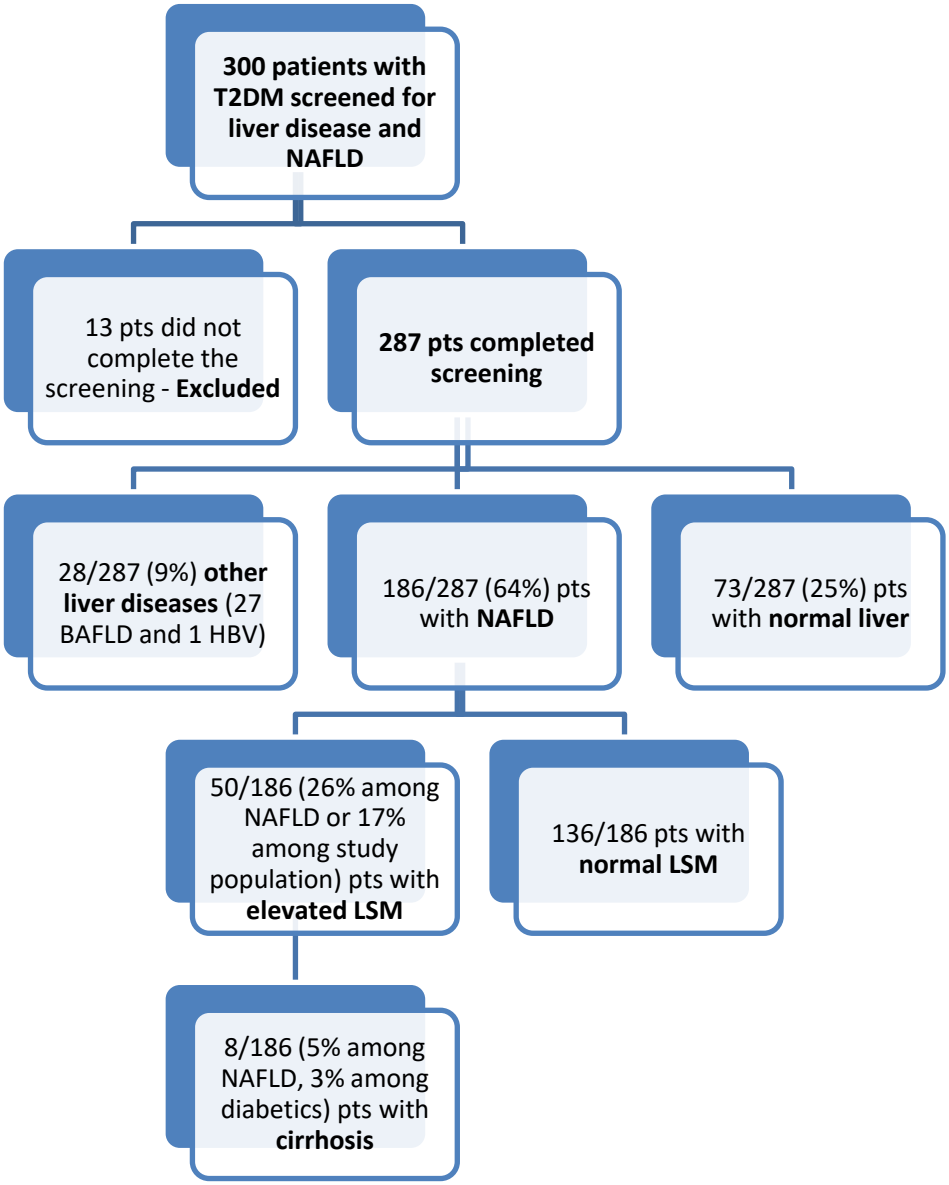

Figure 3.1. Flowchart showing the patients enrolled in the study. The flowchart of the study illustrates the total number (n=300) of patients enrolled in the study and the breakdown of the overall prevalence of NAFLD (64%) and other liver disease (9%) in the population. Patients with NAFLD were stratified according to LSM in those with elevated LSM (LSM≥8.1 kPa, n=50) and those with normal LSM (LSM < 8 kPa, n=136).
Abbreviations: T2DM: type-2 diabetes mellitus, NAFLD: non-alcoholic fatty liver disease, HBV: hepatitis B virus, BAFLD: both alcoholic and non-alcoholic fatty liver disease, LSM: liver stiffness measurement.

	Study population N=287	NAFLD N=186	Normal liver N=73	
	Median (IQR)	**Median (IQR)**	**Median (IQR)**	**P value***
Age, *years*	59 (59-66)	60 (54-66)	59 (53-65)	0.83
Waist circum, *cm*	107 (107-116)	**108 (101-118)**	**98 (92-106)**	**0.0001**
Hip circum, *cm*	110 (102-119)	**112 (105-122)**	**103 (98-108)**	**0.0001**
BMI, kg/m^2	30.8 (26.9-34.4)	**31.4 (28.4-35.8)**	**26.9 (24.8-30.3)**	**0.0001**
PLT, $x\ 10^9/\mu L$	250 (202-290)	245 (212-287)	249 (206-298)	0.88
ALT, *IU/L*	35 (22-45)	**34 (23-49)**	**24 (18-28)**	**0.0001**
AST, *IU/L*	31 (22-35)	**28 (23-37)**	**24 (19-27)**	**0.0001**
GGT, *IU/L*	47 (19-50)	**32 (22-52)**	**19 (17-27)**	**0.0001**
ALP, *IU/L*	88 (70-103)	84 (72-105)	85 (63-99)	0.7
Albumin, *g/L*	40 (39-42)	41 (39-42)	40 (39-42)	0.83
Bilirubin, *µmol/L*	10.6 (6-12)	9 (6-12)	8 (6-14)	0.55
Total Cholesterol, *mmol/l*	4.1 (3.5-4.7)	4.1 (3.4-4.7)	4 (3.6-4.5)	0.58
TRG, *mmol/l*	2.3 (1.02-2.08)	1.4 (1.07-2.1)	1.2 (0.98-1.5)	0.25
HDL, *mmol/l*	1.1 (0.9-1.3)	1.1 (0.9-1.2)	1.16 (1.06-1.39)	0.25
LDL, *mmol/l*	2.3 (1.6-2.7)	2.2 (1.6-2.8)	2.1 (1.7-2.6)	0.68
Ferritin, *ng/ml*	124 (43-155)	82 (39-140)	70 (28-178)	0.91
Diabetes characteristics				
	Median (IQR)	**Median (IQR)**	**Median (IQR)**	**P value***
Fasting glucose, *mmol/l*	7.9 (5.5)	**7.4 (5.6-10.2)**	**6.2 (4.8-7.8)**	**0.001**
HbA1c, *mmol/mol*	60 (49-70)	**60 (50-74)**	**55 (48-61)**	**0.0001**
Insulin, *µU/ml*	24 (8.1-26.5)	**15.3 (9.8-28.2)**	**7.2 (5.8-12.2)**	**0.028**

Homa index	8 (1.9-8.95)	**4.6 (2.2-10.3)**	**2.1 (1.35-4.8)**	**0.0001**
Duration DM, *years*	11 (4-16)	10 (3-16)	13 (7-16)	0.16
	N (%)	**N (%)**	**N (%)**	**P value***
Diet controlled	39 (13)	25 (13)	13 (18)	0.11
On oral agents	227 (79)	170 (91)	55 (75)	0.16
On GLP-1RA	37 (13)	31 (16)	6 (8)	0.08
On insulin	74 (25)	51 (28)	23 (31)	0.18
Diabetic complications	45 (16)	26 (14)	15 (21)	0.82
Ethnic background and comorbidities				
	N (%)	**N (%)**	**N (%)**	**P value***
Male gender	160 (53)	104 (56)	34 (45)	0.07
White, Caucasian	102 (32)	**64 (34)**	**15 (20)**	**0.02**
White, Hispanic	6 (2)	3 (1)	2 (2)	0.43
Black African, Afro-Caribbean	33 (12)	22 (12)	10 (13)	0.41
Arab	74 (28)	52 (28)	20 (26)	0.52
South Asian	47 (17)	31 (17)	16 (21)	0.2
East Asian	24 (8)	14 (7)	10 (13)	0.09
Hypertension	191 (67)	120 (64)	50 (66)	0.32
Dyslipidaemia	148 (52)	98 (53)	39 (52)	0.51
Psychiatric disorder	41 (15)	27 (14)	11 (14)	0.53
Previous ACE	28 (10)	16 (8)	11 (14)	0.98
On statin	214 (75)	138 (74)	57 (76)	0.31

Table 3.1. Characteristics of the study population and differences between patients with and without NAFLD. The table shows the differences between patients with (n=186) and without (n=73) NAFLD in the whole study population (n=287). Variables are expressed as median and IQR or relative percentages. * p-value refers to differences between patients with NAFLD and normal liver.
Abbreviations: IQR: interquartile range, BMI: Body mass index, PLT: platelet, ALT: alanine aminotransferase, AST: aspartate aminotransferase, GGT: gamma-glutamyl transferase, ALP: alkaline phosphatase, TRG: triglycerides, HDL: high density lipoprotein, LDL: low density lipoprotein, HbA1c: glycated haemoglobin, GLP-1RA: glucagon like peptide-1 receptor agonist

	Study population N=287	NAFLD N=186	Normal liver N=73	
	Median (IQR)	**Median (IQR)**	**Median (IQR)**	**P value***
Overall IMD	12090 (4855-22794)	10451 (4311-19881)	11080 (6506-23403)	0.67
Income rank	9010 (3543-21051)	8121 (2735-18772)	7859 (4465-21047	0.52
Employment rank	11453 (4262-25693)	9654 (3109-22898)	10762 (6120-26319)	0.41
Education rank	22924 (14331-27622)	22301 (14025-27522)	20753 (14157-26996)	0.42
Health and disability rank	19527 (12063-30517)	18655 (10506-27522)	20218 (12449-31764)	0.12
Crime rank	15996 (7882-22418)	15345 (2848-22453)	14655 (7803-21262)	0.2
Barriers to housing services rank	11758 (8643-14719)	11698 (8646-14434)	11580 (8497-14586)	0.57
Living environment rank	5832 (3228-8143)	5775 (3232-8116)	5338 (3729-7867)	0.97
	N (%)	**N (%)**	**N (%)**	**P value***
Overall IMD				0.23
1st tertile	119 (41)	83 (44)	30 (41)	
3rd tertile	70 (24)	36 (19)	19 (26)	
Income rank				0.65
1st tertile	149 (51)	100 (53)	40 (54)	
3rd tertile	66 (23)	36 (19)	17 (23)	
Employment rank				0.42

1st tertile	136 (47)	93 (50)	35 (48)	
3rd tertile	80 (27)	46 (24)	20 (27)	
Education rank				0.56
1st tertile	25 (8)	19 (10)	5 (7)	
3rd tertile	142 (49)	90 (48)	30 (41)	
Health and disability rank				0.76
1st tertile	45 (15)	34 (18)	7 (10)	
3rd tertile	124 (43)	76 (41)	29 (39)	
Crime rank				0.81
1st tertile	88 (31)	55 (29)	29 (39)	
3rd tertile	66 (23)	43 (23)	12 (16)	
Barriers to housing services rank				0.72
1st tertile	84 (29)	53 (28)	27 (37)	
3rd tertile	10 (3)	1 (5)	1 (1)	
Living environment rank	239 (83)	152 (81)	61 (83)	0.44
1st tertile	1 (0)	1 (5)	0 (0)	
3rd tertile				

Table 3.2. Socio-economic status of the study population and differences between patients with and without NAFLD. Socio-economic status is expressed as Index of multiple deprivation and relative single domains. The table shows the differences between patients with (n=186) and without (n=73) NAFLD in the whole study population (n=287). Variables are expressed as median and IQR or relative percentages. * p-value refers to differences between patients with NAFLD and normal liver.
Abbreviations: NAFLD: non-alcoholic fatty liver disease, IQR: interquartile range, IMD: index of multiple deprivation.

3.3.2 The prevalence of NAFLD and other liver disease in the diabetic community

The overall prevalence of NAFLD, based on ultrasound, was 64% (186/287), while the prevalence of other liver diseases was 9% (28/287, 27 BAFLD and 1 with chronic hepatitis B). The Number needed to treat/screen (NNT) in this population was 4.56.

Among those with NAFLD (n=186), median age was 60 (54-66) years, median BMI 31.4 (28.4-35.8) kg/m2 and 56% (104/186) were men. In terms of ethnic background, 34% (64/186) of the patients are White Caucasian, 28% (52/186) Arab, 17% (31/186) South Asian, 12% (22/186) Black African or Caribbean, 7% (14/186) East Asian and 1% (3/186) White Hispanic. As per comorbidities, 64% (120/186) had hypertension, 53% (98/186) dyslipidaemia and 14% (27/186) a psychiatric disorder. Moreover, 8% (16/186) reported history of ACE, while 74% (138/186) were on statin treatment for either primary or secondary CV prophylaxis (**Table 3.1**).

In terms of diabetes control, median HbA1c was 60 (50-74) mmol/mol, insulin level 15.3 (9.8-28.2) μU/ml and HOMA index 4.6 (2.2-10.3). Furthermore, the median time from diagnosis was 10 (3-16) years, with 14% (26/186) of the patients having at least one known diabetic complication. In terms of anti-diabetic treatment, 6% (13/186) of the patients were on diet only, 72% (134/186) on oral agents and/or GLP-1RA and 21% (39/186) on insulin treatment.

Compared to those with normal liver (n=73), patients with NAFLD had higher BMI (31.4 vs 26.9 kg/m^2, p=0.0001) and larger waist (108 vs 98 cm, p=0.0001) and hip (112 vs 103 cm, p=0.0001) circumferences. Those with NAFLD also presented with higher levels of ALT (34 vs 24 IU/L, p=0.0001), AST (28 vs 24 IU/L, p=0.0001) and gamma-glutamyl transferase (GGT, 32 vs 19 IU/L, p=0.0001). In terms of diabetes control, patients with NAFLD showed higher median HbA1c (60 vs 55 mmol/mol, p=0.0001), fasting glucose (7.4 vs 6.2 mmol/l, p=0.001), insulin level (15.3 vs 7.2 μU/ml, p=0.028) and HOMA index (4.6 vs 2.1, p=0.0001). There was no difference in terms of duration of diabetes, anti-diabetic medications or presence of diabetic complications. In terms of socio-economic status, there was no difference between the two groups in median IMD (and related single domain), as well as in distribution in tertile of IMD (and related single domains) (**Table 3.2**).

3.3.3 The prevalence of significant liver disease secondary to NAFLD in the diabetic community

The overall prevalence of significant liver disease, as defined by LSM ≥ 8.1 kPa, was 17% (50/287) in the whole diabetic population and 26% (50/186) in the NAFLD subgroup. The prevalence of newly diagnosed cirrhosis (either histologically or clinically) secondary to NAFLD was 3% (8/287) in the whole diabetic population and 5% (8/184) in the NAFLD subgroup. All patients diagnosed with liver disease were referred to tertiary care, while the other participants were advised for lifestyle changes.

Compared to those with normal LSM (n=136), patients with elevated LSM (n=50) presented higher BMI (36.8 vs 30.3 kg/m2, p=0.0001), larger hip (123 vs 110 cm, p=0.0001) and waist circumferences (120 vs 105 cm, p=0.0001). Those with significant liver disease also presented with higher ALT (46 vs 30 IU/L, p=0.0001), AST (37 vs 26 IU/L, p=0.0001) and GGT (62 vs 27 IU/L, p=0.0001) levels. Of note, although there was an increase in LFTs across the study groups, up to 42% patients with LSM between 8 and 12 kPa and up to 38% patients with LSM greater than 12.1 kPa presented with normal LFTs (**Figure 3.2**). In terms of metabolic control, patients with NAFLD showed higher median HbA1c (71 vs 59 mmol/mol, p=0.0001), fasting glucose (9.4 vs 6.7 mmol/l, p=0.001), insulin level (21 vs 12.4 µU/ml, p=0.001) and HOMA index (8.1 vs 3.3, p=0.001). There was no difference in terms of duration of diabetes, anti-diabetic medication or presence of diabetic complications (**Table 3.3**). In terms of socio-economic status, those with NAFLD and elevated LSM lived in more deprived neighbourhoods according to median education rank (18789 vs 23148, p=0.03). However, there was no difference in terms of distribution of the patients within most deprived (1st tertile) and least deprived (3rd tertile) areas as per education ranks (**Table 3.4**).

On multivariate analysis, waist circumference (crude OR 1.086, 95%CI 1.021-1.154, p=0.008), BMI (crude OR 1.17, 95%CI 1.008-1.358, p=0.04), AST (crude OR 1.071, 95%CI 1.07-1.01, p=0.022) and education rank (crude OR 0.857, 95%CI 0.744-0.987) were independent predictors of significant liver disease in the whole diabetic population (**Table 3.5**). Of these patients with elevated LSM (n=50), 11 patients underwent a liver biopsy. As per NASH CRN scoring system,

one (9%) patient showed fibrosis 1a, 3 (27%) had fibrosis stage 2, 5 (45%) had bridging fibrosis and 2 (18%) had cirrhosis. As per NAS score, 9 patients had “probable NASH” (3 < NAS score< 5) while 2 “definite NASH” (NAS score ≥5).

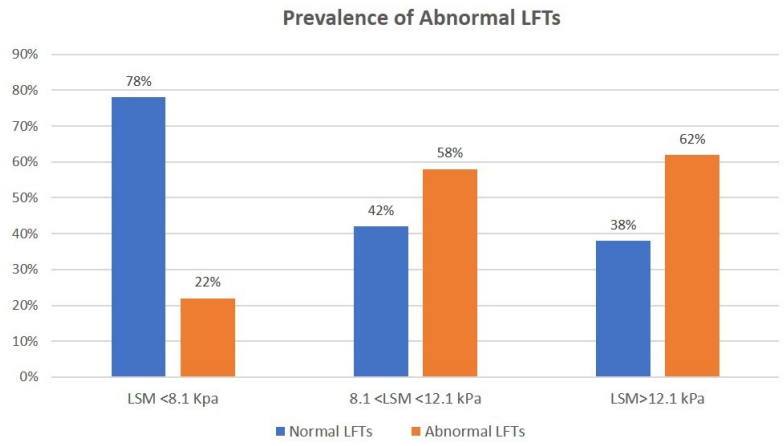

ALT cut-off: 0-45 U/L (men), 0-34 (women)

AST cut-off: 0-40 U/L

Figure 3.2. Prevalence of abnormal liver function tests in the NAFLD cohort stratified per liver stiffness measurement. The bar chart illustrates the percentage of NAFLD patients with normal and abnormal LFTs, stratified per LSM cut-off 8.1 kPa (significant fibrosis) and 12.1 kPa (advanced fibrosis). Abnormal LFTs was defined using ALT and AST cut-offs applied at Imperial College NHS Trust are also included.
Abbreviations: LFTs: liver function tests; ALT: alanine aminotransferase; AST: aspartate aminotransferase

	NAFLD, elevated LSM N=50	NAFLD, normal LSM N=136	
	Median (IQR)	**Median (IQR)**	**P value***
Age, *years*	60 (51-65)	61 (54-65)	0.49
Waist circum, *cm*	**120 (112-127)**	**105 (99-113)**	**0.0001**
Hip circum, *cm*	**123 (123-132)**	**110 (103-119)**	**0.0001**
BMI, kg/m^2	**36.8 (32-39.7)**	**30.3 (27.6-33.6)**	**0.0001**
PLT, $x\ 10^9/uL$	231 (198-266)	255 (215-300)	0.3
ALT, *IU/L*	**46 (25-60)**	**30 (22-43)**	**0.0001**
AST, *IU/L*	**37 (28-48)**	**26 (22-32)**	**0.0001**
GGT, *IU/L*	**62 (35-96)**	**27 (19-39)**	**0.0001**
ALP, *IU/L*	83 (70-110)	84 (72-101)	0.62
Albumin, *g/L*	40 (38-41)	41 (39-42)	0.06
Bilirubin, *µmol/L*	10 (7-16)	8 (6-11)	0.55
Total Cholesterol, *mmol/l*	3.9 (3.4-4.4)	4.1 (3.5-4.8)	0.14
TRG, *mmol/l*	1.3 (1.08-2.2)	1.5 (1.06-2.1)	0.92
HDL, *mmol/l*	1.1 (0.9-1.2)	1.08 (0.9-1.3)	0.51
LDL, *mmol/l*	1.9 (1.6-2.6)	2.2 (1.6-2.8)	0.42
Ferritin, *ng/ml*	108 (48-182)	81 (36-124)	0.31
Diabetes characteristics			
	Median (IQR)	**Median (IQR)**	**P value***
Fasting glucose, *mmol/l*	**9.4 (6.2-13.4)**	**6.7 (5.2-9.2)**	**0.001**
HbA1c, *mmol/mol*	**71 (56-84)**	**59 (49-68)**	**0.0001**

Insulin, *μU/ml*	**21 (14-37.2)**	**12.4 (9-25)**	**0.001**
Homa index	**8.1 (4.5-14.1)**	**3.3 (2.1-8.4)**	**0.001**
Duration DM, *years*	10 (4-16)	10 (3-16)	0.46
	N (%)	**N (%)**	**P value***
Diet controlled	1 (2)	24 (17)	0.052
On oral agents	43 (86)	127 (93)	0.051
On GLP-1-RA	10 (20)	21 (15)	0.07
On insulin	15 (30)	36 (26)	0.25
Diabetic complications	10 (20)	16 (12)	0.82
Ethnic background and comorbidities			
	N (%)	**N (%)**	**P value***
Male gender	29 (58)	75 (55)	0.44
White, Caucasian	20 (40)	45 (33)	0.22
White, Hispanic	1 (2)	2 (1)	0.61
Black African, Afro-Caribbean	4 (8)	18 (13)	0.23
Arab	15 (30)	37 (27)	0.43
South Asian	8 (16)	22 (16)	0.47
East Asian	2 (4)	12 (9)	0.21
Hypertension	33 (66)	87 (63)	0.45
Dyslipidaemia	27 (54)	71 (52)	0.46
Psychiatric disorder	9 (18)	19 (13)	0.28
Previous ACE	3 (6)	13 (9)	0.29
On statin	39 (78)	99 (76)	0.32

Table 3.3. Differences between NAFLD patients stratified per liver stiffness measurement greater than 8.1 kPa. The table shows the differences between patients with NAFLD with elevated (n=50) and normal (n=136) LSM. Variables are expressed as median and IQR or relative percentages. * p-value: differences between patients with NAFLD with elevated LSM and normal LSM.
Abbreviations: IQR: interquartile range, BMI: Body mass index, PLT: platelet, ALT: alanine aminotransferase, AST: aspartate aminotransferase, GGT: gamma-glutamyl transferase, ALP: alkaline phosphatase, TRG:

triglycerides, HDL: high density lipoprotein, LDL: low density lipoprotein, HbA1c: glycated haemoglobin, GLP-1RA: glucagon like peptide-1 receptor agonist

	NAFLD, elevated LSM N=50	NAFLD, normal LSM N=136	
	Median (IQR)	**Median (IQR)**	**P value***
Overall IMD	10043 (4098-18528)	11858 (4851-21254)	0.1
Income rank	6767 (1872-16991)	8336 (3218-20084)	0.19
Employment rank	8171 (3109-19674)	10511 (3110-24241)	0.22
Education rank	**18789 (13721-26362)**	**23148 (14665-28792)**	**0.03**
Health and disability rank	16806 (9800-27198)	20105 (12063-29788)	0.13
Crime rank	14692 (7268-20746)	16118 (8228-22680)	0.63
Barriers to housing services rank	11292 (8067-13945)	11728 (9393-14434)	0.29
Living environment rank	5923 (2769-9394)	5599 (3289-8107)	0.99
	N (%)	**N (%)**	**P value***
Overall IMD			0.2
1st tertile	27 (54)	56 (41)	
3rd tertile	7 (14)	29 (21)	
Income rank			0.06
1st tertile	27 (54)	73 (53)	

3rd tertile	36 (51)	27 (20)	
Employment rank			0.42
1st tertile	27 (54)	66 (48)	
3rd tertile	9 (16)	37 (27)	
Education rank			0.08
1st tertile	6 (12)	13 (10)	
3rd tertile	18 (36)	71 (52)	
Health and disability rank			0.54
1st tertile	13 (25)	21 (15)	
3rd tertile	15 (30)	61 (44)	
Crime rank			0.71
1st tertile	17 (34)	38 (27)	
3rd tertile	10 (20)	33 (24)	
Barriers to housing services rank			0.65
1st tertile	18 (36)	35 (25)	
3rd tertile	0 (0)	1 (0)	
Living environment rank			0.73
1st tertile	38 (76)	114 (83)	
3rd tertile	1 (2)	0 (0)	

Table 3.4. Differences in socio-economic status between NAFLD patients stratified per liver stiffness measurement greater than 8.1 kPa. Socio-economic status is expressed as Index of multiple deprivation and relative single domains. The table shows the differences between patients with NAFLD with elevated (n=50) and normal (n=136) LSM. Variables are expressed as median and IQR or relative percentages. * p-value: differences between patients with NAFLD with elevated LSM and normal LSM.
Abbreviations: NAFLD: non-alcoholic fatty liver disease, LSM: liver stiffness measurement, IQR: interquartile range, IMD: index of multiple deprivation.

	Sign.	Crude OR	95% C.I.	
			Lower	Upper
Waist Circumf., *cm*	**0,008**	**1,086**	**1,021**	**1,154**
Hip Circumf., *cm*	0.659	0.992	0.956	1.029
BMI, *kg/m2*	**0.040**	**1.170**	**1.008**	**1.358**
ALT, *IU/L*	0.693	0.992	0.952	1.033
AST, *IU/L*	**0.022**	**1.071**	**1.010**	**1.135**
Insulin, *µU/ml*	0.600	0.986	0.934	1.041
Glucose, *mmol/l*	0.796	0.967	0.752	1.244
Homa- index*	0.442	1.048	0.930	1.181
HbA1c, *mmol/mol*	0.095	1.035	0.994	1.079
Education rank	**0.033**	**0.857**	**0.744**	**0.987**

Table 3.5. Predictive factors for the presence of significant liver disease in the whole diabetic population. The table shows predictive factors for LSM ≥8.1 kPa on multivariate analysis. Education rank is derived from the Index of multiple deprivation.
**Homa-index was calculated only in those not on insulin treatment.*
Abbreviations: OR: odds ratio, 95%CI: 95% confidence interval, BMI: Body Mass Index, ALT: Alanine aminotransferase, AST: aspartate aminotransferase, HbA1c: glycated haemoglobin

3.3.4 The derivation of the BIMAST score

Overall, the whole study population was split into a derivation (n=194) and a validation (n=93) cohort, following a 2:1 random allocation. The derivation and the validation cohorts were similar in terms of clinical features (**Table 3.6**). Moreover, the proportion of patients with significant NAFLD (LSM≥8.1 kPa) was also similar between the groups (33/194=17% vs 17/93=18%, p=0.44).

The predictive factors for the presence of fibrosis (**Table 3.5**) were moved forward to calculate a dedicate predictive score. The BIMAST score was therefore derived from the the derivation cohort, based on BMI and AST. Such score was computed by binary logistic regression and for predicting the presence of LSM≥ 8.1 kPa among the diabetics:

$$0.17*(\text{BMI, kg/m}^2) + 0.054*(\text{AST, IU/L}) - 8.771$$

Of note, waist circumference and education attainment wwere omitted *a priori* to increase the potential usability of the score. Indeed, waist circumference and education attainment are not routinely calculated in clinical practice and would be relatively time consuming for the GPs to assess.

The Hosmer-Lemeshow test and Brier score for the BIMAST score were 0.9 and 0.12, confirming that the derived model fitted well the derivation cohort and had good calibration. In the derivation cohort, the BIMAST score was able to predict the presence of significant fibrosis (LSM≥8.1 kPa, n=33) accurately, with an AUROC of 0.81 (95%CI: 0.72-0.9, p<0.0001) (**Figure 3.3A**). A cut-off of 0.063 gave 94% sensitivity and 44% specificity, with PPV 22% and NPV 97%. Moreover, the BIMAST score was able to predict the presence of advanced fibrosis (LSM≥12.1 kPa, n=17) accurately, with an AUROC of 0.84 (95%CI: 0.72-0.95, p<0.0001) (**Figure 3.3B**). A cut-off of 0.102 carried sensitivity 94%, specificity 50%, PPV 20% and NPV 99%.

	Derivation cohort N=194	Internal validation cohort N=93	
	Median (IQR)	**Median (IQR)**	**P value***
Age, *years*	60 (54-66)	61 (54-65)	0.46
Waist circum, *cm*	106 (98-116)	106 (100-107)	0.38
Hip circum, *cm*	109 (102-118)	112 (105-121)	0.16
BMI, kg/m^2	30 (26.7-34.4)	31.1 (28.1-34.4)	0.39
PLT, $x\ 10^9/uL$	254 (212-292)	234 (192-275)	0.055
ALT, *IU/L*	28 (20-43)	32 (26-48)	0.07
AST, *IU/L*	27 (22-34)	28 (23-39)	0.18
GGT, *IU/L*	27 (18-46)	31 (19-59)	0.31
ALP, *IU/L*	83 (69-100)	85 (23-39)	0.1
Total Cholesterol, *mmol/l*	4.1 (3.5-4.7)	4.1 (3.4-4.8)	0.9
TRG, *mmol/l*	1.3 (1-2)	1.4 (1-2)	0.93
HDL, *mmol/l*	1.1 (0.9-1.3)	1.1 (0.9-1.3)	0.69
LDL, *mmol/l*	2.1 (1.2-2.7)	2.1 (1.5-2.8)	0.77
Ferritin, *ng/ml*	81 (40-155)	108 (46-156)	0.37
LSM, *kPa*	5.6 (4.4-7.3)	5.5 (4-7.5)	0.56
CAP score, *dB/m*	309 (255-292)	308 (260-347)	0.81
Diabetes characteristics			
	Median (IQR)	**Median (IQR)**	**P value***
Fasting glucose, *mmol/l*	6.8 (5.2-9.4)	6.9 (5.8-9.9)	0.07
HbA1c, *mmol/mol*	57 (49-70)	59 (47-71)	0.75
Insulin, *µU/ml*	14 (9-27)	12.4 (7.4-22)	0.17
Homa index	4.1 (2.1-8.4)	3.2 (1.8-9.6)	0.47
Duration DM, *years*	10 (4-18)	10 (4-15)	0.055

Table 3.6. Differences between derivation and internal validation cohort. The table shows the differences between patients from the derivation (n=194) vs internal validation (n=93) cohort. Variables are expressed as median and IQR or relative percentages. * p-value: differences between patients from the derivation vs internal validation cohort.
Abbreviations: IQR: interquartile range, BMI: Body mass index, PLT: platelet, ALT: alanine aminotransferase, AST: aspartate aminotransferase, GGT: gamma-glutamyl transferase, ALP: alkaline phosphatase, TRG: triglycerides, HDL: high density lipoprotein, LDL: low density lipoprotein, HbA1c: glycated haemoglobin.

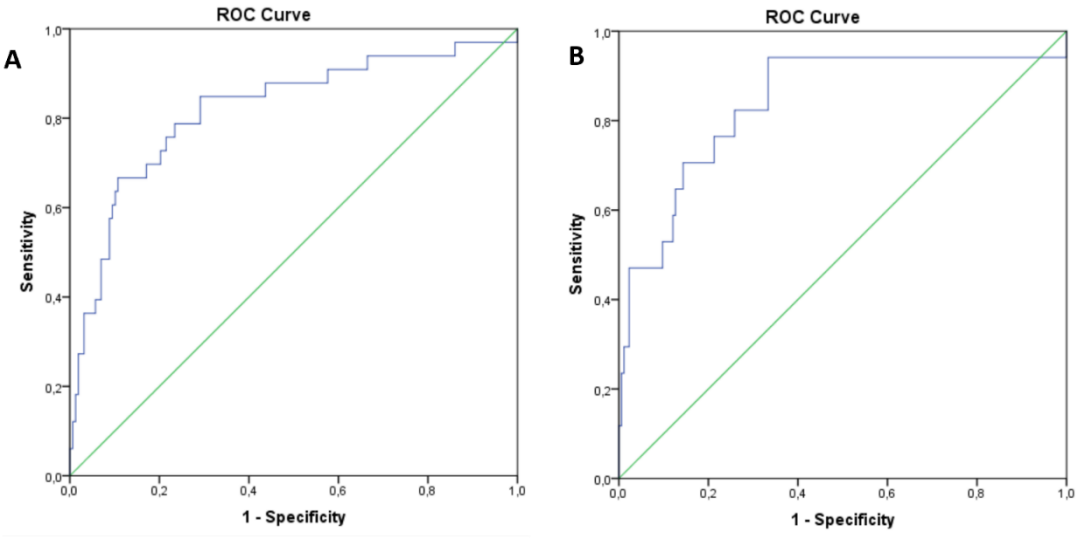

Figure 3.3. Diagnostic performance of the BIMAST score for predicting significant and advanced fibrosis in the derivation cohort (diabetes primary care). The figure illustrates the receiver operating characteristic curve of the BIMAST score for predicting LSM ≥ 8.1 kPa (Figure 3.3A) and for predicting LSM ≥ 12.1 kPa (Figure 3.3B) in the derivation cohort (n=194, diabetes primary care).
Abbreviations: LSM: liver stiffness measurement.

3.3.5 Internal validation of the BIMAST score and performance against established screening methods in the whole diabetic primary care population

In the validation cohort, the BIMAST score showed a Hosmer-Lemeshow test and Brier score of 0.89 and 0.13, confirming that the derived model fitted well the validation cohort and had good calibration. In the validation cohort, the BIMAST score was able to predict the presence of significant fibrosis (LSM≥8.1 kPa, n=17) accurately, with an AUROC 0.91 (95%CI: 0.82-0.99, p<0.0001) (**Figure 3.4A**). A cut-off of 0.063 gave 70% sensitivity and 90% specificity, with PPV 63% and NPV 94%. Similarly, the BIMAST score predicted the presence of advanced fibrosis (LSM≥12.1 kPa, n=14) accurately, with an AUROC 0.908 (95%CI: 0.81-0.99, p<0.0001) (**Figure 3.4B**). A cut-off of 0.102 carried sensitivity 63%, specificity 95%, PPV 66% and NPV 99%.

In the whole population, when compared to established methods for screening liver disease, the BIMAST score performed better. Specifically, the AUROC for diagnosing LSM≥8.1 kPa (n=50) was 0.86 (95%CI 0.8-0.92, p<0.0001) for the BIMAST score, 0.74 (95%CI 0.65-0.82, p=0.0001) for US plus LFTs, 0.72 (95%CI 0.65-0.8, p=0.0001) for NAFLD fibrosis score and 0.62 (95%CI 0.53-0.7, p=0.001) for FIB-4. The pairwise comparison of AUROC curves, as per the DeLong method, confirmed that the BIMAST score was better than US plus LFTs (p=0.01), NAFLD fibrosis score

(p=0.009) and FIB-4 (p<0.0001) in diagnosing the significant fibrosis in the community (**Figure 3.5A**). Similarly, the ROC curve for GGT to PLT ratio were 0.68 (95%CI 0.58-0.74, p=0.001) and 0.71 (95%CI 0.64-0.77, p=0.02) for diagnosing significant and advanced fibrosis respectively.

Furthermore, the AUROC for diagnosing LSM≥12.1 kPa (n=31) were 0.9 (95%CI 0.84-0.95, p=0.0001) for the BIMAST score, 0.76 (95%CI 0.66-0.85, p=0.0001) for US plus abnormal LFTs, 0.73 (95%CI 0.64-0.82, p=0.0001) for NAFLD fibrosis score and 0.61 (95%CI 0.51-0.72, p=0.001) for FIB-4. The pairwise comparison of AUROC curves, as per the DeLong method, confirmed that the BIMAST score performed better than US plus abnormal LFTs (p=0.01), NAFLD fibrosis score (p<0.0001) and FIB-4 (p<0.0001) (**Figure 3.5B)**. Specifically, among those with NAFLD, 40% (20/50) of the patients with LSM ≥ 8.1 kPa were misclassified as low-risk group by FIB-4 (FIB-4 <1.3). Specifically, those who were misclassified by FIB-4 were significantly younger (57 vs 62 years, p=0.03) and had lower AST (35 vs 41 IU/L, p=0.034) compared to those correctly classified as low-risk group. Similarly, up to 66% (91/136) of patients with normal LSM were misclassified as either intermediate (1.31<FIB-4<3.24, 89/136) or high-risk group (FIB-4>3.25, 2/136) by FIB-4. In this case, those who were misclassified by FIB-4 were significantly older (63 vs 58 years, p<0.0001) and had higher AST (30 vs 24 IU/L, p<0.0001) compared to those correctly classified as intermediate-high risk group.

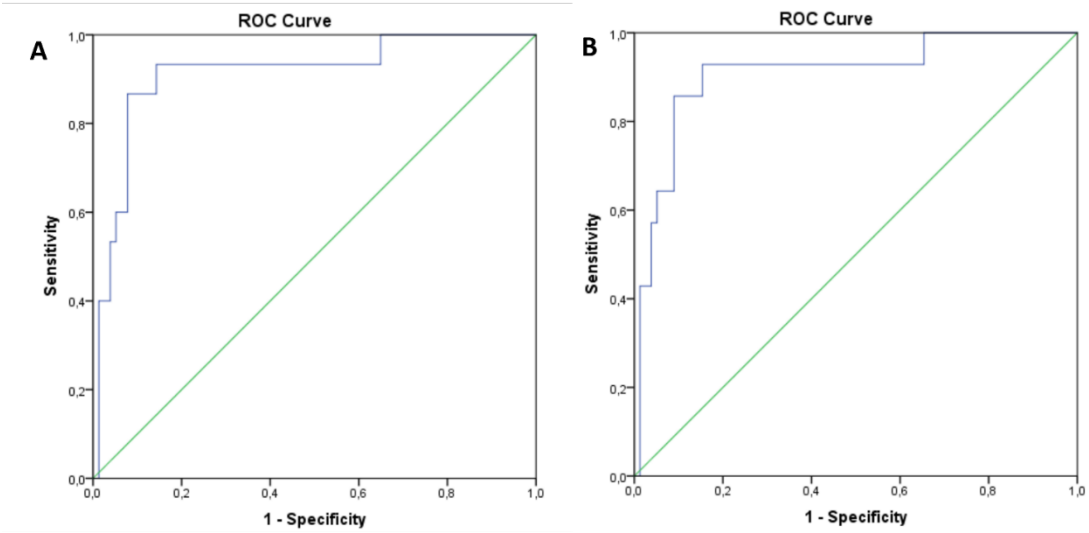

Figure 3.4. Diagnostic performance of the BIMAST score for predicting significant and advanced fibrosis in the internal validation cohort (diabetes primary care). The figure illustrates the receiver operating characteristic curve of the BIMAST score for predicting LSM ≥ 8.1 kPa (Figure 3.4A) and for predicting LSM ≥ 12.1 kPa (Figure 3.4B) in the internal validation cohort (n=93, diabetes primary care).
Abbreviations: LSM: liver stiffness measurement.

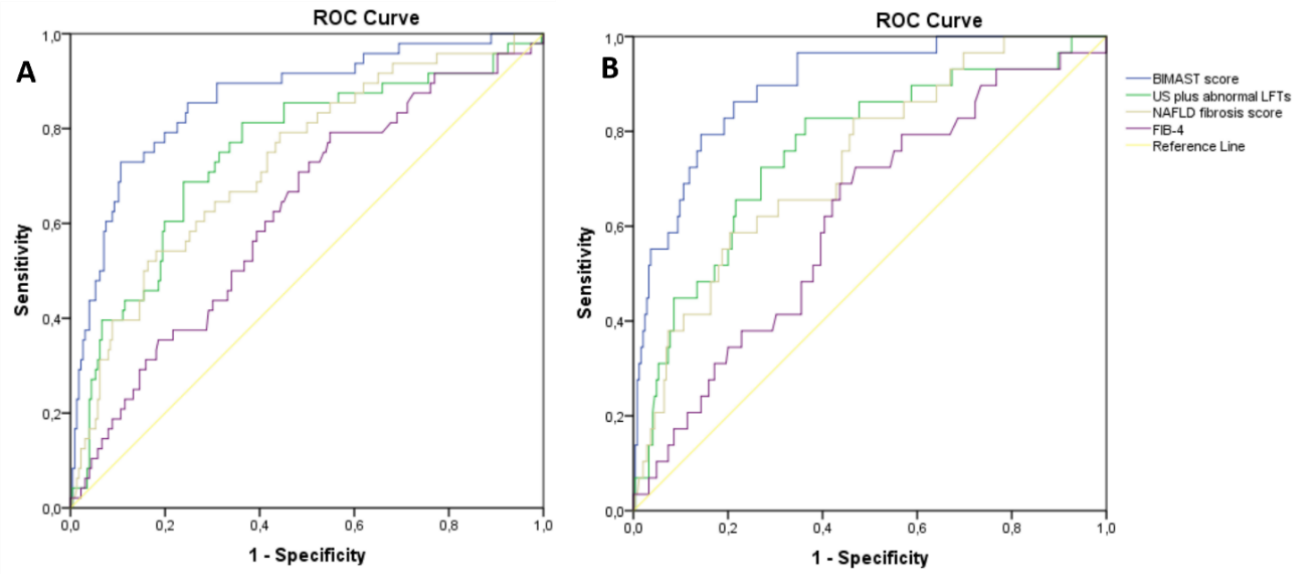

Figure 3.5. BIMAST score vs conventional screening methods for predicting significant and advanced fibrosis in the diabetic primary care population (whole study population). The figure illustrates the receiver operating characteristic curve of the BIMAST score vs conventional methods for predicting LSM ≥ 8.1 kPa (Figure 3.5A) and for predicting LSM ≥ 12.1 kPa (Figure 3.5B) in the whole study population (n=287, diabetes primary care).
Abbreviations: LSM: liver stiffness measurement.

3.3.6 Identification rates for screening NAFLD in diabetes primary care

Overall, the whole population was stratified according to LSM≥8.1 kPa (significant fibrosis) and 12 kPa (advanced fibrosis), being those with other liver diseases excluded (N=259). The identification rates were calculated for US and abnormal LFTs, FIB-4 and BIMAST score.

The number of patients with LSM≥8.1 kPa who were missed by FIB-4 and US plus abnormal LFTs strategy (false negative) was 19 (19/50=38%) and 19 (19/50=38%) vs 5 (5/50=10%) by BIMAST score. Moreover, the number of patients with LSM≤8 kPa who could potentially undergo avoidable investigations (false positive) was 34 (34/209=16%) for US and abnormal LFTs, 78 (78/209=38%) for FIB-4 and 80 (80/209=38%) for BIMAST score (**Figure 3.6, Figure 3.7,** and **Figure 3.8**).

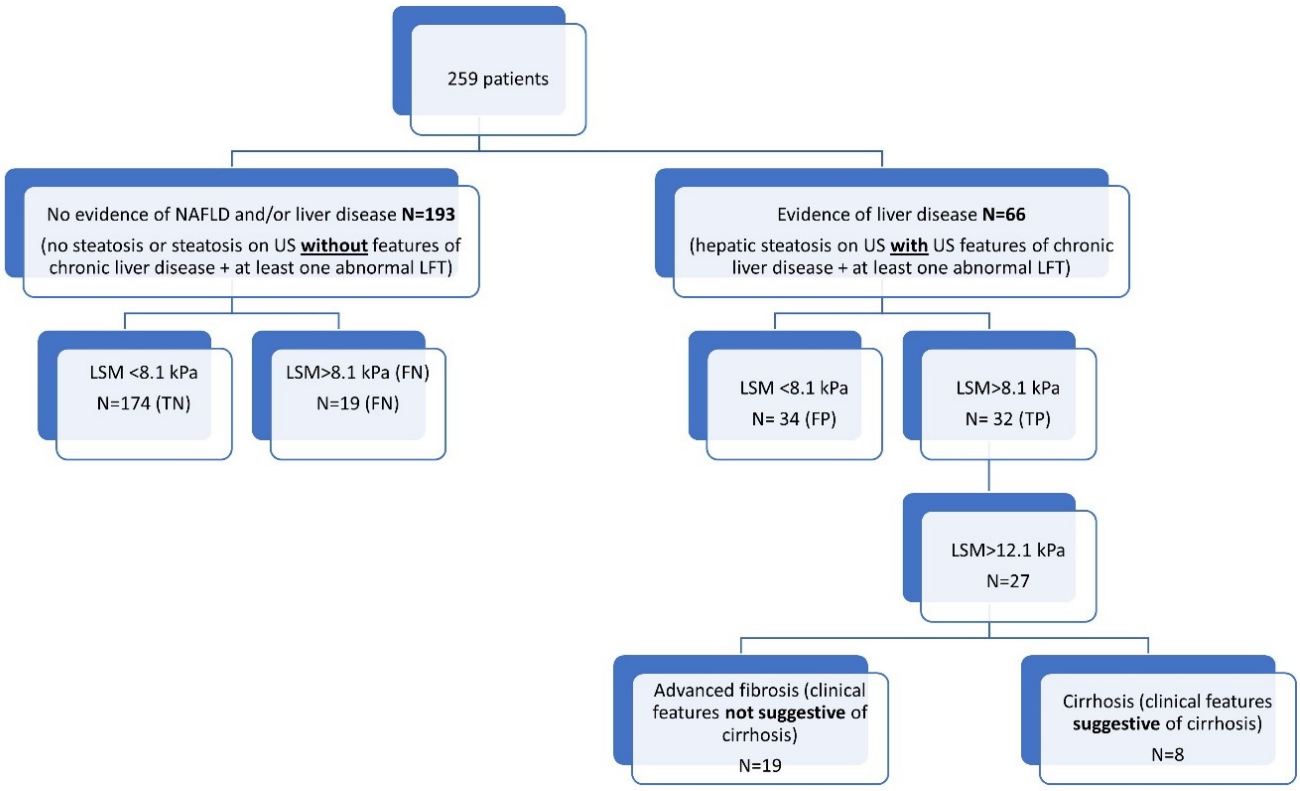

Figure 3.6. Identification rates for significant and advanced liver disease due to NAFLD among diabetic patients in primary care using US and LFTs.
Abbreviations: NAFLD: non-alcoholic fatty liver disease, LSM: liver stiffness measurement, TP: true positive, TN: true negative, FP: false positive, FN: false negative, US: ultrasound, LFT: liver function test

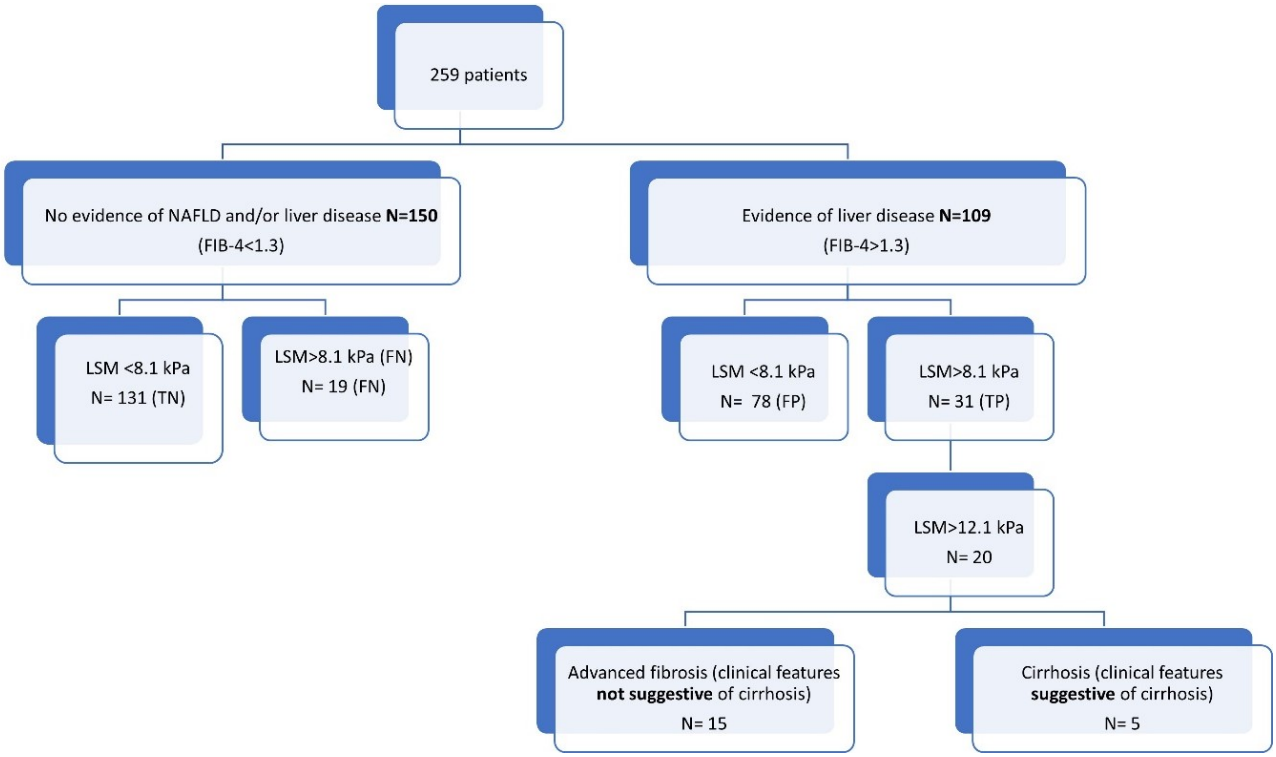

Figure 3.7. Identification rates for significant and advanced liver disease due to NAFLD among diabetic patients in primary care using FIB-4.
Abbreviations: NAFLD: non-alcoholic fatty liver disease, LSM: liver stiffness measurement, TP: true positive, TN: true negative, FP: false positive, FN: false negative, FIB-4: fibrosis score-4

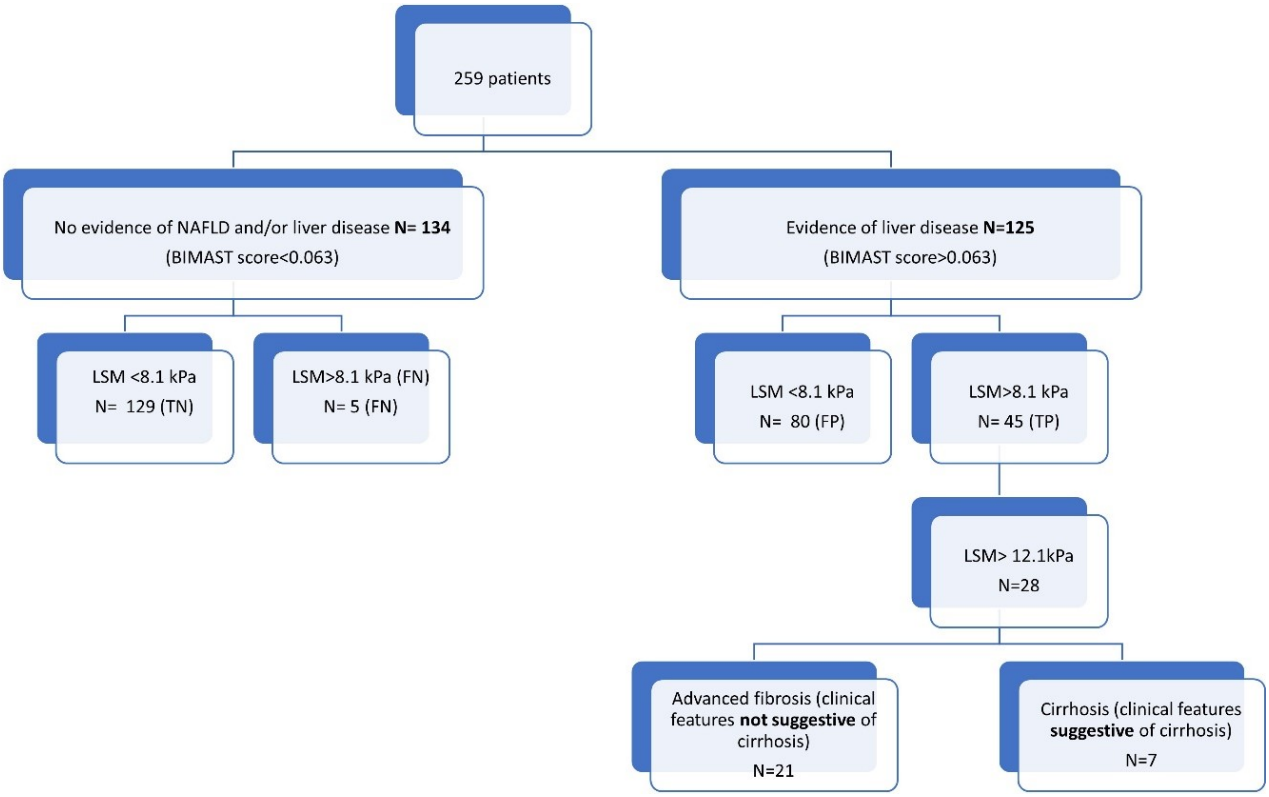

Figure 3.8. Identification rates for significant and advanced liver disease due to NAFLD among diabetic patients in primary care using the BIMAST score.
Abbreviations: NAFLD: non-alcoholic fatty liver disease, LSM: liver stiffness measurement, TP: true positive, TN: true negative, FP: false positive, FN: false negative.

3.3.7 The validation of the BIMAST score: the Royal free cohort

Overall, the Royal Free cohort (n=218) presented significantly larger waist circumference (111 vs 106 cm, p=0.006) and higher BMI (32.4 vs 30.4 kg/m^2, p=0.0001) compared to the derivation cohort. Also, the Royal Free cohort had higher ALT (49 vs 30 IU/L, p=0.0001) and AST (34 vs 27 IU/L, p=0.0001) and lower PLT (230 vs 243 x 10^9/μL, p=0.0001). Furthermore, the patients from the Royal Free cohort had significantly higher LSM (7.9 vs 5.6 kPa, p=0.0001) compared to the derivation cohort (**Table 3.7**). When the patients were stratified per LSM cut-offs, the distribution of the Royal Free cohort was shifted towards high LSM ranges compared to the derivation cohort (**Figure 3.9**).

The Hosmer-Lemeshow test and the Brier score for the BIMAST score were 0.67 and 0.31, suggesting that the BIMAST score had a moderate goodness-of-fit and calibration in the Royal Free

cohort. Specifically, the AUROC of BIMAST score for diagnosing LSM≥ 8.1 kPa (n=105) was 0.7 (95%CI: 0.63-0.77, p<0.0001) vs 0.68 (95%CI: 0.61-0.75, p<0.0001) of FIB-4 (**Figure 3.10A**). The pairwise comparison between AUROC curves (De Long method) confirmed that the BIMAST score and FIB-4 performed similarly well (p=0.69). With a cut-off of 0.063, the BIMAST score predicted the presence of LSM ≥ 8.1 kPa with sensitivity 34%, specificity 91%, PPV 76% and NPV 40%.

The AUROC of BIMAST score for diagnosing LSM≥ 12.1 kPa (n=66) was 0.72 (95%CI: 0.65-0.8, p<0.0001) vs 0.68 (95%CI: 0.6-0.76, p<0.0001) of FIB-4 (**Figure 3.10B**). The pairwise comparison between AUROC curves (De Long method) confirmed that the BIMAST score performed similarly to the FIB-4 (p=0.41) in this cohort. With a cut-off of 0.102, the BIMAST score predicted the presence of LSM ≥ 12.1 kPa with sensitivity 43%, specificity 89%, PPV 62% and NPV 23%.

	Primary care cohort N=287	Validation cohort Royal Free N=218	Validation cohort Sicily N=168		
	Median (IQR)	**Median (IQR)**	**Median (IQR)**	**P value***	**P value****
Age, *years*	61 (54-66)	61 (53-68)	56 (50-63)	0.58	**0.0001**
Waist circum, *cm*	106 (98-116)	111 (100-120)	109 (100-118)	**0.006**	0.09
BMI, kg/m^2	30.4 (26.9-34.4)	32.4 (28.1-37.7)	31.8 (28.9-35.5)	**0.0001**	**0.004**
PLT, $x\ 10^9/\mu L$	243 (202-290)	230 (181-276)	229 (178-267)	**0.001**	**0.01**
ALT, *IU/L*	30 (22-45)	49 (33-68)	56 (37-82)	**0.0001**	**0.0001**
AST, *IU/L*	27 (22-35)	34 (24-48)	38 (28-51)	**0.0001**	**0.0001**
LSM, *kPa*	5.6 (4.4-7.3)	7.9 (5.4-14)	11 (7.8-16.8)	**0.0001**	**0.0001**

Table 3.7. Differences between the derivation cohort and the validation cohorts. The table shows the differences between the primary care cohort (n=287) and cohorts from Royal Free Hospital (n=218) and Sicily (n=168). Variables are expressed as median and IQR. * p value for difference between derivation cohort and validation cohort from Royal Free. ** p value for difference between derivation cohort and validation cohort from Sicily.
Abbreviations: IQR: interquartile range, BMI: Body Mass Index, PLT: platelet, ALT: Alanine aminotransferase, AST: aspartate aminotransferase, LSM: Liver stiffness measurement

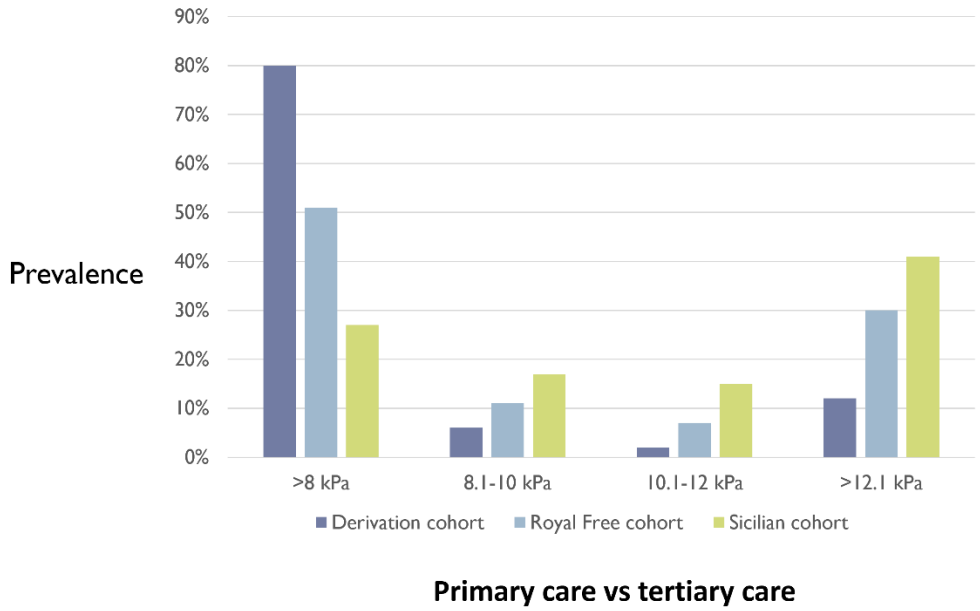

Figure 3.9. Primary care and external validation cohorts stratified per LSM ranges. The bar chart illustrates the prevalence of patients with different ranges of LSM in the three groups: primary care cohort (n=287), Royal free cohort (n=218) and Sicilian cohort (n=168).
Abbreviations: LSM: liver stiffness measurement.

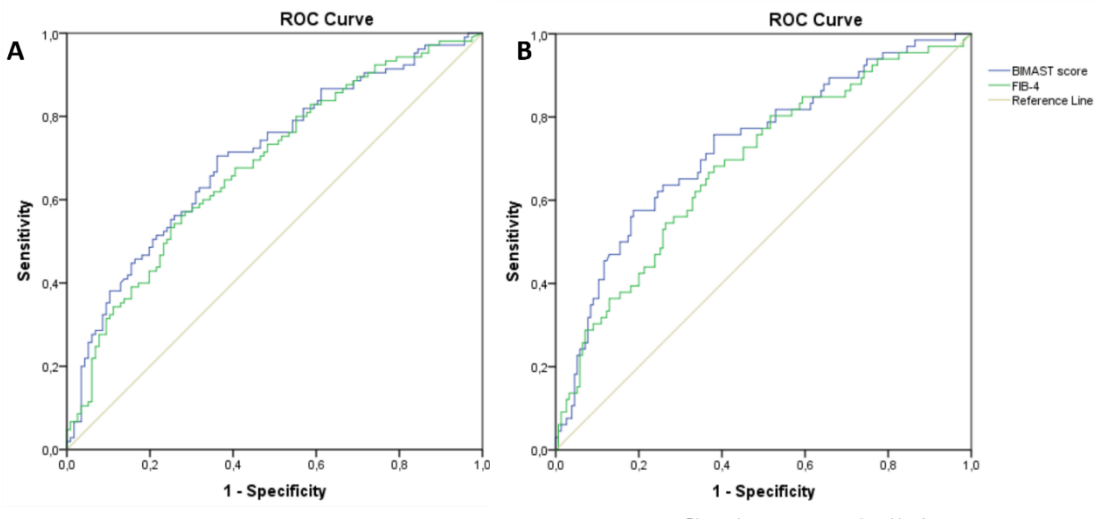

Figure 3.10. BIMAST score vs FIB-4 for predicting significant and advanced fibrosis in the Royal Free cohort. The figure shows the receiver operating characteristic curve of BIMAST score vs FIB-4 for predicting LSM≥ 8.1 kPa (Figure 3.10A) and LSM ≥12.1 kPa (Figure 3.10B) in the Royal Free cohort (n=218).
Abbreviations: FIB-4: fibrosis score-4, LSM: liver stiffness measurement.

3.3.8 The validation of the BIMAST score: the Sicilian cohort

Overall, the Sicilian cohort (n=168) was significantly younger (56 vs 61 years, p>0.0001) and showed higher median BMI (31.8 vs 30.4 kg/m^2, p=0.004) compared to the derivation cohort. In terms of blood tests, the Sicilian cohort presented significantly higher AST (38 vs 27 IU/L, p>0.0001)

and ALT (56 vs 30 IU/L, p<0.0001) and lower PLT (229 vs 243 x 10^9/uL, p=0.01) levels. Moreover, the patients from the Sicilian cohort had significantly higher LSM (11 vs 5.6 kPa, p>0.0001) compared to the primary care cohort (**Table 3.7**). When the patients were stratified per LSM cut-offs, the distribution of the Sicilian cohort was shifted towards high LSM ranges compared to the derivation cohort (**Figure 3.9**).

The Hosmer-Lemeshow test and the Brier score for the BIMAST score were 0.6 and 0.38, suggesting that the BIMAST score had a moderate goodness-of-fit and calibration in the Sicilian cohort. Specifically, the AUROC of BIMAST score for diagnosing LSM≥ 8.1 kPa (n=114) was 0.608 (95%CI: 0.5-0.71, p=0.037) vs 0.64 (0.54-0.74, p=0.006) FIB-4 (**Figure 3.11A**). The pairwise comparison between AUROC curves (De Long test) confirmed that FIB-4 (p=0.003) performed better than the BIMAST score in this cohort. With a cut-off of 0.063, the BIMAST score predicted the presence of LSM≥ 8.1 kPa with a sensitivity 27%, specificity 86%, PPV 83% and NPV 30%.

The AUROC of BIMAST score for diagnosing LSM≥ 12.1 kPa (n=65) was 0.602 (95%CI: 0.51-0.69, p=0.0001) vs 0.69 (95%CI: 0.609-0.77, p=0.0001) of FIB-4 (**Figure 3.11B**). The pairwise comparison between AUROC curves (De Long method) confirmed that FIB-4 performed better than the BIMAST score (p=0.0.01) in this cohort. With a cut-off of 0.102, the BIMAST score predicted the presence of LSM ≥ 12.1 kPa with sensitivity 20%, specificity 85%, PPV 48% and NPV 40%.

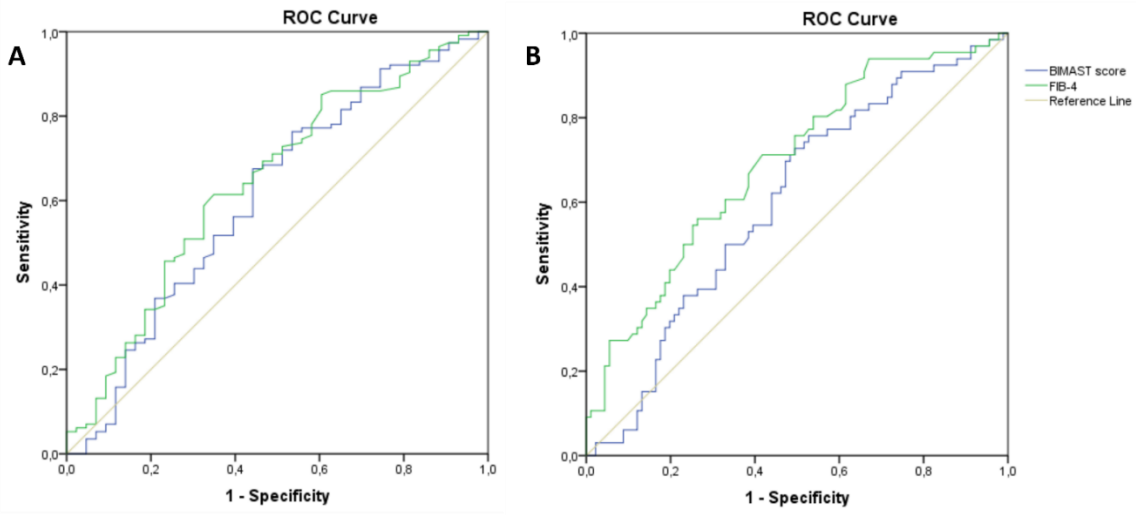

Figure 3.11. BIMAST score vs FIB-4 for predicting significant and advanced fibrosis in the Sicilian cohort. The figure shows the receiver operating characteristic curve of BIMAST score vs FIB-4 for predicting LSM≥ 8.1 kPa (Figure 3.11A) and LSM ≥12.1 kPa (Figure 3.11B) in the Sicilian cohort (n=168).
Abbreviations: LSM: liver stiffness measurement.

3.4 Discussion

Non-alcoholic fatty liver disease represents the leading cause of chronic liver disease worldwide and the commonest cause of abnormal liver function tests in the UK (Williams et al., 2014). In patients with NAFLD, T2DM represents an independent predictor of advanced fibrosis/cirrhosis and of more progressive disease (Hossain et al., 2009). Notably, in the UK, almost 4.9 million people are diagnosed with T2DM, while 13.5 million people are identified as being at increased risk for developing T2DM in the near future (source Diabetes UK). As such, a large number of diabetic patients is expected to develop significant liver disease in the next years with subsequent burden on the healthcare services (Younossi et al., 2019d).

Primary care clinicians play an essential role in identifying patients with NAFLD who are at risk of significant liver disease and may require further evaluation in a specialist setting. Specifically, managing NAFLD is perceived as a challenging task by the GPs in the UK (Sheridan et al., 2017) as well as worldwide (Younossi et al., 2021), mainly due to the lack of clarity around screening and referral/managing pathways. Moreover, diagnosing NAFLD in primary care currently relies on the presence and entity of abnormal LFTs, leaving a considerable proportion of those with significant liver disease with normal LFTs undiagnosed in the community (Blais et al., 2015). Interestingly, a recent study has shown that up to two/thirds of the new referral to NAFLD liver clinics are discharged once received their first assessment, confirming that current risk-stratification requires implementation (Elangovan et al., 2020).

Screening for significant NAFLD in the general population is still under debate, as there is still not enough evidence on cost-effective strategies. Moreover, the treatment options which could be offered to the patients are currently limited, as there is still no licensed treatment for the condition. A previous study simulating the use of pioglitazone as therapeutical option, concluded that screening for NAFLD was not cost-effective, as screening was dominated by the cost of treatment (Corey et al., 2016). However, this scenario could easily change in the next future, as new promising, well-tolerated agents may come to the market. Furthermore, more recent studies have suggested that

screening high-risk population with optimised algorithms may be highly cost-effective (Noureddin et al., 2020).

The most updated EASL guidelines recommend screening patients at risk for NAFLD using a 2-tiers system. FIB-4 should be tested in the first instance in primary care, followed by further assessment with TE in a specialist setting. Of note, the latest EASL guidelines also recommend referring patients with LSM≥8.1 kPa to specialist care, as this identifies those who are at moderate-high risk for significant liver disease (European Association for the Study of the Liver. Electronic address et al., 2021).

3.4.1 NAFLD is highly prevalent among diabetics in the community and significant fibrosis is associated with visceral obesity, AST and education attainment

The study population presented here is a cohort of patients with T2DM who were systematically screened for liver disease and NAFLD in the community. Specifically, these patients had their T2DM followed up in general practice and community clinics (Tier 1 and Tier 2 of the UK Diabetes levels of care(England, June 2018)), reflecting a true primary care without any *a priori* selection. This population also captures a wide range of antidiabetic treatments, comorbidities, ranges of glycaemic control and length of disease. Furthermore, this cohort is very diverse in terms of ethnic background, as this reflects the general population of a large urban city, such as London (**Table 3.1**).

In this cross-sectional study, the overall prevalence of NAFLD based on US was 64%, while the prevalence of other liver disease (mainly from BAFLD and HBV) was 9%. Interestingly, those with NAFLD had significantly higher BMI (31.4 vs 26.9 kg/m^2, p=0.0001) and had greater visceral adiposity (waist circumference, 108 vs 98 cm, p=0.0001) compared to diabetics without NAFLD. Moreover, patients with NAFLD tend to have higher LFTs and worse glycaemic control (HbA1c 60 vs 55 mmol/mol, p=0.0001) (**Table 3.1**). There was no difference in terms other diabetic features, such as diabetic complications, antidiabetic treatment and length of disease (**Table 3.1**). There was also no difference in terms of socio-economic status, as expressed as IMD (**Table 3.2**).

In the whole diabetic population, the prevalence of significant liver disease and cirrhosis secondary to NAFLD were 17% and 3% respectively. On a clinical perspective, patients with NAFLD and significant liver disease presented with greater visceral obesity (expressed as BMI, waist and hip circumferences), higher liver blood tests (ALT, AST and GGT) and worse diabetic control (HbA1c, glucose level and HOMA index) compared to those with NAFLD but without significant liver disease (normal LSM) (**Table 3.3**). In terms of socio-economic status, those with NAFLD and significant liver disease lived in more deprived neighbourhoods as per education attainment (education rank, 18789 vs 23148, p=0.03) (**Table 3.4**). Nevertheless, only waist circumference (crude OR 1.086, 95%CI: 1.021-1.154, p=0.008), BMI (crude OR 1.17, 95%CI: 1.008-1.358, p=0.04), AST (crude OR 1.071, 95%CI: 1.01-1.135, p=0.022) and education rank (crude OR 0.857, 95%CI 0.744-0.987) were associated with the presence of significant liver disease secondary to NAFLD on multivariate analysis (**Table 3.5**). Of note, glycaemic control did not emerge as a predictor for negative outcome in this population.

The prevalence of NAFLD reported here (64%) mirrors the results of a recent metanalysis by Younossi et al (Younossi et al., 2019b), where the pooled NAFLD prevalence was 68% (95%CI:62.1-73) among diabetics in the European countries. Interestingly, the prevalence of liver disease secondary to NAFLD described in current study population (17%) is higher compared to the one reported in the same metanalysis (4.8%, 95%CI: 0.00-17.46). It should be noted that a significant proportion of the studies included in (Younossi et al., 2019b) were derived from tertiary care. As such, the findings from the present work raise the concern on the potential large number of clinically relevant NAFLD cases which remain undetected in the community.

Another interesting finding from this cross-sectional study was that visceral obesity, rather than HbA1c, was strongly associated with significant liver disease due to NAFLD in the diabetes community. Notably, several studies have pointed out that being overweight/obese is a strong predictor for sub-optimal glycaemic control *per se* (Bae et al., 2016). As such, in these patients, visceral obesity may reflect an overall adverse “metabolic status” which includes the glycaemic

control. Moreover, it has been described that visceral adipose tissue plays a central role in promoting liver inflammation and fibrosis development (Du Plessis et al., 2013).

Another interesting finding was the correlation of education attainment, as defined by education rank from IMD, with significant liver disease in patients with diabetes (**Table 3.5**). Previous studies have demonstrated how education and health are entangled towards socio-economic status, health awareness and health behaviours/lifestyle (Chandola et al., 2006, Lleras-Muney, 2005). Specifically, inequalities in education have been strongly associated with poorer diet (Rippin et al., 2020) and obesity (Bernard et al., 2019). Furthermore, educational gradients were found to influence self-care activities, monitoring and glycaemic control in patients with T2DM in primary care (Silva-Tinoco et al., 2020). However, when interpreting these results, it should be noted that the IMD education rank is an area-specific rather than patient-specific measurement. As such, this parameter provides an overall snapshot of the average educational level from the area where the patient lives. These results, although preliminary, suggest that the average socio-cultural environment may be contributing to the severity of NAFLD in the general diabetic population. Educational status may be particularly relevant in a metabolic disorder which is strictly influenced by lifestyle pattern.

3.4.2 The BIMAST score predicts accurately the presence of significant and advanced fibrosis secondary to NAFLD, outperforming traditional screening strategies

The BIMAST score combines BMI and AST to predict the presence of significant and advanced fibrosis. In the derivation cohort (primary care), the BIMAST score predicted the presence of significant liver disease (LSM≥8.1 kPa) accurately, with an AUROC of 0.81 (95%CI 0.72-0.9, p>0.0001) and had excellent calibration and goodness-of-fit (Brier score and Hosmer-Lemeshow test) (**Figure 3.3A**). Moreover, with a cut-off of 0.063, the BIMAST score showed NPV 97%, making it a good test at *ruling out* the presence of liver disease. Furthermore, the BIMAST score predicted advanced fibrosis (LSM≥ 12.1 kPa) excellently, with an AUROC of 0.84 (95%CI 0.72-0.95, p=0.0001) (**Figure 3.3B**). The BIMAST score was then validated internally and predicted the presence of significant fibrosis and advanced fibrosis accurately, confirming a high NPV (**Figure 3.4A and 3.4B**). Moreover, in the whole diabetic population, the BIMAST score predicted significant and advanced

fibrosis better than other screening methods, such as US plus abnormal LFTs, FIB-4 and NAFLD fibrosis score (De Long method) (**Figure 3.5A and 3.5B)**. Notably, when applying the BIMAST score, the percentage of patients with significant fibrosis missed at screening was lower compared to the other screening strategies, such as FIB-4 and ultrasound plus LFTs (10 vs 38%).

3.4.3 The BIMAST score is validated externally, although the diagnostic performance is impacted by the spectrum effect

Ideally, new screening tests should be derived from a cohort which mirrors the target population for the test, so that spectrum biases could be minimised (Usher-Smith et al., 2016). From an epidemiological perspective, the *spectrum effect* describes the variation in the diagnostic performance of predictive tests when applied to populations with different disease prevalence. To current knowledge, the BIMAST score represents the first screening test which has been designed from a diabetic primary care population (low-prevalence disease). Conversely, the FIB-4 and NAFLD fibrosis score were previously derived from a tertiary care cohort (high-prevalence disease).

The BIMAST score was then tested and validated in two external cohorts of diabetic patients with NAFLD. Specifically, the Royal Free cohort was an intermediate care cohort of patients triaged from primary care based on either FIB-4>1.3 or ELF, while the Sicilian cohort was from a pure tertiary care setting. As such, these patients' phenotype was typical of those referred to specialist care, i.e. characterised by higher liver function tests and higher LSM values compared to the derivation cohort (**Table 3.7**). When tested in the Royal Free cohort, the BIMAST score's performance was lower but still acceptable (AUROC > 0.7) and performed similarly to the FIB-4 (**Figure 3.10**). Moreover, the BIMAST score showed a good calibration (Brier score) and a moderate goodness-of-fit (Hosmer-Lemeshow test) in this cohort. Conversely, the BMAST score performed poorly in the cohort from Sicily and was outperformed by FIB-4 (**Figure 3.11**). Secondary to the spectrum effect, there was also a typical decrease in the sensitivity and increase in the specificity, when the BIMAST score was applied to the external testing sets, with a switch from high NPV to high PPV (Usher-Smith et al., 2016). Nevertheless, calibration and goodness-of-fit tests, rather than AUROC curves alone, may provide more useful information when comparing different populations, as these tests reflect the

relationship between the predictive model and the population independently from the disease prevalence (Crossan et al., 2015). Notably, the BIMAST score showed a good calibration (Brier score) and a moderate goodness-of-fit as (Hosmer-Lemeshow test) in both the validation cohorts.

Overall, these results suggest that the BIMAST score and the FIB-4 are both victims of spectrum effect but in an opposite way. Specifically, the BIMAST score outperformed FIB-4 and the other screening methods in the primary care cohort (**Figure 3.5**), while the FIB-4 performed significantly better than the BIMAST score in the validation cohorts (**Figure 3.10 and 3.11**). According to the results of this study, applying FIB-4 with a cut-off of 1.3 in this population would miss up to 38% of the patients with significant liver disease. Specifically, age and LFTs level were the main factors behind the patients being misclassified as either low-risk or intermediate-high risk by FIB-4. These findings raise a specific concern that young patients with normal LFTs may be missed at screening with current screening pathways for NAFLD.

Engaging with primary care is crucial, as GPs are at the forefront for identifying patients with NAFLD in need for further evaluation. Of note, several studies have highlighted the importance of increasing the awareness for diagnosing and managing NAFLD among the primary care providers (Sheridan et al., 2017, Younossi et al., 2021). There is need for a simple, pragmatical referral/management pathway which performs well in primary care and that could be easily implemented by the GPs. In this sense, the BIMAST score represents an accurate, easy-to-use option that could be calculated by the clinicians without any additional test, and therefore cost, to standard of care.

3.5 Strengths and limitations

This part of the study has many strengths. Firstly, I describe a population of consecutive, well phenotyped patients from diabetes primary care without any *a priori* selection. All patients underwent systematic screening for NAFLD and other liver disease, allowing for an accurate estimation of the prevalence of NAFLD and clinically significant fibrosis. Secondly, this population is diverse in terms of ethnicity and characteristics of diabetes mirroring the diversity of the population in North-West

London, making the results potentially significant on a larger scale. Furthermore, the here-presented BIMAST score is so far the first score developed directly from primary care based on the risk factors associated with NAFLD with significant fibrosis. The BIMAST score is accurate, easy-to-use and does not carry any additional cost or test from a GP perspective.

The current study presents some limitations. Firstly, the number of liver biopsies obtained from this cohort was low, whereas histology is considered the gold standard for staging NAFLD and for validating non-invasive markers. Unfortunately, the number of elective procedures carried out in the study had been significantly impacted by the restrictions put in place as a response to the COVID-19 pandemic. Nevertheless, we chose LSM ≥ 8.1 kPa and 12.1 kPa secondary to NAFLD as the main endpoints of the study, as these identify significant and advanced fibrosis respectively and a reason for referral to specialist care. Secondly, it might be argued that elevated BMI and AST may falsely increase LSM. However, BMI is also a well-known factor associated with liver disease severity and this cannot be easily disentangled from the analysis. In terms of liver function tests, the majority of patients from the derivation cohort had AST well below 100 IU/L, as such a flare in transaminases was unlikely associated with false positives on LSM in this cohort. Finally, another limitation of the BIMAST score may be that AST is currently not part of the standard LFTs panel in many areas of the UK.

3.6 Future work

Future work is required to validate the BIMAST in an external cohort of diabetic patients in primary care. It would be also of interest to test the BIMAST score in a non-diabetic population, as this could increase the applicability of the score on a GP perspective. Finally, further research should focus on comparing the cost-effectiveness of applying BIMAST score vs conventional screening techniques in the diabetes community.

3.7 Conclusions

To summarise, in this study, the prevalence of NAFLD was 64%, while the prevalence of significant liver disease secondary to NAFLD was 17% in a cohort of diabetics from primary care.

The BIMAST score is the first score which has been developed in primary care and has been validated both internally and externally. Such score is accurate and easy-to-use from a GP perspective. Moreover, the BIMAST score outperformed conventional screening methods, such as FIB-4 and NAFLD fibrosis score, in the community and demonstrated a reduction in false negatives, which could be missed at screening to date. Furthermore, these results suggest that a risk-stratification based on FIB-4 may leave liver disease undetected in young patients with normal LFTs. Further work is required to validate the BIMAST score in an external primary care cohort and to establish the cost-effectiveness to support its use in clinical practice.

4. ANALYSIS OF METABOLIC PROFILE AND GUT MICROBIOTA IN DIABETIC PATIENTS SCREENED FOR NAFLD

4.1 Introduction

Considerable advances have been made in understanding the role of metabolomics and gut microbiota in the pathogenesis of NAFLD (Younes and Bugianesi, 2019). Despite the increasing incidence of NAFLD worldwide and the endeavours made in drug development, there is still no licensed treatment at present. In this sense, the analysis of metabolomics and gut microbiome may provide new potential therapeutical targets for treating the disease, along with new insights into the pathogenesis of the disease.

The term “gut-liver axis” refers to the bidirectional relationship between the gut and the liver, resulting from the interactions between diet, microbiome, genetic and environmental factors (Albillos et al., 2020). Several studies have shown how gut microbiome could modulate the body response to diet and calories intake, as well as regulate the availability of nutrients. Specifically, the intestinal microbiome could influence the host metabolism through the release of specific substances, such as SCFA, LPS and peptides, as well as thought the modulation of the pool of BAs (Arslan, 2014). There is growing evidence suggesting that a reduced microbiome diversity as well as a increased *Firmicutes* to *Bacteroides* ratio is associated with the presence of hepatic steatosis and NASH (Grabherr et al., 2019). Moreover, results from preliminary studies involving administration of probiotics or FMT have proved effective in improving hepatic fat content as well as metabolic profile in patients with NAFLD.

Moreover, metabolomic techniques have been widely employed to elucidate the role of small metabolites and metabolic products in the development and progression of NAFLD (Dumas et al., 2014). It is well known that the metabolism of AA is strictly linked to hepatic synthetic function but it is also known that metabolic disturbances may occur with IR and metabolic syndrome. Of note, a number of studies published in the field have focused on differences between NASH and simple steatosis. However, it would be clinically important to explore the presence of specific gut microbiota

changes and metabolic profiles with regards to liver fibrosis, as this represents the main prognostic factor in these patients.

Therefore, the main objectives of this part of the project were:

- to compare the metabolic profile and gut microbiome between diabetics with normal liver vs diabetics with NAFLD and different liver disease severity, all confounders included

- to compare the metabolic profile and gut microbiome between diabetics with normal liver vs diabetics with NAFLD and different liver disease severity, correcting for metabolic risk factors

- to compare the metabolic profile and gut microbiome between diabetics with and without NAFLD, correcting for metabolic risk factors

4.2 Materials and methods

4.2.1 Study population and sample collection

Serum and urine samples were collected on the same day the clinical assessment and after 3 hours of fasting. Stool samples were collected within one week from the clinical assessment and delivered within 3 hours from being produced. There was no specific dietary restriction or recommendation before collecting the faecal samples, while stool from patients who had received antibiotic treatment for the previous 2 weeks were excluded from the analysis. Samples were collected, processed and stored as per SOP.

4.2.2 Metabolic profiling and gut microbiota analysis

In this study, targeted and untargeted metabolic profile was carried out in serum, urine and faecal extracts using NMR (Gratton et al., 2016, Beckonert et al., 2007), while bile acid profile was obtained from serum and faecal extracts using UPLC-MS (Sarafian et al., 2015, Mullish et al., 2018). NMR and UPLCS were performed at the MRC-NHR National Phenome centre, Imperial College London, UK. Gut microbiome was analysed in stool samples by 16s rRNA gene sequencing.

The full list of metabolites detected by NMR in the biological samples for this study is provided in **Table 4.1.,** while the full list of bile acids detected by UPLC-MS in the biological samples of this study is provided in **Table 4.2.**

NMR		
Serum	Urine	Faecal water
2-Aminobutyric acid	1-Methylhistidine	Acetic acid
2-Hydroxybutyric acid	1-Methylnicotineamide	Alanine
2-Oxoglutaric acid	2-Methylsuccinic acid	Butyric acid
3-Hydroxybutyric acid	2-Oxoglutaric acid	Ethanol
Acetic acid	3-Hydroxybutiric acid	Formic acid
Acetoacetic acid	4-Aminobutyric acid	Fumaric acid
Acetone	Acetic acid	Glutamic acid
Alanine	Acetoacetic acid	Glycine
Asparagine	Acetone	Isoleucine
Ca-EDTA	Adenosin	Leucine
Choline	Alanine	N-Methylamine
Citric acid	Allantoin	N-Trimethylamine (TMA)
Creatine	Allopurinol	Nicotinic acid
Creatinine	Arginine	Phenylacetate
D-Galactose	Benzoic acid	Propionic acid
Dimethylsulfone	Betaine	Succinic acid
Ethanol	Caffeine	Tyrosine
Formic acid	Citric acid	Uracil
Glucose	Creatine	Valine
Glutamic acid	Creatinine	Valeric acid
Glutamine	D-Galactose	
Glycerol	D-Glucose	
Glycine	D-Lactose	
Histidine	D-Mandelic acid	
Isoleucine	D-Mannitol	
K-EDTA	D-Mannose	
Lactic acid	Dimethylamine	
Leucine	Formic acid	
Lysine	Fumaric acid	
Methionine	Guanidinoacetic acid	
N, N-Dimethylglycine	Glycine	
Ornithine	Hippuric acid	
Phenylalanine	Imidazole	
Proline	Inosine	
Pyruvic acid	Lactic acid	
Sarcosine	Methionine	
Succinic acid	Myo-Inositol	
Threonine	N, N-Dimethylglycine	
Trimethylamine-N-oxide	Oxaloacetic acid	
Tyrosine	Proline betaine	
Valine	Pyruvic acid	
	Sarcosine	
	Succinic acid	
	Tartaric acid	
	Taurine	
	Trigonellin	
	Trimethylamine	
	Valine	

Table 4.1 Metabolites detected using Nuclear Magnetic Resonance in the biological samples from current study.

Liquid chromatography - Mass spectrometry		
Serum	Stool	
3-Ketocholanic Acid	23-Norcholic Acid	Glycocholic Acid
3-alpha-Hydroxy-7 Ketolithocholic Acid	3-Ketocholanic Acid	Glycodeoxycholic Acid
5-beta-Cholanic Acid-3-beta, 12-alpha-diol	3-alpha-Hydroxy-7 Ketolithocholic Acid	Glycodeoxycholic Acid-3-Sulfate
5-beta-Cholanic Acid 12-alpha-ol-3-one	3-alpha-Hydroxy-7,12-Diketocholanic Acid	Glycolithocholic Acid
5-Cholenic Acid-3-beta-ol	3-alpha-Hydroxy-12 Ketolithocholic Acid	Glycolithocholic Acid-3-Sulfate
12-Dehydrocholic Acid|7-Dehydrocholic Acid	3-alpha,12-alpha, 23-Nordeoxycholic Acid	Glycoursodeoxycholic Acid
Chenodeoxycholic Acid	3-Dehydrocholic Acid	Glycoursodeoxycholic Acid-3-Sulfate
Cholic acid|Ursocholic acid	3,6-Diketocholanic Acid| 3,12-Diketocholanic Acid	Hyocholic acid
Deoxycholic Acid	5-alpha-Cholanic Acid-3-one	Hyodeoxycholic Acid
Deoxycholic Acid-3-Sulfate	5-alpha-Cholanic Acid-3-alpha-ol-6-one	Isolithocholic Acid
Glycochenodeoxycholic Acid	5-beta-Cholanic Acid-3-alpha, 6-alpha-diol-7-one	Isoallolithocholic Acid
Glycochenodeoxycholic Acid-3-Sulfate	5-beta-Cholanic Acid-3-beta, 12-alpha-diol	Lithocholic Acid
Glycocholic Acid	5-beta-Cholanic Acid 12-alpha-ol-3-one	Lithocholic Acid 3-Sulfate
Glycodeoxycholic Acid	5-Cholenic Acid-3-beta-ol	Murocholic Acid
Glycodeoxycholic Acid-3-Sulfate	5-beta-Cholenic Acid-7-alpha-ol-3-one	Taurocholic Acid
Glycolithocholic Acid	6-Oxolithocholic Acid	Taurolithocholic Acid
Glycolithocholic Acid-3-Sulfate	7-Dehydrocholic Acid	Taurochenodeoxycholic Acid
Glycoursodeoxycholic Acid	8(14),(5-beta)-Cholenic Acid-3-alpha, 12-alpha-diol	Taurochenodeoxycholic Acid-3-Sulfate
Glycoursodeoxycholic Acid-3-Sulfate	9(11), (5-beta)-Cholenic Acid-3-alpha-ol-12-one	Taurodeoxycholic Acid
Isolithocholic Acid	Alpha Muricholic Acid	Taurodeoxycholic Acid-3-Sulfate
Lithocholic Acid	Beta Muricholic Acid	Taurohyocholic Acid
Lithocholic Acid 3-Sulfate	Chenodeoxycholic Acid	Taurocholic Acid-3-Sulfate
Murocholic Acid	Chenodeoxycholic Acid-3-Sulfate	Tauro omega-Muricholic Acid
Taurocholic Acid	Cholic Acid-3-Sulfate	Tauroursodeoxycholic Acid
Taurolithocholic Acid	Cholic Acid 7-Sulfate	Ursodeoxycholic Acid
Taurochenodeoxycholic Acid	Cholic acid|Ursocholic acid	Ursodeoxycholic Acid-3-Sulfate
Taurodeoxycholic Acid	Deoxycholic Acid	
Tauro omega-Muricholic Acid	Deoxycholic Acid-3-Sulfate	
Ursodeoxycholic Acid	Glycochenodeoxycholic Acid	

Table 4.2 Bile acids detected with UP-LCMS in the biological samples from current study.

4.2.3 Histological assessment and image analysis

Metabolic profile was then compared against liver histology. As liver biopsies from the present study were limited in number, a group of serum samples matched with liver biopsies were included from the cohort of patients followed-up in the specialist NAFLD clinic, based at St Mary's Hospital, Imperial college NHS Trust, London, UK. Metabolic profile was analysed in serum samples from this population using NMR, while liver histology was assessed using NASH CRN scoring system and automated quantitation of histological features (Forlano et al., 2020).

4.2.4 Statistical analysis and regulatory approval

The data table obtained as output from NMR and UPLCMS were introduced to SIMCA v 14.1 (MKS Umetrics AB), with UPLCMS data were pareto-scaled. A principal component analysis (PCA) was performed so that clustering of the samples could be visualised in a unsupervised fashion. Afterwards, a supervised analysis, called orthogonal projections to latent structures discriminant analysis (OPLS-DA), was carried out to demonstrate the features responsible for the discrimination between two groups. OPLS-DA models were validated using cross-validated residuals ANOVA (CV-ANOVA) (Eriksson et al., 2000), while S-plots were used to visualise the most-influential features discriminating the groups which are typically located at the far ends of the plot (Wiklund et al., 2008). Heatmap were produced based on R Pearson coefficient of bile acids against microbial abundances and reporting with a false discovery rate 10% threshold. More complex modelling was performed on Software R, using linear regression analysis with mixed effect model. Differences between groups were adjusted with post-hoc Benjamini test and values were reported with a 10% significance threshold.

4.3 Results

4.3.1 Patient samples

From a total of the 300 patients enrolled in the study, 254 serum samples, 254 urine samples and 98 stool samples were collected. Among the serum and urine samples, 67 (26%) were obtained

from patients with normal liver, 124 (48%) from those with NAFLD and normal LSM, while 37 (14%) from those with NAFLD and elevated LSM. The 26 (10%) samples from patients with other liver diseases (BAFLD or HBV) were excluded from this analysis.

Among the stool samples, 17 (17%) were from patients with normal liver, 54 (55%) from those with NAFLD and normal LSM, while 17 (17%) from those with NAFLD and elevated LSM. There were also 9 (9%) samples from patients with other liver diseases (BAFLD and HBV), which were also excluded from this analysis.

4.3.2 Statistical models

4.3.2.1 Analysis of the metabolic profile and gut microbiome in the whole cohort

This analysis was carried out in the whole study population, with no correction applied, so that all possible (metabolic and non-metabolic) confounders could be included. The main study groups were normal liver, NAFLD with normal LSM and NAFLD with elevated LSM.

4.3.2.2 Analysis of the metabolic profile and gut microbiome in matched sub-populations

In a sub-analysis, patients with NAFLD were matched for metabolic factors, such as BMI, glucose, insulin, HbA1c and HOMA index. The purpose of this analysis was to identify differences between patients with NAFLD and elevated LSM (n=10) vs those with normal liver (n=20). The resulting differences would be independent of metabolic risk factors and, therefore, highly specific for the presence of significant liver fibrosis (elevated LSM).

In a subsequent sub-analysis, patients were matched for metabolic factors, such as BMI, total cholesterol, LDL, HDL, HOMA, insulin level, HbA1c, and for severity of liver disease, as expressed as LSM. The purpose of this analysis was to identify differences between patients with NAFLD (n=12) vs those with normal liver (n=18). The resulting differences would be independent of metabolic risk factors and LSM and, therefore, specific for the presence of NAFLD.

4.3.3 Serum metabolic profile

In the whole population, those with NAFLD and elevated LSM (n=37) had significantly higher levels of serum 3-hydroxybutyric acid, acetone, citric acid, phenylalanine, pyruvic acid, lactic acid, glutamic acid and glucose, and significantly lower levels of glycine and glutamine compared to those with normal liver (n=67) (**Figure 4.1**). On OPLS-DA model (supervised, multivariate analysis), low levels of glycine and glutamine with increased glucose and glutamate could separate those with NAFLD (n=158) vs those with normal liver (n=67) accurately (CV-ANOVA, p=0.002) (**Figure 4.2**). Decreased glutamine and elevated glutamate were able to separate those with NAFLD and elevated LSM vs those with NAFLD and normal LSM accurately (CV-ANOVA, p<0.0001) (**Figure 4.4**). Similarly, reduced glutamine and increased glutamate could distinguish those with NAFLD and elevated LSM vs those with normal liver accurately (CV-ANOVA, p<0.0001) (**Figure 4.3**). When patients with NAFLD (n=158) were stratified according to cut-offs of LSM of 8.1 kPa (significant fibrosis) and 12.1 kPa (advanced fibrosis), there was a significant decrease in serum glycine and an increase in glutamate/glutamine across the groups (**Figure 4.5**). Moreover, the AUROC of glutamate/glutamine for predicting LSM >8.1 kPa (significant fibrosis) was 0.74 (95%CI: 0.65-0.82, p=0.002), while the AUROC for predicting LSM >12.1 kPa was 0.78 (95%CI: 0.68-0.88, p=0.004) in the whole population (**Figure 4.6**).

When metabolites were analysed against clinical features, glycine was not associated with metabolic factors, such as waist circumference (p=0.48), BMI (p=0.22), HbA1c (p=0.78) or HOMA index (p=0.26). However, glycine showed significant inverse correlation with liver markers, such as CAP score (Rho= -0.15 p=0.23), AST (Rho= -0.24, p=0.001) and ALT (Rho= -0.12, p=0.05). Conversely, glutamate/glutamine showed a significant positive correlation with metabolic factors, such as waist circumference (Rho=0.14, p=0.014), BMI (Rho=0.18, p=0.), HOMA (Rho=0.38, p=0.0001) and HbA1c (Rho=0.19, p=0.003). There was also a significant association between glutamate/glutamine ratio with AST (Rho=0.19, p=0.003), ALT (Rho=0.16, p=0.013) and CAP score (Rho=0.27, p=0.0001).

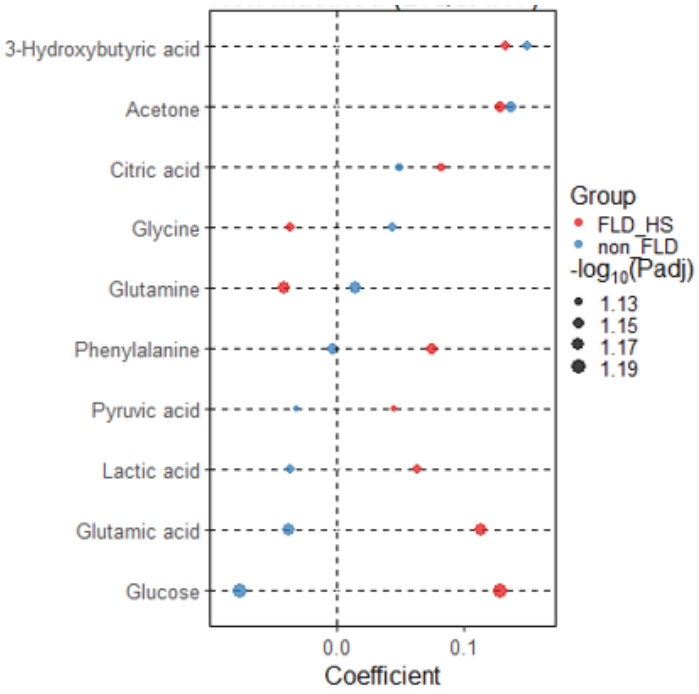

Figure 4.1. Differences in serum metabolites between those with NAFLD and elevated LSM vs normal liver in the whole population. This coefficient plot shows coefficient values of linear regression analysis for single metabolites and their distribution in the two comparison groups: NAFLD with elevated LSM (n=37) vs normal liver (n=67). Coefficients located to the right of the reference line (line 0.0) are positive, while coefficients locate to the left of the reference line are negative. Coefficients for the group NAFLD with elevated LSM are highlighted in red, while those for the group normal liver are highlighted in blue. The size of the coefficient refers to the $-\log_{10}$ (adjusted p-value).
Abbreviations: NAFLD: non-alcoholic fatty liver disease, LSM: liver stiffness measurement.

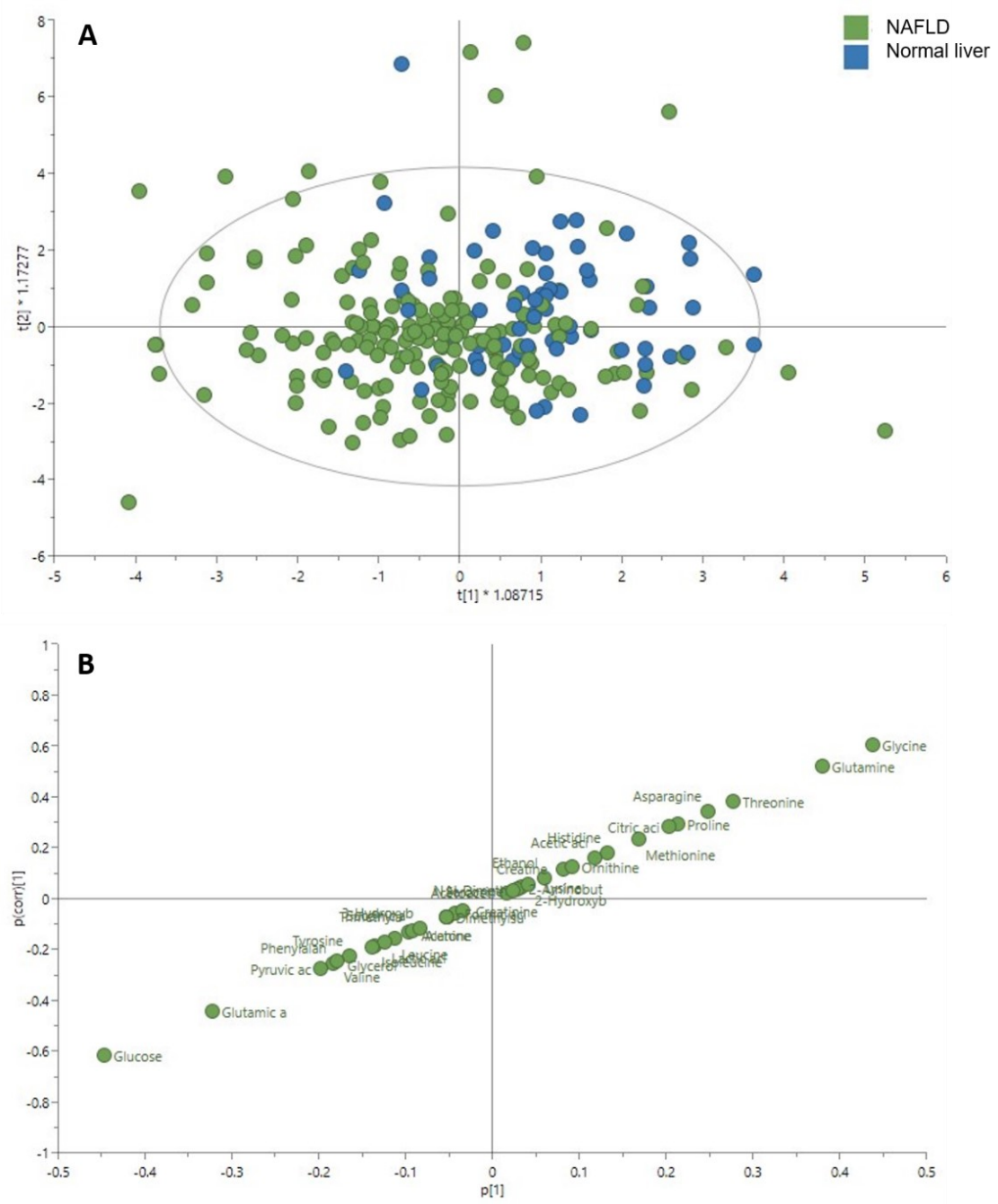

Figure 4.2. Multivariate model (OPLS-DA) showing differences in serum metabolites between those with NAFLD vs those with normal liver in the whole population. Figure 2A shows a scatter plot of the derived OPLS-DA model between NAFLD (n=161) vs normal liver (n=67). There is small overlap between those with NAFLD (green) vs those with normal liver (dark blue), meaning that the model was good at separating the groups. **Figure 2B** shows a S-plot which highlights the distribution of the metabolites compared to the group normal liver. Metabolites increased in the group normal liver are located at the top end (glycine and glutamine), while those decreased in the group normal liver are located at the bottom end (glucose and glutamic acid).

Abbreviations: OPLS-DA: Orthogonal Projections to Latent Structures Discriminant Analysis, NAFLD: non-alcoholic fatty liver disease, LSM: liver stiffness measurement.

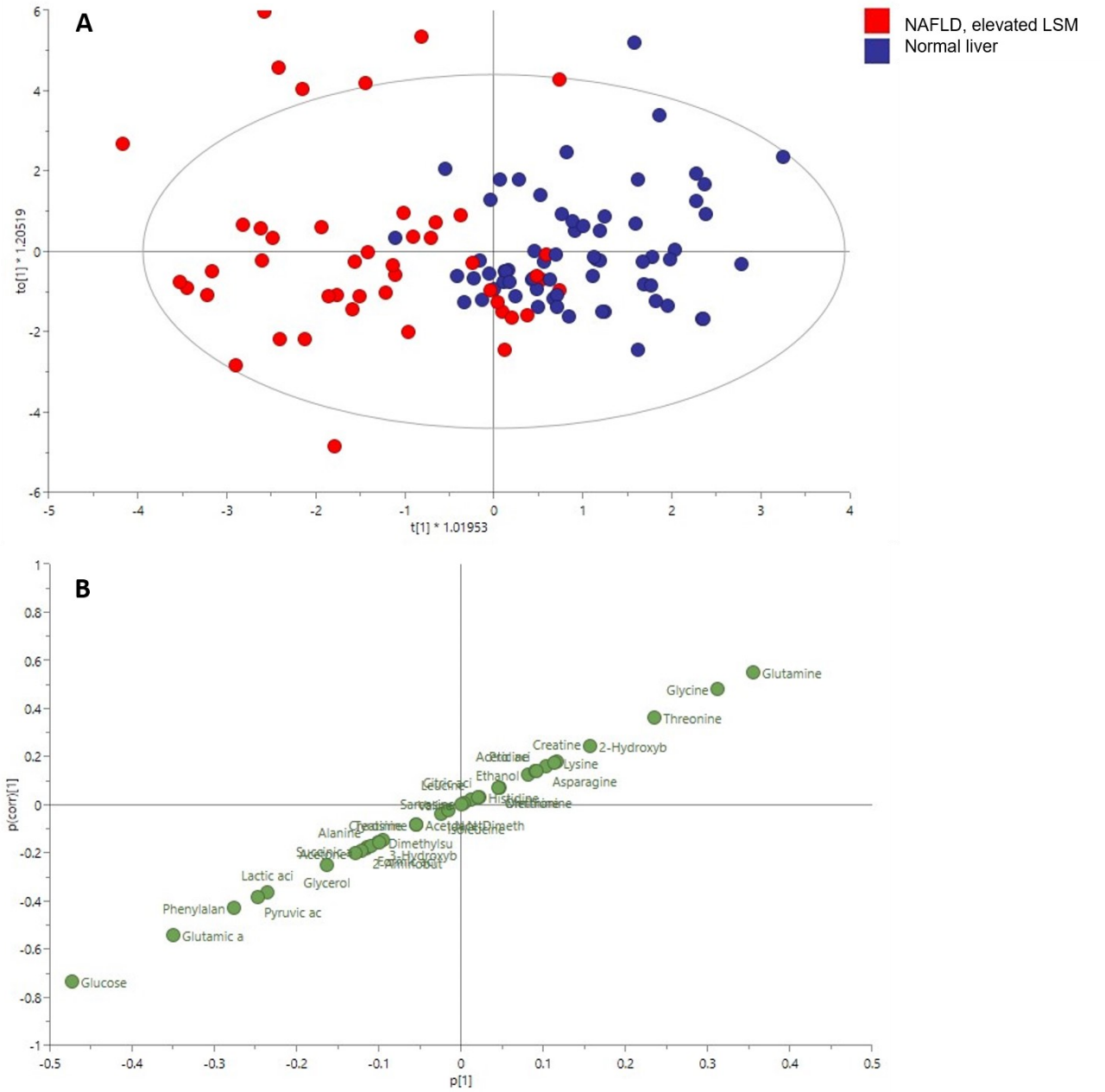

Figure 4.3. Multivariate model (OPLS-DA) showing differences in serum metabolites between NAFLD and elevated LSM vs normal liver in the whole population. Figure 3A shows a scatter plot of the derived OPLS-DA model between NAFLD and elevated LSM (n=37) vs normal liver (n=67). There is small overlap between those with NAFLD and elevated LSM (red) vs those with normal liver (dark blue), meaning that the model was good at separating the groups. **Figure 3B** shows a S-plot which highlights the distribution of the metabolites compared to the group normal liver. Metabolites increased in the group normal liver are located at the top right (glutamine and glycine), while those decreased in the group normal liver are located at the bottom left (glucose and glutamic acid).
Abbreviations: OPLS-DA: Orthogonal Projections to Latent Structures Discriminant Analysis, NAFLD: non-alcoholic fatty liver disease, LSM: liver stiffness measurement.

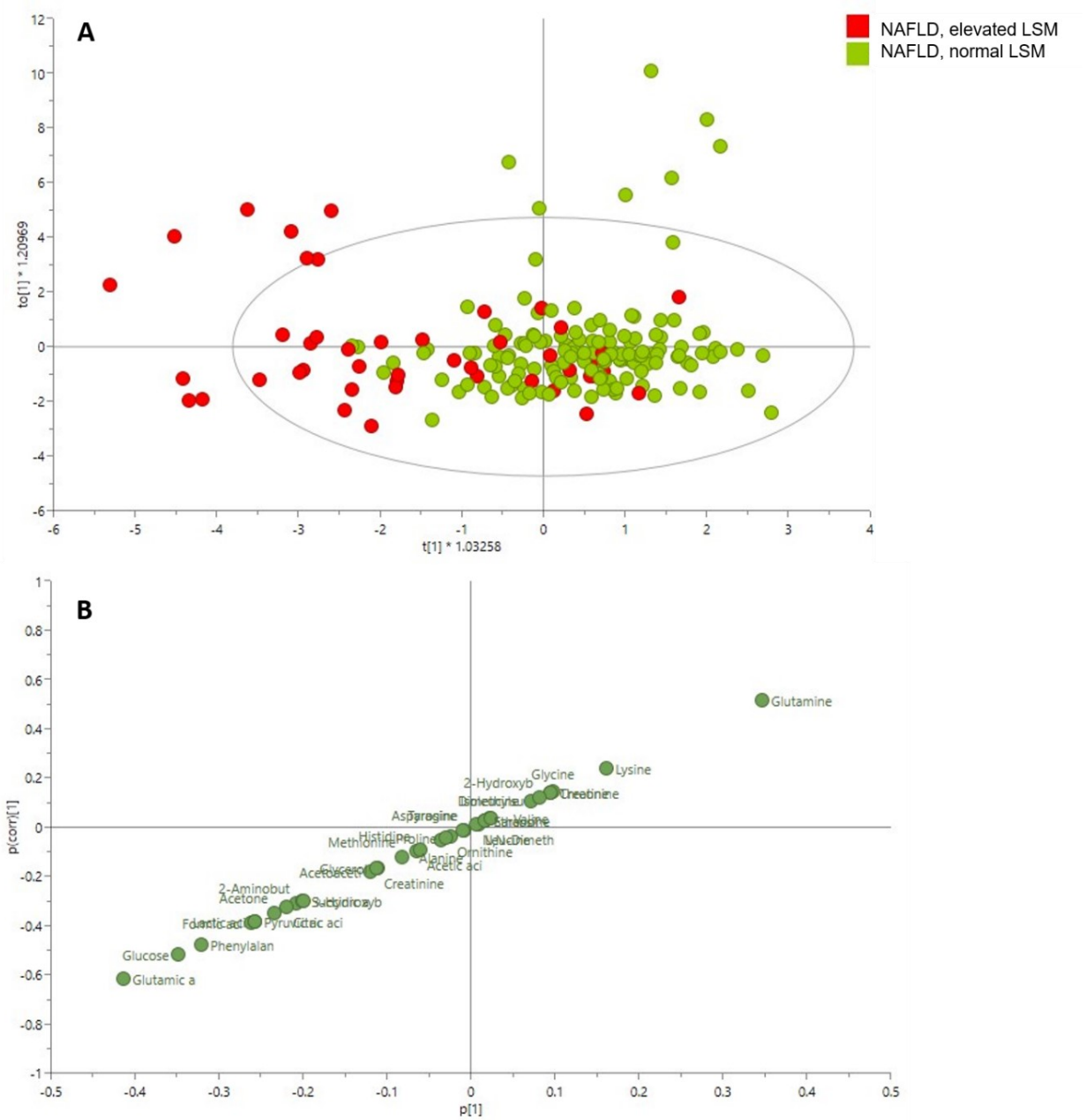

Figure 4.4. Multivariate model (OPLS-DA) showing differences in serum metabolites between NAFLD and elevated LSM vs NAFLD and normal LSM in the whole population. Figure 4A shows a scatter plot of the derived OPLS-DA model between NAFLD and elevated LSM (n=37) vs NAFLD and normal LSM (n=124). There is small overlap between those with NAFLD and elevated LSM (red) vs those with NAFLD and normal LSM (green), meaning that the model was good at separating the groups. **Figure 4B** shows a S-plot which highlights the distribution of the metabolites compared to the group NAFLD with normal LSM. Metabolites increased in the groups NAFLD with normal LSM are located at the top end (lysine and glutamine), while those decreased in the group NAFLD with normal LSM are located at the bottom end (glucose and glutamic acid).
Abbreviations: OPLS-DA: Orthogonal Projections to Latent Structures Discriminant Analysis, NAFLD: non-alcoholic fatty liver disease, LSM: liver stiffness measurement.

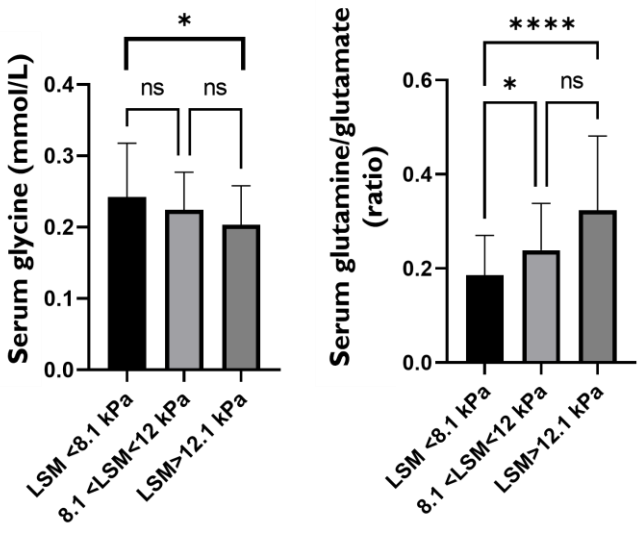

Figure 4.5. Serum glycine and glutamate to glutamine ratio in patients with NAFLD stratified per liver stiffness measurements. Figure 5A is a bar chart illustrating levels of serum glycine expressed as median with 95%CI. Figure 5A is a bar chart illustrating levels of serum glutamate to glutamine ratio expressed as median with 95%CI.
Abbreviations: LSM: liver stiffness measurement, 95%CI: 95% confidence interval.

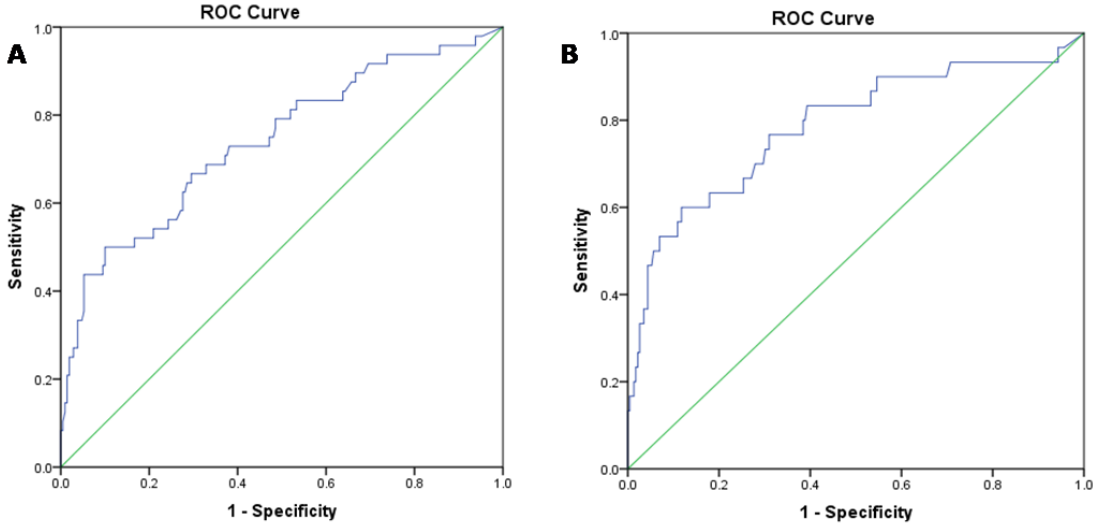

Figure 4.6. ROC curves of glutamate to glycine ratio for predicting the presence of significant and advanced fibrosis from NAFLD in the whole population. Figure 4.6A shows the AUROC for glutamate/glutamine for predicting LSM ≥8.1 kPa (significant fibrosis), while Figure 4.6B shows the AUROC for glutamate/glutamine for predicting LSM ≥12.1 kPa (advanced fibrosis) in the whole population (n=254).
Abbreviations: NAFLD: non-alcoholic fatty liver disease. ROC: Receiver operating characteristic curve, LSM: liver stiffness measurement.

When patients were matched for metabolic factors, those with NAFLD and elevated LSM showed significantly higher levels of serum lysine compared to those with normal liver (**Figure 4.7**). In this sub-analysis, there was no difference in terms of glycine, glutamine and glutamate between the groups.

Finally, when patients were matched for metabolic factors and LSM, there was no difference in terms of serum metabolites between those with NAFLD and normal liver. In this sub-analysis, there was no difference in glycine, glutamine and glutamate levels between the groups.

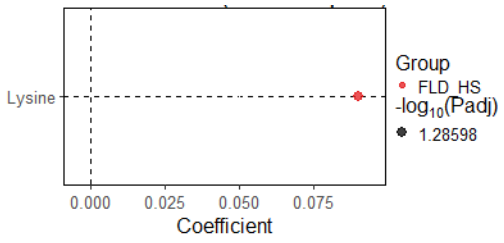

Figure 4.7. Differences in serum lysine between those with NAFLD and elevated LDM vs those with normal liver, matched for metabolic risk factors. This coefficient plot shows coefficient values of regression analysis for lysine and distribution within two groups: NAFLD with elevated LSM (n=10) vs normal liver (n=20). Coefficients located to the right of the reference line (line 0.0) are positive, while coefficients locate to the left of the reference line are negative. Coefficients for the group NAFLD and normal LSM are highlighted in blue, while those for the group normal liver are highlighted in red. The size of the coefficient refers to the $-\log_{10}$ (adjusted p-value).
Abbreviations: NAFLD: non-alcoholic fatty liver disease, LSM: liver stiffness measurement.

4.3.4 Serum and faecal bile acid profile

In the whole population, those with NAFLD and elevated LSM showed significantly higher levels of taurocholic acid, glycoursodeoxycholic acid-3-sulfate and glychochenodeoxycholic acid-3-sulfate (GCDA-3S) compared to those with normal liver (**Figure 4.8** and **Figure 4.9**).

When patients were matched for metabolic risk factors, only GCDA-3S remained significantly higher in those with NAFLD and elevated LSM compared to those with normal liver (**Figure 4.10**).

Finally, when patients were matched for metabolic factors and LSM, those with NAFLD presented significantly higher levels of glycolithocholic acid, isolithocholic acid, taurolithocholic acid, 3-ketocholanic acid, 3-alpha-hydroxy-12 ketolithocholic acid and lithocholic acid compared to those with normal liver. Moreover, those with NAFLD had significantly lower levels of GCDA-3S, murcholic acid, glycoursodeoxycholic acid and glycoursodeoxycholic acid-3-sulfate (**Figure 4.11** and **4.12**).

There was no significant difference in terms of faecal bile acids profile across study groups in all the analyses.

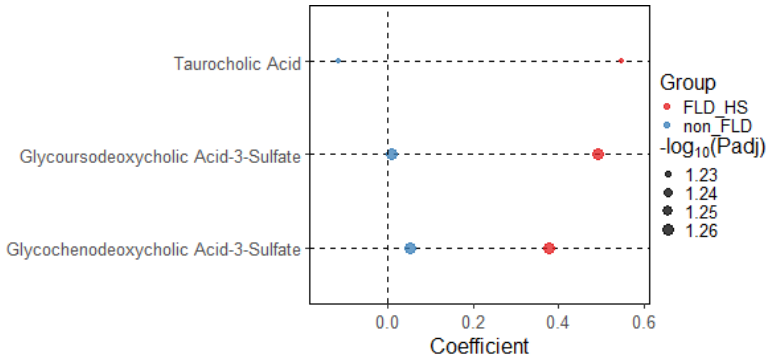

Figure 4.8. Differences in serum bile acid profile between those with NAFLD and elevated LDM vs those with normal liver, in the whole population. This coefficient plot shows coefficient values of linear regression for metabolites and their distribution within two groups: NAFLD with elevated LSM (n=37) vs normal liver (n=67). Coefficients located to the right of the reference line (line 0.0) are positive, while coefficients locate to the left of the reference line are negative. Coefficients for the group NAFLD with elevated LSM are highlighted in red, while those for the group normal liver are highlighted in blue. The size of the coefficient refers to the -$\log_{10}$ (adjusted p-value).
Abbreviations: NAFLD: non-alcoholic fatty liver disease, LSM: liver stiffness measurement.

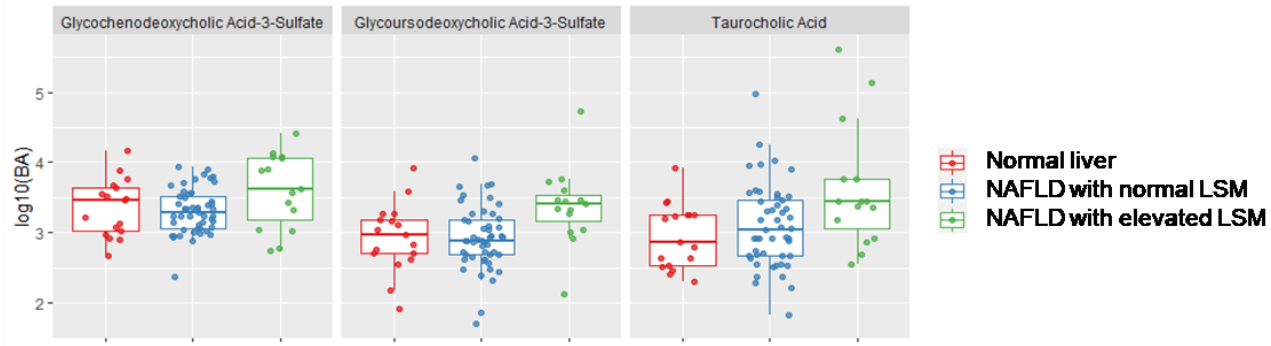

Figure 4.9. Differences between study groups for serum bile acid profile in the whole population. This box plot shows individual values with relative median and 95%CI for glycochenodeoxycholic acid-3 sulfate, glycoursodeoxucholic acid 3-sulfate and taurocholic acid in three study groups: those with NAFLD and elevated LSM (n=37), NAFLD and normal LSM (n=124) and normal liver (n=67).
Abbreviations: NAFLD: non-alcoholic fatty liver disease, LSM: liver stiffness measurement.

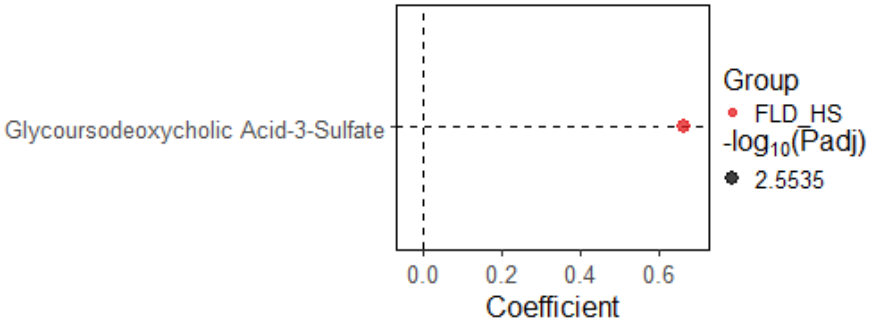

Figure 4.10. Differences in serum bile acid between those with NAFLD and elevated LSM vs those with normal liver, matched for metabolic risk factors. This coefficient plot shows coefficiens values of linear

regression for glycoursodeoxycholic acid-3 sulfate and its distribution in two groups: NAFLD with elevated LSM (n=10) vs normal liver (n=20). Coefficients located to the right of the reference line (line 0.0) are positive, while coefficients locate to the left of the reference line are negative. Coefficients for the group NAFLD and elevated LSM are highlighted in red. The size of the coefficient refers to the -$\log_{10}$ (adjusted p-value)
Abbreviations: NAFLD: non-alcoholic fatty liver disease, LSM: liver stiffness measurement.

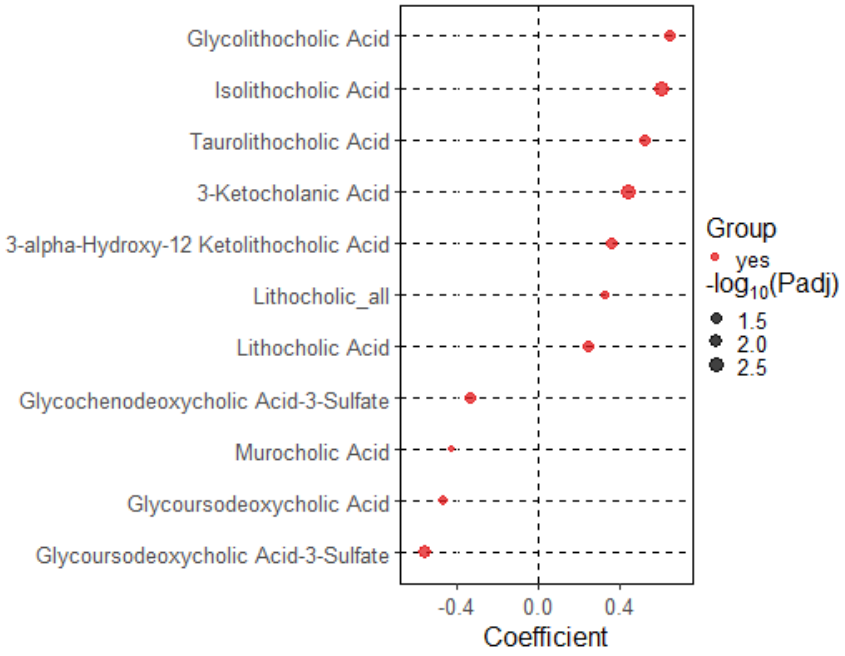

Figure 4.11. Differences in serum bile acid between those with NAFLD vs those with normal liver, matched for metabolic risk factors and LSM. This coefficient plot shows coefficients values of linear regression for bile acids and their distribution within two groups: NAFLD (n=12) vs normal liver (n=18). Coefficients located to the right of the reference line (line 0.0) are positive, while coefficients locate to the left of the reference line are negative. Coefficients for the group NAFLD are highlighted in red. The size of the coefficient refers to the -$\log_{10}$ (adjusted p-value)
Abbreviations: NAFLD: non-alcoholic fatty liver disease, LSM: liver stiffness measurement.

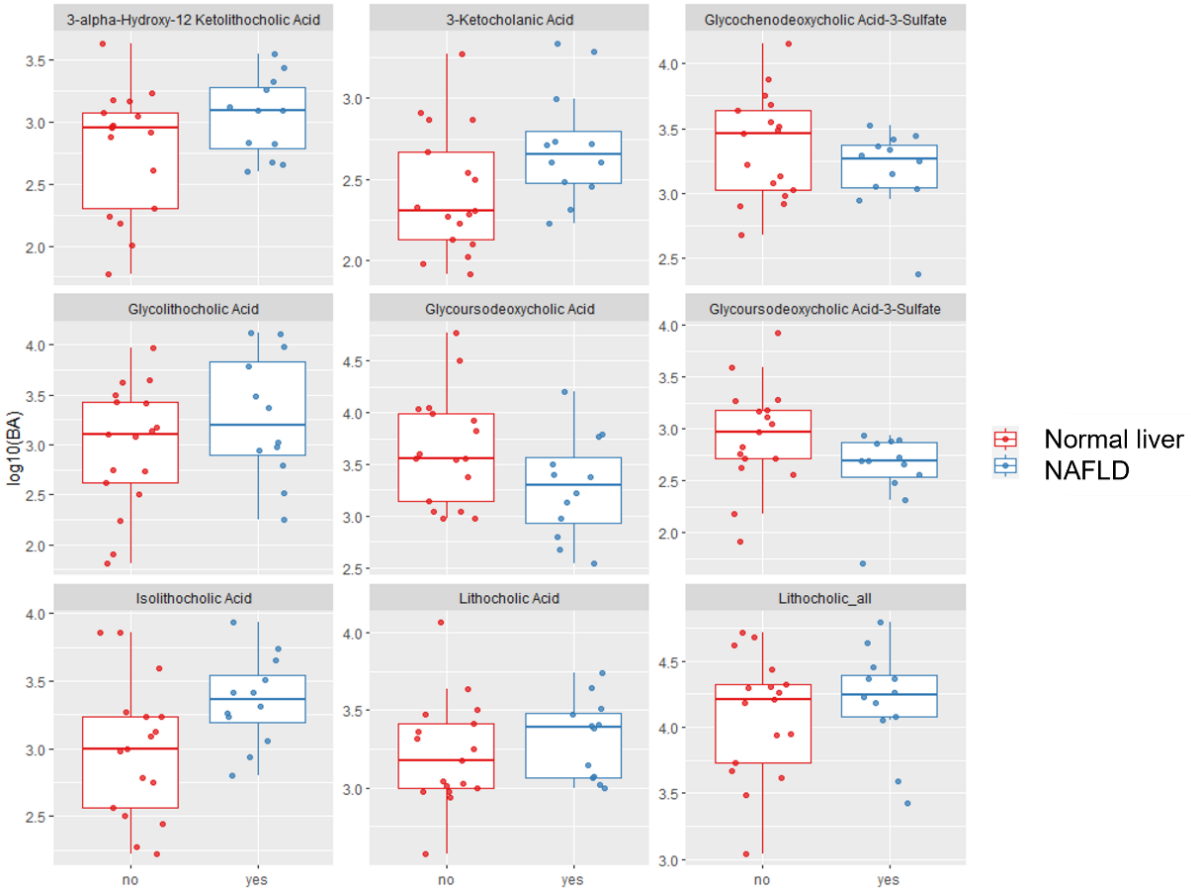

Figure 4.12. Distribution of serum bile acid in those with NAFLD vs those with normal liver, matched for metabolic risk factors and LSM. This box plot shows individual values with relative median and 95%CI of serum bile acids in those with NAFLD (n=12) vs normal liver (n=18). The variable lithocholic all includes all lithocholic derived bile acids.
Abbreviations: NAFLD: non-alcoholic fatty liver disease, LSM: liver stiffness measurement, 95%CI: 95% confidence interval.

4.3.5 Urinary metabolic profile

In the whole population, patients with NAFLD and elevated LSM presented significantly higher levels of alanine, valine, citric acid and creatinine compared to those with normal liver (**Figure 4.13**). No valid OPLS-DA model based on urinary metabolites could separate those with normal liver vs NAFLD (CV-ANOVA, p=0.23), NAFLD with elevated LSM vs normal liver (CV-ANOVA, p=0.72) and NAFLD with elevated LSM vs NAFLD and normal LSM (CV-ANOVA, p=0.45).

When urinary metabolites were analysed against clinical features, urinary alanine and valine levels were significantly associated with HOMA index (Rho= 0.24, p=0.001 and Rho=0.17, p=0.021) and HbA1c (Rho=0.15, p=0.02 and Rho=0.16, p=0.015). Similarly, citric acid and creatinine were significantly associated with HbA1c (Rho=0.203, p=0.002 and Rho=0.12, p=0.05) but not with HOMA

(p=0.82 and p=0.43). There was no association between urinary alanine, valine, citric acid and creatinine with liver markers (AST, ALT, LSM and CAP score).

On a similar note, when patients were matched for metabolic factors, there was no difference in urinary metabolic profile between NAFLD and elevated LDM vs normal liver. Similarly, there was no difference in urinary metabolic profile between NAFLD and normal liver when patients were matched for metabolic factors and LSM.

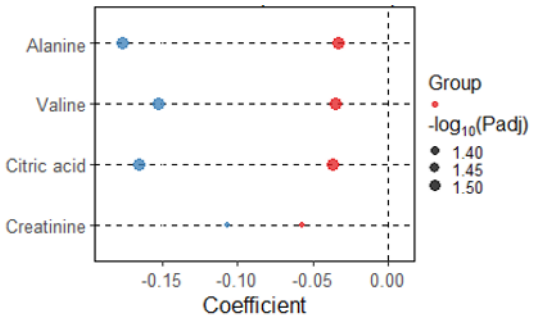

Figure 4.13. Differences in urinary metabolites between those with NAFLD and elevated LDM vs those with normal liver, in the whole population. This coefficient plot shows coefficients values of linear regression for metabolites in two groups: NAFLD with elevated LSM (n=37) vs normal liver (n=67). Coefficients located to the right of the reference line (line 0.0) are positive, while coefficients locate to the left of the reference line are negative. Coefficients for the group normal liver are highlighted in blue, while those for the group NAFLD with elevated LSM are highlighted in red. The size of the coefficient refers to the $-\log_{10}$ (adjusted p-value)
Abbreviations: NAFLD: non-alcoholic fatty liver disease, LSM: liver stiffness measurement.

4.3.6 Faecal metabolic profile

In the whole population, there was no significant difference between the groups in terms of faecal metabolic profile. Specifically, there was no difference in terms of tryptophane metabolites (**Figure 4.14**) and SCFA. When patients were matched for metabolic factors, those with NAFLD and elevated LSM showed significantly lower faecal glycine compared to those with normal liver (**Figure 4.15**). Finally, when patients were matched for metabolic factors and LSM, there was no difference between those with NAFLD vs normal liver.

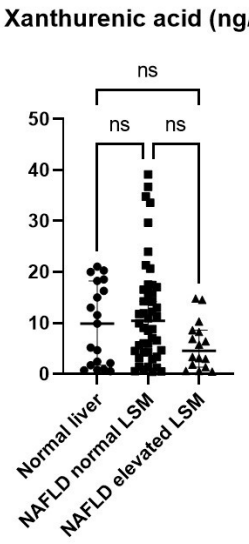
Xanthurenic acid (ng/ml)
ns
ns
ns
50
40
30
20
10
0
Normal liver
NAFLD normal LSM
NAFLD elevated LSM

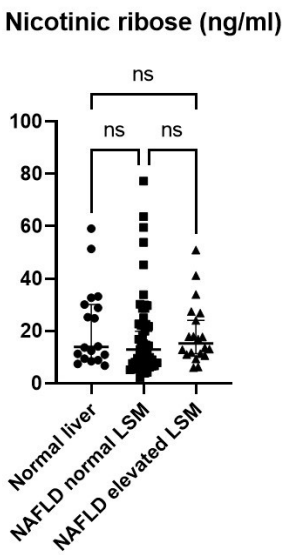
Nicotinic ribose (ng/ml)
ns
ns
ns
100
80
60
40
20
0
Normal liver
NAFLD normal LSM
NAFLD elevated LSM

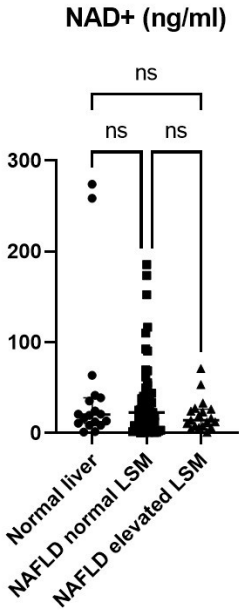
NAD+ (ng/ml)
ns
ns
ns
300
200
100
0
Normal liver
NAFLD normal LSM
NAFLD elevated LSM

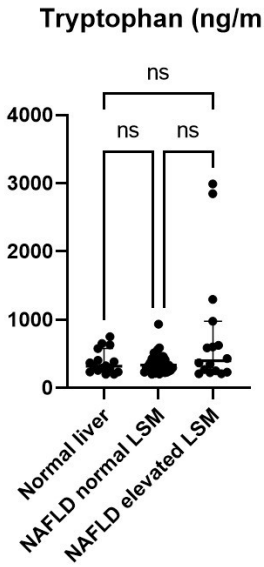
Tryptophan (ng/ml)
ns
ns
ns
4000
3000
2000
1000
0
Normal liver
NAFLD normal LSM
NAFLD elevated LSM

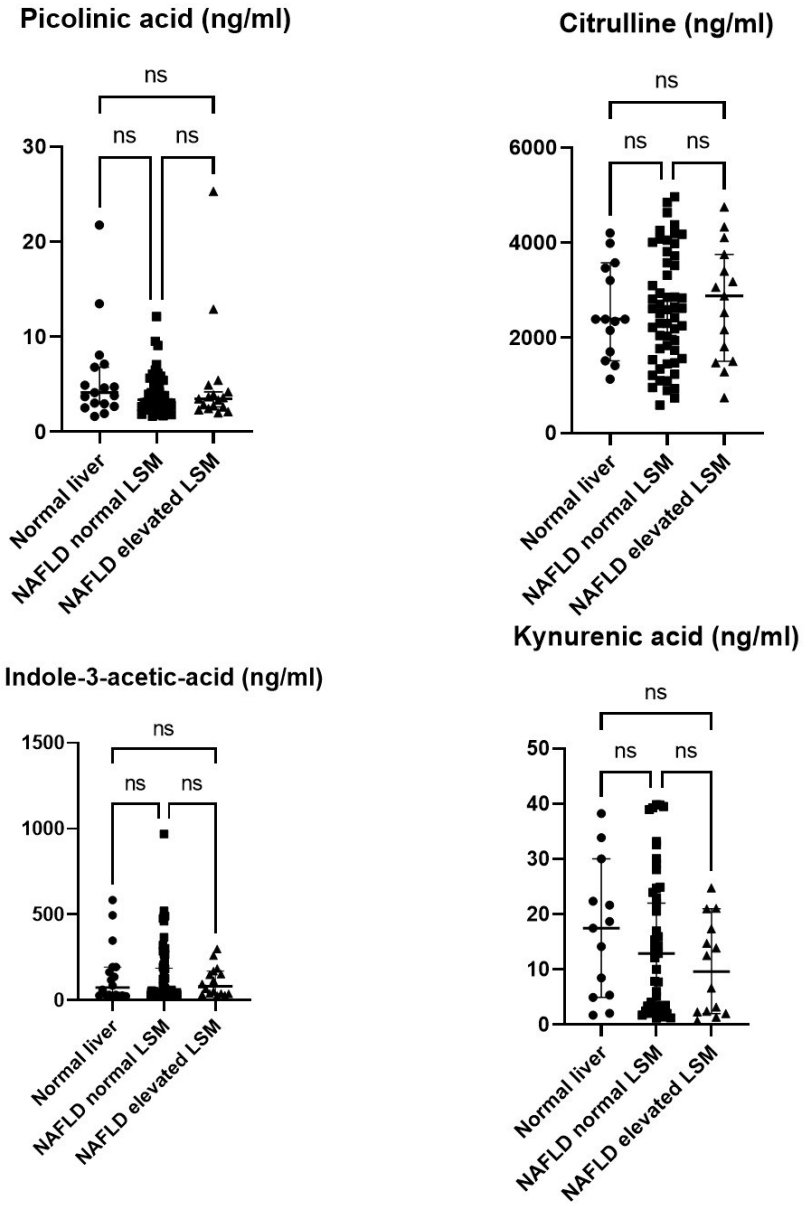

Figure 4.14. Differences in faecal tryptophan metabolites between study groups. This figure includes scatter dots showing single values of metabolites, together with associated median and 95%CI. P-values refer to differences between the study groups: NAFLD and elevated LSM (n=17), NAFLD and normal LSM (n=54) and normal liver (n=17).
Abbreviations: NAFLD: non-alcoholic fatty liver disease, LSM: liver stiffness measurement, 95%CI: 95% confidence interval.

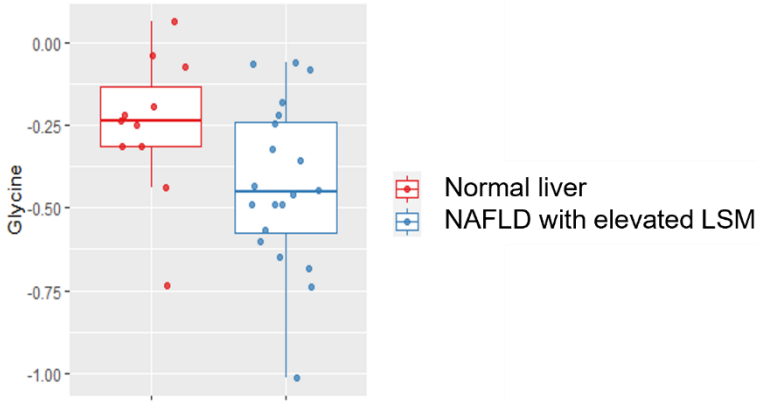

Figure 4.15. Difference in faecal glycine between NAFLD with elevated LSM vs normal liver, matched for metabolic factors. This box plot shows individual values with relative median and 95%CI for faecal glycine comparing those with NAFLD and elevated LSM (n=10) vs normal liver (n=20).
Abbreviations: NAFLD: non-alcoholic fatty liver disease, LSM: liver stiffness measurement, 95%CI: 95% confidence interval.

4.3.7 Microbiome profiling

In the whole population, on a phylum level, *Proteobacteria* and *Firmicutes* were relatively more abundant, while *Bacteroidetes* (*Bacteroidota*) less abundant in those with NAFLD and elevated LSM compared to those with normal liver (**Figure 4.16A**). On a lower level (order level), *Anaeroplasma* and *Escherichia/Shigella* were significantly less abundant in those with NAFLD and elevated LSM compared to those with normal liver (**Figure 4.16B**).

When patients were matched for metabolic factors, on a phylum level, *Bacteroidetes* were less abundant in those with NAFD and elevated LSM compared to those with normal liver. On a lower level (order level), *Monoglobus* was significantly less abundant in those with NAFLD and elevated LSM compared to those with NAFLD and normal LSM (**Figure 4.17**).

Finally, when patients were matched for metabolic factors and LSM, *Verrucomicrobiales* were more abundant in those with NAFLD compared to those without (phylum level). On a lower level (order level) *Faecalibacterium* genus, *Veillonella* genus, *Subdoligranulum* genus, *Rikenella* genus and *Coprobacter* genus were significantly more abundant in those with NAFLD compared to those with normal liver. Conversely, *Bacteroides* genus, *Escherichia/Shigella* genus and *Prevotella* genus were significantly more abundant in those with normal liver compared to those with NAFLD (**Figure 4.18**).

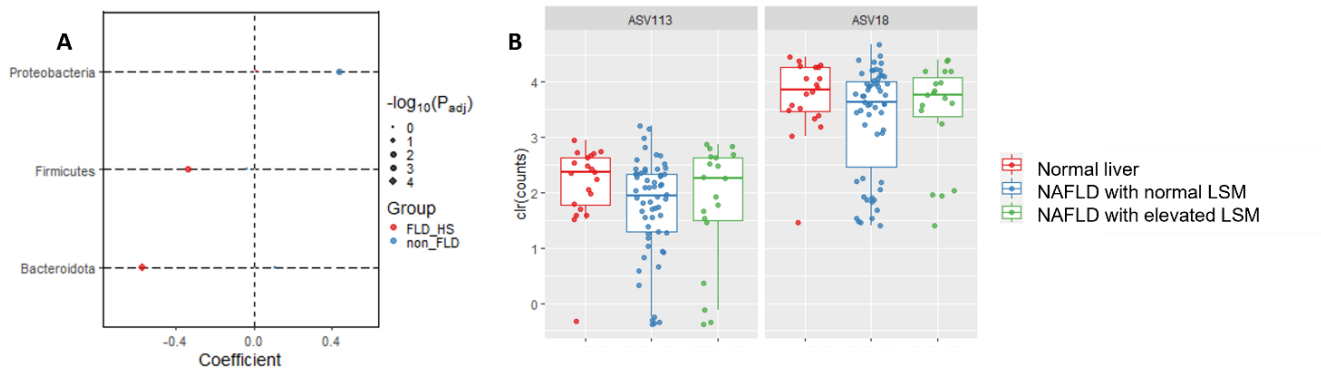

Figure 4.16. Differences in gut microbiome between different study groups in the whole population. Figure 4.16A) This coefficient plot shows coefficients values of linear regression for relative abundance (phylum level) between two groups: NAFLD with elevated LSM (n=17) vs normal liver (n=17). Coefficients located to the right of the reference line (line 0.0) are positive, while coefficients locate to the left of the reference line are negative. Coefficients for the group NAFLD with elevated LSM are highlighted in red, while those for the group normal liver are highlighted in blue. The size of the coefficient refers to the -$\log_{10}$ (adjusted p-value) Figure 4.16B) This box plot shows individual values with relative median and 95%CI for *Anaeroplasma* genus (ASV113) and *Escherichia/Shigella* genus (ASV18) (order level).
Abbreviations: NAFLD: non-alcoholic fatty liver disease, LSM: liver stiffness measurement, 95%CI: 95% confidence interval.

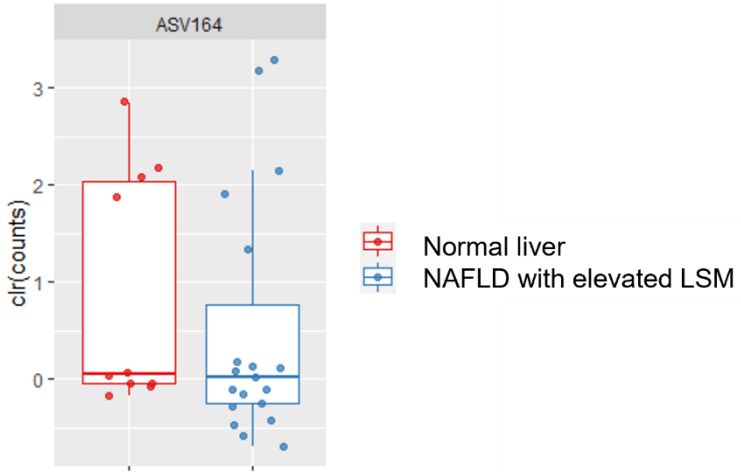

Figure 4.17. Difference in relative abundance of *Monoglobus genus* between NAFLD with elevated LSM vs normal liver, matched for metabolic factors. This box plot shows individual values with relative median and 95%CI for *Monoglobus genus* (ASV164) and difference between NAFLD with elevated LSM (n=17) and normal liver (n=17).
Abbreviations: NAFLD: non-alcoholic fatty liver disease, LSM: liver stiffness measurement, 95%CI: 95% confidence interval.

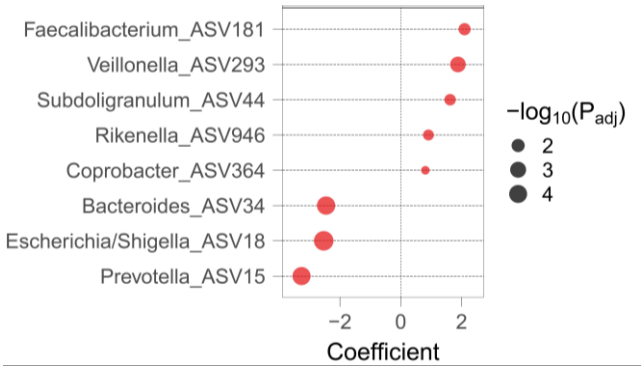

Figure 4.18. Difference in relative abundance of genus between patients with NAFLD vs those with normal liver, matched for metabolic factors and LSM. This coefficient plot shows coefficients of linear regression for specific genus and their relative abundance compared to the reference group (NAFLD with elevated LSM). Coefficient located to the right of the reference line are more abundant in the reference group, while those located to the left are less abundant in the reference group. The size of the coefficient refers to the -$\log_{10}$ (adjusted p-value).
Abbreviations: NAFLD: non-alcoholic fatty liver disease, LSM: liver stiffness measurement.

4.3.8 Faecal bile acids and gut microbiota composition

In the whole population, the association between faecal BA and the composition of microbiome was analysed on different taxonomic levels, from ASV to family level. Of note, although there was no difference in terms of levels of faecal BA across study groups (**paragraph 4.3.6**), some BA were significantly influenced by microbiome composition.

Overall, glycine-conjugated BA were relatively lower in stool of patients with higher abundance of *Firmicutes* (*Tuzerella*) and *Verrucomicrobiales* (Akkermansiacee). Moreover, sulphated BAs (cholic acid-7-sulfate, cholic acid-3-sulfate, deoxycholic acid-3-sulfate, chenodeoxycholic acid-3-sulfate) and lithocolic acid-3-sulfate were elevated in stool samples of patients enriched with *Firmicutes* (**Figure 4.19**).

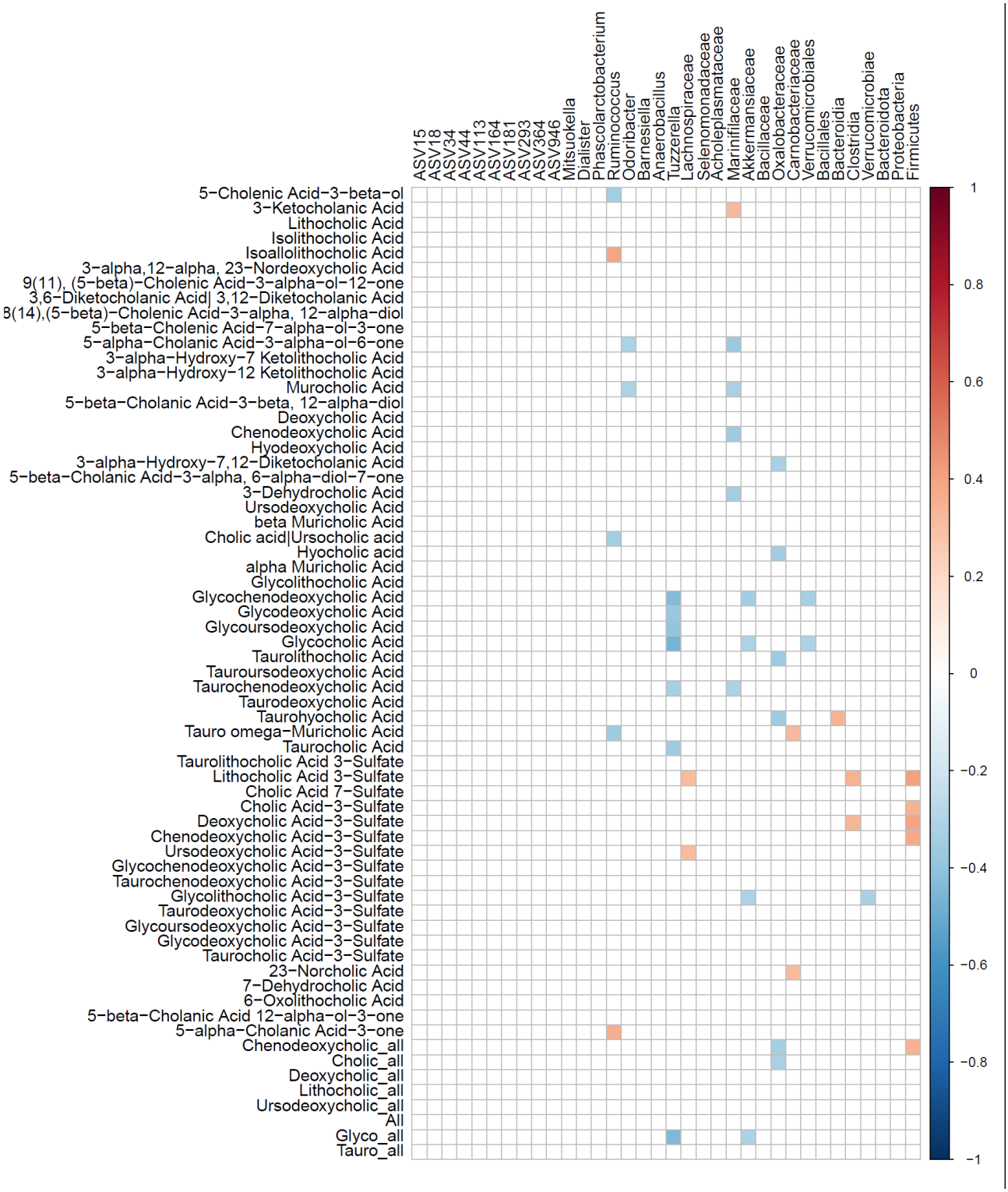

Figure 4.19. Faecal bile acids against microbiome composition. This figure shows a correlation heatmap based on the R Pearson coefficients between faecal bile acids concentration and relative microbial abundances, analysed from ASV to family level. A positive effect is highlighted in red, while a negative effect in blue.

4.3.9 Serum metabolic profile of patients from NAFLD clinic

In this study, 59 serum samples from patients followed up in liver clinic (tertiary care), based at St Mary's Hospital, were included in the analysis in an attempt to analyse metabolic profile against histology. Overall, this population had a median age of 48 (38-57) years, BMI 29.8 (28-32.4) kg/m^2, AST (36-61) IU/L and ALT 75 (48-106) IU/L. Of note, 28 (47%) patients had T2DM, while median HbA1c was 43 (36-53) mmol/mol (**Table 4.3**). Histology, expressed as NASH CRN scoring system as well as automated quantitation, is displayed in **Table 4.4**. Overall, 25 (41%) patients had advanced fibrosis (F≥3), while 18 (31%) had definite NASH (NAS≥5).

When metabolic profile was analysed against quantitative features, glycine showed an inverse, linear relationship with fat% (R^2=0.35, p=0.006) and steatosis grade (R^2=0.25, p=0.05) (**Figure 4.20**). However, there was no association between glycine and inflammation%, ballooning% or collagen. Interestingly, there was no significant association between glutamate/glutamine and histological features, specifically with regards to fibrosis stage and collagen (**Figure 4.21**). Finally, serum lysine showed a significant, inverse association with collagen (R^2=0.37, p=0.008) but not with fibrosis stage, as per NASH CRN scoring system (R^2=0.15, p=0.18) (**Figure 4.22**). There was no association between lysine and steatosis, inflammation or ballooning.

NAFLD liver clinic (N=59)			
	Median (IQR)		**N (%)**
Age, *years*	48 (38-57)	**Male gender**	42 (71)
BMI, kg/m^2	29.8 (28-32.4)	**White, Caucasian**	19 (32)
ALT, *IU/L*	75 (48-106)	**White, Hispanic**	6 (10)
AST, *IU/L*	46 (36-61)	**Black African, Afro-Caribbean**	3 (5)
GGT, *IU/L*	54 (35-97)	**Arab**	4 (7)
Total Cholesterol, *mmol/l*	4.7 (4-5.3)	**South Asian**	19 (33)
TRG, *mmol/l*	1.7 (1.2-2.8)	**Unknown ethnicity**	8 (14)
HDL, *mmol/l*	1.01 (0.8-1.2)	**T2DM**	28 (47)
LDL, *mmol/l*	2.8 (1.9-3.6)	**Hypertension**	17 (29)
Ferritin, *ng/ml*	206 (87-307)	**Dyslipidaemia**	21 (36)
HbA1c, *mmol/mol*	43 (36-53)		
LSM, *kPa*	9.4 (6.7-13.5)		
CAP score, *dB/m*	334 (299-367)		

Table 4.3 Clinical characteristics of the population from the NAFLD liver clinic. The table shows the clinical characteristics of the patients from the NAFLD liver clinic. Variables are expressed as median and IQR or relative percentages.
Abbreviations: IQR: interquartile range, BMI: Body mass index, ALT: alanine aminotransferase, AST: aspartate aminotransferase, GGT: gamma-glutamyl transferase, TRG: triglycerides, HDL: high density lipoprotein, LDL: low density lipoprotein, HbA1c: glycated haemoglobin, T2DM: type-2 diabetes mellitus.

NAFLD liver clinic (N=59)					
	N (%)	**Median fat% (IQR)**		**N (%)**	**Median CPA (IQR)**
Steatosis grade			**Fibrosis stage**		
Mild	16 (27)	7 (3-15)	Stage 1	15 (25)	2.7 (1.6-3.6)
Moderate	30 (51)	15 (7-10)	Stage 2	19 (32)	2.9 (1.7-4.3)
Severe	13 (22)	22 (12-25)	Stage 3	21 (35)	5.2 (4.3-6.9)
			Stage 4	4 (6)	16.1 (13-19.4)
Lobular Inflammation	**N (%)**	**Median inflammation% (IQR)**			
Absent	3 (5)	0.5 (0.5-1.8)			
In < 2 foci	51 (86)	1.2 (0.49-2.2)			
2-4 foci	5 (8)	1.5 (0.73.1)			
3- 4 foci	0 (0)	-			
Hepatocellular ballooning	**N (%)**	**Median ballooning% (IQR)**			
Absent	9 (15)	8.9 (6.2-9.6)			
Few cells	36 (61)	29.2 (16-40.7)			
Many cells	14 (28)	34.2 (16.9-39.3)			

Table 4.4 Histological characteristics of the population from the NAFLD liver clinic. The table shows the histological characteristics of the patients from the NAFLD liver clinic. The table also shows correspondent median fat%, inflammation%, ballooning% and CPA to NASH CRN scores. Stage 1 of the NASH CRN scoring system includes 1a, 1b and 1c. Variables are expressed as median and IQR or relative percentages.
Abbreviations: NAFLD: non-alcoholic fatty liver disease, IQR: interquartile range, CPA: collagen proportionate area.

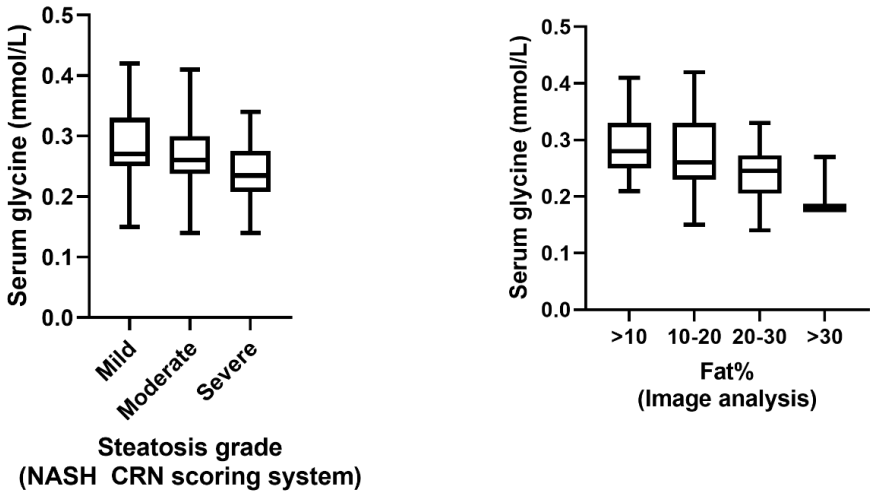

Figure 4.20. Distribution of serum glycine against steatosis grade and fat% categories. This box plot illustrates median values of serum glycine and relative 95%CI. Steatosis grade was assigned as per NASH CRN scoring system, while Fat% was measured using image analysis on images of liver biopsies stained in H&E (n=59).
Abbreviations: 95%CI: 95% confidence interval, NASH CRN scoring system: NASH clinical research network scoring system, H&E: Haematoxylin and eosin.

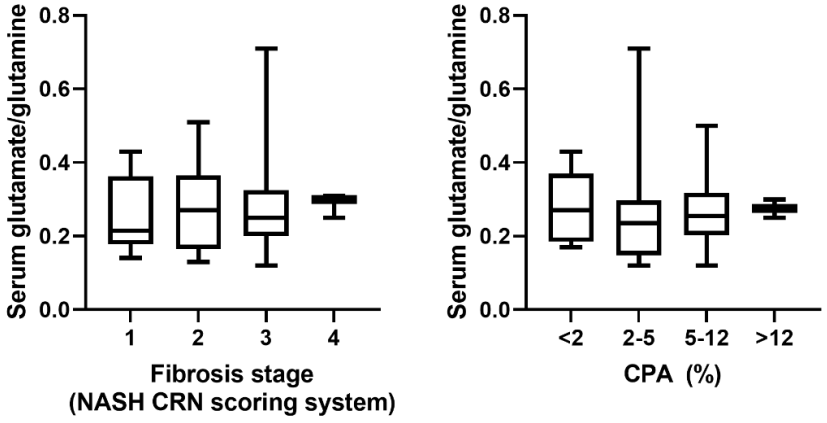

Figure 4.21. Distribution of serum glutamate to glutamine ratio across fibrosis stage and CPA categories. This box plot illustrates median values of glutamate/glutamine and relative 95%CI. Fibrosis stage was assigned as per NASH CRN scoring system, while CPA was measured using image analysis on images of liver biopsies stained in Sirius Red (n=59). Fibrosis 1 includes fibrosis stage 1a, 1b and 1c.
Abbreviations: 95%CI: 95% confidence interval, NASH CRN scoring system: NASH clinical research network scoring system, CPA: collagen proportionate area.

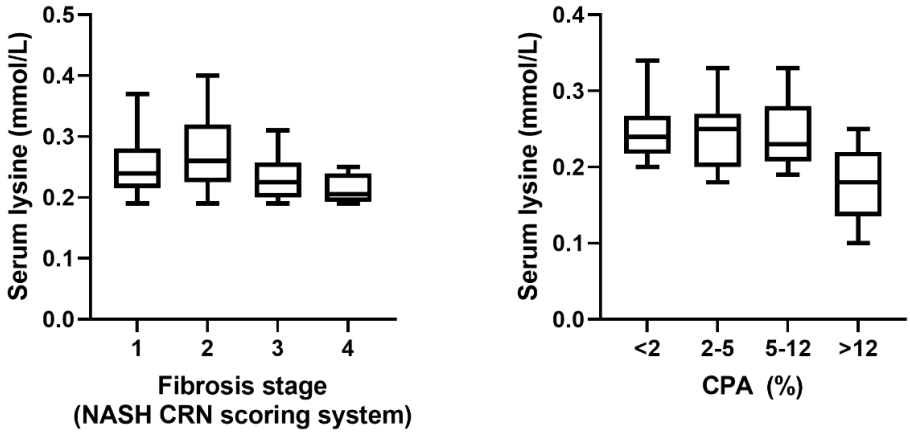

Figure 4.22. Distribution of serum lysine across fibrosis stage and CPA categories. This box plot illustrates median values of lysine and relative 95%CI. Fibrosis stage was assigned as per NASH CRN scoring system, while CPA was measured using image analysis on images of liver biopsies stained in Sirius Red (n=59). Fibrosis 1 includes fibrosis stage 1a, 1b and 1c.
Abbreviations: 95%CI: 95% confidence interval, NASH CRN scoring system: NASH clinical research network scoring system, CPA: collagen proportionate area.

4.4 Discussion

4.4.1 Glycine deficiency is associated with hepatic steatosis but not severity of liver disease in diabetic patients with NAFLD

Glycine is a nonessential amino acid, mainly synthesized in the liver, whose deficiency has been repeatedly described in NAFLD and metabolic disorders. Specifically, few studies have demonstrated that glycine deficiency may be associated with oxidative stress related damage in beta-pancreatic cells (Chen et al., 2018) as well with insulin-resistance systemically (El-Hafidi et al., 2018). Supporting these findings, glycine-based treatment was able to restore fatty acid oxidation, glutathione synthesis and gut microbiome in a mouse model (Rom et al., 2018).

In line with previous studies, lower levels of serum glycine were strongly associated with the presence of hepatic steatosis due to NAFLD in the whole diabetic population (**Figure 4.2**). Moreover, glycine was inversely associated with CAP score and LFTs and was significantly decreased in those with NAFLD and advanced fibrosis (LSM ≥12.1 kPa) compared to those without fibrosis (LSM < 8 kPa). Nevertheless, when the levels of glycine were compared to liver histology, glycine levels decreased along with hepatic fat content but not with disease activity (inflammation and ballooning) or disease severity (fibrosis) (**Figure 4.20**).

Several studies have suggested that a significant proportion of the total body glycine derives from a combination of endogenous synthesis from serine and hepatic de-novo glycine synthesis. In this sense, glycine de-novo synthesis seems to be downregulated by high glucagon levels, which may be particularly relevant in patients with insulin resistance and T2DM. Moreover, dietary patterns (i.e. vegetarian or vegan vs meat- or fish-eaters) rather than specific dietary glycine content have been shown to influence glycine availability and uptake (Alves et al., 2019). Moreover, the bioavailability of dietary glycine has been shown to be strictly modulated by the gut microbiome, as approximately 30% of dietary glycine is used or degraded in the small intestine by the intestinal flora. Specifically, few studies have shown how gut microbiota from patients with T2DM may be particularly enriched in genes involved in glycine degradation. On a similar note, an interesting study showed that urinary glycine excretion could be modulated by changes in gut microbiome. In this study, those with NAFLD had lower levels of faecal glycine, but there was no difference in urinary glycine metabolites (i.e. hippurate), compared to their counterpart without NAFLD. Of note, lower faecal levels of glycine were associated with NAFLD *per se*, independently of metabolic risk factors and liver disease severity (**Figure 4.15**). As such, these findings suggest that changes in dietary intake and/or intestinal availability of glycine (i.e. through changes in the microbiome) represent the main contributing factors to glycine deficiency in this population.

Taken together, these findings suggest that glycine deficiency is associated with the presence of hepatic steatosis but not with the severity of liver disease in diabetic patients screened for NAFLD. Moreover, these results suggest that altered glycine intake and/or availability, rather than increased urinary excretion, may contribute to the lower levels of the metabolite in this population.

4.4.2 Increased glutaminolysis predicts the presence of liver fibrosis in diabetic patients, but this reflects the host metabolic status rather than the severity of liver disease

Glutamate is a non-essential amino acid, derived endogenously via the direct or indirect catabolism of glutamine (glutaminolysis) in the liver (Cynober, 2018). Of note, increased glutamine catabolism (glutaminolysis) is a key metabolic characteristic of rapidly proliferating cells and is controlled primarily by the enzymes glutaminase (for glutamine catabolism) and glutamine synthetase (for glutamine anabolism). Interestingly, a recent study from Du et al has demonstrated that the liver isoform of glutaminase may be upregulated by the hepatic stellate cells, as they require glutaminolysis to satisfy their energetic demand (Du et al., 2020).

In this study, patients with significant liver disease due to NAFLD presented increased glutamate and reduced glutamine level compared to those with NAFLD and normal LSM, as well as compared to those with normal liver (**Figure 4.3** and **4.4**). Moreover, when the NAFLD patients were stratified for liver disease severity, those with even more advanced fibrosis (LSM ≥12.1 kPa) had significantly higher levels of glutamate/glutamine compared to those with normal LSM (LSM< 8.1 kPa) (**Figure 4.5**). Moreover, glutamate/glutamine ratio was a good predictor for the presence of significant and advanced fibrosis in the whole population (**Figure 4.6**). Interestingly, glutamate/glutamine ratio was also strongly associated with BMI, waist circumference, glycaemic status and severity of insulin resistance. When patients were matched for metabolic factors, there was no difference in terms of glutamate/glutamine level between those with elevated LSM and those with normal liver. On a similar note, there was no actual association between glutamate/glutamine and histological features in the NAFLD liver clinic population (**Figure 4.21**).

Taken together, these results suggest that glutamate to glutamine ratio predicts the presence of significant and advanced liver disease in diabetic patients screened for NAFLD. However, this metabolic alteration reflects a more general worse “metabolic status” rather than histological damage *per se*.

4.4.3 Lysine deficiency is associated with liver fibrosis from NAFLD in diabetics, independently of the host metabolic risk factors

Lysine is an essential amino acid which is mainly catabolised in the liver. Interestingly, lysine represents a key component of fatty acid metabolism, proteinogenesis and connective tissue deposition/remodelling. On this note, previous studies have associated lower lysine levels with collagen disturbances, as a result of over-expression of the enzyme lysil oxidases (Ortiz et al., 2021). Under physiological condition, lysil oxidases deaminates lysine residues for maintaining the structural integrity of the extra-cellular matrix. In pathological condition such as fibrogenesis, such enzyme is overexpressed and promotes collagen cross-linking and stabilization against proteolytic degradation, maintaining hepatic stellate cells in an activated state (Kagan and Li, 2003). Moreover, higher levels of pipecolic acid, one of lysine's catabolites, were previously described in patients with chronic liver disease and cirrhosis (Kawasaki et al., 1988).

In this study, when patients were matched for metabolic factors, those with NAFLD and increased LSM had significantly lower level of serum lysine compared to those with normal liver (**Figure 4.7**). Moreover, when compared to liver biopsies from the tertiary care cohort, lysine levels decreased along with augmented hepatic collagen content in liver biopsies (**Figure 4.22**). However, there was no difference of levels of serum lysine between study groups in the whole population. These results suggest a limited role in the use of lysine levels as fibrosis marker in large groups of the patients.

Collectedly, these findings suggest that low lysine levels are strongly associated with the presence of fibrosis in diabetic patients with NAFLD, and this is independent of the overall metabolic status of the patient. However, the use of lower lysine level as biomarker could be explored in tertiary care rather than primary care setting.

4.4.4 Urinary metabolic profile reflects glycosuria and insulin resistance in diabetic patients with NAFLD

Previous works have explored the effects of insulin on the regulation of aminoacids and protein kinetics in diabetic patients, with particular focus on the relationship between circulating insulin concentrations and protein turnover. Specifically, the metabolism of valine, among other branched chain aminoacids, has been reported as impaired in a cohort of patients with NAFLD, associated with lipotoxicity and oxidative stress in the liver (Masoodi et al., 2021). Moreover, the extent of glycosuria has been associated with increased levels of metabolites (i.e. citric acid and creatinine) in urine samples from patients treated with dapagliflozin, suggesting a possible disruption in the tubular reabsorption and/or metabolism in those patients secondary to increased urinary glucose loss (Bletsa et al., 2021, Ferslew et al., 2015).

In this study, patients with significant fibrosis from NAFLD had higher levels of urinary valine, alanine, creatinine and citric acid compared to those without NAFLD (**Figure 4.13**). Interestingly, when analysed against clinical features, these metabolites were strongly associated with glycaemic control rather than with liver markers. On a similar note, when patients were matched for metabolic status, there was no difference in terms of urinary profile between those with NAFLD and elevated LSM vs those with normal liver.

Taken together, these results suggest that increased levels of urinary aminoacids reflect worse glycaemic control (and glycosuria), and proteolysis related to insulin resistance in diabetic patients screened for NAFLD.

4.4.5 Specific bile acid profile is associated with significant fibrosis and changes in gut microbiome in diabetic patients with NAFLD

Recent work revealed that patients with NASH have higher fasting and post-prandial exposure to bile acids. These changes are mainly driven by increase in both taurine and glycine-conjugates primary and secondary bile acid (Ferslew et al., 2015) and possibly reflective of increased faecal bile acids losses with stools (Mouzaki et al., 2016). It has been hypothesized that specific bile

acids may exert not only a toxic effect directly on the liver parenchyma, but they may also influence the hepatic lipid oxidation and the gut permeability (Arab et al., 2017).

In this study, patients with NAFLD had higher levels of serum conjugated and unconjugated litocholic acid (LCA) compared to those with normal liver (**Figure 4.11** and **Figure 4.12**). Of note, recent studies have suggested that LCA may exert a hepatotoxic effect (Staudinger et al., 2001) but also that its serum concentration may be modulated by specific changes in the gut microbiome, such as a reduction in *Bacteroitedes* spp (Mouzaki et al., 2016). Interestingly, those with NAFLD also had a higher *Firmicutes* and lower *Bacteroides*, even though faecal LCA did not directly correlate with microbiome composition. Moreover, stools from patients with higher abundance of Firmicutes (i.e. *Tuzerella* and *Akkermansiaceae*) had lower level of glycine derived BAs, possibly as a result of a relatively lower Bacteroides' glycine deconjugation activity (**Figure 4.19**). Finally, higher abundance of Firmicutes was proportionally associated with sulphated BAs in the stool, where also patients with NAFLD and those with NAFLD and liver disease had elevated sulphate BAs in the serum. Of note, sulfation of BAs increases their solubility, decreases their intestinal absorption, and leads to increased faecal loss.

Among other bile acids, higher levels of serum GDCA-3S were highly specific for significant fibrosis due to NAFLD, and this finding was controlled for glycaemic control and obesity (**Figure 4.10**). From previous works, very little is known about GDCA-3S and its role in health as well as in pathological status. In this, there was no difference in GDCA-3S in stool samples across groups and there was no association with microbial abundances in stools. As such, GDCA-3S does not seem to be influenced by gut microbiota or gut environment overall. It would be interesting to explore whether the increase in serum levels may be driven by impaired hepatic metabolism and/or hepatic inflammation.

Taken together, these results suggest that diabetic patients with NAFLD tend to have a specific serum bile acid profile associated with NAFLD, favouring conjugated and unconjugated LCA and reducing glycine-conjugated bile acid. Moreover, these patients have higher levels of serum

sulphated bile acids. Faecal levels of LCA, glycine-conjugated and sulphated bile acids are influenced by the composition of the intestinal microbiome.

4.4.6 Lower abundance of pectin-dependent species in the gut is associated with the presence and severity of NAFLD in diabetics

Pectins are mainly indigestible by human enzymes, however, they can be easily digested by gut microbes with production of SCFA and other active metabolites. Among other beneficial effects of pectins, delayed gastric emptying and improved glucose tolerance have been described (Schwartz et al., 1988). Moreover, pectins have shown to modulate the composition of gut microbiome and improve the integrity of intestinal barrier (Fukunaga et al., 2003).

In this study, the genus *Anaeroplasma* and *Monoglobus* were less abundant in those with liver fibrosis due to NAFLD compared to those with a normal liver (**Figure 4.16** and **figure 4.17**). Interestingly, *Anaeroplasma* is a newly discovered bacterial genus, with a putative probiotic and anti-inflammatory effect on gut epithelium (Beller et al., 2018). Similarly, *Monoglobus* is another recently identified genus with marked pectin-degrading activity in the human colon (Kim et al., 2019). On a similar trend, when compared to those with normal liver, patients with NAFLD presented lower abundance of other well-known pectin-degrading species, such as *Bacteroides* and *Prevotella* (*Bacteroitedes* phylum). Conversely, in those with NAFLD, there was higher abundance of *Rikenella* spp and *Coprobacter* spp, which were previously associated with high-fat and high-proteins diet (Daniel et al., 2014) and increased response to dietary carbohydrates (Korem et al., 2017) (**Figure 4.18**). Few studies have proved that diet in general, and pectin levels specifically, *per se* may modulate the proliferation of pectin-degrading species, suggesting a bidirectional influence between pectin-intake and microbiome composition (Onumpai et al., 2011, Aguirre et al., 2014).

On a higher level, patients with NAFLD and fibrosis showed a relatively higher abundance of *Firmicutes,* while lower *Bacteroidetes*, in line with previously published data (Stojanov et al., 2020, Crovesy et al., 2020). Moreover, specific changes in the *Bacteroides* and *Firmicutes* were associated

with different BA profile in the stools, such as reduced Bacteroidetes being associated with increased levels of LCA as observed in this population and in the literature.

Taken together, lower abundance of *Bacteroides* and pectin-degrading species with increased abundance of *Firmicutes* were associated with the presence of NAFLD and severity of liver disease in diabetic patients screened for NAFLD. On a more specific level, *Monoglobus* was associated with clinically significant NAFLD, independent of metabolic factors.

4.5 Strengths and limitations

This part of the project presents several strengths. Firstly, the population included in this study has been well-phenotyped. Specifically, the metabolomics analysis was comprehensive and carried out on several biological levels, and the results from such analysis were also matched with accurate gut microbiome profiling. Thirdly, a detailed statistical analysis allowed for the identification of factors associated with NAFLD and severity of liver disease in the whole population, with all confounders included as well as on an independent level (matched subsets, controlled for metabolic confounders).

This part of the work has also several limitations. Firstly, the sub-analysis of matched subjects included only small number of patients compared to the whole population. Secondly, limited information was available on dietary patterns from these patients, as such analysis against diet could not be included. Finally, liver disease severity was defined based on LSM and not histology.

4.6 Future work

Future research should be considered to explore more in depth the role of serum lysine as biomarker for liver fibrosis in specific NAFLD populations, for example in tertiary care. Future work could also focus on elucidating the biological effect of GCDA-3S in liver diseases and NAFLD, starting from *in-vitro* models of fibroblasts and/or other cell-lines. Finally, specific changes in diet and/or gut microbiota towards pectin-degrading species may be explored as possible therapeutical option to treat the disease. Specifically, targeting specific bacteria, such as *Monoglobus*, may offer

a therapeutical approach as its lower abundance was associated with significant fibrosis, independently of metabolic risk factors.

4.7 Conclusions

In this study, glycine deficiency was associated with hepatic steatosis, but not with the severity of liver disease in diabetics screened for NAFLD. Serum glutamate to glutamine ratio, despite being a good predictor for clinically significant NAFLD, reflects metabolic status rather than histological changes *per se*. Nevertheless, levels of lysine in sera may be explored as possible biomarker for liver fibrosis in NAFLD as this was strongly associated with collagen content, independently of metabolic status. In terms of bile acid profile, higher levels of conjugated and unconjugated LCA were characteristic of patients with NALD, while serum GDCA-3S was highly specific for significant fibrosis but was not influenced by intestinal microbial composition. Finally, specific changes in pectin-degrading species and *Firmicutes* characterise those with clinically significant NAFLD among diabetics, supporting the role of diet and microbiome modulation as potential therapeutic targets for the disease.

5. ASSESSMENT OF GUT PERMEABILITY IN DIABETIC PATIENTS SCREENED FOR NAFLD

5.1 Introduction

The GI mucosa is a semi-permeable barrier with multiple properties, such as the absorption of nutrients and immune sensing. The gut barrier also plays an important role in limiting the passage of potentially pathological molecules and microorganisms into the systemic circulation. Among others, tight junctions represent the main structures forming the complex for cell-to-cell adhesion that polarizes the intestinal epithelium, as they regulate the passage of ions and, therefore, create a potential difference at either side of the tissue. Of note, products may cross the epithelium from the lumen using different pathways, based on their chemical properties, such as size and hydrophobicity. Various mediators may influence TJ structure and, therefore, paracellular permeability, such as cytokines, microbiota, diet and bacterial or host-produced proteases (Van Spaendonk et al., 2017).

Several techniques have been employed to measure the intestinal permeability both in-vitro and in-vivo. Commonly, permeability has been assessed as Trans-epithelial electric resistance (TEER) measured across monolayers of specific cell lines or biopsies from GI mucosa. The TEER is usually measured in ohms and it is a quantitative measure of the gut barrier integrity. Other techniques for measuring the permeability across cell monolayer use probe molecules, such as dextran 4 or 40, exploiting a similar concept. In vivo, intestinal permeability may be measured as the urinary excretion of indigested probes (Camilleri and Vella, 2021) as well as serum levels of occluding. In the field of liver disease, individuals with CHB and CHC have shown higher plasma levels of FABP-2 compared to controls, suggesting some degree of enterocytes death (Sandler et al., 2011).

The presence of T2DM is known to be associated with low-grade inflammation as well as with alterations in the intestinal barrier function. When compared to non-diabetics, patients with T2DM show significantly higher levels of LPS (Gomes et al., 2017). Moreover, LPS levels were also predictive of developing T2DM within 10 years follow-up, in the FINRISK97 cohort (Pussinen et al., 2011). Changes in the composition of the gut microbiota have also been described as contributing

to an impaired mucosal barrier (Dabke et al., 2019). Moreover, in patients with T2DM, decreased levels of GLP-2 have also been associated with disruption of zonulin-1, occluding and claudin-1, resulting in abnormalities in the TJ barrier (Yu et al., 2016). Of note, hyperglycaemia can damage the intestinal epithelial cells directly by altering TJ integrity, via a mechanism which is GLUT2-dependant (Thaiss et al., 2018).

Evidence has also revealed that plasma endotoxin concentrations are increased in the early stages of liver disease from NAFLD in a paediatric population, suggesting the presence of some degree of increased gut permeability in the initial phases of the disease (Nier et al., 2017). Not only excessive food intake but also specific dietary patterns have proved to be strongly associated with alterations in the intestinal barrier (Alvarez-Mercado et al., 2019). Intestinal dysbiosis may also impact upon the expression of TJ, increasing gut permeability and translocation of bacterial products (Yoshida et al., 2018). The composition of gut microbiota may also modulate the abundance of SCFA, which in turn may have protective effect on the intestinal epithelium, as they promote epithelial cell proliferation and adhesion as well as anti-inflammatory effect (Mailing et al., 2019). Overall, small intestinal permeability increases with the degree of hepatic steatosis, while there is no clear association with severity of liver disease (such as hepatic inflammation, ballooning or fibrosis) (De Munck et al., 2020, Miele et al., 2009).

To conclude, there is evidence suggesting that patients with NAFLD may have increased gut permeability. A combination of diet, changes in gut microbiota, hyperglycaemia and hormonal status may be responsible of such changes in the intestinal epithelium in diabetic patients with NAFLD. However, a clear association between gut permeability and severity of liver disease in NAFLD has not been demonstrated so far.

Therefore, the main objectives of this part of the project were

1. To explore gut permeability in diabetic patients with and without NAFLD and with different stages of liver disease severity using an in-vitro model

2. To explore the factors associated with increased gut permeability in diabetic patients screened for NAFLD

5.2 Materials and methods

5.2.1 Biological samples

Serum and stool samples were collected, processed and stored as per the Hepatology and Gastroenterology divisional standard operating procedure. Faecal water was obtained from the faecal samples from patients enrolled in the study, while protein concentration and quantification were performed using a BCA assay. A Pierce Fluorescent Protease assay kit (Thermo Scientific, UK) was used to measure total protease activity with and without the addition of commercial bacterial protease inhibitor cocktail (Protease inhibitor cocktail powder for use with bacterial cells extracts, lyophilized powder, Merck Life Science UK Limited, UK). Clinical data and metabolic profile were matched with correspondent FW samples.

5.2.2 In-vitro model of gut-permeability with MDCK cell culture

Aliquots of 1-2 x 10^5 MDCK cells were cultured on Transwell inserts in a 24 well plate at 37°C, 5% CO_2, for 72-96 hours to allow for monolayer formation. The integrity of individual monolayers was assessed by measuring TEER using an EVOM (**Figure 2.3**). Monolayers were considered intact when TEER measurements were stable after at least 2 days from seeding. Monolayers with TEER values < 150 Ωcm^2 after 72 hours were not considered intact and were excluded. At time zero, HBSS from the apical compartment of each well was removed and replaced by equal volume of either PBS (as negative control), *Enterococcus faecalis* (*E. faecalis*) spent medium (as positive control) or faecal water (FW) derived from the faecal samples of patients enrolled in the study. Specifically, *E.faecalis* was chosen as positive control, given its peculiar proteolytic activity through the production of specific gelatinases and serine proteases (Nesuta et al., 2017). Once PBS, *E. faecalis* and FW were added to the wells (time zero), TEER was then measured at a sequence of 5, 30, 90, 120 mins and 24

hours. Experiments were replicated with the addition of a commercial bacterial protease inhibitor cocktail to differentiate the contribution from host and microbial proteases.

5.2.3 Measurement of serum FABP-2 and faecal cytokines

The serum level of FABP-2 was measured in serum samples from the patients enrolled in the study, using a Human FABP2/I-FABP Quantikine ELISA Kit, which is essentially a sandwich ELISA. The faecal levels of IFN-γ, IL-1β, IL-2, IL-4, IL-6, IL-8, IL-10, IL-12p70, IL-13, and TNF were measured in the FW obtained from samples of the patients enrolled in the study, using the V-plex Proinflammatory Panel 1 (MSD) - essentially a sandwich immunoassay.

5.2.4 Statistical analysis and regulatory approval

The distribution of variables was explored using the Shapiro-Wilk test. Continuous variables were reported as medians and IQR, while categorical variables were expressed as relative frequencies and percentages. Univariate analysis was carried out using Mann-Whitney for continuous, and chi-square test for categorical variables respectively. Kruskal-Wallis or ANOVA with post-hoc corrections was used for comparison between multiple groups. Spearman correlation and logistic regression carried out to explore the relationship between variables. All tests were two-sided and a *P* value 0.05 was considered significant. Statistical analysis was performed by GraphPad Prism (version 9.1) and SPSS (version 24.0; SPSS Inc Chicago, IL).

.

5.3 Results

5.3.1 *In-vitro* model of gut-permeability

5.3.1.1 Patient samples

For this experiment, FW was obtained from the stool samples of 12 patients enrolled in the study. Specifically, 5 patients had normal liver, 3 patients were diagnosed with NAFLD and normal LSM and 4 patients with NAFLD and elevated LSM. The clinical characteristics of the patients whose samples were used in the model are shown in **Table 5.1**.

	Normal liver N=5	NAFLD, normal LSM N=3	NAFLD, elevated LSM N=4
	Median (IQR)	**Median (IQR)**	**Median (IQR)**
Age, *years*	59 (52-61)	61 (54-65)	62 (60-67)
Waist circum, *cm*	96 (73-103)	105 (99-13)	121 (113-128)
BMI, kg/m^2	26.7 (19.4-30.6)	30.3 (27.6-33.6)	40.3 (38.2-44)
PLT, $x\ 10^9/\mu L$	225 (186-266)	255 (215-300)	255 (197-328)
ALT, *IU/L*	18 (15-41)	30 (22-43)	22 (19-51)
AST, *IU/L*	22 (22-28)	26 (22-32)	29 (23-45)
GGT, *IU/L*	17 (15-56)	27 (19-39)	32 (19-78)
Total Cholesterol, *mmol/l*	3.8 (3.6-4)	4.1 (3.5-4.8)	4 (3.6-5.3)
Ferritin, *ng/ml*	62 (24-76)	82 (36-124)	129 (54-139)
CAP score, *dB/m*	208 (175-244)	324 (300-394)	356 (332-391)
LSM, *kPa*	4.4 (4.1-6.3)	5.4 (4.5-6.4)	18.2 (11-22.2)
Diabetes characteristics			
	Median (IQR)	**Median (IQR)**	**Median (IQR)**
Fasting glucose, *mmol/l*	4.4 (4.3-8.4)	6.7 (5.2-9.2)	5.9 (5.1-8.1)
HbA1c, *mmol/mol*	57 (55-61)	59 (49-68)	67 (44-74)
Homa index	3.7 (0.5-3.8)	3.3 (2.1-8.4)	2.3 (0.4-8.8)

Table 5.1. Characteristics of patients whose samples were used in the in-vitro model of gut permeability. Variables are expressed as median and IQR or relative percentages. * p-value refers to differences between patients with NAFLD and normal liver.
Abbreviations: IQR: interquartile range, BMI: Body mass index, PLT: platelet, ALT: alanine aminotransferase, AST: aspartate aminotransferase, GGT: gamma-glutamyl transferase, ALP: alkaline phosphatase, TRG: triglycerides, HDL: high density lipoprotein, LDL: low density lipoprotein, CAP score: controlled attenuation parameter score, LSM: liver stiffness measurement, HbA1c: glycated haemoglobin

5.3.1.2 MDCK cultivation and maintenance of a monolayer

TEER values were determined for all MDCK monolayers to ensure the cells had formed a monolayer. Following at least 48 hours in culture, TEER values were typically in the range of 250-300 Ωcm^2 when confluence was reached. The successful cultivation of the monolayer, from seeding to confluence, is shown in **Figure 5.1**.

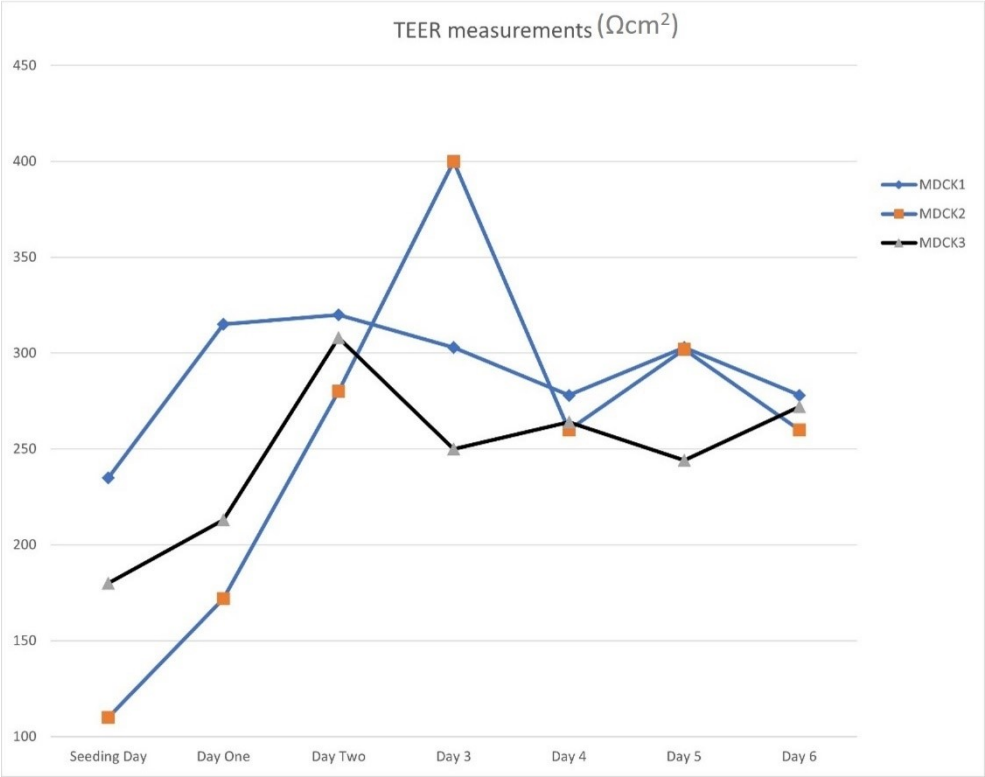

Figure 5.1. TEER values during the formation of the monolayer of MDCK cell line. Each point (expressed as Ωcm^2) represents the median value of triplicate readings for each well at determinate time point. *Abbreviations: TEER: transepithelial electric resistance, MDCK: Madin-Darby canine kidney cell.*

5.3.1.3 Effect of faecal water on MDCK monolayers

The effect that FW, PBS (negative control) and E. *faecalis* (positive control) exerted on MDCK monolayers was monitored at 5, 30, 90, 120 mins and 24 hours from incubation (time zero). Overall, the samples from patients with NAFLD and elevated LSM caused the greatest change in the TEER compared to those with normal liver. Specifically, when comparing monolayers incubated with samples from patients with NAFLD and elevated LSM vs samples from those with normal liver, TEER was 185 vs 258 Ωcm^2 (p=0.04) at five minutes, 132 vs 247 Ωcm^2 (p=0.032) at 30 mins, 172 vs 250 Ωcm^2 (p=0.037) at 90 mins, 175 vs 245 Ωcm^2 (p=0.026) at 120 mins and 164 vs 252 Ωcm^2 (p=0.002)

at 24 hours (**Figure 5.2** and **Table 5.2**). Furthermore, the TEER across the monolayer of MDCK incubated with faecal samples from patients with NAFLD and normal LSM, was significantly lower compared to those incubated with faecal water from those with normal liver at 24 hours (162 vs 252 Ωcm^2, p=0.03) (**Figure 5.2** and **Table 5.2**).

To explore whether bacterial proteases were associated with the decrease in the monolayer resistance, a commercial cocktail of bacterial protease inhibitors was added to FW (inhibited FW), and the TEER experiments were replicated under the same conditions. Of note, inhibited FW caused a significant lower decrease in TEER compared to uninhibited FW in those with NAFLD and normal LSM, and in those with NAFLD and elevated LSM. Interestingly, there was no significant change in TEER when using inhibited or uninhibited FW from patients with normal liver (**Figure 5.3** and **Table 5.3**).

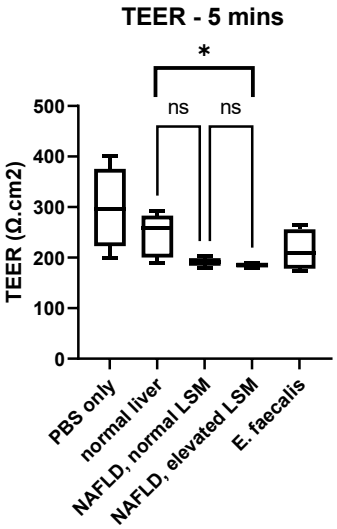
TEER - 5 mins
TEER (Ω.cm2)
500
400
300
200
100
0
*
ns
ns
PBS only
normal liver
NAFLD, normal LSM
NAFLD, elevated LSM
E. faecalis

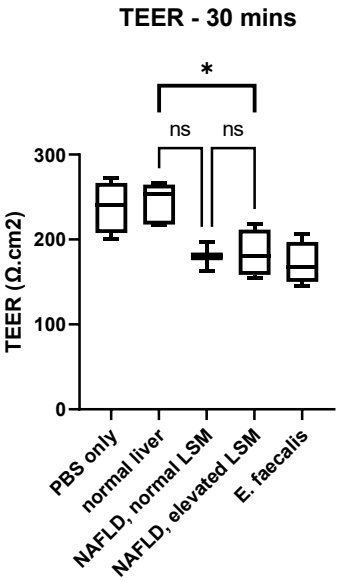
TEER - 30 mins
TEER (Ω.cm2)
300
200
100
0
*
ns
ns
PBS only
normal liver
NAFLD, normal LSM
NAFLD, elevated LSM
E. faecalis

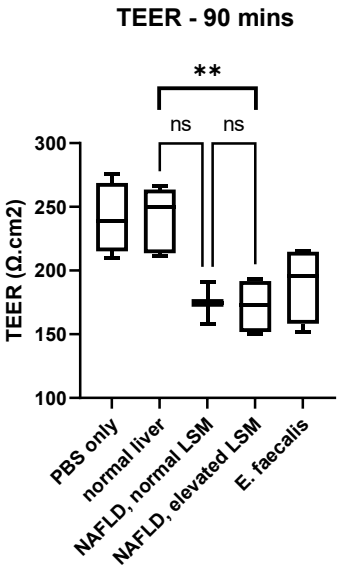
TEER - 90 mins
TEER (Ω.cm2)
300
250
200
150
100
**
ns
ns
PBS only
normal liver
NAFLD, normal LSM
NAFLD, elevated LSM
E. faecalis

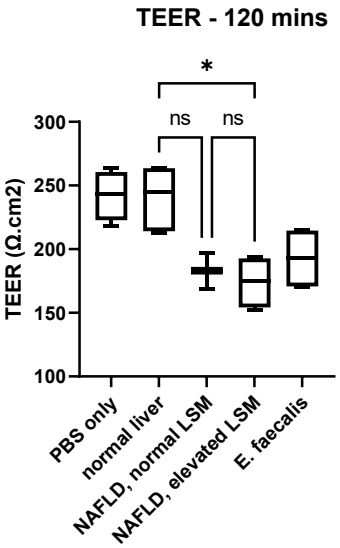
TEER - 120 mins
TEER (Ω.cm2)
300
250
200
150
100
*
ns
ns
PBS only
normal liver
NAFLD, normal LSM
NAFLD, elevated LSM
E. faecalis

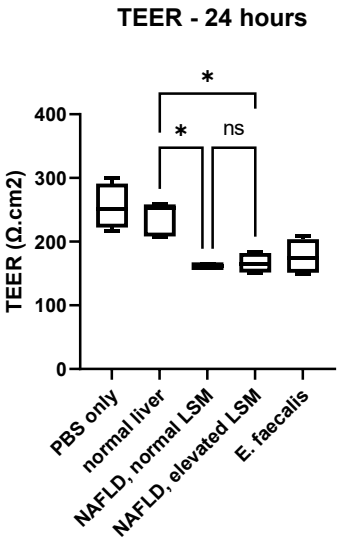
TEER - 24 hours
TEER (Ω.cm2)
400
300
200
100
0
*
*
ns
PBS only
normal liver
NAFLD, normal LSM
NAFLD, elevated LSM
E. faecalis

Figure 5.2. Effect of uninhibited faecal water, positive and negative controls on TEER of MDCK monolayers. The box plot illustrates median values of triplicate measurements of TEER and corresponding 95%CI and difference between study groups: normal liver (n=5), NAFLD with normal LSM (n=3) and NAFLD with elevated LSM (n=4).
Abbreviations: 95%CI: 95% confidence interval, TEER: trans-epithelium electric resistance.

	PBS (N=4)	NORMAL LIVER (N=5)	NAFLD WITH NORMAL LSM (N=3)	NAFLD WITH ELEVATED LSM (N=4)	E. FAECALIS (N=4)
			Median (IQR)		
TEER 5 MIN (ΩCM^2)	296 (167-327)	258 (210-273)	191 (185-203)	185 (181-189)	209 (186-238)
TEER 30 MIN (ΩCM^2)	240 (222-255)	247 (215-255)	135 (130-145)	132 (128-137)	167 (160-179)
TEER 90 MIN (ΩCM^2)	238 (225-254)	250 (216-261)	174 (166-191)	172 (155-189)	195 (172-214)
TEER 120 MIN (ΩCM^2)	243 (232-253)	245 (215-263)	183 (176-197)	175 (158-190)	193 (172-213)
TEER 24 HOURS (ΩCM^2)	251 (232-273)	252 (209-258)	161 (159-165)	164 (152-178)	174 (155-195)

Table 5.2. Effect of uninhibited faecal water, positive and negative controls on TEER of MDCK monolayers. The experiments for each FW were repeated in triplicates, i.e. incubating three adjacent wells with the same FW. Moreover, in each well, TEER was measured in triplicates at all time points. The table shows median values of TEER and correspondent IQR.
Abbreviations: PBS: Phosphate buffer saline, LSM: liver stiffness measurement, IQR: interquartile range, NAFLD: non-alcoholic fatty liver disease, TEER: trans-epithelium electric resistance.

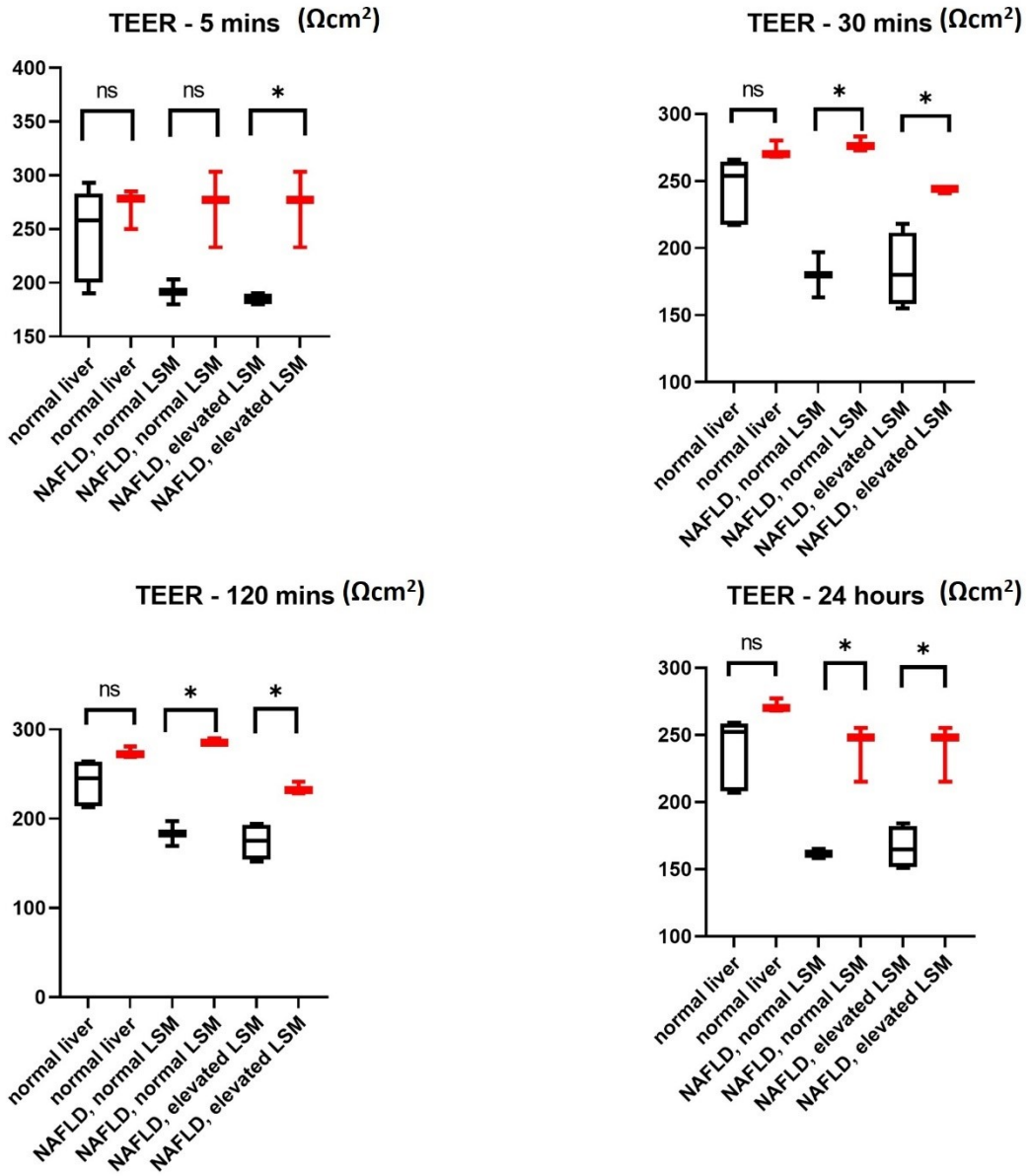

Figure 5.3. Effect of uninhibited and inhibited faecal water on TEER of MDCK monolayer. The box plot illustrates median values of triplicate measurements of TEER and corresponding 95%CI among study groups: normal liver (n=5), NAFLD with normal LSM (n=3) and NAFLD with elevated LSM (n=4). TEER measurement in presence of uninhibited faecal water are represented in black, while TEER measurement in presence of inhibited faecal water are represented in red.
Abbreviations: 95%CI: 95% confidence interval, TEER: trans-epithelium electric resistance, T2DM: type-2 diabetes, NAFLD: non-alcoholic fatty liver disease.

	NORMAL LIVER (N=5)			NAFLD WITH NORMAL LSM (N=3)			NAFLD WITH ELEVATED LSM (N=4)		
	Median (IQR)								
	Uninhibited FW	Inhibited FW	p-value	Uninhibited FW	Inhibited FW	p-value	Uninhibited FW	Inhibited FW	p-value
TEER 5 MIN (ΩCM^2)	258 (210-273)	278 (264-281)	0.65	**191 (185-203)**	**277 (255-290)**	**0.12**	**185 (181-189)**	**277 (255-290)**	**0.007**
TEER 30 MIN (ΩCM^2)	247 (215-255)	270 (269-275)	0.15	**135 (130-145)**	**276 (274-279)**	**0.006**	**132 (128-137)**	**244 (242-244)**	**0.017**
TEER 120 MIN (ΩCM^2)	245 (215-263)	272 (270-276)	0.22	**183 (176-197)**	**285 (284-287)**	**0.007**	**175 (158-190)**	**232 (230-236)**	**0.002**
TEER 24 HOURS (ΩCM^2)	252 (209-258)	270 (269-273)	0.35	**161 (159-165)**	**248 (231-251)**	**0.005**	**164 (152-178)**	**248 (231-251)**	**0.001**

Table 5.3. Differences in the effect of uninhibited and inhibited faecal water on TEER of MDCK cell line. The table shows median values of triplicate measurements of TEER and corresponding IQR. * p-value differences in TEER between uninhibited and inhibited faecal water.
Abbreviations: FW: faecal water, IQR: interquartile range, TEER: trans-epithelium electric resistance, NAFLD: non-alcoholic fatty liver disease, LSM: liver stiffness measurement.

5.3.1.4 Analysis of TEER against clinical features

An overall median TEER was calculated for each well as the median of the TEER measurements from 5 minutes to 24 hours. With regards to the association between TEER and clinical features, clinical data and metabolic profile were matched with the samples used for the in-vitro model. There was a strong, inverse linear relationship between the overall TEER and BMI (Rho= -0.78, p=0.01 and R^2=0.43, p=0.029) and between overall TEER and waist circumference (Rho= -0.69, p=0.026 and R^2=0.51, p=0.019) (**Figure 5.4A and 5.4B**). Moreover, there was a strong, inverse linear relationship between overall TEER and AST (Rho= -0.65, p=0.03 and R^2=0.402, p=0.036) and

between overall TEER and LSM (Rho= -0.88, p=0.0001 and R^2=0.55, p=0.009) (**Figure 5.4C and 5.4D**). Nevertheless, there was no relationship between overall TEER and HbA1c (p=0.069), between TEER and HOMA index (p=0.88) or between TEER and ALT (p=0.07).

In terms of faecal metabolites, TEER showed a strong, negative association with valerate levels (Rho= -0.65, p=0.029). Specifically, faecal valerate was significantly lower in NAFLD with elevated LSM vs normal liver (0.28 vs 0.47, p=0.007) (**Figure 5.5**).

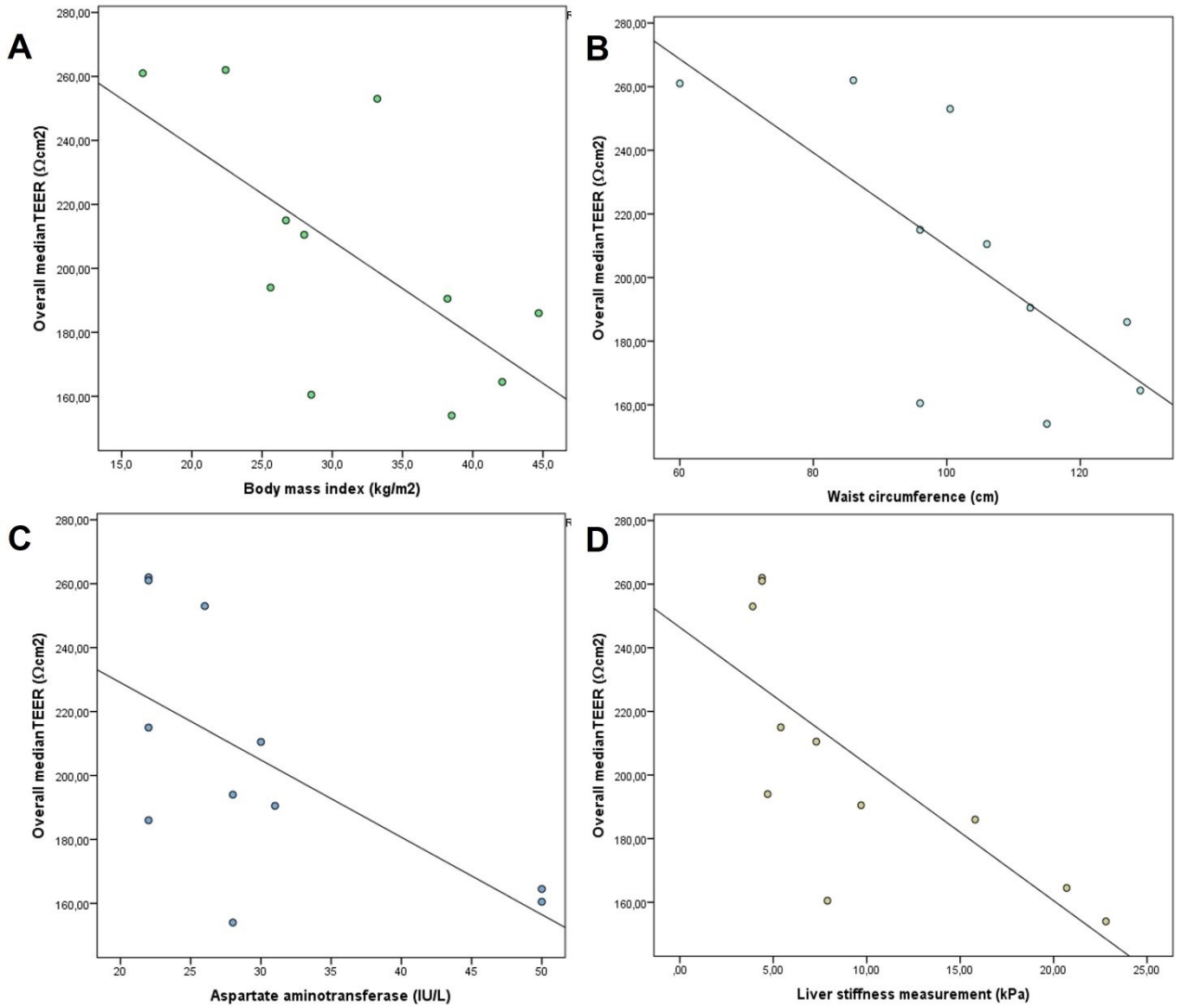

Figure 5.4. Correlation between overall TEER and clinical features of the study patients. The scatter dot plots illustrate single dots corresponding to single cases of patients whose FW was used for the TEER measurements (n=12). Figure 5.4A) illustrates the correlation between overall TEER and BMI. Figure 5.4B) illustrates the correlation between overall TEER and waist circumference. Figure 5.4C) illustrates the correlation between overall TEER and AST. Figure 5.4D) illustrates the correlation between overall TEER and LSM.
Abbreviations: 95%CI: 95% confidence interval, TEER: trans-epithelium electric resistance. AST: aspartate aminotransferase, LSM: liver stiffness measurement.

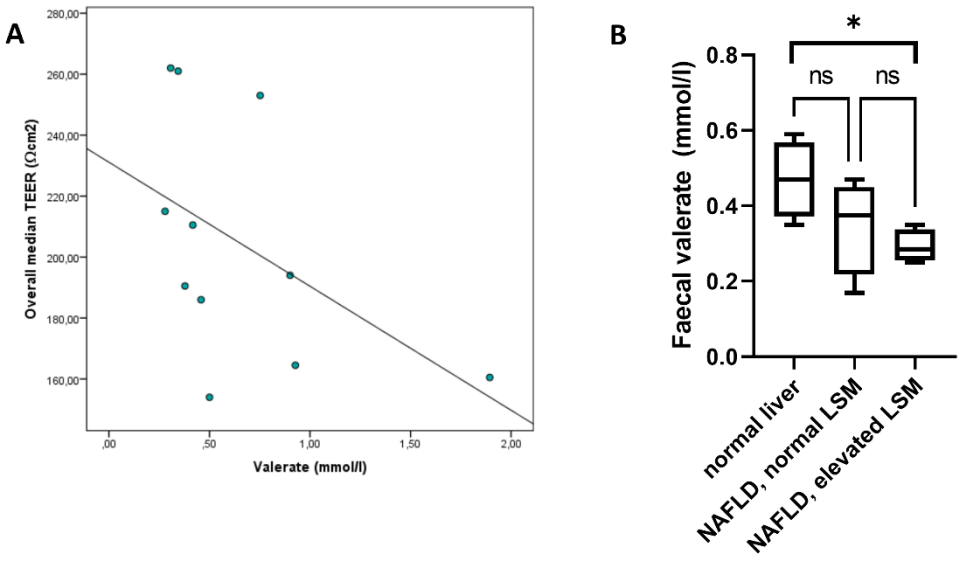

Figure 5.5. Association between overall TEER and faecal valerate. Figure 5.5A) The scatter dot plot illustrates single cases of patients whose FW was used for the TEER measurements (n=12) and correlation with valerate. Figure 5.5B) this box plot illustrates median values and corresponding 95%CI for valerate among samples used for TEER experiment.
Abbreviations: 95%CI: 95% confidence interval, TEER: trans-epithelium electric resistance. NAFLD: non-alcoholic fatty liver disease, LSM: liver stiffness measurement.

5.3.2 Assessment of ex-vivo protease activity

5.3.2.1 Patient samples

For this experiment, FW water was obtained from the stool samples of 24 patients enrolled in the study. Specifically, 8 patients had normal liver, 7 patients NAFLD and normal LSM and 9 patients NAFLD and elevated LSM. Of note, 12 out of the 24 samples used for this experiment, were the same samples used for the in-vitro gut-permeability model. The protease activity within the FW was measured with (inhibited FW) and without (uninhibited FW) the addition of a commercial cocktail of bacterial proteases inhibitor.

5.3.2.2 Assessment of protease activity

Overall, the protease concentration in the uninhibited FW tended to increase from normal liver to NAFLD and elevated LSM, although the difference was not statistically significant (**Figure 5.6A**). Similarly, when the protease concentration was measured in inhibited FW, the difference across the groups was not statistically significant (**Figure 5.6B**). Finally, delta protease concentration was calculated as (protease concentration in uninhibited FW – protease concentration in inhibited

FW) / protease concentration in uninhibited FW) *100 and expressed as percentage. There was no difference in terms of delta protease concentration across the groups (**Figure 5.6C**).

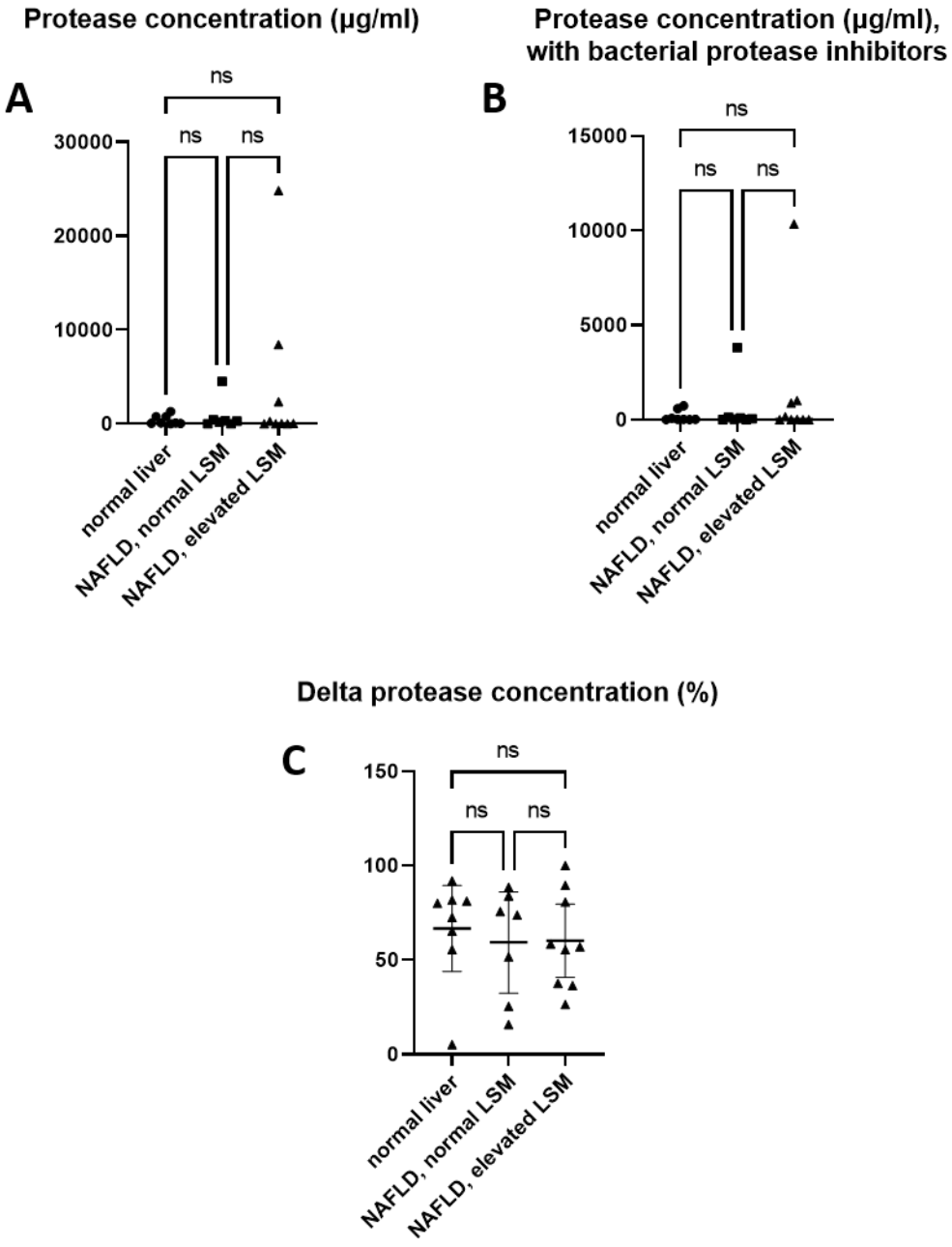

Figure 5.6. Assessment of protease concentration in uninhibited and inhibited FW. The scatter dot plot illustrates single dots corresponding to single cases of protease concentration and median with 95%CI. Figure 5.6A) illustrates the protease concentration in uninhibited FW. Figure 5.6B) illustrates the protease concentration in inhibited FW. Figure 5.6C) illustrates the delta protease concentration between uninhibited and inhibited FW. Differences are shown among study groups: normal liver (n=8), NAFLD with normal LSM (n=7) and NAFLD with elevated LSM (n=9).
Abbreviations: FW: faecal water, 95%CI: 95% confidence interval, TEER: trans-epithelium electric resistance, NAFLD: non-alcoholic fatty liver disease, LSM: liver stiffness measurement.

5.3.3 Fatty acid binding protein 2

5.3.3.1 Patients samples

A total of 49 serum samples were analysed for FABP-2. Specifically, 17 (34%) patients had normal liver, 22 (45%) patients had NAFLD and normal LSM, while 10 (20%) patients NAFLD and elevated LSM. Fifteen serum samples from healthy controls were also included as a comparator for the analysis.

5.3.3.2 Serum levels of FABP-2

Median serum concentration for FABP-2 was 2662.8 (1342.2-3595.3) pg/ml in those with normal liver, 1608.5 (992.4-2782.7) pg/ml in those with NAFLD and normal LSM, 3112.2 (1987.5-3900.3) pg/ml in those with NAFLD and elevated LSM. Overall, there was no difference in terms of levels of serum FABP-2 across study groups (**Figure 5.7**). There was also no difference against healthy controls. Moreover, there was no direct association between FABP and metabolic factors, such as BMI (p=0.9), waist circumference (p=0.87), HOMA index (p=0.72) and HbA1c (p=0.65).

When patients were matched for metabolic factors, FABP-2 levels were not significantly different between significant liver disease due to NAFLD vs those with normal liver (p=0.33). Moreover, when patients were matched for metabolic factors and LSM, there was no difference in terms of FABP-2 levels between NAFLD vs normal liver (p=0.059).

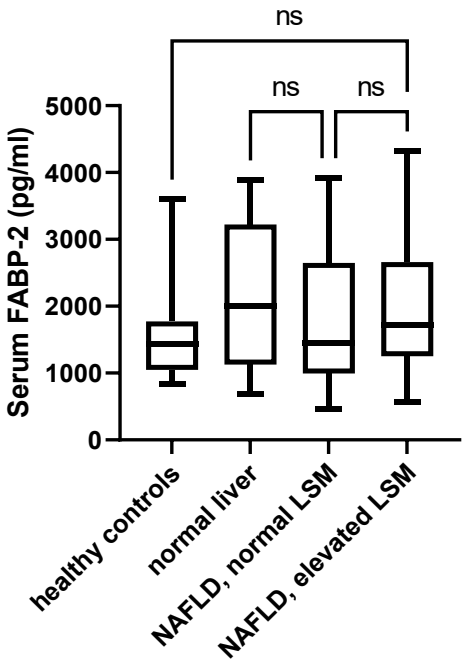

Figure 5.7. Fatty acid binding protein-2 measurement in serum samples and difference between study groups. The box plot illustrates median values of FABP-2 in serum samples and corresponding 95%CI. Differences are shown among study groups: normal liver (n=17), NAFLD with normal LSM (n=22) and NAFLD with elevated LSM (n=10).
Abbreviations: 95%CI: 95% confidence interval, NAFLD: non-alcoholic fatty liver disease, LSM: liver stiffness measurement, FAPB-2: fatty acid binding protein-2.

5.3.4 Faecal cytokines

5.3.4.1 Patient samples

A total of 76 FW samples were tested for faecal cytokines using the V-plex proinflammatory panel 1. Specifically, 18 (23%) patients had normal liver, 38 (50%) patients had NAFLD and normal LSM, while 20 (26%) patients NAFLD and elevated LSM.

5.3.4.2 Levels of faecal cytokines

Overall, those with NAFLD and elevated LSM showed significantly lower levels of faecal IFN-γ compared to those with normal liver (0.45 vs 0.79 pg/ml, p=0.02) and compared to normal liver (0.45 vs 0.79 pg/ml, p=0.01) (**Figure 5.8**). However, there was no difference in terms of levels of faecal IL-1β, IL-2, IL-4, IL-6, IL-8 (CXCL8), IL-10, IL-12p70, IL-13, and TNF-α across study groups (**Figure 5.9** and **Figure 5.10**). Median values of faecal cytokines are displayed in **Table 5.4**. Results were normalised per protein content of each FW sample.

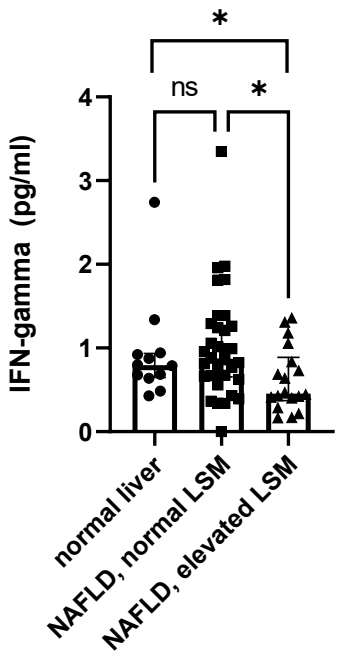

Figure 5.8. Levels of IFN-γ in FW samples and comparison between study groups. The scatter plot graph illustrates single values of faecal IFN-γ and differences across study groups: normal liver (n=18), NAFLD with normal LSM (n=38) and NAFLD with elevated LSM (n=20).
Abbreviations: FW: faecal water, NAFLD: non-alcoholic fatty liver disease, LSM: liver stiffness measurement, IFN-γ: interferon-gamma.

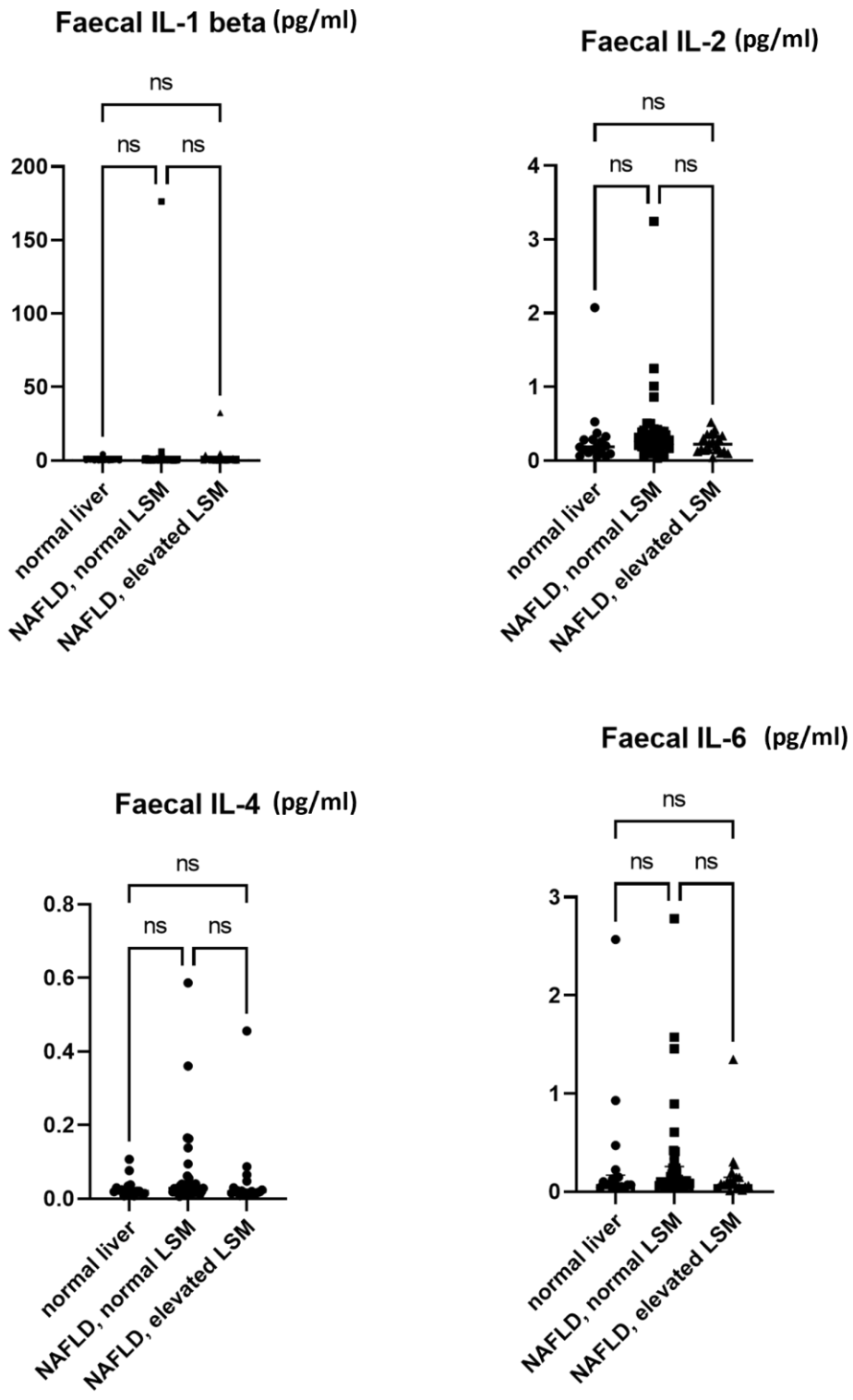

Figure 5.9. Levels of IL-1β, IL-2, IL-4 and IL-6 in FW samples and comparison between study groups. The scatter plot graph illustrates single values of faecal IL-1β, IL-2, IL-4 and IL-6 and differences across study groups: normal liver (n=18), NAFLD with normal LSM (n=38) and NAFLD with elevated LSM (n=20).

Abbreviations: FW: faecal water, NAFLD: non-alcoholic fatty liver disease, LSM: liver stiffness measurement, IL-1β: interleukin-1 beta, IL-2: interleukin-2, IL-4: interleukin-4, IL-6: interleukin-6.

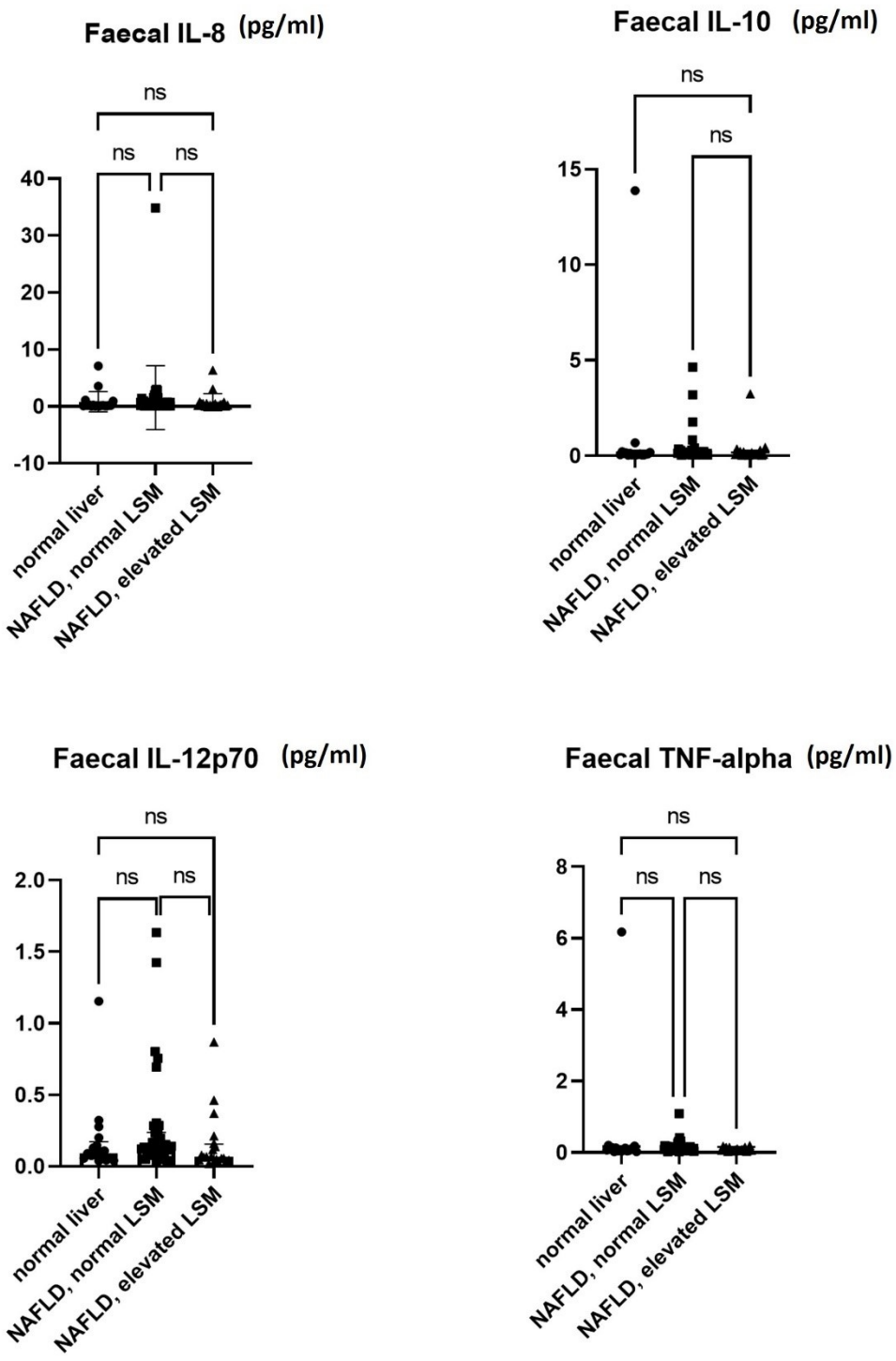

Figure 5.10. Levels of IL-8, IL-10, IL-12p70 and TNF-α in FW samples and comparison between study groups. The scatter plot graph illustrates single values of faecal IL-8, IL-10, IL-12p70 and TNF-α and differences across study groups: normal liver (n=18), NAFLD with normal LSM (n=38) and NAFLD with elevated LSM (n=20).
Abbreviations: FW: faecal water, NAFLD: non-alcoholic fatty liver disease, LSM: liver stiffness measurement, IL-8: interleukin-8, IL-10: interleukin-10, IL-12p70: interleukin-12p70, TNFα: tumour necrosis factor alpha.

	Normal liver (N=18)	NAFLD, normal LSM (N=38)	NAFLD, elevated LSM (N=20)
		MEDIAN (IQR)	
IFN-Γ, *pg/ml*	0.79 (0.64-0.93)	0.87 (0.65-1.2)	0.45 (0.3-0.8)
IL-1β, *pg/ml*	0.34 (0.12-0.69)	0.23 (0.09-0.81)	0.2 (0.09-0.87)
IL-2, *pg/ml*	0.18 (0.1-0.29)	0.29 (0.18-0.39)	0.22 (0.12-0.35)
IL-4, *pg/ml*	0.02 (0.01-0.03)	0.02 (0.01-0.04)	0.01 (0.01-0.02)
IL-6, *pg/ml*	0.07 (0.04-0.16)	0.1 (0.06-0.25)	0.07 (004-0.14)
IL-8, *pg/ml*	0.18 (0.1-0.4)	0.19 (0.11-0.86)	0.29 (0.11-0.5)
IL-10, *pg/ml*	0.08 (0.04-0.14)	0.14 (0.09-0.23)	0.1 (0.06-0.21)
IL-12p70, *pg/ml*	0.09 (0.05-0.17)	0.13 (0.09-0.23)	0.06 (0.04-0.15)
IL-13, *pg/ml*	0.36 (0.25-0.54)	0.5 (0.32-0.66)	0.36 (0.24-0.44)
TNF-α, *pg/ml*	0.08 (0.04-0.12)	0.11 (0.06-0.16)	0.07 (0.04-0.13)

Table 5.4 Concentrations of faecal cytokines in the study groups. This table shows median values and related IQR of faecal cytokines in the study groups.
Abbreviations: IQR: interquartile range, IFN-γ: interferon gamma, IL-1β: interleukin-1beta, IL-2: interleukin-2, IL-interleukin, IL-4: interleukin-4, IL-6: interleukin-6, IL-8: interleukin-8, IL-10:interleukin-10, IL-12p70: interleukin-12p70, IL-13: interleukin-13, TNF-α: tumour necrosis factor alpha.

5.4 Discussion

5.4.1 Gut permeability is increased and associated with liver disease severity in diabetic patients with NAFLD

A certain degree of increased gut permeability has been previously demonstrated in the small intestine of patients with NAFLD (De Munck et al., 2020). According to a recent metanalysis, those with NAFLD have an increased risk of leaky gut compared to healthy controls. Also, those with NASH have a greater risk of leaky gut compared to those with simple steatosis (Luther et al., 2015). Of note, the majority of the studies now available in the field have been carried out with experiments in vivo (De Munck et al., 2020), using either the lactulose:mannitol test or the measurement of serum zonulin levels, showing an improvement in gut permeability after FMT (Craven et al., 2020). It has not been elucidated whether or not gut permeability may be worsening with liver disease severity, as most of the studies have focused on differences between steatosis grades and/or NASH rather than fibrosis stage and mainly in paediatric setting (Pacifico et al., 2014, Nobili et al., 2015).

In this study, an *in-vitro* model was set up to replicate the gut barrier based on monolayers of MDCK cells. MDCK cells have been extensively used to evaluate epithelial permeability, intestinal absorption and to assess active transport of molecules. When compared to Caco-2 cells, MDCK demonstrate similar performances as barrier models (Volpe, 2011), although MDCK is not a GI-derived cell line. Moreover, MDCK cells have the advantage of having faster replication rates, reaching confluence in 48-72 hours compared to 1-2 weeks for Caco-2. Here, the integrity of the epithelial layer was estimated using TEER, a widely accepted technique for assessing the integrity of cell barriers. Monolayers were cultured on Transwell so that the model could mirror the intestinal compartmentalisation into an apical and a baso-lateral compartment (**Figure 2.3**).

In this model, TEER was measured at different timepoints to detect changes in permeability when faecal samples were added to the apical (luminal) compartment of the model. Interestingly, the samples from patients with NAFLD and elevated LSM caused the greatest change in the TEER compared to those with normal liver. Of note, the drop in TEER was significant after 5 mins from incubation and was observed until 24 hours (**Figure 5.2**). After 24 hours, TEER was also significantly lower in samples with NAFLD and normal LSM compared to normal liver. When TEER was analysed

against clinical features, TEER *per se* had a strong, negative linear relationship with liver fibrosis, defined by liver stiffness (**Figure 5.4D**). Furthermore, TEER had a strong, negative relationship with AST values (**Figure 5.4C**).

Collectedly, these findings suggest that patients with liver disease due to NAFLD have increased gut permeability. Moreover, the extent of permeability seems to be inversely associated with the severity of liver fibrosis, as expressed by liver stiffness. Despite previous works focusing mainly on steatosis and NASH, these results show evidence that gut permeability correlates with fibrosis, which is the main clinical predictor in these patients (Estes et al., 2018).

5.4.2 Increased gut permeability is associated with visceral obesity, not glycaemic control in diabetic patients with NAFLD

Previous studies suggested that increased gut permeability may be associated with obesity and metabolic risk factors. One of the most accepted theories suggests that a leaky gut is both cause and consequence of obesity, glycaemic control and hypercholesterolaemia, with subsequent bacterial translocation and systemic pro-inflammatory status secondary to LPS (Boulange et al., 2016, Ding and Lund, 2011). In this study, there was a strong, inverse correlation between TEER and BMI (**Figure 5.4A**) as well as an inverse correlation between TEER and waist circumference (**Figure 5.4B**), suggesting a strong relationship between intestinal permeability and visceral obesity. In this sense, it has been previously described that Western diet may be responsible for changes in the gut microbiome towards a more efficient intestinal absorption of calories and increased lipid deposition, which may influence body weight (Bruel et al., 2011). Moreover, obese adults appear to have increased levels of zonulin, which are dependent on insulin resistance and are mediated by obesity-related IL-6, a cytokine which modulates the expression of zonulin in TJs (Moreno-Navarrete et al., 2012). Moreover, previous evidence suggested a link between gut permeability and host glucose levels (Gerard and Vidal, 2019). In this study, the presence and entity of gut permeability was not influenced by glycaemic control, as expressed by HbA1c.

Altogether, these results suggest a strong association between increased gut permeability and visceral adiposity. Interestingly, glycaemic control *per se* did not emerge as contributing factor in this population.

5.4.3 Increased gut permeability may be associated with bacterial proteases in diabetic patients with NAFLD

Various mediators may influence TJ structure and, therefore, paracellular permeability, such as growth factors, cytokines, intestinal bacteria, diet and proteases (Van Spaendonk et al., 2017). Specifically, proteases may exert a direct proteolytic effect on TJ proteins. Interestingly, different microorganism and/or cellular sub-types, such as bacteria, epithelial cells, inflammatory infiltrates, may contribute to the pool of proteases present within the gut.

In this in-vitro model of gut permeability, the effect of FW on membrane potential was significantly attenuated when inhibitors of bacterial proteases were added to FW from study patients, in particularly in those with NAFLD and elevated LSM (**Figure 5.3**). These results suggested that bacterial proteases were - to some extent - responsible of the suppressive effect that FW had on TEER. However, when the actual activity of protease was measured in uninhibited and inhibited FW, there was no difference across the groups in terms of absolute value and in terms of change (delta protease) (**Figure 5.6**). Of note, when interpreting such results, it should be considered that the profile of proteases detected by the protease assay kit does not necessarily overlap with the profile of proteases which are inhibited by the commercial cocktail used in this study. For instance, the protease assay detects activity from chymotrypsin, elastase, plasminogen, subtilisin, thermolysin and trypsin. Nevertheless, the cocktail of protease inhibitors targets a wider range of proteases, including aminopeptidase, cysteine and acid-protease. As such, it might be argued that some bacterial proteases among those which were not detected by the assay, could still be relevant to the model.

Taken together, these results suggest that bacterial proteases may play a role in modulating the gut permeability in diabetic patients with NAFLD and different disease severity. A more targeted approach should be used to identify the main bacterial proteases influencing the model.

5.4.4 Increased gut permeability is associated with lower faecal valerate and IFN-γ in diabetic patients with NAFLD

Overall, intestinal permeability has also been associated with specific faecal metabolites, such as glutamine, glycine and tryptophane. SCFA are also known to modulate intestinal permeability through a direct effect on TJ (Li and Neu, 2009). Moreover, experimental studies have demonstrated that SCFA can modulate regulatory cell expansion and enhance neutrophil chemotaxis in mice models (Vinolo et al., 2009, Vinolo et al., 2011).

In the whole study population, there was no difference in terms of faecal SCFA as well as in terms of metabolites of tryptophane across study groups. However, when the analysis was narrowed to the only samples used for the in-vitro model, the levels of valerate were significantly lower in those with significant fibrosis due to NAFLD compared to normal liver (**Figure 5.5**). Interestingly, specific changes in gut microbiome, such as lower abundance of *Bacteroides* and increased *Firmicutes* spp, have been previously associated with disturbances in the SCFA production, with a similar profile being observed in this population (**paragraph 4.4.6**). It might be argued that changes in gut microbiome may also contribute to the gut permeability in this model, via disturbances of specific SCFA, i.e. valerate. Interestingly, it is known from a previous study that SCFA and valerate in particular may modulate inflammation as it is a potent inhibitor of the histone deacetylases, a transcriptor factor for pro-inflammatory genes (Yuille et al., 2018).

A pro-inflammatory gut environment may also lead to an increased intestinal permeability (Fava and Danese, 2011) and susceptibility to invasive pathogens (Thiennimitr et al., 2011). However, it is currently unclear whether intestinal inflammation is at the dispensing/receiving or at both ends of gut microbiome shifts culminating in increased bacterial translocation (Riva et al., 2020). Here, the levels of IFN-γ in the stool samples of patients with significant fibrosis were significantly lower compared to those with normal liver (**Figure 5.8**). Of note, IFN-γ has emerged as a crucial modulator of the intestinal homeostasis as it limits the recruitment of inflammatory cells (Beaurepaire et al., 2009, Ost and Round, 2017) . Moreover, IFN-γ is known to regulate the MLC and therefore may enhance the paracellular permeability to molecules up to 10 kDa (Watson et al., 2005). As such, altered levels of IFN-γ may results in further accentuation in the increased gut permeability in diabetic

patients with liver disease from NAFLD. Finally, in this study, FABP-2 levels did not differ among groups, suggesting the presence of an intact intestinal epithelium in the study groups (**Figure 5.7**). Nevertheless, compared to other studies, the patients from the current study might have milder liver disease to be able to detect changes in serum FABP-2 (Graupera et al., 2017).

Collectedly, these findings suggest that increased gut permeability is associated with lower levels of valerate, which may be driven by specific changes in gut microbiome. Moreover, patients with significant fibrosis due to NAFLD show lower intestinal IFN-γ levels, which may potentially contribute to impair the intestinal barrier even further.

5.5 Strengths and limitations

This part of the project has several strengths. Firstly, the in-vitro model presented here is based on an established assessment to study epithelial permeability. Secondly, this project provides a comprehensive analysis of many factors which could be potentially associated with gut permeability, such as bacterial proteases activity, faecal metabolites and SCFA, intestinal intraluminal inflammation and integrity of the intestinal epithelium.

This study has also several limitations. Firstly, TEER is designed to measure the flow of small ions and water, as such it is suitable for the assessment of TJ but not the passage of macromolecules. Secondly, it should be noted that cell monolayers represent an established, yet simplistic model of the GI tract, as they do not include other important structures, such as Goblet cells, Paneth or neuroendocrine cells. Thirdly, ex-vivo LPS and zonulin levels were not measured in this study, due to reduced availability of samples.

5.6 Future work

Future work should focus on further characterising the determinants of this in-vitro model. Specifically, monolayers of MDCK could be stained for specific TJ proteins, such as zonulin, so that the actual differences in their expression could be assessed when exposed to FW from patients of different study groups. Moreover, repeating the experiments with TEER targeting specific bacterial protease may provide further insight. Further research should also investigate gut permeability in-

vivo in patients with NAFLD and different disease severity with regards to fibrosis and matched with gut microbiome and metabolic profiling.

5.7 Conclusions

The results from this in-vitro model of gut barrier suggest that diabetic patients with significant fibrosis duet NAFLD have an increased gut permeability. Moreover, the degree of permeability mirrors the severity of liver disease, as defined by liver stiffness. An increased gut permeability in these patients may result from a combination of factors, such as the effect of specific bacterial proteases as well as altered level of specific SCFA and intestinal inflammation.

6. SYSTEMIC INFLAMMATORY STATUS IN DIABETIC PATIENTS WITH NAFLD

6.1 Introduction

The term “metabolic inflammation” (or meta-inflammation) identifies the activation of pro-inflammatory signalling pathways and cytokine production in metabolic tissue, i.e. adipose tissue, in presence of IR and obesity. The gut-liver axis is one of the main contributors to the meta-inflammation in NAFLD. Not only a gut dysbiosis is associated with intestinal inflammation, but also with systemic inflammatory response via the translocation of bacterial products (Grabherr et al., 2019). A large number of gut metabolites have been proved to elicit a chronic inflammatory status, including ethanol production, changes in SCFA, secondary bile acids, BCAA and PAMPs (Zmora et al., 2017).

Adipose tissue also plays an important role in the development of IR and NAFLD. The rapid expansion of the adipose tissue leads to adipocyte cell death, which results into further production of inflammatory cytokines and activation of ATMs. In addition to an increase in the numbers of ATM, obesity is also associated with a change in their phenotype towards a pro-inflammatory M1 state (Lumeng et al., 2008). Moreover, it has been shown that the severity of ATM correlated with the degree of hepatic steatosis, inflammation and fibrosis in the liver (Kolak et al., 2007, Tordjman et al., 2009). Interestingly, adipose tissue may also contribute to an increased gut permeability directly, producing TNF-α, IL-1β and IL-6 and perpetuating bacterial translocation.

Hepatic inflammation results from the complex interaction of different cells populations (Luci et al., 2020, Cai et al., 2019). Briefly, the hepatocytes and the Kupffer cells interact with portal and systemic metabolites and initiate a cascade of inflammatory events and metabolic dysfunction, whereby the liver transitions from an immune-tolerant to an immune-active state (Cai et al., 2019, Hammoutene and Rautou, 2019). Overall, an altered balance between pro-inflammatory and anti-inflammatory macrophages seems to play a crucial role in the development and progression of NAFLD (Wan et al., 2014). In this sense, bacterial products, toxic lipids and adipokines may shift the

balance towards a pro-inflammatory polarization and the recruitment of further immune cells, which is the hallmark characteristic of NASH and fibrogenesis (Krawczyk et al., 2018).

To conclude, NAFLD is characterised by a systemic low-grade inflammatory status which translates into disease progression. Both the gut and the adipose tissue contribute to the maintenance of such pro-inflammatory status, and therefore to liver injury. However, the complex interplay between gut, adipose tissue and liver has not been fully elucidated.

Therefore, the main objectives of this part of the project were

1. To analyse the inflammatory status of diabetic patients screened for NAFLD

2. To explore the clinical and metabolic factors associated with the inflammatory status in diabetic patients screened for NAFLD

6.2 Materials and methods

6.2.1 Biological samples

Serum samples were collected, processed and stored as per the Hepatology and Gastroenterology divisional standard operating procedure.

6.2.2 Measurement of serum cytokines and PAI-1 level

The serum levels of IFN-γ, IL-1β, IL-2, IL-4, IL-6, IL-8 (CXCL8), IL-10, IL-12p70, IL-13, and TNF-α were measured using the V-plex Proinflammatory Panel 1 (MSD), which is essentially a sandwich immunoassay. The serum level of PAI-1 was measured using a Human Serpin E1/PAI-1 Quantikine ELISA Assay (R&D systems, USA) Kit, which is essentially a sandwich ELISA.

6.2.3 Statistical analysis and regulatory approval

The distribution of variables was explored using the Shapiro-Wilk test. Continuous variables were reported as medians and IQR, while categorical variables were expressed as relative

frequencies and percentages. Univariate analysis was carried out using Mann-Whitney for continuous, and chi-square test for categorical variables respectively. Kruskal-Wallis or ANOVA with post-hoc corrections was used for comparison between multiple groups. Spearman correlation and logistic regression carried out to explore the relationship between variables. All tests were two-sided and a *P* value 0.05 was considered significant. Statistical analysis was performed by GraphPad Prism (version 9.1) and SPSS (version 24.0; SPSS Inc Chicago, IL).

6.3 Results

6.3.1 Serum cytokines

6.3.1.1 Patient samples

A total of 139 serum samples were tested for cytokines level using the V-plex proinflammatory panel 1. Specifically, 42 (30%) patients had normal liver, 57 (41%) patients NAFLD and normal LSM, while 40 (28%) patients NAFLD and elevated LSM.

6.3.1.2 Measurement of cytokines in serum samples

Overall, those with NAFLD and elevated LSM showed significantly higher levels of serum IFN-γ compared to those with NAFLD and normal LSM (7.09 vs 3.5 pg/ml, p=0.02) and compared to normal liver (7.09 vs 4.2 pg/m, p=0.003) (**Figure 6.1**). Moreover, patients with significant fibrosis showed significantly higher serum levels of IL-2 (p=0.02), IL-4 (p=0.04) and IL-6 (1.6 vs 0.77 pg/ml, p<0.0001) (**Figure 6.1**). Similarly, serum levels of IL-8 (18.7 vs 14.7 pg/ml, p=0.0001), IL-10 (0.07 vs 0.0 pg/ml, p=0.001) and TNF-α (0.4 vs 0.9 pg/ml, p=0.004) were also significantly higher in those with NAFLD and elevated LSM compared to normal liver (**Figure 6.2**). However, there was no difference in terms of levels of serum IL-1β, IL-12p70 and IL-13 across study groups. Median values of serum cytokines are displayed in **Table 6.1**.

When patients were matched for metabolic factors (i.e HbA1c, HOMA index, BMI), only IFN-γ (p=0.04), IL-6 (p=0.009), IL-8 (p=0.009) and TNF-α (p=0.05) were still significantly higher in those with significant liver disease due to NAFLD compared to those with normal liver. Overall, IL-2 and IL-4 correlated with HOMA index (Rho=0.21, p=0.013 and Rho=0.23, p=0.003), while IL-10 was associated with waist circumference (Rho=0.26, p=0.002), BMI (Rho=0.21, p=0.012) and HOMA index (Rho=0.22, p<0.0001). In terms of LFTs, IL-6 and TNF-alpha correlated with AST (Rho=0.24, p=0.004 and Rho=0.22, p=0.009) but not ALT.

On multivariate analysis, only IL-6 was able to predict the presence of significant (LSM≥8.1 kPa) and advanced (LSM≥12.1 kPa) fibrosis with crude OR 1.97 (95%CI 1.24-3.14, p=0.04) and OR 1.86 (95%CI 1.18-2.94, p=0.007) respectively (**Table 6.2**).

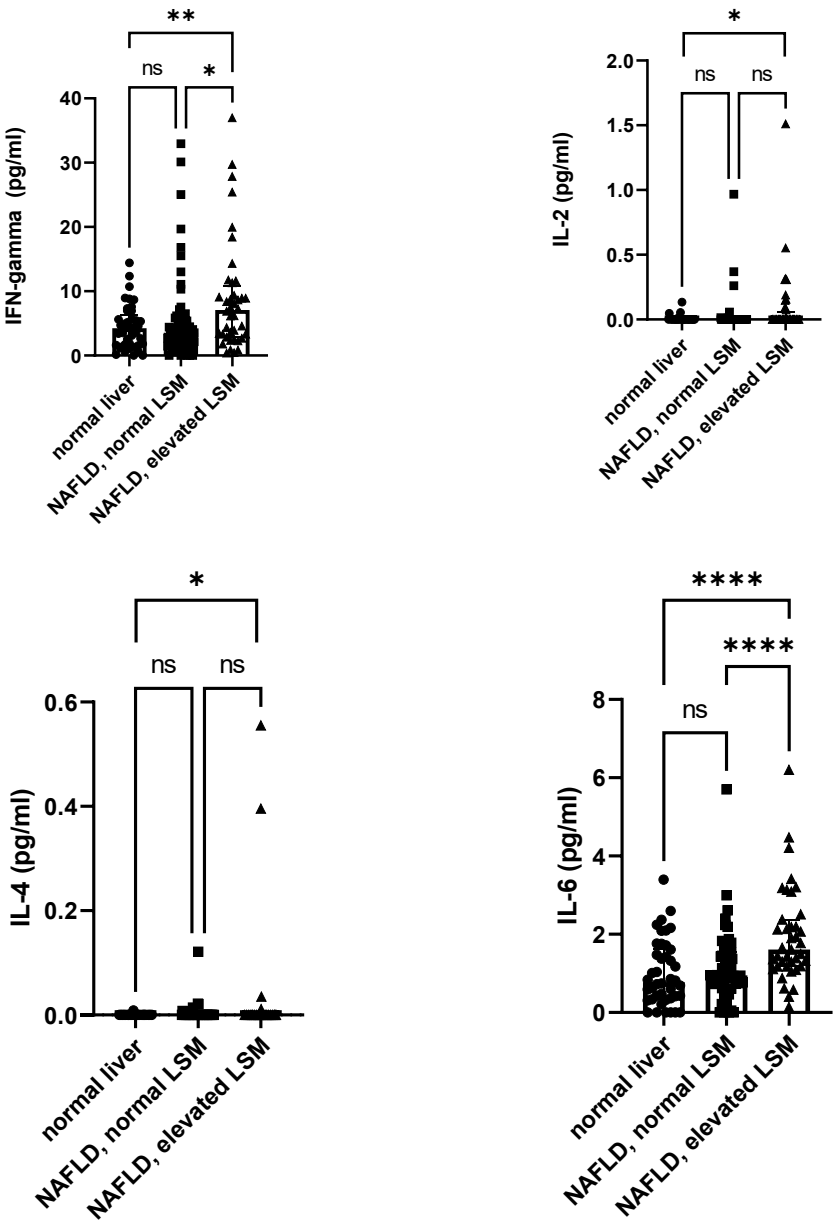

Figure 6.1. Levels of IFN-γ, IL-2, IL-4 and IL-6 in serum samples and comparison between study groups. The scatter plot graph illustrates single values of serum IFN-γ, IL-2, IL-4 and IL-6 and differences among study groups: normal liver (n=42), NAFLD with normal LSM (n=57) and NAFLD with elevated LSM (n=401).
Abbreviations: NAFLD: non-alcoholic fatty liver disease, LSM: liver stiffness measurement, IFN-γ: interferon gamma, IL-2: interleukin-2, IL-4: interleukin-4, IL-6: interleukin-6.

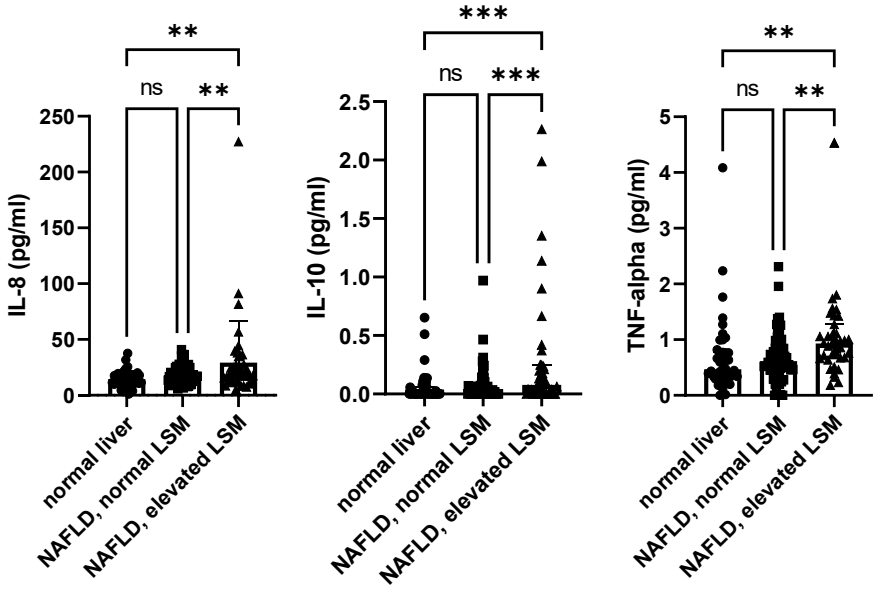

Figure 6.2. Levels of IL-8, IL-10 and TNF-α in serum samples and comparison between study groups. The scatter plot graph illustrates single values of faecal IL-8, IL-10 and TNF-α: normal liver (n=42), NAFLD with normal LSM (n=57) and NAFLD with elevated LSM (n=401).
Abbreviations: NAFLD: non-alcoholic fatty liver disease, LSM: liver stiffness measurement, IL-8: interleukin-8, IL-10: interleukin-10, TNFα-tumour necrosis factor-alpha.

	Normal liver (N=42)	NAFLD, normal LSM (N=57)	NAFLD, elevated LSM (N=40)
		MEDIAN (IQR)	
IFN-Γ, *pg/ml*	4.2 (1.5-6.2)	3.5 (1.5-5.9)	7.09 (2.9-10.8)
IL-1β, *pg/ml*	0.05 (0.05-0.05)	0.05 (0.05-0.05)	0.05 (0.05-0.05)
IL-2, *pg/ml*	0.09 (0.09-0.09)	0.09 (0.09-0.09)	0.09 (0.09-0.09)
IL-4, *pg/ml*	0.02 (0.02-0.02)	0.02 (0.02-0.02)	0.02 (0.02-0.02)
IL-6, *pg/ml*	0.7 (0.3-1.6)	0.9 (0.6-1.5)	1.6 (1.1-2.3)
IL-8, *pg/ml*	14.7 (10.2-17.4)	16.5 (12.4-24.3)	18.7 (12.2-32.9)
IL-10, *pg/ml*	0.04 (0.04-0.06)	0.04 (0.04-0.07)	0.07 (0.04-0.2)
IL-12p70, *pg/ml*	0.11 (0.11-0.11)	0.11 (0.11-0.11)	0.11 (0.11-0.11)
IL-13, *pg/ml*	0.24 (0.24-0.24)	0.24 (0.24-0.24)	0.24 (0.24-0.24)
TNF-α, *pg/ml*	0.4 (0.32-0.78)	0.61 (0.45-0.84)	0.9 (0.67-1.2)

Table 6.1 Concentrations of serum cytokines. This table shows median values and related IQR of levels of serum cytokines in the study groups.
Abbreviations: IQR: interquartile range, IFN-γ: interferon gamma, IL-1β: interleukin-1beta, IL-2: interleukin-2, IL-4: interleukin-4, IL-6: interleukin-6, IL-8: interleukin-8, IL-10:interleukin-10, IL-12p70: interleukin-12p70, IL-13: interleukin-13, TNF-α: tumor necrosis factor alpha.

	MULTIVARIATE ANALYSIS			
	LSM≥8.1 kPa		**LSM≥12.1 kPa**	
	OR (95%CI)	**p-value**	**OR (95%CI)**	**p-value**
IFN-Γ, *pg/ml*	0.98 (1-0.96)	NS	1.007 (0.97-1.04)	NS
IL-6, *pg/ml*	**1.97 (1.24-3.14)**	**0.04**	**1.86 (1.18-2.93)**	**0.007**
IL-10, *pg/ml*	8.9 (0.8-32.8)	NS	1.31 (0.35-4.7)	NS
TNF-α, *pg/ml*	1.2 (0.8-1.89)	NS	1-12 (0.65-1.92)	NS

Table 6.2 Multivariate analysis showing serum cytokines associated with significant or advanced fibrosis. This table shows OR for multivariate analysis to predict the presence of significant (LSM≥8.1 kPa) and advanced (LSM≥12.1 kPa) fibrosis in the diabetic population (n=139).
Abbreviations: OR: odds ratio, LSM: liver stiffness measurement, IFN-γ: interferon gamma, IL-6: interleukin-6, IL-10: interleukin-10, TNF-α: tumour necrosis factor alpha.

6.3.1.3 Systemic inflammatory status and metabolic profile

Serum metabolites and cytokines from the same study samples were matched and analysed. Overall, TNF-α was positively associated with glutamate/glutamine (Rho=0.14, p=0.04), mainly driven by association with glutamate (Rho= 0.21, p=0.01) rather than glutamine (Rho= -0.15, p=0.07) (**Figure 6.3**). Of note, IL-6 (Rho= -0.27, p=0.001) and TNF-α (Rho= -0.21, p=0.014) were inversely associated with serum lysine levels (**Figure 6.4**).

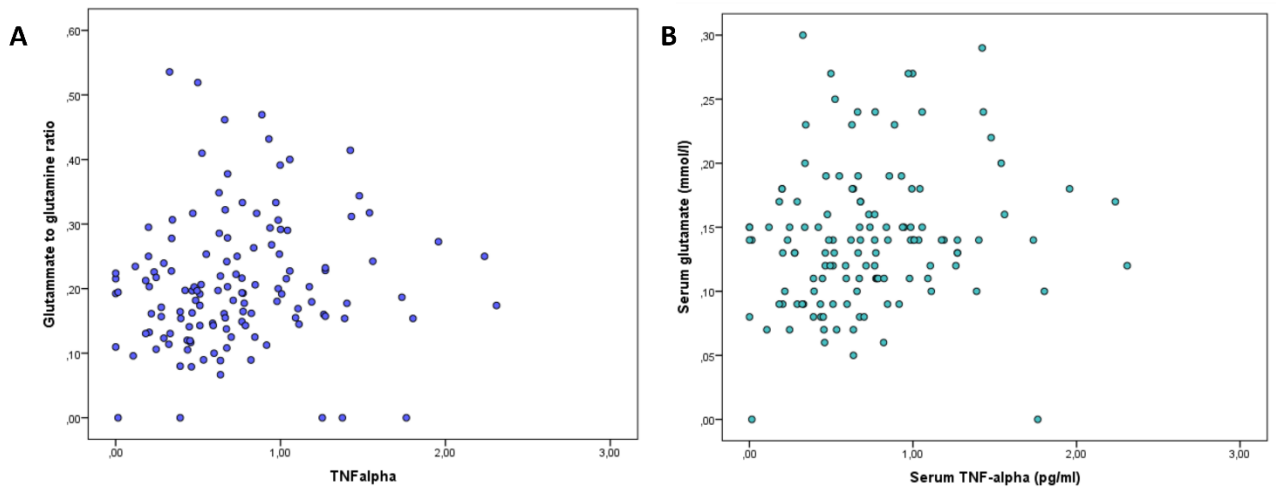

Figure 6.3. Association between serum TNF-α and glutaminolysis. This scatter dot graph illustrates values for single samples. Figure 6.3A) illustrates TNF-α vs glutamate to glutamine ratio, while Figure 6.3B) illustrates TNF-α vs glutamate.
Abbreviations: TNF-α: tumour necrosis factor-alpha.

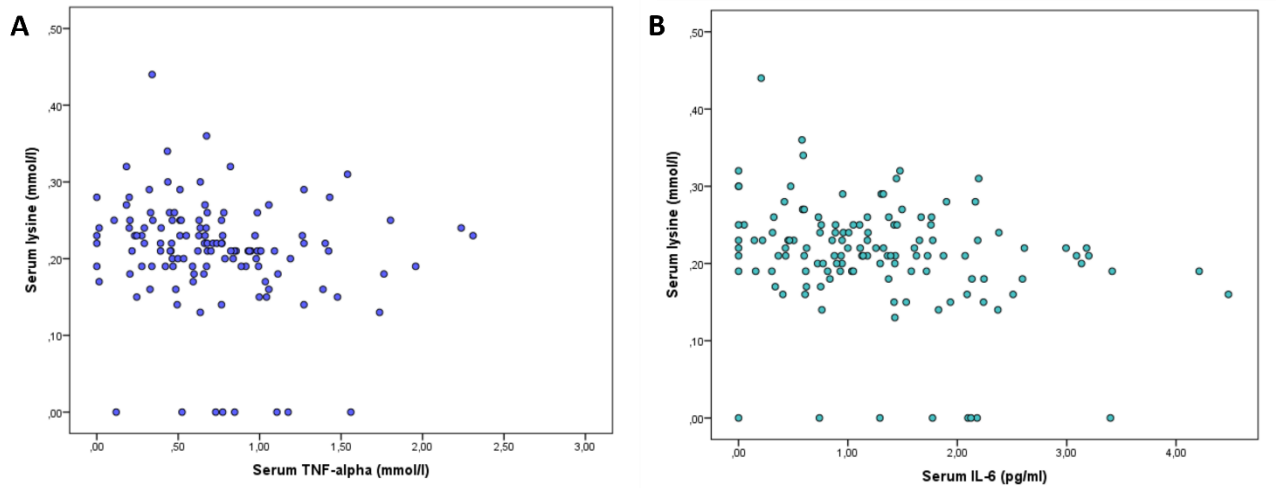

Figure 6.4. Association between serum cytokines and lysine. This scatter dot graph illustrates values for single samples. Figure 6.4A) illustrates TNF-α vs lysine, while Figure 6.4B) illustrates IL-6 vs lysine.
Abbreviations: TNF-α: tumour necrosis factor-alpha, IL-6: interleukin-6.

6.3.2 Plasminogen activator inhibitor-1

6.3.2.1 Patient samples

A total of 92 serum samples were tested for PAI-1. Specifically, 30 (32%) patients were diagnosed with normal liver, 33 (36%) patients with NAFLD and normal LSM, while 33 (36%) patients with NAFLD and elevated LSM. Fifteen serum samples from healthy controls were also included as a comparator for the analysis.

6.3.2.2 Measurement of PAI-1 in serum samples

Median serum concentration for PAI-1 was 6.4 (2.7-12.8) ng/ml in those with normal liver, 9.5 (2.5-14.3) ng/ml in those with NAFLD and normal LSM, 8.2 (1.2-13.7) ng/ml in those with NAFLD and elevated LSM. Overall, there was no difference in terms of levels of serum PAI-1 across study groups (**Figure 6.5**). However, healthy controls showed significantly higher PAI-1 levels compared to all study groups.

When patients were matched for metabolic factors, PAI-1 levels were not significantly different between those with significant liver disease due to NAFLD vs those with normal liver (p=0.81). Moreover, when patients were matched for metabolic factors and LSM, there was no difference in terms of PAI-1 levels between NAFLD vs normal liver (p=0.18). In terms of other clinical features, PAI *per se* only correlated with CAP score (Rho=0.27, p=0.022), HOMA index (Rho=0.36, p=0.002) and HbA1c (Rho=0.023, p=0.05).

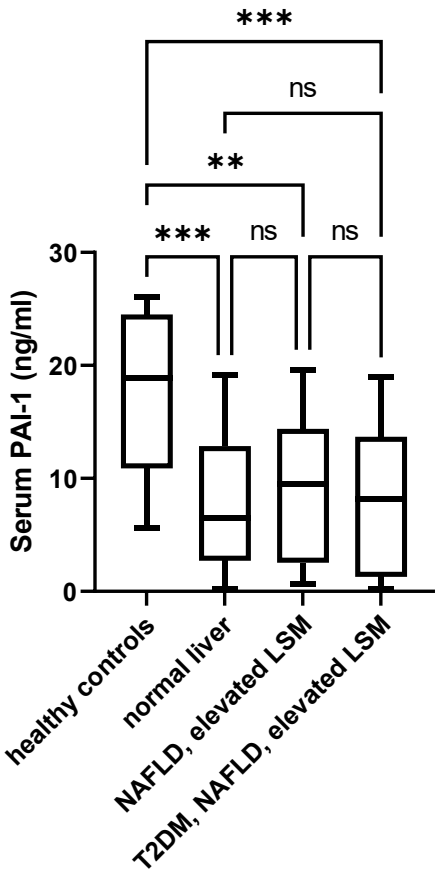

Figure 6.5. Plasminogen activator inhibitor-1 measurement in serum samples and difference between study groups. The box plot illustrates median values of PAI-1 in serum samples and corresponding 95%CI with differences among study groups: normal liver (n=30), NAFLD with normal LSM (n=33) and NAFLD with elevated LSM (n=33).
Abbreviations: 95%CI: 95% confidence interval, NAFLD: non-alcoholic fatty liver disease, LSM: liver stiffness measurement, PAI-1: plasminogen activator inhibitor-1

6.4 Discussion

6.4.1 Serum cytokine profile suggests an underlying macrophages activation in diabetic patients with NAFLD and liver fibrosis

In a status of normal BMI, the ATM are located throughout the adipose tissue and show predominant M2-like phenotype (Lumeng et al., 2008). Conversely, models of diet-induced obesity demonstrated that fat remodelling is associated with changes towards the M1 phenotype activation and proliferation (Lumeng et al., 2008). In humans, visceral adipose tissue has been shown to be enriched by clusters of macrophages producing IL-6 and TNF-alpha. In obese patients with NAFLD, crown-like structures of macrophages from the subcutaneous adipose tissue correlated with liver

fibrosis scores (Tordjman et al., 2009). Moreover, portal inflammation, a hepatic histological feature previously associated with disease progression in human patients, is mainly constituted of macrophages (Wan et al., 2014). Interestingly, sCD163, a marker of liver macrophages activation, was increased proportionally with severity of liver disease and improved along with metabolic profile in patients undergoing bariatric procedures and weight loss (Kazankov et al., 2015).

In this study, patients with significant fibrosis due to NAFLD showed a cytokine profile suggestive of a M1 macrophage activation, with higher IFN-γ, TNF-α, IL-4, IL-6 and IL-8. Furthermore, the inflammatory status was associated with specific metabolites in the serum. Specifically, TNF-α correlated with increased glutamate to glutamine ratio, while TNF-α and IL-6 had an inverse relationship with serum lysine. In terms of glutaminolysis, a combination of metabolic risk factors as well as an increased macrophage activation may be driving the increase glutamate to glutamine ratio in those with significant fibrosis, although this does not necessarily reflect an increased hepatic fibrosis. Interestingly, both TNF-α and IL-6 were associated with lower levels of serum lysine, which has previously been identified as the only metabolite associated with fibrosis in this population, independently of metabolic risk factors.

As metabolic syndrome *per se* carries a certain degree of low-grade chronic inflammation, it is difficult to disentangle the independent association between liver fibrosis due to NAFLD and the inflammatory status. As an attempt to overcome this issue, patients were matched for metabolic risk factors so that a specific cytokine profile associated with liver fibrosis could be identified. In this sub-analysis, only IFN-γ, IL-6, IL-10 and TNF-α remained still significantly enhanced in those with significant liver disease due to NAFLD. Of note, TNF-α has been shown to increase gut permeability, via a disturbance of TJs which may increase bacterial products translocation and therefore perpetuate the inflammatory crosstalk between gut and the liver (Wigg et al., 2001).

Collectedly, these results suggest that patients with more severe liver disease have an overall M1 macrophage activation. Not only such inflammatory milieu may influence metabolic status but may also sustain a dysfunctional gut-liver crosstalk via modulating the gut permeability.

6.4.2 Levels of serum IL-6 are strongly associated with liver fibrosis in diabetic patients with NAFLD

IL-6 plays a crucial role in modulating the relationship between adipose tissue and the liver. Of note, IL-6 represents the major inducer of the hepatic acute phase proteins in the liver. It also plays a crucial role in liver regeneration. Previous studies demonstrated that both subcutaneous and visceral adipose tissue represent the major sources of IL-6 in humans (Bastard et al., 2002), while the liver represents the main target (Moschen et al., 2010). Specifically, IL-6 signalling seems to be directly involved in modulating hepatic metabolism and insulin resistance, mainly via the activation of insulin associated pathways, such as JNK1 and SOC3.

In this population of patients with T2DM, IL-6 levels increased proportionally with BMI and HOMA index, suggesting a direct association with worsening metabolic syndrome. Interestingly, previous studies showed that adipose tissue, rather than the liver is the main producer of circulating IL-6 (Moschen et al., 2010). Among all serum cytokines, IL-6 was the only one associated with significant and advanced fibrosis in NAFLD, with an OR of 1.97 (95%CI 1.24-3.14, p=0.04) and 1.86 (95%CI 1.18-2.93, p=0.007) respectively. Interestingly, IL-6 also correlated with AST but not ALT levels, suggesting a link between pro-inflammatory status and abnormal liver function tests. It was previously shown that drastic weight loss may result into decreased IL-6 production and into an increase in adiponectin levels in the liver (Moschen et al., 2010) . In a clinical perspective, decreased IL-6 levels may explain the improvement in AST which is usually observed in patient with NAFLD who report weight loss. Moreover, similarly to TNF-α, IL-6 may also induce disturbances in TJs in the intestinal epithelium, perpetuating an increased gut permeability even further (Suzuki et al., 2011).

Taken together, these results suggest that higher levels of serum IL-6 are independently associated with fibrosis in diabetic patients screened for NAFLD. In these patients, IL-6 is involved at the crosstalk between gut-liver axis and adipose-tissue liver axis.

6.5 Strengths and limitations

This part of the project presents some limitations. Overall, the inflammatory status was analysed as serum cytokine levels only, while there were no functional studies or immunohistochemistry experiments. However, studying the inflammatory status *per se* was not among the primary objectives of the study. Conversely, a general overview of the cytokine levels was included to allow for a more comprehensive interpretation of the clinical as well as the metabolic profile of the patients – which is therefore a strength of the study. Future works are required to explore more in details the effect of inflammation in modulating adipose tissue-liver axis as well as the gut-liver axis.

6.6 Conclusions

In this population of diabetics from primary care, patients with liver fibrosis from NAFLD have a cytokine profile in keeping with macrophage activation. Among other cytokines, IL-6 is the main predictor of advanced liver disease in these patients.

7. SUMMARY AND CONCLUSIONS

This thesis aimed to explore the prevalence of clinically significant NAFLD in patients with type 2 diabetes mellitus in primary care and to elaborate a risk-stratification for NAFLD in this population. Moreover, this work aimed to explore the metabolic profiles and potential abnormalities of the gut-liver axis which identify patients with more severe liver disease and/or reveal pathogenetic mechanism.

The work in chapter 3 reported a high prevalence of NAFLD and clinically significant liver disease in patients with diabetes in primary care. This work reports the results of a comprehensive screening of diabetic patients from primary care. In this population, visceral adiposity (as expressed with BMI and waist circumference), AST and education attainment (as expressed by education rank from the Index of Multiple Deprivation) were found to correlate with the presence of liver fibrosis in this population. A new score (the BIMAST score) could accurately identify those with significant and advanced fibrosis. The score was validated both internally and in two external cohorts. When compared to established screening methods, the BIMAST score performed better and improved false negative scores, translated to patients with liver disease who could have been missed by screening.

Chapter 4, 5 and 6 explored the metabolic profile and the alterations of the gut-liver axis against severity of liver disease in this population. In chapter 4, a wide range of metabolites was analysed in an attempt to identify possible biomarkers for the disease. Overall, glycine deficiency was characteristically associated with the presence of steatosis but did not correlate with severity of liver disease. Despite being a strong predictor of liver fibrosis, an increased hepatic glutaminolysis, and glutamate to glutamine ratio, were mainly reflective of worse metabolic risk factors (glycaemic control, visceral adiposity, insulin resistance) rather than hepatic collagen content *per se*. Conversely, lysine deficiency did mirror the extent of hepatic fibrosis and this was independent from the presence of other metabolic risk factors. However, these significant findings emerged only in a matched-group analysis, suggesting that measuring serum lysine may be of limited use as biomarker

in a large, unselected primary care population. Finally, urinary metabolites were probably more reflective of glycaemic control and, possibly, glycosuria, rather than of liver disease severity.

The work in chapter 5 focused on investigating factors associated with gut permeability using an in-vitro model as well as *ex-vivo* analyses of samples obtained from the patients enrolled in the study. Overall, there was evidence suggesting that gut permeability increases with the severity of liver disease, defined by liver stiffness measurement. Interestingly, a leakier gut was associated with worsening visceral obesity, a mechanism which could potentially be mediated by higher levels of circulating IL-6 and TNF-alpha and their effect on intestinal TJs. Moreover, an intestinal milieu with lower level of specific short chain fatty acid (valerate) and impaired cytokine levels (IFN-gamma) might favour the development of a leakier gut in these patients. Finally, these data also suggested that an augmented activity of bacterial proteases on the luminal side may contribute to a reduced epithelial integrity. Specific changes in the gut microbiota, i.e. lower abundance of pectin-degraders and higher abundance of Firmicutes may translate into altered production of short chain fatty acids and release of intraluminal cytokines. Furthermore, microbial changes in the gut were also associated with shifts in bile acid profile in the stools, while conjugated lithocholic acid was increased in the serum samples of patients with more severe liver disease.

Finally, chapter 6 reported the analysis of systemic inflammatory status in patients with different disease severity. Overall, cytokine profile suggested a macrophage activation, which was independent of the presence of metabolic risk factors. Moreover, IL-6 was the main cytokine associated with severity of liver disease and this may be an important player in the gut-liver-adipose tissue axis.

7.1 Is it possible to improve the risk-stratification in patients with T2DM with regards to screening for NAFLD in primary care?

The results from this study confirm that clinically significant NAFLD is highly prevalent in the diabetic community. With 4.95 million people expected to have T2DM by 2030 in the UK, almost 3.16 million will have NAFLD, including 841.000 with significant liver disease and 14.800 with cirrhosis. There is a strong need for diagnosing liver disease early in the community, with GPs being at the forefront for identifying these cases. Current EASL guidelines suggest using non-invasive markers of fibrosis for screening such as FIB-4 in diabetic patients and refer those with FIB-4>1.3 to secondary/tertiary care for a fibroscan; if liver stiffness is greater than 8.1 kPa they should be seen by hepatologists. According to the results of this study, applying FIB-4 with a cut-off of 1.3 in this population would miss up to 38% of the patients with significant liver disease. Of note, those misclassified by FIB-4 were on average younger and had lower, within-normal-limit AST compared to those who were classified by FIB-4 correctly. These observations highlight a limitation of the FIB-4, as this was developed in tertiary care population and, therefore, performs well in identifying patients with abnormal LFTs and in their middle age. This is the first study demonstrating such limitation in a well phenotyped population with type 2 diabetes patients screened in primary care. The first step was to develop a tailored, primary-care derived score, the BIMAST score. Of note, the BIMAST score has been shaped based on a diabetic population from a large and multi-ethnic urban area, which also represents different lengths of disease, diabetic complications and glycaemic status. Overall, the BIMAST score outperformed other screening methods for identifying both significant and advanced fibrosis. Moreover, applying the BIMAST score would reduce the percentage of patients missed at screening from 38% to 10% compared to current risk-stratification and management pathway (**Figure 7.1**).

To conclude, the BIMAST score could potentially improve the risk-stratification for NAFLD in patients with T2DM in the community. A cost-effectiveness analysis will be required to further support the use of the score in clinical practice. Further validation in other primary care populations is also warranted.

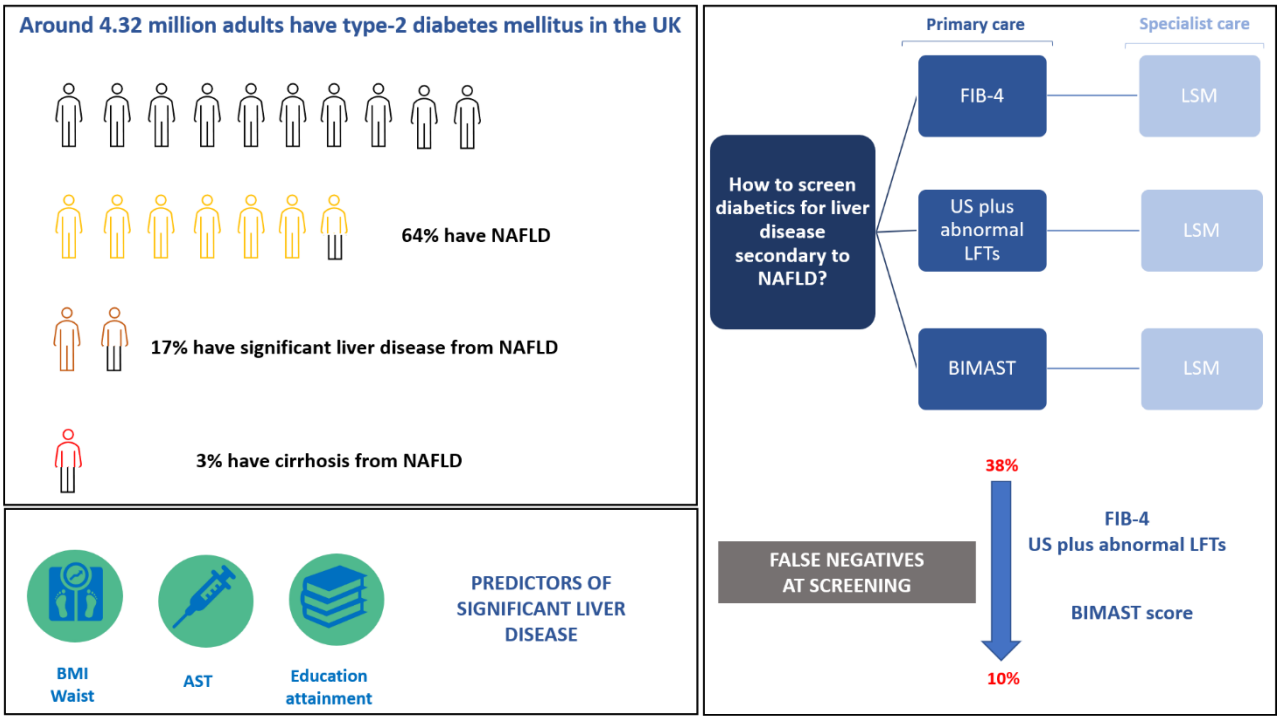

Figure 7.1. Prevalence of clinically significant NAFLD and screening pathway for diabetics in primary care. Around 4.32 million adults have T2DM in the UK. In this study, the prevalence of NAFLD, based on US, was 64%. The prevalence of significant liver disease (defined as LSM≥8.1 kPa) and cirrhosis (either clinically diagnosed or histology proven) was 3%. In this population, predictors of significant liver disease were BMI, waist circumference, AST levels and education attainment (expressed as IMD education rank). Current screening strategies include performing FIB-4 or US plus LFTs, according to different guidelines. Both strategies show a 38% rate of false negative who are missed at screening. Using the BIMAST score, a score derived from this population, the rate of false negatives reduces to 10%.
Abbreviations: NAFLD: non-alcoholic fatty liver disease, LSM: liver stiffness measurement, T2DM: type-2 diabetes mellitus, IMD: index of multiple deprivation, US: ultrasound, LFTs: liver function tests, FN: false negative.

7.2 Clinical translation and therapeutical targets

The results from this study confirm that the gut-liver axis plays an important role in the pathogenesis of NAFLD. It also represents an important therapeutical target for treatment. One of the key findings of this study was that intestinal permeability increased proportionally with severity of liver disease, defined by liver stiffness measurement. On a pathophysiological point of view, an increased intestinal permeability leads to an augmented translocation of bacterial products and, therefore, increased systemic inflammatory response and intrahepatic inflammation and fibrogenesis.

Unfortunately, there are no therapeutic targets available at present, aiming at gut barrier. One could, however, manipulate the factors associated with increased gut permeability, as they could have an impact on progression of liver disease in these patients. In terms of microbiome

composition, interventions aimed at increasing the abundance of pectin-degrading species should be explored, such as administration of rich in fibres dietary products, faecal transplantation or probiotics. Moreover, changing the microbiome towards a lower *Firmicutes/Bacteroidetes* ratio may restore the production of short chain fatty acids (i.e. valerate or its precursor, propionate) and intestinal cytokines (i.e IFN-gamma) which are crucial for the preservation of the intestinal barrier integrity. Future studies should aim on identifying specific bacterial proteases that could impact gut permeability. Inhibiting specific proteases may be another therapeutical target to restore the intestinal barrier in these patients (**Figure 7.2**).

Finally, measuring the gut permeability in-vivo may become part of the clinical work-up in patients with NAFLD, as this could identify patients with liver disease who may benefit the most from intestinal barrier interventions.

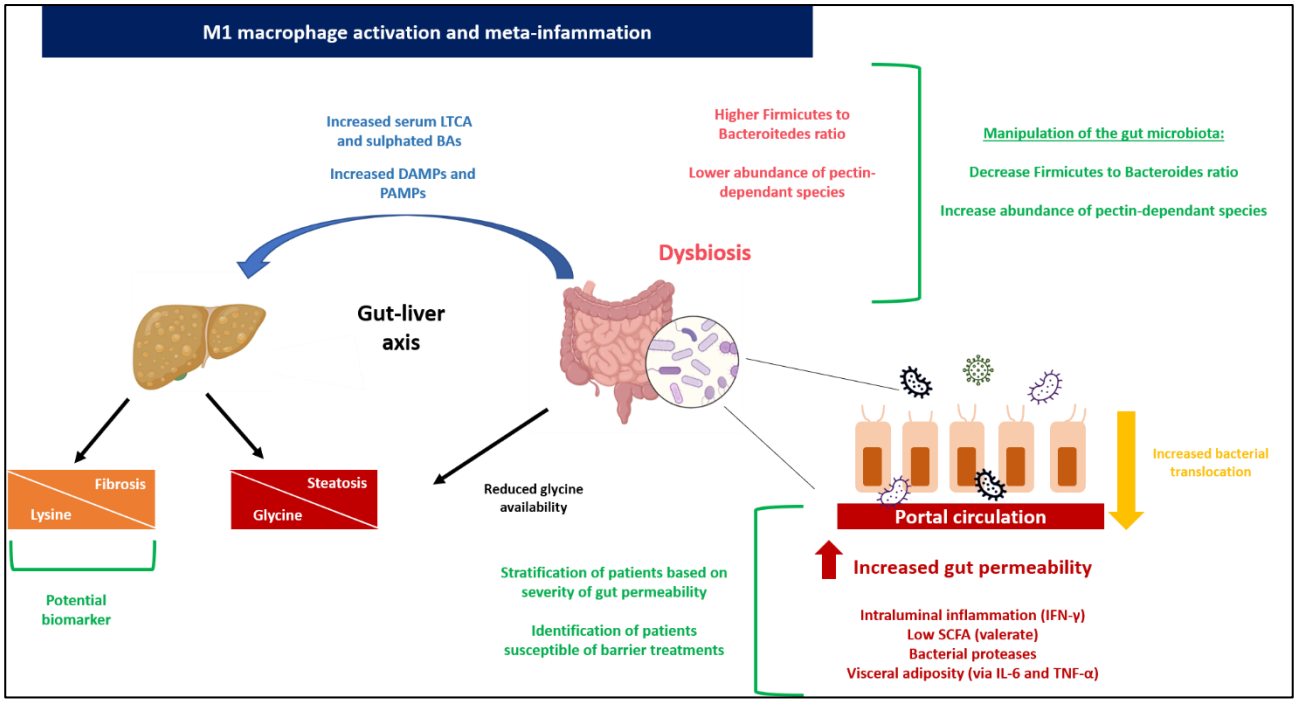

Figure 7.2. Clinical translation and therapeutic targets. This figure illustrates the main findings arising from this study with regards to metabolic profile and the alterations of the gut-liver axis in diabetic patients screened for NAFLD in primary care. Glycine deficiency in serum was associated with greater hepatic fat content and likely resulted from reduced glycine availability. Lysine deficiency in serum was associated with increased hepatic collagen content and likely associated with consumption of lysine during fibrogenesis. Specific dysbiosis as higher Firmicutes to Bacteroitedes ratio as well as lower abundance of pectin-dependant species were observed in those with more severe liver disease. Moreover, intestinal permeability was increased in those with more severe liver disease, as a result of impaired intraluminal inflammation (IFN-γ), SCFA level (valerate), bacterial proteases and visceral adiposity (mediated via IL-6 and TNF-α). Dysbiosis translates into changes in bile acid profile (increased serum LTCA and sulphated Bas) as well as hypothesized increased release of DAMPs and PAMPs. Overall, there was a M1 macrophage activation and meta-inflammation, as

assessed by systemic cytokine levels. Possible clinical translation and therapeutical targets are highlighted in green.
Abbreviations: LTCA: litocholic acid, DAMP: damage-associated molecular pattern, PAMP: pathogen-associated molecular pattern, IFN-γ: interferon-gamma, SCFA: short chain fatty acid, IL-6: interleukin-6, TNF-α: tumour necrosis factor-alpha.

REFERENCES

ABADIE, C., HUG, M., KUBLI, C. & GAINS, N. 1994. Effect of cyclodextrins and undigested starch on the loss of chenodeoxycholate in the faeces. *Biochem J,* 299 (Pt 3)**,** 725-30.

ABELES, R. D., MULLISH, B. H., FORLANO, R., KIMHOFER, T., ADLER, M., TZALLAS, A., GIANNAKEAS, N., YEE, M., MAYET, J., GOLDIN, R. D., THURSZ, M. R. & MANOUSOU, P. 2019. Derivation and validation of a cardiovascular risk score for prediction of major acute cardiovascular events in non-alcoholic fatty liver disease; the importance of an elevated mean platelet volume. *Aliment Pharmacol Ther,* 49**,** 1077-1085.

ABEYSEKERA, K. W. M., FERNANDES, G. S., HAMMERTON, G., PORTAL, A. J., GORDON, F. H., HERON, J. & HICKMAN, M. 2020. Prevalence of steatosis and fibrosis in young adults in the UK: a population-based study. *Lancet Gastroenterol Hepatol,* 5**,** 295-305.

ACALOVSCHI, M., TIRZIU, S., CHIOREAN, E., KRAWCZYK, M., GRUNHAGE, F. & LAMMERT, F. 2009. Common variants of ABCB4 and ABCB11 and plasma lipid levels: a study in sib pairs with gallstones, and controls. *Lipids,* 44**,** 521-6.

ADAMS, L. A., HARMSEN, S., ST SAUVER, J. L., CHARATCHAROENWITTHAYA, P., ENDERS, F. B., THERNEAU, T. & ANGULO, P. 2010. Nonalcoholic fatty liver disease increases risk of death among patients with diabetes: a community-based cohort study. *Am J Gastroenterol,* 105**,** 1567-73.

ADAMS, L. A., ROBERTS, S. K., STRASSER, S. I., MAHADY, S. E., POWELL, E., ESTES, C., RAZAVI, H. & GEORGE, J. 2020. Nonalcoholic fatty liver disease burden: Australia, 2019-2030. *J Gastroenterol Hepatol,* 35**,** 1628-1635.

AGUIRRE, M., JONKERS, D. M., TROOST, F. J., ROESELERS, G. & VENEMA, K. 2014. In vitro characterization of the impact of different substrates on metabolite production, energy extraction and composition of gut microbiota from lean and obese subjects. *PLoS One,* 9**,** e113864.

AHMAD, R., RAH, B., BASTOLA, D., DHAWAN, P. & SINGH, A. B. 2017. Obesity-induces Organ and Tissue Specific Tight Junction Restructuring and Barrier Deregulation by Claudin Switching. *Sci Rep,* 7**,** 5125.

AL-SADI, R., GUO, S., YE, D., DOKLADNY, K., ALHMOUD, T., EREIFEJ, L., SAID, H. M. & MA, T. Y. 2013. Mechanism of IL-1beta modulation of intestinal epithelial barrier involves p38 kinase and activating transcription factor-2 activation. *J Immunol,* 190**,** 6596-606.

ALBHAISI, S. A. M. & SANYAL, A. J. 2021. New drugs for NASH. *Liver Int,* 41 Suppl 1**,** 112-118.

ALBILLOS, A., DE GOTTARDI, A. & RESCIGNO, M. 2020. The gut-liver axis in liver disease: Pathophysiological basis for therapy. *J Hepatol,* 72**,** 558-577.

ALVAREZ-MERCADO, A. I., NAVARRO-OLIVEROS, M., ROBLES-SANCHEZ, C., PLAZA-DIAZ, J., SAEZ-LARA, M. J., MUNOZ-QUEZADA, S., FONTANA, L. & ABADIA-MOLINA, F. 2019. Microbial Population Changes and Their Relationship with Human Health and Disease. *Microorganisms,* 7.

ALVES, A., BASSOT, A., BULTEAU, A. L., PIROLA, L. & MORIO, B. 2019. Glycine Metabolism and Its Alterations in Obesity and Metabolic Diseases. *Nutrients,* 11.

ANDERSON, J. L., EDNEY, R. J. & WHELAN, K. 2012. Systematic review: faecal microbiota transplantation in the management of inflammatory bowel disease. *Aliment Pharmacol Ther,* 36**,** 503-16.

ANDO, Y. & JOU, J. H. 2021. Nonalcoholic Fatty Liver Disease and Recent Guideline Updates. *Clin Liver Dis (Hoboken),* 17**,** 23-28.

ANGULO, P., HUI, J. M., MARCHESINI, G., BUGIANESI, E., GEORGE, J., FARRELL, G. C., ENDERS, F., SAKSENA, S., BURT, A. D., BIDA, J. P., LINDOR, K., SANDERSON, S. O., LENZI, M., ADAMS, L. A., KENCH, J., THERNEAU, T. M. & DAY, C. P. 2007. The NAFLD fibrosis score: a noninvasive system that identifies liver fibrosis in patients with NAFLD. *Hepatology,* 45**,** 846-54.

ARAB, J. P., KARPEN, S. J., DAWSON, P. A., ARRESE, M. & TRAUNER, M. 2017. Bile acids and nonalcoholic fatty liver disease: Molecular insights and therapeutic perspectives. *Hepatology,* 65**,** 350-362.

ARANHA, M. M., CORTEZ-PINTO, H., COSTA, A., DA SILVA, I. B., CAMILO, M. E., DE MOURA, M. C. & RODRIGUES, C. M. 2008. Bile acid levels are increased in the liver of patients with steatohepatitis. *Eur J Gastroenterol Hepatol,* 20**,** 519-25.

ARMSTRONG, M. J., HOULIHAN, D. D., BENTHAM, L., SHAW, J. C., CRAMB, R., OLLIFF, S., GILL, P. S., NEUBERGER, J. M., LILFORD, R. J. & NEWSOME, P. N. 2012. Presence and severity of non-alcoholic fatty liver disease in a large prospective primary care cohort. *J Hepatol,* 56**,** 234-40.

ARON-WISNEWSKY, J., VIGLIOTTI, C., WITJES, J., LE, P., HOLLEBOOM, A. G., VERHEIJ, J., NIEUWDORP, M. & CLEMENT, K. 2020. Gut microbiota and human NAFLD: disentangling microbial signatures from metabolic disorders. *Nat Rev Gastroenterol Hepatol,* 17**,** 279-297.

ARSLAN, N. 2014. Obesity, fatty liver disease and intestinal microbiota. *World J Gastroenterol,* 20**,** 16452-63.

ASCHA, M. S., HANOUNEH, I. A., LOPEZ, R., TAMIMI, T. A., FELDSTEIN, A. F. & ZEIN, N. N. 2010. The incidence and risk factors of hepatocellular carcinoma in patients with nonalcoholic steatohepatitis. *Hepatology,* 51**,** 1972-8.

ASTBURY, S., ATALLAH, E., VIJAY, A., AITHAL, G. P., GROVE, J. I. & VALDES, A. M. 2020. Lower gut microbiome diversity and higher abundance of proinflammatory genus Collinsella are associated with biopsy-proven nonalcoholic steatohepatitis. *Gut Microbes,* 11**,** 569-580.

BACKHED, F., DING, H., WANG, T., HOOPER, L. V., KOH, G. Y., NAGY, A., SEMENKOVICH, C. F. & GORDON, J. I. 2004. The gut microbiota as an environmental factor that regulates fat storage. *Proc Natl Acad Sci U S A,* 101**,** 15718-23.

BAE, J. P., LAGE, M. J., MO, D., NELSON, D. R. & HOOGWERF, B. J. 2016. Obesity and glycemic control in patients with diabetes mellitus: Analysis of physician electronic health records in the US from 2009-2011. *J Diabetes Complications,* 30**,** 212-20.

BASTARD, J. P., MAACHI, M., VAN NHIEU, J. T., JARDEL, C., BRUCKERT, E., GRIMALDI, A., ROBERT, J. J., CAPEAU, J. & HAINQUE, B. 2002. Adipose tissue IL-6 content correlates with resistance to insulin activation of glucose uptake both in vivo and in vitro. *J Clin Endocrinol Metab,* 87**,** 2084-9.

BEAUREPAIRE, C., SMYTH, D. & MCKAY, D. M. 2009. Interferon-gamma regulation of intestinal epithelial permeability. *J Interferon Cytokine Res,* 29**,** 133-44.

BECKONERT, O., KEUN, H. C., EBBELS, T. M., BUNDY, J., HOLMES, E., LINDON, J. C. & NICHOLSON, J. K. 2007. Metabolic profiling, metabolomic and metabonomic procedures for NMR spectroscopy of urine, plasma, serum and tissue extracts. *Nat Protoc,* 2**,** 2692-703.

BELLER, A., KRUGLOV, A., DUREK, P., VON GOETZE, V., HOFFMANN, U., MAIER, A., HEIKING, K., SIEGMUND, B., HEINZ, G., MASHREGHI, M.-F., RADBRUCH, A. & CHANG, H.-D. 2018. P104 Anaeroplasma, a potential anti-inflammatory probiotic for the treatment of chronic intestinal inflammation. *Annals of Rheumatic Diseases,* 78.

BERG, R. D. & OWENS, W. E. 1979. Inhibition of translocation of viable Escherichia coli from the gastrointestinal tract of mice by bacterial antagonism. *Infect Immun,* 25**,** 820-27.

BERGHEIM, I., WEBER, S., VOS, M., KRAMER, S., VOLYNETS, V., KASEROUNI, S., MCCLAIN, C. J. & BISCHOFF, S. C. 2008. Antibiotics protect against fructose-induced hepatic lipid accumulation in mice: role of endotoxin. *J Hepatol,* 48**,** 983-92.

BERNARD, M., FANKHANEL, T., RIEDEL-HELLER, S. G. & LUCK-SIKORSKI, C. 2019. Does weight-related stigmatisation and discrimination depend on educational attainment and level of income? A systematic review. *BMJ Open,* 9**,** e027673.

BESERRA, B. T., FERNANDES, R., DO ROSARIO, V. A., MOCELLIN, M. C., KUNTZ, M. G. & TRINDADE, E. B. 2015. A systematic review and meta-analysis of the prebiotics and synbiotics effects on glycaemia, insulin concentrations and lipid parameters in adult patients with overweight or obesity. *Clin Nutr,* 34**,** 845-58.

BIOLATO, M., MANCA, F., MARRONE, G., CEFALO, C., RACCO, S., MIGGIANO, G. A., VALENZA, V., GASBARRINI, A., MIELE, L. & GRIECO, A. 2019. Intestinal permeability after Mediterranean diet and low-fat diet in non-alcoholic fatty liver disease. *World J Gastroenterol,* 25**,** 509-520.

BLAIS, P., HUSAIN, N., KRAMER, J. R., KOWALKOWSKI, M., EL-SERAG, H. & KANWAL, F. 2015. Nonalcoholic fatty liver disease is underrecognized in the primary care setting. *Am J Gastroenterol,* 110**,** 10-4.

BLETSA, E., FILIPPAS-DEKOUAN, S., KOSTARA, C., DAFOPOULOS, P., DIMOU, A., PAPPA, E., CHASAPI, S., SPYROULIAS, G., KOUTSOVASILIS, A., BAIRAKTARI, E., FERRANNINI, E. & TSIMIHODIMOS, V. 2021. Effect of Dapagliflozin on Urine Metabolome in Patients with Type 2 Diabetes. *J Clin Endocrinol Metab,* 106**,** 1269-1283.

BOLLRATH, J. & POWRIE, F. 2013. Immunology. Feed your Tregs more fiber. *Science,* 341**,** 463-4.

BOULANGE, C. L., NEVES, A. L., CHILLOUX, J., NICHOLSON, J. K. & DUMAS, M. E. 2016. Impact of the gut microbiota on inflammation, obesity, and metabolic disease. *Genome Med,* 8**,** 42.

BOURSIER, J., ZARSKI, J. P., DE LEDINGHEN, V., ROUSSELET, M. C., STURM, N., LEBAIL, B., FOUCHARD-HUBERT, I., GALLOIS, Y., OBERTI, F., BERTRAIS, S., CALES, P. & MULTICENTRIC GROUP FROM, A. H. C. E. P. F. S. 2013. Determination of reliability criteria for liver stiffness evaluation by transient elastography. *Hepatology,* 57**,** 1182-91.

BROWNING, J. D., BAXTER, J., SATAPATI, S. & BURGESS, S. C. 2012. The effect of short-term fasting on liver and skeletal muscle lipid, glucose, and energy metabolism in healthy women and men. *J Lipid Res,* 53**,** 577-586.

BROWNING, J. D., WEIS, B., DAVIS, J., SATAPATI, S., MERRITT, M., MALLOY, C. R. & BURGESS, S. C. 2008. Alterations in hepatic glucose and energy metabolism as a result of calorie and carbohydrate restriction. *Hepatology,* 48**,** 1487-96.

BRUEL, L., SULZENBACHER, G., CERVERA TISON, M., PUJOL, A., NICOLETTI, C., PERRIER, J., GALINIER, A., ROPARTZ, D., FONS, M., POMPEO, F. & GIARDINA, T. 2011. alpha-Galactosidase/sucrose kinase (AgaSK), a novel bifunctional enzyme from the human microbiome coupling galactosidase and kinase activities. *J Biol Chem,* 286**,** 40814-23.

BRUNT, E. M., KLEINER, D. E., CARPENTER, D. H., RINELLA, M., HARRISON, S. A., LOOMBA, R., YOUNOSSI, Z., NEUSCHWANDER-TETRI, B. A., SANYAL, A. J. & AMERICAN ASSOCIATION FOR THE STUDY OF LIVER DISEASES, N. T. F. 2021. NAFLD: Reporting Histologic Findings in Clinical Practice. *Hepatology,* 73**,** 2028-2038.

BUGIANESI, E., MOSCATIELLO, S., CIARAVELLA, M. F. & MARCHESINI, G. 2010. Insulin resistance in nonalcoholic fatty liver disease. *Curr Pharm Des,* 16**,** 1941-51.

BUZZETTI, E., PINZANI, M. & TSOCHATZIS, E. A. 2016. The multiple-hit pathogenesis of non-alcoholic fatty liver disease (NAFLD). *Metabolism,* 65**,** 1038-48.

CAI, J., ZHANG, X. J. & LI, H. 2019. The Role of Innate Immune Cells in Nonalcoholic Steatohepatitis. *Hepatology,* 70**,** 1026-1037.

CAI, J. S. & CHEN, J. H. 2014. The mechanism of enterohepatic circulation in the formation of gallstone disease. *J Membr Biol,* 247**,** 1067-82.

CALLAHAN, B. J., MCMURDIE, P. J., ROSEN, M. J., HAN, A. W., JOHNSON, A. J. & HOLMES, S. P. 2016. DADA2: High-resolution sample inference from Illumina amplicon data. *Nat Methods,* 13**,** 581-3.

CAMILLERI, M. & VELLA, A. 2021. What to do about the leaky gut. *Gut*.

CAMPBELL, J. E. & DRUCKER, D. J. 2013. Pharmacology, physiology, and mechanisms of incretin hormone action. *Cell Metab,* 17**,** 819-837.

CANI, P. D., AMAR, J., IGLESIAS, M. A., POGGI, M., KNAUF, C., BASTELICA, D., NEYRINCK, A. M., FAVA, F., TUOHY, K. M., CHABO, C., WAGET, A., DELMEE, E., COUSIN, B., SULPICE, T., CHAMONTIN, B., FERRIERES, J., TANTI, J. F., GIBSON, G. R., CASTEILLA, L., DELZENNE, N. M., ALESSI, M. C. & BURCELIN, R. 2007. Metabolic endotoxemia initiates obesity and insulin resistance. *Diabetes,* 56**,** 1761-72.

CANI, P. D., BIBILONI, R., KNAUF, C., WAGET, A., NEYRINCK, A. M., DELZENNE, N. M. & BURCELIN, R. 2008. Changes in gut microbiota control metabolic endotoxemia-induced inflammation in high-fat diet-induced obesity and diabetes in mice. *Diabetes,* 57**,** 1470-81.

CANI, P. D., POSSEMIERS, S., VAN DE WIELE, T., GUIOT, Y., EVERARD, A., ROTTIER, O., GEURTS, L., NASLAIN, D., NEYRINCK, A., LAMBERT, D. M., MUCCIOLI, G. G. & DELZENNE, N. M. 2009. Changes in gut microbiota control inflammation in obese mice through a mechanism involving GLP-2-driven improvement of gut permeability. *Gut,* 58**,** 1091-103.

CASSINOTTO, C., BOURSIER, J., DE LEDINGHEN, V., LEBIGOT, J., LAPUYADE, B., CALES, P., HIRIART, J. B., MICHALAK, S., BAIL, B. L., CARTIER, V., MOURIES, A., OBERTI, F., FOUCHARD-HUBERT, I., VERGNIOL, J. & AUBE, C. 2016. Liver stiffness in nonalcoholic fatty liver disease: A comparison of supersonic shear imaging, FibroScan, and ARFI with liver biopsy. *Hepatology,* 63**,** 1817-27.

CHALASANI, N., YOUNOSSI, Z., LAVINE, J. E., DIEHL, A. M., BRUNT, E. M., CUSI, K., CHARLTON, M. & SANYAL, A. J. 2012. The diagnosis and management of non-alcoholic fatty liver disease: practice Guideline by

the American Association for the Study of Liver Diseases, American College of Gastroenterology, and the American Gastroenterological Association. *Hepatology,* 55**,** 2005-23.

CHANDOLA, T., DEARY, I. J., BLANE, D. & BATTY, G. D. 2006. Childhood IQ in relation to obesity and weight gain in adult life: the National Child Development (1958) Study. *Int J Obes (Lond),* 30**,** 1422-32.

CHEN, H. T., HUANG, H. L., LI, Y. Q., XU, H. M. & ZHOU, Y. J. 2020a. Therapeutic advances in non-alcoholic fatty liver disease: A microbiota-centered view. *World J Gastroenterol,* 26**,** 1901-1911.

CHEN, K., SNG, W. K., QUAH, J. H., LIU, J., CHONG, B. Y., LEE, H. K., WANG, X. F., TAN, N. C., CHANG, P. E., TAN, H. C., BEE, Y. M. & GOH, G. B. B. 2020b. Clinical spectrum of non-alcoholic fatty liver disease in patients with diabetes mellitus. *PLoS One,* 15**,** e0236977.

CHEN, L., ZHANG, J., LI, C., WANG, Z., LI, J., ZHAO, D., WANG, S., ZHANG, H., HUANG, Y. & GUO, X. 2018. Glycine Transporter-1 and glycine receptor mediate the antioxidant effect of glycine in diabetic rat islets and INS-1 cells. *Free Radic Biol Med,* 123**,** 53-61.

CHIANG, J. Y. 2017. Recent advances in understanding bile acid homeostasis. *F1000Res,* 6**,** 2029.

CHITTURI, S., WONG, V. W., CHAN, W. K., WONG, G. L., WONG, S. K., SOLLANO, J., NI, Y. H., LIU, C. J., LIN, Y. C., LESMANA, L. A., KIM, S. U., HASHIMOTO, E., HAMAGUCHI, M., GOH, K. L., FAN, J., DUSEJA, A., DAN, Y. Y., CHAWLA, Y., FARRELL, G. & CHAN, H. L. 2018. The Asia-Pacific Working Party on Non-alcoholic Fatty Liver Disease guidelines 2017-Part 2: Management and special groups. *J Gastroenterol Hepatol,* 33**,** 86-98.

CHOE, S. S., HUH, J. Y., HWANG, I. J., KIM, J. I. & KIM, J. B. 2016. Adipose Tissue Remodeling: Its Role in Energy Metabolism and Metabolic Disorders. *Front Endocrinol (Lausanne),* 7**,** 30.

COREY, K. E., KARTOUN, U., ZHENG, H. & SHAW, S. Y. 2016. Development and Validation of an Algorithm to Identify Nonalcoholic Fatty Liver Disease in the Electronic Medical Record. *Dig Dis Sci,* 61**,** 913-9.

CRAVEN, L., RAHMAN, A., NAIR PARVATHY, S., BEATON, M., SILVERMAN, J., QUMOSANI, K., HRAMIAK, I., HEGELE, R., JOY, T., MEDDINGS, J., URQUHART, B., HARVIE, R., MCKENZIE, C., SUMMERS, K., REID, G., BURTON, J. P. & SILVERMAN, M. 2020. Allogenic Fecal Microbiota Transplantation in Patients With Nonalcoholic Fatty Liver Disease Improves Abnormal Small Intestinal Permeability: A Randomized Control Trial. *Am J Gastroenterol,* 115**,** 1055-1065.

CROSNIER, C., STAMATAKI, D. & LEWIS, J. 2006. Organizing cell renewal in the intestine: stem cells, signals and combinatorial control. *Nat Rev Genet,* 7**,** 349-59.

CROSSAN, C., TSOCHATZIS, E. A., LONGWORTH, L., GURUSAMY, K., DAVIDSON, B., RODRIGUEZ-PERALVAREZ, M., MANTZOUKIS, K., O'BRIEN, J., THALASSINOS, E., PAPASTERGIOU, V. & BURROUGHS, A. 2015. Cost-effectiveness of non-invasive methods for assessment and monitoring of liver fibrosis and cirrhosis in patients with chronic liver disease: systematic review and economic evaluation. *Health Technol Assess,* 19**,** 1-409, v-vi.

CROVESY, L., MASTERSON, D. & ROSADO, E. L. 2020. Profile of the gut microbiota of adults with obesity: a systematic review. *Eur J Clin Nutr,* 74**,** 1251-1262.

CYNOBER, L. 2018. Metabolism of Dietary Glutamate in Adults. *Ann Nutr Metab,* 73 Suppl 5**,** 5-14.

DA, B. L. & SATAPATHY, S. K. 2021. Semaglutide or Placebo for Nonalcoholic Steatohepatitis. *N Engl J Med,* 385**,** e6.

DABKE, K., HENDRICK, G. & DEVKOTA, S. 2019. The gut microbiome and metabolic syndrome. *J Clin Invest,* 129**,** 4050-4057.

DAI, W., YE, L., LIU, A., WEN, S. W., DENG, J., WU, X. & LAI, Z. 2017. Prevalence of nonalcoholic fatty liver disease in patients with type 2 diabetes mellitus: A meta-analysis. *Medicine (Baltimore),* 96**,** e8179.

DAMMS-MACHADO, A., LOUIS, S., SCHNITZER, A., VOLYNETS, V., RINGS, A., BASRAI, M. & BISCHOFF, S. C. 2017. Gut permeability is related to body weight, fatty liver disease, and insulin resistance in obese individuals undergoing weight reduction. *Am J Clin Nutr,* 105**,** 127-135.

DANIEL, H., GHOLAMI, A. M., BERRY, D., DESMARCHELIER, C., HAHNE, H., LOH, G., MONDOT, S., LEPAGE, P., ROTHBALLER, M., WALKER, A., BOHM, C., WENNING, M., WAGNER, M., BLAUT, M., SCHMITT-KOPPLIN, P., KUSTER, B., HALLER, D. & CLAVEL, T. 2014. High-fat diet alters gut microbiota physiology in mice. *ISME J,* 8**,** 295-308.

DASARATHY, S., YANG, Y., MCCULLOUGH, A. J., MARCZEWSKI, S., BENNETT, C. & KALHAN, S. C. 2011. Elevated hepatic fatty acid oxidation, high plasma fibroblast growth factor 21, and fasting bile acids in nonalcoholic steatohepatitis. *Eur J Gastroenterol Hepatol,* 23**,** 382-8.

DAVIES, M. J., D'ALESSIO, D. A., FRADKIN, J., KERNAN, W. N., MATHIEU, C., MINGRONE, G., ROSSING, P., TSAPAS, A., WEXLER, D. J. & BUSE, J. B. 2018. Management of hyperglycaemia in type 2 diabetes, 2018. A consensus report by the American Diabetes Association (ADA) and the European Association for the Study of Diabetes (EASD). *Diabetologia,* 61**,** 2461-2498.

DAVIS, N. M., PROCTOR, D. M., HOLMES, S. P., RELMAN, D. A. & CALLAHAN, B. J. 2018. Simple statistical identification and removal of contaminant sequences in marker-gene and metagenomics data. *Microbiome,* 6**,** 226.

DAWES, E. A. & FOSTER, S. M. 1956. The formation of ethanol in Escherichia coli. *Biochim Biophys Acta,* 22**,** 253-65.

DE MUNCK, T. J. I., XU, P., VERWIJS, H. J. A., MASCLEE, A. A. M., JONKERS, D., VERBEEK, J. & KOEK, G. H. 2020. Intestinal permeability in human nonalcoholic fatty liver disease: A systematic review and meta-analysis. *Liver Int,* 40**,** 2906-2916.

DE WIT, N., DERRIEN, M., BOSCH-VERMEULEN, H., OOSTERINK, E., KESHTKAR, S., DUVAL, C., DE VOGEL-VAN DEN BOSCH, J., KLEEREBEZEM, M., MULLER, M. & VAN DER MEER, R. 2012. Saturated fat stimulates obesity and hepatic steatosis and affects gut microbiota composition by an enhanced overflow of dietary fat to the distal intestine. *Am J Physiol Gastrointest Liver Physiol,* 303**,** G589-99.

DEN BESTEN, G., BLEEKER, A., GERDING, A., VAN EUNEN, K., HAVINGA, R., VAN DIJK, T. H., OOSTERVEER, M. H., JONKER, J. W., GROEN, A. K., REIJNGOUD, D. J. & BAKKER, B. M. 2015. Short-Chain Fatty Acids Protect Against High-Fat Diet-Induced Obesity via a PPARgamma-Dependent Switch From Lipogenesis to Fat Oxidation. *Diabetes,* 64**,** 2398-408.

DESAI, M. S., SEEKATZ, A. M., KOROPATKIN, N. M., KAMADA, N., HICKEY, C. A., WOLTER, M., PUDLO, N. A., KITAMOTO, S., TERRAPON, N., MULLER, A., YOUNG, V. B., HENRISSAT, B., WILMES, P., STAPPENBECK, T. S., NUNEZ, G. & MARTENS, E. C. 2016. A Dietary Fiber-Deprived Gut Microbiota Degrades the Colonic Mucus Barrier and Enhances Pathogen Susceptibility. *Cell,* 167**,** 1339-1353 e21.

DING, S. & LUND, P. K. 2011. Role of intestinal inflammation as an early event in obesity and insulin resistance. *Curr Opin Clin Nutr Metab Care,* 14**,** 328-33.

DLUGOSZ, A., NOWAK, P., D'AMATO, M., MOHAMMADIAN KERMANI, G., NYSTROM, J., ABDURAHMAN, S. & LINDBERG, G. 2015. Increased serum levels of lipopolysaccharide and antiflagellin antibodies in patients with diarrhea-predominant irritable bowel syndrome. *Neurogastroenterol Motil,* 27**,** 1747-54.

DONA, A. C., JIMENEZ, B., SCHAFER, H., HUMPFER, E., SPRAUL, M., LEWIS, M. R., PEARCE, J. T., HOLMES, E., LINDON, J. C. & NICHOLSON, J. K. 2014. Precision high-throughput proton NMR spectroscopy of human urine, serum, and plasma for large-scale metabolic phenotyping. *Anal Chem,* 86**,** 9887-94.

DU, K., CHITNENI, S. K., SUZUKI, A., WANG, Y., HENAO, R., HYUN, J., PREMONT, R. T., NAGGIE, S., MOYLAN, C. A., BASHIR, M. R., ABDELMALEK, M. F. & DIEHL, A. M. 2020. Increased Glutaminolysis Marks Active Scarring in Nonalcoholic Steatohepatitis Progression. *Cell Mol Gastroenterol Hepatol,* 10**,** 1-21.

DU PLESSIS, J., VANHEEL, H., JANSSEN, C. E., ROOS, L., SLAVIK, T., STIVAKTAS, P. I., NIEUWOUDT, M., VAN WYK, S. G., VIEIRA, W., PRETORIUS, E., BEUKES, M., FARRE, R., TACK, J., LALEMAN, W., FEVERY, J., NEVENS, F., ROSKAMS, T. & VAN DER MERWE, S. W. 2013. Activated intestinal macrophages in patients with cirrhosis release NO and IL-6 that may disrupt intestinal barrier function. *J Hepatol,* 58**,** 1125-32.

DUMAS, M. E., KINROSS, J. & NICHOLSON, J. K. 2014. Metabolic phenotyping and systems biology approaches to understanding metabolic syndrome and fatty liver disease. *Gastroenterology,* 146**,** 46-62.

DUNCAN, S. H., LOUIS, P., THOMSON, J. M. & FLINT, H. J. 2009. The role of pH in determining the species composition of the human colonic microbiota. *Environ Microbiol,* 11**,** 2112-22.

DYSON, J., JAQUES, B., CHATTOPADYHAY, D., LOCHAN, R., GRAHAM, J., DAS, D., ASLAM, T., PATANWALA, I., GAGGAR, S., COLE, M., SUMPTER, K., STEWART, S., ROSE, J., HUDSON, M., MANAS, D. & REEVES, H. L. 2014. Hepatocellular cancer: the impact of obesity, type 2 diabetes and a multidisciplinary team. *J Hepatol,* 60**,** 110-7.

DYSON, J. K., ANSTEE, Q. M. & MCPHERSON, S. 2015. Republished: Non-alcoholic fatty liver disease: a practical approach to treatment. *Postgrad Med J,* 91**,** 92-101.

EKSTEDT, M., HAGSTROM, H., NASR, P., FREDRIKSON, M., STAL, P., KECHAGIAS, S. & HULTCRANTZ, R. 2015. Fibrosis stage is the strongest predictor for disease-specific mortality in NAFLD after up to 33 years of follow-up. *Hepatology,* 61**,** 1547-54.

EL-HAFIDI, M., FRANCO, M., RAMIREZ, A. R., SOSA, J. S., FLORES, J. A. P., ACOSTA, O. L., SALGADO, M. C. & CARDOSO-SALDANA, G. 2018. Glycine Increases Insulin Sensitivity and Glutathione Biosynthesis and Protects against Oxidative Stress in a Model of Sucrose-Induced Insulin Resistance. *Oxid Med Cell Longev,* 2018**,** 2101562.

ELANGOVAN, H., RAJAGOPAUL, S., WILLIAMS, S. M., MCKILLEN, B., BRITTON, L., MCPHAIL, S. M., HORSFALL, L. U., VALERY, P. C., HAYWARD, K. L. & POWELL, E. E. 2020. Nonalcoholic Fatty Liver Disease: Interface Between Primary Care and Hepatology Clinics. *Hepatol Commun,* 4**,** 518-526.

ENGLAND, P. H. June 2018. NHS RightCare Pathway: Diabetes.

ERIKSSON, J., CHAIT, B. T. & FENYO, D. 2000. A statistical basis for testing the significance of mass spectrometric protein identification results. *Anal Chem,* 72**,** 999-1005.

ESTES, C., RAZAVI, H., LOOMBA, R., YOUNOSSI, Z. & SANYAL, A. J. 2018. Modeling the epidemic of nonalcoholic fatty liver disease demonstrates an exponential increase in burden of disease. *Hepatology,* 67**,** 123-133.

EUROPEAN ASSOCIATION FOR STUDY OF, L. & ASOCIACION LATINOAMERICANA PARA EL ESTUDIO DEL, H. 2015. EASL-ALEH Clinical Practice Guidelines: Non-invasive tests for evaluation of liver disease severity and prognosis. *J Hepatol,* 63**,** 237-64.

EUROPEAN ASSOCIATION FOR THE STUDY OF THE, L., EUROPEAN ASSOCIATION FOR THE STUDY OF, D. & EUROPEAN ASSOCIATION FOR THE STUDY OF, O. 2016. EASL-EASD-EASO Clinical Practice Guidelines for the Management of Non-Alcoholic Fatty Liver Disease. *Obes Facts,* 9**,** 65-90.

EUROPEAN ASSOCIATION FOR THE STUDY OF THE LIVER. ELECTRONIC ADDRESS, E. E. E., CLINICAL PRACTICE GUIDELINE, P., CHAIR, REPRESENTATIVE, E. G. B. & PANEL, M. 2021. EASL Clinical Practice Guidelines on non-invasive tests for evaluation of liver disease severity and prognosis - 2021 update. *J Hepatol,* 75**,** 659-689.

FARQUHAR, M. G. & PALADE, G. E. 1963. Junctional complexes in various epithelia. *J Cell Biol,* 17**,** 375-412.

FASANO, A. 2012. Intestinal permeability and its regulation by zonulin: diagnostic and therapeutic implications. *Clin Gastroenterol Hepatol,* 10**,** 1096-100.

FAVA, F. & DANESE, S. 2011. Intestinal microbiota in inflammatory bowel disease: friend of foe? *World J Gastroenterol,* 17**,** 557-66.

FEROLLA, S. M., SILVA, L. C., FERRARI MDE, L., DA CUNHA, A. S., MARTINS FDOS, S., COUTO, C. A. & FERRARI, T. C. 2015. Dietary approach in the treatment of nonalcoholic fatty liver disease. *World J Hepatol,* 7**,** 2522-34.

FERSLEW, B. C., XIE, G., JOHNSTON, C. K., SU, M., STEWART, P. W., JIA, W., BROUWER, K. L. & BARRITT, A. S. T. 2015. Altered Bile Acid Metabolome in Patients with Nonalcoholic Steatohepatitis. *Dig Dis Sci,* 60**,** 3318-28.

FISCHER, J. E., ROSEN, H. M., EBEID, A. M., JAMES, J. H., KEANE, J. M. & SOETERS, P. B. 1976. The effect of normalization of plasma amino acids on hepatic encephalopathy in man. *Surgery,* 80**,** 77-91.

FORLANO, R., HARLOW, C., MULLISH, B. H., THURSZ, M. R., MANOUSOU, P. & YEE, M. 2021. Binge-eating disorder is associated with an unfavorable body mass composition in patients with non-alcoholic fatty liver disease. *Int J Eat Disord*.

FORLANO, R., MULLISH, B. H., GIANNAKEAS, N., MAURICE, J. B., ANGKATHUNYAKUL, N., LLOYD, J., TZALLAS, A. T., TSIPOURAS, M., YEE, M., THURSZ, M. R., GOLDIN, R. D. & MANOUSOU, P. 2020. High-Throughput, Machine Learning-Based Quantification of Steatosis, Inflammation, Ballooning, and Fibrosis in Biopsies From Patients With Nonalcoholic Fatty Liver Disease. *Clin Gastroenterol Hepatol,* 18**,** 2081-2090 e9.

FUKUNAGA, T., SASAKI, M., ARAKI, Y., OKAMOTO, T., YASUOKA, T., TSUJIKAWA, T., FUJIYAMA, Y. & BAMBA, T. 2003. Effects of the soluble fibre pectin on intestinal cell proliferation, fecal short chain fatty acid production and microbial population. *Digestion,* 67**,** 42-9.

FURUSAWA, Y., OBATA, Y., FUKUDA, S., ENDO, T. A., NAKATO, G., TAKAHASHI, D., NAKANISHI, Y., UETAKE, C., KATO, K., KATO, T., TAKAHASHI, M., FUKUDA, N. N., MURAKAMI, S., MIYAUCHI, E., HINO, S., ATARASHI, K., ONAWA, S., FUJIMURA, Y., LOCKETT, T., CLARKE, J. M., TOPPING, D. L., TOMITA, M., HORI, S., OHARA, O., MORITA, T., KOSEKI, H., KIKUCHI, J., HONDA, K., HASE, K. & OHNO, H. 2013. Commensal microbe-derived butyrate induces the differentiation of colonic regulatory T cells. *Nature,* 504**,** 446-50.

FURUSE, M. & TSUKITA, S. 2006. Claudins in occluding junctions of humans and flies. *Trends Cell Biol,* 16**,** 181-8.

GAGGINI, M., CARLI, F., ROSSO, C., BUZZIGOLI, E., MARIETTI, M., DELLA LATTA, V., CIOCIARO, D., ABATE, M. L., GAMBINO, R., CASSADER, M., BUGIANESI, E. & GASTALDELLI, A. 2018. Altered amino acid concentrations in NAFLD: Impact of obesity and insulin resistance. *Hepatology,* 67**,** 145-158.

GALSGAARD, K. D. 2020. The Vicious Circle of Hepatic Glucagon Resistance in Non-Alcoholic Fatty Liver Disease. *J Clin Med,* 9.

GAO, Z., HWANG, D., BATAILLE, F., LEFEVRE, M., YORK, D., QUON, M. J. & YE, J. 2002. Serine phosphorylation of insulin receptor substrate 1 by inhibitor kappa B kinase complex. *J Biol Chem,* 277**,** 48115-21.

GASTALDELLI, A., REPETTO, E., GUJA, C., HARDY, E., HAN, J., JABBOUR, S. A. & FERRANNINI, E. 2020. Exenatide and dapagliflozin combination improves markers of liver steatosis and fibrosis in patients with type 2 diabetes. *Diabetes Obes Metab,* 22**,** 393-403.

GERARD, C. & VIDAL, H. 2019. Impact of Gut Microbiota on Host Glycemic Control. *Front Endocrinol (Lausanne),* 10**,** 29.

GIORGIO, V., MIELE, L., PRINCIPESSA, L., FERRETTI, F., VILLA, M. P., NEGRO, V., GRIECO, A., ALISI, A. & NOBILI, V. 2014. Intestinal permeability is increased in children with non-alcoholic fatty liver disease, and correlates with liver disease severity. *Dig Liver Dis,* 46**,** 556-60.

GLEN, J., FLOROS, L., DAY, C., PRYKE, R. & GUIDELINE DEVELOPMENT, G. 2016. Non-alcoholic fatty liver disease (NAFLD): summary of NICE guidance. *BMJ,* 354**,** i4428.

GOLLIN, G., MARKS, C. & MARKS, W. H. 1993. Intestinal fatty acid binding protein in serum and urine reflects early ischemic injury to the small bowel. *Surgery,* 113**,** 545-51.

GOMES, J. M. G., COSTA, J. A. & ALFENAS, R. C. G. 2017. Metabolic endotoxemia and diabetes mellitus: A systematic review. *Metabolism,* 68**,** 133-144.

GRABHERR, F., GRANDER, C., EFFENBERGER, M., ADOLPH, T. E. & TILG, H. 2019. Gut Dysfunction and Non-alcoholic Fatty Liver Disease. *Front Endocrinol (Lausanne),* 10**,** 611.

GRATTON, J., PHETCHARABURANIN, J., MULLISH, B. H., WILLIAMS, H. R., THURSZ, M., NICHOLSON, J. K., HOLMES, E., MARCHESI, J. R. & LI, J. V. 2016. Optimized Sample Handling Strategy for Metabolic Profiling of Human Feces. *Anal Chem,* 88**,** 4661-8.

GRAUPERA, I., COLL, M., POSE, E., ELIA, C., PIANO, S., SOLA, E., BLAYA, D., HUELIN, P., SOLE, C., MOREIRA, R., DE PRADA, G., FABRELLAS, N., JUANOLA, A., MORALES-RUIZ, M., SANCHO-BRU, P., VILLANUEVA, C. & GINES, P. 2017. Adipocyte Fatty-Acid Binding Protein is Overexpressed in Cirrhosis and Correlates with Clinical Outcomes. *Sci Rep,* 7**,** 1829.

GRUZDEVA, O., BORODKINA, D., UCHASOVA, E., DYLEVA, Y. & BARBARASH, O. 2019. Leptin resistance: underlying mechanisms and diagnosis. *Diabetes Metab Syndr Obes,* 12**,** 191-198.

GRZYCH, G., VONGHIA, L., BOUT, M. A., WEYLER, J., VERRIJKEN, A., DIRINCK, E., CHEVALIER CURT, M. J., VAN GAAL, L., PAUMELLE, R., FRANCQUE, S., TAILLEUX, A., HAAS, J. T. & STAELS, B. 2020. Plasma BCAA Changes in Patients With NAFLD Are Sex Dependent. *J Clin Endocrinol Metab,* 105.

GUIDELINES, N. 2010. Alcohol-use disorders: prevention.

GUILHERME, A., VIRBASIUS, J. V., PURI, V. & CZECH, M. P. 2008. Adipocyte dysfunctions linking obesity to insulin resistance and type 2 diabetes. *Nat Rev Mol Cell Biol,* 9**,** 367-77.

HAMMOUTENE, A. & RAUTOU, P. E. 2019. Role of liver sinusoidal endothelial cells in non-alcoholic fatty liver disease. *J Hepatol,* 70**,** 1278-1291.

HAN, M. A., SAOUAF, R., AYOUB, W., TODO, T., MENA, E. & NOUREDDIN, M. 2017. Magnetic resonance imaging and transient elastography in the management of Nonalcoholic Fatty Liver Disease (NAFLD). *Expert Rev Clin Pharmacol,* 10**,** 379-390.

HARRISON, S. A., GAWRIEH, S., ROBERTS, K., LISANTI, C. J., SCHWOPE, R. B., CEBE, K. M., PARADIS, V., BEDOSSA, P., ALDRIDGE WHITEHEAD, J. M., LABOURDETTE, A., MIETTE, V., NEUBAUER, S., FOURNIER, C., PAREDES, A. H. & ALKHOURI, N. 2021. Prospective evaluation of the prevalence of non-alcoholic fatty liver disease and steatohepatitis in a large middle-aged US cohort. *J Hepatol,* 75**,** 284-291.

HARTE, A. L., VARMA, M. C., TRIPATHI, G., MCGEE, K. C., AL-DAGHRI, N. M., AL-ATTAS, O. S., SABICO, S., O'HARE, J. P., CERIELLO, A., SARAVANAN, P., KUMAR, S. & MCTERNAN, P. G. 2012. High fat intake leads to acute postprandial exposure to circulating endotoxin in type 2 diabetic subjects. *Diabetes Care,* 35**,** 375-82.

HAUFE, S., WITT, H., ENGELI, S., KAMINSKI, J., UTZ, W., FUHRMANN, J. C., REIN, D., SCHULZ-MENGER, J., LUFT, F. C., BOSCHMANN, M. & JORDAN, J. 2016. Branched-chain and aromatic amino acids, insulin resistance and liver specific ectopic fat storage in overweight to obese subjects. *Nutr Metab Cardiovasc Dis,* 26**,** 637-642.

HEALTH AND SOCIAL CARE INFORMATION CENTRE (HSCIC), P. H. E. April 2014. National child measurement programme: England 2012/2013 school year.

HENAO-MEJIA, J., ELINAV, E., JIN, C., HAO, L., MEHAL, W. Z., STROWIG, T., THAISS, C. A., KAU, A. L., EISENBARTH, S. C., JURCZAK, M. J., CAMPOREZ, J. P., SHULMAN, G. I., GORDON, J. I., HOFFMAN, H. M. & FLAVELL, R. A. 2012. Inflammasome-mediated dysbiosis regulates progression of NAFLD and obesity. *Nature,* 482**,** 179-85.

HERNAEZ, R., LAZO, M., BONEKAMP, S., KAMEL, I., BRANCATI, F. L., GUALLAR, E. & CLARK, J. M. 2011. Diagnostic accuracy and reliability of ultrasonography for the detection of fatty liver: a meta-analysis. *Hepatology,* 54**,** 1082-1090.

HOSSAIN, N., AFENDY, A., STEPANOVA, M., NADER, F., SRISHORD, M., RAFIQ, N., GOODMAN, Z. & YOUNOSSI, Z. 2009. Independent predictors of fibrosis in patients with nonalcoholic fatty liver disease. *Clin Gastroenterol Hepatol,* 7**,** 1224-9, 1229 e1-2.

HOTAMISLIGIL, G. S. 2017. Inflammation, metaflammation and immunometabolic disorders. *Nature,* 542**,** 177-185.

HOYLES, L., FERNANDEZ-REAL, J. M., FEDERICI, M., SERINO, M., ABBOTT, J., CHARPENTIER, J., HEYMES, C., LUQUE, J. L., ANTHONY, E., BARTON, R. H., CHILLOUX, J., MYRIDAKIS, A., MARTINEZ-GILI, L., MORENO-NAVARRETE, J. M., BENHAMED, F., AZALBERT, V., BLASCO-BAQUE, V., PUIG, J., XIFRA, G., RICART, W., TOMLINSON, C., WOODBRIDGE, M., CARDELLINI, M., DAVATO, F., CARDOLINI, I., PORZIO, O., GENTILESCHI, P., LOPEZ, F., FOUFELLE, F., BUTCHER, S. A., HOLMES, E., NICHOLSON, J. K., POSTIC, C., BURCELIN, R. & DUMAS, M. E. 2018. Molecular phenomics and metagenomics of hepatic steatosis in non-diabetic obese women. *Nat Med,* 24**,** 1070-1080.

HU, H., LIN, A., KONG, M., YAO, X., YIN, M., XIA, H., MA, J. & LIU, H. 2020. Intestinal microbiome and NAFLD: molecular insights and therapeutic perspectives. *J Gastroenterol,* 55**,** 142-158.

HUANG, W., METLAKUNTA, A., DEDOUSIS, N., ZHANG, P., SIPULA, I., DUBE, J. J., SCOTT, D. K. & O'DOHERTY, R. M. 2010. Depletion of liver Kupffer cells prevents the development of diet-induced hepatic steatosis and insulin resistance. *Diabetes,* 59**,** 347-57.

JAN, A., NARWARIA, M. & MAHAWAR, K. K. 2015. A Systematic Review of Bariatric Surgery in Patients with Liver Cirrhosis. *Obes Surg,* 25**,** 1518-26.

JOHANSSON, M. E., PHILLIPSON, M., PETERSSON, J., VELCICH, A., HOLM, L. & HANSSON, G. C. 2008. The inner of the two Muc2 mucin-dependent mucus layers in colon is devoid of bacteria. *Proc Natl Acad Sci U S A,* 105**,** 15064-9.

JUMPERTZ, R., LE, D. S., TURNBAUGH, P. J., TRINIDAD, C., BOGARDUS, C., GORDON, J. I. & KRAKOFF, J. 2011. Energy-balance studies reveal associations between gut microbes, caloric load, and nutrient absorption in humans. *Am J Clin Nutr,* 94**,** 58-65.

KAGAN, H. M. & LI, W. 2003. Lysyl oxidase: properties, specificity, and biological roles inside and outside of the cell. *J Cell Biochem,* 88**,** 660-72.

KANDA, T., FUJII, H., TANI, T., MURAKAMI, H., SUDA, T., SAKAI, Y., ONO, T. & HATAKEYAMA, K. 1996. Intestinal fatty acid-binding protein is a useful diagnostic marker for mesenteric infarction in humans. *Gastroenterology,* 110**,** 339-43.

KANDA, T., NAKATOMI, Y., ISHIKAWA, H., HITOMI, M., MATSUBARA, Y., ONO, T. & MUTO, T. 1992. Intestinal fatty acid-binding protein as a sensitive marker of intestinal ischemia. *Dig Dis Sci,* 37**,** 1362-7.

KAWASAKI, H., HORI, T., NAKAJIMA, M. & TAKESHITA, K. 1988. Plasma levels of pipecolic acid in patients with chronic liver disease. *Hepatology,* 8**,** 286-9.

KAZANKOV, K., TORDJMAN, J., MOLLER, H. J., VILSTRUP, H., POITOU, C., BEDOSSA, P., BOUILLOT, J. L., CLEMENT, K. & GRONBAEK, H. 2015. Macrophage activation marker soluble CD163 and non-alcoholic fatty liver disease in morbidly obese patients undergoing bariatric surgery. *J Gastroenterol Hepatol,* 30**,** 1293-300.

KEATING, S. E., HACKETT, D. A., GEORGE, J. & JOHNSON, N. A. 2012. Exercise and non-alcoholic fatty liver disease: a systematic review and meta-analysis. *J Hepatol,* 57**,** 157-66.

KEIRNS, B. H., KOEMEL, N. A., SCIARRILLO, C. M., ANDERSON, K. L. & EMERSON, S. R. 2020. Exercise and intestinal permeability: another form of exercise-induced hormesis? *Am J Physiol Gastrointest Liver Physiol,* 319**,** G512-G518.

KEITA, A. V. & SODERHOLM, J. D. 2010. The intestinal barrier and its regulation by neuroimmune factors. *Neurogastroenterol Motil,* 22**,** 718-33.

KHALID, Q. B. I., PATEL B. V. 2015. Non-Alcoholic Fatty Liver Disease: The Effect of Bile Acids and Farnesoid X Receptor Agonists on Pathophysiology and Treatment. *Liver res open j*.

KIM, C. C., HEALEY, G. R., KELLY, W. J., PATCHETT, M. L., JORDENS, Z., TANNOCK, G. W., SIMS, I. M., BELL, T. J., HEDDERLEY, D., HENRISSAT, B. & ROSENDALE, D. I. 2019. Genomic insights from Monoglobus pectinilyticus: a pectin-degrading specialist bacterium in the human colon. *ISME J,* 13**,** 1437-1456.

KIM, J., LEE, M., KIM, S. Y., KIM, J. H., NAM, J. S., CHUN, S. W., PARK, S. E., KIM, K. J., LEE, Y. H., NAM, J. Y. & KANG, E. S. 2021. Non-Laboratory-Based Simple Screening Model for Nonalcoholic Fatty Liver Disease in Patients with Type 2 Diabetes Developed Using Multi-Center Cohorts. *Endocrinol Metab (Seoul),* 36**,** 823-834.

KIM, J. J. & SEARS, D. D. 2010. TLR4 and Insulin Resistance. *Gastroenterol Res Pract,* 2010.

KIRPICH, I. A., MARSANO, L. S. & MCCLAIN, C. J. 2015. Gut-liver axis, nutrition, and non-alcoholic fatty liver disease. *Clin Biochem,* 48**,** 923-30.

KLEINER, D. E., BRUNT, E. M., VAN NATTA, M., BEHLING, C., CONTOS, M. J., CUMMINGS, O. W., FERRELL, L. D., LIU, Y. C., TORBENSON, M. S., UNALP-ARIDA, A., YEH, M., MCCULLOUGH, A. J., SANYAL, A. J. & NONALCOHOLIC STEATOHEPATITIS CLINICAL RESEARCH, N. 2005. Design and validation of a histological scoring system for nonalcoholic fatty liver disease. *Hepatology,* 41**,** 1313-21.

KLEINER, D. E. & MAKHLOUF, H. R. 2016. Histology of Nonalcoholic Fatty Liver Disease and Nonalcoholic Steatohepatitis in Adults and Children. *Clin Liver Dis,* 20**,** 293-312.

KOLAK, M., WESTERBACKA, J., VELAGAPUDI, V. R., WAGSATER, D., YETUKURI, L., MAKKONEN, J., RISSANEN, A., HAKKINEN, A. M., LINDELL, M., BERGHOLM, R., HAMSTEN, A., ERIKSSON, P., FISHER, R. M., ORESIC, M. & YKI-JARVINEN, H. 2007. Adipose tissue inflammation and increased ceramide content characterize subjects with high liver fat content independent of obesity. *Diabetes,* 56**,** 1960-8.

KONIKOFF, M. R. & DENSON, L. A. 2006. Role of fecal calprotectin as a biomarker of intestinal inflammation in inflammatory bowel disease. *Inflamm Bowel Dis,* 12**,** 524-34.

KOREM, T., ZEEVI, D., ZMORA, N., WEISSBROD, O., BAR, N., LOTAN-POMPAN, M., AVNIT-SAGI, T., KOSOWER, N., MALKA, G., REIN, M., SUEZ, J., GOLDBERG, B. Z., WEINBERGER, A., LEVY, A. A., ELINAV, E. & SEGAL, E. 2017. Bread Affects Clinical Parameters and Induces Gut Microbiome-Associated Personal Glycemic Responses. *Cell Metab,* 25**,** 1243-1253 e5.

KRAWCZYK, M., MACIEJEWSKA, D., RYTERSKA, K., CZERWINKA-ROGOWSKA, M., JAMIOL-MILC, D., SKONIECZNA-ZYDECKA, K., MILKIEWICZ, P., RASZEJA-WYSZOMIRSKA, J. & STACHOWSKA, E. 2018. Gut Permeability Might be Improved by Dietary Fiber in Individuals with Nonalcoholic Fatty Liver Disease (NAFLD) Undergoing Weight Reduction. *Nutrients,* 10.

KRENKEL, O., PUENGEL, T., GOVAERE, O., ABDALLAH, A. T., MOSSANEN, J. C., KOHLHEPP, M., LIEPELT, A., LEFEBVRE, E., LUEDDE, T., HELLERBRAND, C., WEISKIRCHEN, R., LONGERICH, T., COSTA, I. G., ANSTEE, Q. M., TRAUTWEIN, C. & TACKE, F. 2018. Therapeutic inhibition of inflammatory monocyte recruitment reduces steatohepatitis and liver fibrosis. *Hepatology,* 67**,** 1270-1283.

KRISHNAN, S., DING, Y., SAEDI, N., CHOI, M., SRIDHARAN, G. V., SHERR, D. H., YARMUSH, M. L., ALANIZ, R. C., JAYARAMAN, A. & LEE, K. 2018. Gut Microbiota-Derived Tryptophan Metabolites Modulate Inflammatory Response in Hepatocytes and Macrophages. *Cell Rep,* 23**,** 1099-1111.

KRUMSIEK, J., MITTELSTRASS, K., DO, K. T., STUCKLER, F., RIED, J., ADAMSKI, J., PETERS, A., ILLIG, T., KRONENBERG, F., FRIEDRICH, N., NAUCK, M., PIETZNER, M., MOOK-KANAMORI, D. O., SUHRE, K., GIEGER, C., GRALLERT, H., THEIS, F. J. & KASTENMULLER, G. 2015. Gender-specific pathway differences in the human serum metabolome. *Metabolomics,* 11**,** 1815-1833.

LAFERRERE, B., REILLY, D., ARIAS, S., SWERDLOW, N., GORROOCHURN, P., BAWA, B., BOSE, M., TEIXEIRA, J., STEVENS, R. D., WENNER, B. R., BAIN, J. R., MUEHLBAUER, M. J., HAQQ, A., LIEN, L., SHAH, S. H., SVETKEY, L. P. & NEWGARD, C. B. 2011. Differential metabolic impact of gastric bypass surgery versus dietary intervention in obese diabetic subjects despite identical weight loss. *Sci Transl Med,* 3**,** 80re2.

LAKE, A. D., NOVAK, P., SHIPKOVA, P., ARANIBAR, N., ROBERTSON, D., REILY, M. D., LU, Z., LEHMAN-MCKEEMAN, L. D. & CHERRINGTON, N. J. 2013. Decreased hepatotoxic bile acid composition and altered synthesis in progressive human nonalcoholic fatty liver disease. *Toxicol Appl Pharmacol,* 268**,** 132-40.

LANTHIER, N., RODRIGUEZ, J., NACHIT, M., HIEL, S., TREFOIS, P., NEYRINCK, A. M., CANI, P. D., BINDELS, L. B., THISSEN, J. P. & DELZENNE, N. M. 2021. Microbiota analysis and transient elastography reveal new extra-hepatic components of liver steatosis and fibrosis in obese patients. *Sci Rep,* 11**,** 659.

LEE, J., HONG, S. W., RHEE, E. J. & LEE, W. Y. 2012. GLP-1 Receptor Agonist and Non-Alcoholic Fatty Liver Disease. *Diabetes Metab J,* 36**,** 262-7.

LEFERE, S., VAN STEENKISTE, C., VERHELST, X., VAN VLIERBERGHE, H., DEVISSCHER, L. & GEERTS, A. 2016. Hypoxia-regulated mechanisms in the pathogenesis of obesity and non-alcoholic fatty liver disease. *Cell Mol Life Sci,* 73**,** 3419-31.

LEGRY, V., FRANCQUE, S., HAAS, J. T., VERRIJKEN, A., CARON, S., CHAVEZ-TALAVERA, O., VALLEZ, E., VONGHIA, L., DIRINCK, E., VERHAEGEN, A., KOUACH, M., LESTAVEL, S., LEFEBVRE, P., VAN GAAL, L., TAILLEUX, A., PAUMELLE, R. & STAELS, B. 2017. Bile Acid Alterations Are Associated With Insulin Resistance, but Not With NASH, in Obese Subjects. *J Clin Endocrinol Metab,* 102**,** 3783-3794.

LEY, R. E., PETERSON, D. A. & GORDON, J. I. 2006. Ecological and evolutionary forces shaping microbial diversity in the human intestine. *Cell,* 124**,** 837-48.

LI, N. & NEU, J. 2009. Glutamine deprivation alters intestinal tight junctions via a PI3-K/Akt mediated pathway in Caco-2 cells. *J Nutr,* 139**,** 710-4.

LLERAS-MUNEY, A. 2005. The relationship between Education and Adult Mortality in the United States. *The review of Economic Studies*.

LONARDO, A., NASCIMBENI, F., MANTOVANI, A. & TARGHER, G. 2018. Hypertension, diabetes, atherosclerosis and NASH: Cause or consequence? *J Hepatol,* 68**,** 335-352.

LUCI, C., BOURINET, M., LECLERE, P. S., ANTY, R. & GUAL, P. 2020. Chronic Inflammation in Non-Alcoholic Steatohepatitis: Molecular Mechanisms and Therapeutic Strategies. *Front Endocrinol (Lausanne),* 11**,** 597648.

LUMENG, C. N., DELPROPOSTO, J. B., WESTCOTT, D. J. & SALTIEL, A. R. 2008. Phenotypic switching of adipose tissue macrophages with obesity is generated by spatiotemporal differences in macrophage subtypes. *Diabetes,* 57**,** 3239-46.

LUTHER, J., GARBER, J. J., KHALILI, H., DAVE, M., BALE, S. S., JINDAL, R., MOTOLA, D. L., LUTHER, S., BOHR, S., JEOUNG, S. W., DESHPANDE, V., SINGH, G., TURNER, J. R., YARMUSH, M. L., CHUNG, R. T. & PATEL, S. J. 2015. Hepatic Injury in Nonalcoholic Steatohepatitis Contributes to Altered Intestinal Permeability. *Cell Mol Gastroenterol Hepatol,* 1**,** 222-232.

MA, J., FOX, C. S., JACQUES, P. F., SPELIOTES, E. K., HOFFMANN, U., SMITH, C. E., SALTZMAN, E. & MCKEOWN, N. M. 2015. Sugar-sweetened beverage, diet soda, and fatty liver disease in the Framingham Heart Study cohorts. *J Hepatol,* 63**,** 462-9.

MA, X., LIU, S., ZHANG, J., DONG, M., WANG, Y., WANG, M. & XIN, Y. 2020. Proportion of NAFLD patients with normal ALT value in overall NAFLD patients: a systematic review and meta-analysis. *BMC Gastroenterol,* 20**,** 10.

MAILING, L. J., ALLEN, J. M., BUFORD, T. W., FIELDS, C. J. & WOODS, J. A. 2019. Exercise and the Gut Microbiome: A Review of the Evidence, Potential Mechanisms, and Implications for Human Health. *Exerc Sport Sci Rev,* 47**,** 75-85.

MALAGUARNERA, M., VACANTE, M., ANTIC, T., GIORDANO, M., CHISARI, G., ACQUAVIVA, R., MASTROJENI, S., MALAGUARNERA, G., MISTRETTA, A., LI VOLTI, G. & GALVANO, F. 2012. Bifidobacterium longum with fructo-oligosaccharides in patients with non alcoholic steatohepatitis. *Dig Dis Sci,* 57**,** 545-53.

MAO, J. W., TANG, H. Y., ZHAO, T., TAN, X. Y., BI, J., WANG, B. Y. & WANG, Y. D. 2015. Intestinal mucosal barrier dysfunction participates in the progress of nonalcoholic fatty liver disease. *Int J Clin Exp Pathol,* 8**,** 3648-58.

MASARONE, M., TROISI, J., AGLITTI, A., TORRE, P., COLUCCI, A., DALLIO, M., FEDERICO, A., BALSANO, C. & PERSICO, M. 2021. Untargeted metabolomics as a diagnostic tool in NAFLD: discrimination of steatosis, steatohepatitis and cirrhosis. *Metabolomics,* 17**,** 12.

MASOODI, M., GASTALDELLI, A., HYOTYLAINEN, T., ARRETXE, E., ALONSO, C., GAGGINI, M., BROSNAN, J., ANSTEE, Q. M., MILLET, O., ORTIZ, P., MATO, J. M., DUFOUR, J. F. & ORESIC, M. 2021. Metabolomics and lipidomics in NAFLD: biomarkers and non-invasive diagnostic tests. *Nat Rev Gastroenterol Hepatol*.

MATTHEWS, D. E. 2007. An overview of phenylalanine and tyrosine kinetics in humans. *J Nutr,* 137**,** 1549S-1555S; discussion 1573S-1575S.

MEMBREZ, M., BLANCHER, F., JAQUET, M., BIBILONI, R., CANI, P. D., BURCELIN, R. G., CORTHESY, I., MACE, K. & CHOU, C. J. 2008. Gut microbiota modulation with norfloxacin and ampicillin enhances glucose tolerance in mice. *FASEB J,* 22**,** 2416-26.

MICHITAKA, K., HIRAOKA, A., KUME, M., UEHARA, T., HIDAKA, S., NINOMIYA, T., HASEBE, A., MIYAMOTO, Y., ICHIRYU, M., TANIHIRA, T., NAKAHARA, H., OCHI, H., TANABE, A., UESUGI, K., TOKUMOTO, Y., MASHIBA, T., ABE, M., HIASA, Y., MATSUURA, B. & ONJI, M. 2010. Amino acid imbalance in patients with chronic liver diseases. *Hepatol Res,* 40**,** 393-8.

MIELE, L., VALENZA, V., LA TORRE, G., MONTALTO, M., CAMMAROTA, G., RICCI, R., MASCIANA, R., FORGIONE, A., GABRIELI, M. L., PEROTTI, G., VECCHIO, F. M., RAPACCINI, G., GASBARRINI, G., DAY, C. P. & GRIECO, A. 2009. Increased intestinal permeability and tight junction alterations in nonalcoholic fatty liver disease. *Hepatology,* 49**,** 1877-87.

MORENO-NAVARRETE, J. M., SABATER, M., ORTEGA, F., RICART, W. & FERNANDEZ-REAL, J. M. 2012. Circulating zonulin, a marker of intestinal permeability, is increased in association with obesity-associated insulin resistance. *PLoS One,* 7**,** e37160.

MORGAN, A., HARTMANIS, S., TSOCHATZIS, E., NEWSOME, P. N., RYDER, S. D., ELLIOTT, R., FLOROS, L., HALL, R., HIGGINS, V., STANLEY, G., CURE, S., VASUDEVAN, S. & PEZZULLO, L. 2021. Disease burden and economic impact of diagnosed non-alcoholic steatohepatitis (NASH) in the United Kingdom (UK) in 2018. *Eur J Health Econ,* 22**,** 505-518.

MORGAN, M. Y., MILSOM, J. P. & SHERLOCK, S. 1978. Plasma ratio of valine, leucine and isoleucine to phenylalanine and tyrosine in liver disease. *Gut,* 19**,** 1068-73.

MOSCHEN, A. R., MOLNAR, C., GEIGER, S., GRAZIADEI, I., EBENBICHLER, C. F., WEISS, H., KASER, S., KASER, A. & TILG, H. 2010. Anti-inflammatory effects of excessive weight loss: potent suppression of adipose interleukin 6 and tumour necrosis factor alpha expression. *Gut,* 59**,** 1259-64.

MOUZAKI, M., COMELLI, E. M., ARENDT, B. M., BONENGEL, J., FUNG, S. K., FISCHER, S. E., MCGILVRAY, I. D. & ALLARD, J. P. 2013. Intestinal microbiota in patients with nonalcoholic fatty liver disease. *Hepatology,* 58**,** 120-7.

MOUZAKI, M., WANG, A. Y., BANDSMA, R., COMELLI, E. M., ARENDT, B. M., ZHANG, L., FUNG, S., FISCHER, S. E., MCGILVRAY, I. G. & ALLARD, J. P. 2016. Bile Acids and Dysbiosis in Non-Alcoholic Fatty Liver Disease. *PLoS One,* 11**,** e0151829.

MULLISH, B. H., PECHLIVANIS, A., BARKER, G. F., THURSZ, M. R., MARCHESI, J. R. & MCDONALD, J. A. K. 2018. Functional microbiomics: Evaluation of gut microbiota-bile acid metabolism interactions in health and disease. *Methods,* 149**,** 49-58.

MUSSO, G., GAMBINO, R. & CASSADER, M. 2010. Obesity, diabetes, and gut microbiota: the hygiene hypothesis expanded? *Diabetes Care,* 33**,** 2277-84.

NALBANTOGLU, I. L. & BRUNT, E. M. 2014. Role of liver biopsy in nonalcoholic fatty liver disease. *World J Gastroenterol,* 20**,** 9026-37.

NAVARRO, L. A., WREE, A., POVERO, D., BERK, M. P., EGUCHI, A., GHOSH, S., PAPOUCHADO, B. G., ERZURUM, S. C. & FELDSTEIN, A. E. 2015. Arginase 2 deficiency results in spontaneous steatohepatitis: a novel link between innate immune activation and hepatic de novo lipogenesis. *J Hepatol,* 62**,** 412-20.

NESUTA, O., BUDESINSKY, M., HADRAVOVA, R., MONINCOVA, L., HUMPOLICKOVA, J. & CEROVSKY, V. 2017. How proteases from Enterococcus faecalis contribute to its resistance to short alpha-helical antimicrobial peptides. *Pathog Dis,* 75.

NEUSCHWANDER-TETRI, B. A. 2010. Hepatic lipotoxicity and the pathogenesis of nonalcoholic steatohepatitis: the central role of nontriglyceride fatty acid metabolites. *Hepatology,* 52**,** 774-88.

NEWGARD, C. B., AN, J., BAIN, J. R., MUEHLBAUER, M. J., STEVENS, R. D., LIEN, L. F., HAQQ, A. M., SHAH, S. H., ARLOTTO, M., SLENTZ, C. A., ROCHON, J., GALLUP, D., ILKAYEVA, O., WENNER, B. R., YANCY, W. S., JR., EISENSON, H., MUSANTE, G., SURWIT, R. S., MILLINGTON, D. S., BUTLER, M. D. & SVETKEY, L. P. 2009. A branched-chain amino acid-related metabolic signature that differentiates obese and lean humans and contributes to insulin resistance. *Cell Metab,* 9**,** 311-26.

NICOLETTI, A., PONZIANI, F. R., BIOLATO, M., VALENZA, V., MARRONE, G., SGANGA, G., GASBARRINI, A., MIELE, L. & GRIECO, A. 2019. Intestinal permeability in the pathogenesis of liver damage: From non-alcoholic fatty liver disease to liver transplantation. *World J Gastroenterol,* 25**,** 4814-4834.

NIER, A., ENGSTLER, A. J., MAIER, I. B. & BERGHEIM, I. 2017. Markers of intestinal permeability are already altered in early stages of non-alcoholic fatty liver disease: Studies in children. *PLoS One,* 12**,** e0183282.

NIEWOLD, T. A., MEINEN, M. & VAN DER MEULEN, J. 2004. Plasma intestinal fatty acid binding protein (I-FABP) concentrations increase following intestinal ischemia in pigs. *Res Vet Sci,* 77**,** 89-91.

NOBILI, V., ALISI, A., CUTRERA, R., CARPINO, G., DE STEFANIS, C., D'ORIA, V., DE VITO, R., CUCCHIARA, S., GAUDIO, E. & MUSSO, G. 2015. Altered gut-liver axis and hepatic adiponectin expression in OSAS: novel mediators of liver injury in paediatric non-alcoholic fatty liver. *Thorax,* 70**,** 769-81.

NOUREDDIN, M., JONES, C., ALKHOURI, N., GOMEZ, E. V., DIETERICH, D. T., RINELLA, M. E. & NASHNET 2020. Screening for Nonalcoholic Fatty Liver Disease in Persons with Type 2 Diabetes in the United States Is Cost-effective: A Comprehensive Cost-Utility Analysis. *Gastroenterology,* 159**,** 1985-1987 e4.

OARADA, M., TAKAHASHI-NAKAGUCHI, A., ABE, T., NIKAWA, T., MIKI, T. & GONOI, T. 2015. Refeeding with glucose rather than fructose elicits greater hepatic inflammatory gene expression in mice. *Nutrition,* 31**,** 757-65.

ODENWALD, M. A. & TURNER, J. R. 2013. Intestinal permeability defects: is it time to treat? *Clin Gastroenterol Hepatol,* 11**,** 1075-83.

OFFICE, G. F. April, 2014. Tackling obesities: future choices - project report 2014.

ONUMPAI, C., KOLIDA, S., BONNIN, E. & RASTALL, R. A. 2011. Microbial utilization and selectivity of pectin fractions with various structures. *Appl Environ Microbiol,* 77**,** 5747-54.

ORTIZ, C., SCHIERWAGEN, R., SCHAEFER, L., KLEIN, S., TREPAT, X. & TREBICKA, J. 2021. Extracellular Matrix Remodeling in Chronic Liver Disease. *Curr Tissue Microenviron Rep***,** 1-12.

OST, K. S. & ROUND, J. L. 2017. A Few Good Commensals: Gut Microbes Use IFN-gamma to Fight Salmonella. *Immunity,* 46**,** 977-979.

PACIFICO, L., BONCI, E., MARANDOLA, L., ROMAGGIOLI, S., BASCETTA, S. & CHIESA, C. 2014. Increased circulating zonulin in children with biopsy-proven nonalcoholic fatty liver disease. *World J Gastroenterol,* 20**,** 17107-14.

PAIS, R., CHARLOTTE, F., FEDCHUK, L., BEDOSSA, P., LEBRAY, P., POYNARD, T., RATZIU, V. & GROUP, L. S. 2013. A systematic review of follow-up biopsies reveals disease progression in patients with non-alcoholic fatty liver. *J Hepatol,* 59**,** 550-6.

PAIS, R., PASCALE, A., FEDCHUCK, L., CHARLOTTE, F., POYNARD, T. & RATZIU, V. 2011. Progression from isolated steatosis to steatohepatitis and fibrosis in nonalcoholic fatty liver disease. *Clin Res Hepatol Gastroenterol,* 35**,** 23-8.

PARLESAK, A., SCHAFER, C., SCHUTZ, T., BODE, J. C. & BODE, C. 2000. Increased intestinal permeability to macromolecules and endotoxemia in patients with chronic alcohol abuse in different stages of alcohol-induced liver disease. *J Hepatol,* 32**,** 742-7.

PATEL, R. & DUPONT, H. L. 2015. New approaches for bacteriotherapy: prebiotics, new-generation probiotics, and synbiotics. *Clin Infect Dis,* 60 Suppl 2**,** S108-21.

PISCAGLIA, F., SVEGLIATI-BARONI, G., BARCHETTI, A., PECORELLI, A., MARINELLI, S., TIRIBELLI, C., BELLENTANI, S. & GROUP, H.-N. I. S. 2016. Clinical patterns of hepatocellular carcinoma in nonalcoholic fatty liver disease: A multicenter prospective study. *Hepatology,* 63**,** 827-38.

POLYZOS, S. A. & MANTZOROS, C. S. 2016. Nonalcoholic fatty future disease. *Metabolism,* 65**,** 1007-16.

POYNARD, T., PARADIS, V., MULLAERT, J., DECKMYN, O., GAULT, N., MARCAULT, E., MANCHON, P., SI MOHAMMED, N., PARFAIT, B., IBBERSON, M., GAUTIER, J. F., BOITARD, C., CZERNICHOW, S., LARGER, E., DRANE, F., CASTILLE, J. M., PETA, V., BRZUSTOWSKI, A., TERRIS, B., VALLET-PICHARD, A., ROULOT, D., LAOUENAN, C., BEDOSSA, P., CASTERA, L., POL, S., VALLA, D. & QUID-NASH, C. 2021. Prospective external validation of a new non-invasive test for the diagnosis of non-alcoholic steatohepatitis in patients with type 2 diabetes. *Aliment Pharmacol Ther,* 54**,** 952-966.

PROMRAT, K., KLEINER, D. E., NIEMEIER, H. M., JACKVONY, E., KEARNS, M., WANDS, J. R., FAVA, J. L. & WING, R. R. 2010. Randomized controlled trial testing the effects of weight loss on nonalcoholic steatohepatitis. *Hepatology,* 51**,** 121-9.

PROPERZI, C., O'SULLIVAN, T. A., SHERRIFF, J. L., CHING, H. L., JEFFREY, G. P., BUCKLEY, R. F., TIBBALLS, J., MACQUILLAN, G. C., GARAS, G. & ADAMS, L. A. 2018. Ad Libitum Mediterranean and Low-Fat Diets Both Significantly Reduce Hepatic Steatosis: A Randomized Controlled Trial. *Hepatology,* 68**,** 1741-1754.

PU, K., WANG, Y., BAI, S., WEI, H., ZHOU, Y., FAN, J. & QIAO, L. 2019. Diagnostic accuracy of controlled attenuation parameter (CAP) as a non-invasive test for steatosis in suspected non-alcoholic fatty liver disease: a systematic review and meta-analysis. *BMC Gastroenterol,* 19**,** 51.

PURI, P., DAITA, K., JOYCE, A., MIRSHAHI, F., SANTHEKADUR, P. K., CAZANAVE, S., LUKETIC, V. A., SIDDIQUI, M. S., BOYETT, S., MIN, H. K., KUMAR, D. P., KOHLI, R., ZHOU, H., HYLEMON, P. B., CONTOS, M. J., IDOWU, M. & SANYAL, A. J. 2018. The presence and severity of nonalcoholic steatohepatitis is associated with specific changes in circulating bile acids. *Hepatology,* 67**,** 534-548.

PUSSINEN, P. J., HAVULINNA, A. S., LEHTO, M., SUNDVALL, J. & SALOMAA, V. 2011. Endotoxemia is associated with an increased risk of incident diabetes. *Diabetes Care,* 34**,** 392-7.

RIDAURA, V. K., FAITH, J. J., REY, F. E., CHENG, J., DUNCAN, A. E., KAU, A. L., GRIFFIN, N. W., LOMBARD, V., HENRISSAT, B., BAIN, J. R., MUEHLBAUER, M. J., ILKAYEVA, O., SEMENKOVICH, C. F., FUNAI, K., HAYASHI, D. K., LYLE, B. J., MARTINI, M. C., URSELL, L. K., CLEMENTE, J. C., VAN TREUREN, W., WALTERS, W. A., KNIGHT, R., NEWGARD, C. B., HEATH, A. C. & GORDON, J. I. 2013. Gut microbiota from twins discordant for obesity modulate metabolism in mice. *Science,* 341**,** 1241214.

RINELLA, M. & CHARLTON, M. 2016. The globalization of nonalcoholic fatty liver disease: Prevalence and impact on world health. *Hepatology,* 64**,** 19-22.

RINNINELLA, E., RAOUL, P., CINTONI, M., FRANCESCHI, F., MIGGIANO, G. A. D., GASBARRINI, A. & MELE, M. C. 2019. What is the Healthy Gut Microbiota Composition? A Changing Ecosystem across Age, Environment, Diet, and Diseases. *Microorganisms,* 7.

RIPPIN, H. L., HUTCHINSON, J., GREENWOOD, D. C., JEWELL, J., BREDA, J. J., MARTIN, A., RIPPIN, D. M., SCHINDLER, K., RUST, P., FAGT, S., MATTHIESSEN, J., NURK, E., NELIS, K., KUKK, M., TAPANAINEN, H., VALSTA, L., HEUER, T., SARKADI-NAGY, E., BAKACS, M., TAZHIBAYEV, S., SHARMANOV, T., SPIROSKI, I., BEUKERS, M., VAN ROSSUM, C., OCKE, M., LINDROOS, A. K., WARENSJO LEMMING, E. & CADE, J. E. 2020. Inequalities in education and national income are associated with poorer diet: Pooled analysis of individual participant data across 12 European countries. *PLoS One,* 15**,** e0232447.

RIVA, A., GRAY, E. H., AZARIAN, S., ZAMALLOA, A., MCPHAIL, M. J. W., VINCENT, R. P., WILLIAMS, R., CHOKSHI, S., PATEL, V. C. & EDWARDS, L. A. 2020. Faecal cytokine profiling as a marker of intestinal inflammation in acutely decompensated cirrhosis. *JHEP Rep,* 2**,** 100151.

RIVERA, C. A., ADEGBOYEGA, P., VAN ROOIJEN, N., TAGALICUD, A., ALLMAN, M. & WALLACE, M. 2007. Toll-like receptor-4 signaling and Kupffer cells play pivotal roles in the pathogenesis of non-alcoholic steatohepatitis. *J Hepatol,* 47**,** 571-9.

ROM, O., VILLACORTA, L., ZHANG, J., CHEN, Y. E. & AVIRAM, M. 2018. Emerging therapeutic potential of glycine in cardiometabolic diseases: dual benefits in lipid and glucose metabolism. *Curr Opin Lipidol,* 29**,** 428-432.

ROSENBERG, W. M., VOELKER, M., THIEL, R., BECKA, M., BURT, A., SCHUPPAN, D., HUBSCHER, S., ROSKAMS, T., PINZANI, M., ARTHUR, M. J. & EUROPEAN LIVER FIBROSIS, G. 2004. Serum markers detect the presence of liver fibrosis: a cohort study. *Gastroenterology,* 127**,** 1704-13.

RYAN, M. C., ITSIOPOULOS, C., THODIS, T., WARD, G., TROST, N., HOFFERBERTH, S., O'DEA, K., DESMOND, P. V., JOHNSON, N. A. & WILSON, A. M. 2013. The Mediterranean diet improves hepatic steatosis and insulin sensitivity in individuals with non-alcoholic fatty liver disease. *J Hepatol,* 59**,** 138-43.

SABERI, M., WOODS, N. B., DE LUCA, C., SCHENK, S., LU, J. C., BANDYOPADHYAY, G., VERMA, I. M. & OLEFSKY, J. M. 2009. Hematopoietic cell-specific deletion of toll-like receptor 4 ameliorates hepatic and adipose tissue insulin resistance in high-fat-fed mice. *Cell Metab,* 10**,** 419-29.

SAID, A., GAGOVIC, V., MALECKI, K., GIVENS, M. L. & NIETO, F. J. 2013. Primary care practitioners survey of non-alcoholic fatty liver disease. *Ann Hepatol,* 12**,** 758-65.

SANCHEZ-RODRIGUEZ, E., EGEA-ZORRILLA, A., PLAZA-DIAZ, J., ARAGON-VELA, J., MUNOZ-QUEZADA, S., TERCEDOR-SANCHEZ, L. & ABADIA-MOLINA, F. 2020. The Gut Microbiota and Its Implication in the Development of Atherosclerosis and Related Cardiovascular Diseases. *Nutrients,* 12.

SANDLER, N. G., KOH, C., ROQUE, A., ECCLESTON, J. L., SIEGEL, R. B., DEMINO, M., KLEINER, D. E., DEEKS, S. G., LIANG, T. J., HELLER, T. & DOUEK, D. C. 2011. Host response to translocated microbial products predicts outcomes of patients with HBV or HCV infection. *Gastroenterology,* 141**,** 1220-30, 1230 e1-3.

SANGSTER, T., MAJOR, H., PLUMB, R., WILSON, A. J. & WILSON, I. D. 2006. A pragmatic and readily implemented quality control strategy for HPLC-MS and GC-MS-based metabonomic analysis. *Analyst,* 131**,** 1075-8.

SARAFIAN, M. H., LEWIS, M. R., PECHLIVANIS, A., RALPHS, S., MCPHAIL, M. J., PATEL, V. C., DUMAS, M. E., HOLMES, E. & NICHOLSON, J. K. 2015. Bile acid profiling and quantification in biofluids using ultra-performance liquid chromatography tandem mass spectrometry. *Anal Chem,* 87**,** 9662-70.

SATHYANARAYANA, P., JOGI, M., MUTHUPILLAI, R., KRISHNAMURTHY, R., SAMSON, S. L. & BAJAJ, M. 2011. Effects of combined exenatide and pioglitazone therapy on hepatic fat content in type 2 diabetes. *Obesity (Silver Spring),* 19**,** 2310-5.

SCHLIEP, K., POTTS, A. J., MORRISON, D. A., GRIMM, G. W. 2017. Intertwining phylogenetic trees and networks. *Methods in Ecology and Evolution*.

SCHNABL, B. 2021. Update on the Role of the Gut Microbiota on Alcohol-Associated Liver Disease. *Gastroenterol Hepatol (N Y),* 17**,** 381-383.

SCHOEPFER, A. M., BEGLINGER, C., STRAUMANN, A., TRUMMLER, M., VAVRICKA, S. R., BRUEGGER, L. E. & SEIBOLD, F. 2010. Fecal calprotectin correlates more closely with the Simple Endoscopic Score for Crohn's disease (SES-CD) than CRP, blood leukocytes, and the CDAI. *Am J Gastroenterol,* 105**,** 162-9.

SCHOULTZ, I. & KEITA, A. V. 2020. The Intestinal Barrier and Current Techniques for the Assessment of Gut Permeability. *Cells,* 9.

SCHWARTZ, S. E., LEVINE, R. A., WEINSTOCK, R. S., PETOKAS, S., MILLS, C. A. & THOMAS, F. D. 1988. Sustained pectin ingestion: effect on gastric emptying and glucose tolerance in non-insulin-dependent diabetic patients. *Am J Clin Nutr,* 48**,** 1413-7.

SENDER, R., FUCHS, S. & MILO, R. 2016. Revised Estimates for the Number of Human and Bacteria Cells in the Body. *PLoS Biol,* 14**,** e1002533.

SHERIDAN, D. A., AITHAL, G., ALAZAWI, W., ALLISON, M., ANSTEE, Q., COBBOLD, J., KHAN, S., FOWELL, A., MCPHERSON, S., NEWSOME, P. N., OBEN, J., TOMLINSON, J. & TSOCHATZIS, E. 2017. Care standards for non-alcoholic fatty liver disease in the United Kingdom 2016: a cross-sectional survey. *Frontline Gastroenterol,* 8**,** 252-259.

SILVA-TINOCO, R., CUATECONTZI-XOCHITIOTZI, T., DE LA TORRE-SALDANA, V., LEON-GARCIA, E., SERNA-ALVARADO, J., OREA-TEJEDA, A., CASTILLO-MARTINEZ, L., GAY, J. G., CANTU-DE-LEON, D. & PRADA, D. 2020. Influence of social determinants, diabetes knowledge, health behaviors, and glycemic control in type 2 diabetes: an analysis from real-world evidence. *BMC Endocr Disord,* 20**,** 130.

SMITH, P. M., HOWITT, M. R., PANIKOV, N., MICHAUD, M., GALLINI, C. A., BOHLOOLY, Y. M., GLICKMAN, J. N. & GARRETT, W. S. 2013. The microbial metabolites, short-chain fatty acids, regulate colonic Treg cell homeostasis. *Science,* 341**,** 569-73.

SRINIVASAN, B., KOLLI, A. R., ESCH, M. B., ABACI, H. E., SHULER, M. L. & HICKMAN, J. J. 2015. TEER measurement techniques for in vitro barrier model systems. *J Lab Autom,* 20**,** 107-26.

SRIVASTAVA, A., GAILER, R., TANWAR, S., TREMBLING, P., PARKES, J., RODGER, A., SURI, D., THORBURN, D., SENNETT, K., MORGAN, S., TSOCHATZIS, E. A. & ROSENBERG, W. 2019. Prospective evaluation of a primary care referral pathway for patients with non-alcoholic fatty liver disease. *J Hepatol,* 71**,** 371-378.

STATISTICS, O. F. N. Mid-2018. Population Estimates for UK, England and Wales, Scotland and NI.

STAUDINGER, J. L., GOODWIN, B., JONES, S. A., HAWKINS-BROWN, D., MACKENZIE, K. I., LATOUR, A., LIU, Y., KLAASSEN, C. D., BROWN, K. K., REINHARD, J., WILLSON, T. M., KOLLER, B. H. & KLIEWER, S. A. 2001. The nuclear receptor PXR is a lithocholic acid sensor that protects against liver toxicity. *Proc Natl Acad Sci U S A,* 98**,** 3369-74.

STEWART, K. E., HALLER, D. L., SARGEANT, C., LEVENSON, J. L., PURI, P. & SANYAL, A. J. 2015. Readiness for behaviour change in non-alcoholic fatty liver disease: implications for multidisciplinary care models. *Liver Int,* 35**,** 936-43.

STEWART, R. A. H. 2018. Primary Prevention of Cardiovascular Disease with a Mediterranean Diet Supplemented with Extra-Virgin Olive Oil or Nuts. *N Engl J Med,* 379**,** 1388.

STIENSTRA, R., SAUDALE, F., DUVAL, C., KESHTKAR, S., GROENER, J. E., VAN ROOIJEN, N., STAELS, B., KERSTEN, S. & MULLER, M. 2010. Kupffer cells promote hepatic steatosis via interleukin-1beta-dependent suppression of peroxisome proliferator-activated receptor alpha activity. *Hepatology,* 51**,** 511-22.

STOJANOV, S., BERLEC, A. & STRUKELJ, B. 2020. The Influence of Probiotics on the Firmicutes/Bacteroidetes Ratio in the Treatment of Obesity and Inflammatory Bowel disease. *Microorganisms,* 8.

SUZUKI, D., TOYODA, M., KIMURA, M., MIYAUCHI, M., YAMAMOTO, N., SATO, H., TANAKA, E., KURIYAMA, Y., MIYATAKE, H., ABE, M., UMEZONO, T. & FUKAGAWA, M. 2013. Effects of liraglutide, a human glucagon-like peptide-1 analogue, on body weight, body fat area and body fat-related markers in patients with type 2 diabetes mellitus. *Intern Med,* 52**,** 1029-34.

SUZUKI, T., YOSHINAGA, N. & TANABE, S. 2011. Interleukin-6 (IL-6) regulates claudin-2 expression and tight junction permeability in intestinal epithelium. *J Biol Chem,* 286**,** 31263-71.

TAKIS, P. G., JIMENEZ, B., SANDS, C. J., CHEKMENEVA, E. & LEWIS, M. R. 2020. SMolESY: an efficient and quantitative alternative to on-instrument macromolecular (1)H-NMR signal suppression. *Chem Sci,* 11**,** 6000-6011.

TANAJEWSKI, L., HARRIS, R., HARMAN, D. J., AITHAL, G. P., CARD, T. R., GKOUNTOURAS, G., BERDUNOV, V., GUHA, I. N. & ELLIOTT, R. A. 2017. Economic evaluation of a community-based diagnostic pathway to stratify adults for non-alcoholic fatty liver disease: a Markov model informed by a feasibility study. *BMJ Open,* 7**,** e015659.

TARGHER, G., BYRNE, C. D., LONARDO, A., ZOPPINI, G. & BARBUI, C. 2016. Non-alcoholic fatty liver disease and risk of incident cardiovascular disease: A meta-analysis. *J Hepatol,* 65**,** 589-600.

TARGHER, G., COREY, K. E., BYRNE, C. D. & RODEN, M. 2021. The complex link between NAFLD and type 2 diabetes mellitus - mechanisms and treatments. *Nat Rev Gastroenterol Hepatol,* 18**,** 599-612.

THAISS, C. A., LEVY, M., GROSHEVA, I., ZHENG, D., SOFFER, E., BLACHER, E., BRAVERMAN, S., TENGELER, A. C., BARAK, O., ELAZAR, M., BEN-ZEEV, R., LEHAVI-REGEV, D., KATZ, M. N., PEVSNER-FISCHER, M., GERTLER, A., HALPERN, Z., HARMELIN, A., AAMAR, S., SERRADAS, P., GROSFELD, A., SHAPIRO, H., GEIGER, B. & ELINAV, E. 2018. Hyperglycemia drives intestinal barrier dysfunction and risk for enteric infection. *Science,* 359**,** 1376-1383.

THIENNIMITR, P., WINTER, S. E., WINTER, M. G., XAVIER, M. N., TOLSTIKOV, V., HUSEBY, D. L., STERZENBACH, T., TSOLIS, R. M., ROTH, J. R. & BAUMLER, A. J. 2011. Intestinal inflammation allows Salmonella to use ethanolamine to compete with the microbiota. *Proc Natl Acad Sci U S A,* 108**,** 17480-5.

TILG, H. 2017. How to Approach a Patient With Nonalcoholic Fatty Liver Disease. *Gastroenterology,* 153**,** 345-349.

TORDJMAN, J., POITOU, C., HUGOL, D., BOUILLOT, J. L., BASDEVANT, A., BEDOSSA, P., GUERRE-MILLO, M. & CLEMENT, K. 2009. Association between omental adipose tissue macrophages and liver histopathology in morbid obesity: influence of glycemic status. *J Hepatol,* 51**,** 354-62.

TORRES, D. M., WILLIAMS, C. D. & HARRISON, S. A. 2012. Features, diagnosis, and treatment of nonalcoholic fatty liver disease. *Clin Gastroenterol Hepatol,* 10**,** 837-58.

TURNBAUGH, P. J., LEY, R. E., MAHOWALD, M. A., MAGRINI, V., MARDIS, E. R. & GORDON, J. I. 2006. An obesity-associated gut microbiome with increased capacity for energy harvest. *Nature,* 444**,** 1027-31.

USHER-SMITH, J. A., SHARP, S. J. & GRIFFIN, S. J. 2016. The spectrum effect in tests for risk prediction, screening, and diagnosis. *BMJ,* 353**,** i3139.

VALLET-PICHARD, A., MALLET, V., NALPAS, B., VERKARRE, V., NALPAS, A., DHALLUIN-VENIER, V., FONTAINE, H. & POL, S. 2007. FIB-4: an inexpensive and accurate marker of fibrosis in HCV infection. comparison with liver biopsy and fibrotest. *Hepatology,* 46**,** 32-6.

VAN SPAENDONK, H., CEULEERS, H., WITTERS, L., PATTEET, E., JOOSSENS, J., AUGUSTYNS, K., LAMBEIR, A. M., DE MEESTER, I., DE MAN, J. G. & DE WINTER, B. Y. 2017. Regulation of intestinal permeability: The role of proteases. *World J Gastroenterol,* 23**,** 2106-2123.

VESELKOV, K. A., VINGARA, L. K., MASSON, P., ROBINETTE, S. L., WANT, E., LI, J. V., BARTON, R. H., BOURSIER-NEYRET, C., WALTHER, B., EBBELS, T. M., PELCZER, I., HOLMES, E., LINDON, J. C. & NICHOLSON, J. K. 2011. Optimized preprocessing of ultra-performance liquid chromatography/mass spectrometry urinary metabolic profiles for improved information recovery. *Anal Chem,* 83**,** 5864-72.

VILAR-GOMEZ, E., MARTINEZ-PEREZ, Y., CALZADILLA-BERTOT, L., TORRES-GONZALEZ, A., GRA-ORAMAS, B., GONZALEZ-FABIAN, L., FRIEDMAN, S. L., DIAGO, M. & ROMERO-GOMEZ, M. 2015. Weight Loss Through Lifestyle Modification Significantly Reduces Features of Nonalcoholic Steatohepatitis. *Gastroenterology,* 149**,** 367-78 e5; quiz e14-5.

VILSBOLL, T., CHRISTENSEN, M., JUNKER, A. E., KNOP, F. K. & GLUUD, L. L. 2012. Effects of glucagon-like peptide-1 receptor agonists on weight loss: systematic review and meta-analyses of randomised controlled trials. *BMJ,* 344**,** d7771.

VINOLO, M. A., RODRIGUES, H. G., HATANAKA, E., HEBEDA, C. B., FARSKY, S. H. & CURI, R. 2009. Short-chain fatty acids stimulate the migration of neutrophils to inflammatory sites. *Clin Sci (Lond),* 117**,** 331-8.

VINOLO, M. A., RODRIGUES, H. G., NACHBAR, R. T. & CURI, R. 2011. Regulation of inflammation by short chain fatty acids. *Nutrients,* 3**,** 858-76.

VOLPE, D. A. 2011. Drug-permeability and transporter assays in Caco-2 and MDCK cell lines. *Future Med Chem,* 3**,** 2063-77.

VRIEZE, A., VAN NOOD, E., HOLLEMAN, F., SALOJARVI, J., KOOTTE, R. S., BARTELSMAN, J. F., DALLINGA-THIE, G. M., ACKERMANS, M. T., SERLIE, M. J., OOZEER, R., DERRIEN, M., DRUESNE, A., VAN HYLCKAMA VLIEG, J. E., BLOKS, V. W., GROEN, A. K., HEILIG, H. G., ZOETENDAL, E. G., STROES, E. S., DE VOS, W. M., HOEKSTRA, J. B. & NIEUWDORP, M. 2012. Transfer of intestinal microbiota from lean donors increases insulin sensitivity in individuals with metabolic syndrome. *Gastroenterology,* 143**,** 913-6 e7.

WALKER, A. W. & PARKHILL, J. 2013. Microbiology. Fighting obesity with bacteria. *Science,* 341**,** 1069-70.

WAN, J., BENKDANE, M., TEIXEIRA-CLERC, F., BONNAFOUS, S., LOUVET, A., LAFDIL, F., PECKER, F., TRAN, A., GUAL, P., MALLAT, A., LOTERSZTAJN, S. & PAVOINE, C. 2014. M2 Kupffer cells promote M1 Kupffer cell apoptosis: a protective mechanism against alcoholic and nonalcoholic fatty liver disease. *Hepatology,* 59**,** 130-42.

WANG, T. J., LARSON, M. G., VASAN, R. S., CHENG, S., RHEE, E. P., MCCABE, E., LEWIS, G. D., FOX, C. S., JACQUES, P. F., FERNANDEZ, C., O'DONNELL, C. J., CARR, S. A., MOOTHA, V. K., FLOREZ, J. C., SOUZA, A., MELANDER, O., CLISH, C. B. & GERSZTEN, R. E. 2011. Metabolite profiles and the risk of developing diabetes. *Nat Med,* 17**,** 448-53.

WANLESS, I. R. & LENTZ, J. S. 1990. Fatty liver hepatitis (steatohepatitis) and obesity: an autopsy study with analysis of risk factors. *Hepatology,* 12**,** 1106-10.

WATSON, C. J., HOARE, C. J., GARROD, D. R., CARLSON, G. L. & WARHURST, G. 2005. Interferon-gamma selectively increases epithelial permeability to large molecules by activating different populations of paracellular pores. *J Cell Sci,* 118**,** 5221-30.

WIGG, A. J., ROBERTS-THOMSON, I. C., DYMOCK, R. B., MCCARTHY, P. J., GROSE, R. H. & CUMMINS, A. G. 2001. The role of small intestinal bacterial overgrowth, intestinal permeability, endotoxaemia, and tumour necrosis factor alpha in the pathogenesis of non-alcoholic steatohepatitis. *Gut,* 48**,** 206-11.

WIKLUND, S., JOHANSSON, E., SJOSTROM, L., MELLEROWICZ, E. J., EDLUND, U., SHOCKCOR, J. P., GOTTFRIES, J., MORITZ, T. & TRYGG, J. 2008. Visualization of GC/TOF-MS-based metabolomics data for identification of biochemically interesting compounds using OPLS class models. *Anal Chem,* 80**,** 115-22.

WILLIAMS, R., ASPINALL, R., BELLIS, M., CAMPS-WALSH, G., CRAMP, M., DHAWAN, A., FERGUSON, J., FORTON, D., FOSTER, G., GILMORE, I., HICKMAN, M., HUDSON, M., KELLY, D., LANGFORD, A., LOMBARD, M., LONGWORTH, L., MARTIN, N., MORIARTY, K., NEWSOME, P., O'GRADY, J., PRYKE, R., RUTTER, H., RYDER, S., SHERON, N. & SMITH, T. 2014. Addressing liver disease in the UK: a blueprint for attaining excellence in health care and reducing premature mortality from lifestyle issues of excess consumption of alcohol, obesity, and viral hepatitis. *Lancet,* 384**,** 1953-97.

WILLIAMSON, R. M., PRICE, J. F., GLANCY, S., PERRY, E., NEE, L. D., HAYES, P. C., FRIER, B. M., VAN LOOK, L. A., JOHNSTON, G. I., REYNOLDS, R. M., STRACHAN, M. W. & EDINBURGH TYPE 2 DIABETES STUDY, I. 2011. Prevalence of and risk factors for hepatic steatosis and nonalcoholic Fatty liver disease in people with type 2 diabetes: the Edinburgh Type 2 Diabetes Study. *Diabetes Care,* 34**,** 1139-44.

WILSON, A. S., KOLLER, K. R., RAMABOLI, M. C., NESENGANI, L. T., OCVIRK, S., CHEN, C., FLANAGAN, C. A., SAPP, F. R., MERRITT, Z. T., BHATTI, F., THOMAS, T. K. & O'KEEFE, S. J. D. 2020. Diet and the Human Gut Microbiome: An International Review. *Dig Dis Sci,* 65**,** 723-740.

WONG, V. W., CHAN, R. S., WONG, G. L., CHEUNG, B. H., CHU, W. C., YEUNG, D. K., CHIM, A. M., LAI, J. W., LI, L. S., SEA, M. M., CHAN, F. K., SUNG, J. J., WOO, J. & CHAN, H. L. 2013a. Community-based lifestyle modification programme for non-alcoholic fatty liver disease: a randomized controlled trial. *J Hepatol,* 59**,** 536-42.

WONG, V. W., TSE, C. H., LAM, T. T., WONG, G. L., CHIM, A. M., CHU, W. C., YEUNG, D. K., LAW, P. T., KWAN, H. S., YU, J., SUNG, J. J. & CHAN, H. L. 2013b. Molecular characterization of the fecal microbiota in patients with nonalcoholic steatohepatitis--a longitudinal study. *PLoS One,* 8**,** e62885.

WONG, V. W., WON, G. L., CHIM, A. M., CHU, W. C., YEUNG, D. K., LI, K. C. & CHAN, H. L. 2013c. Treatment of nonalcoholic steatohepatitis with probiotics. A proof-of-concept study. *Ann Hepatol,* 12**,** 256-62.

WONG, V. W., WONG, G. L., TSANG, S. W., HUI, A. Y., CHAN, A. W., CHOI, P. C., CHIM, A. M., CHU, S., CHAN, F. K., SUNG, J. J. & CHAN, H. L. 2009. Metabolic and histological features of non-alcoholic fatty liver disease patients with different serum alanine aminotransferase levels. *Aliment Pharmacol Ther,* 29**,** 387-96.

WOSTMANN, B. S., LARKIN, C., MORIARTY, A. & BRUCKNER-KARDOSS, E. 1983. Dietary intake, energy metabolism, and excretory losses of adult male germfree Wistar rats. *Lab Anim Sci,* 33**,** 46-50.

XIA, J. & WISHART, D. S. 2010. MetPA: a web-based metabolomics tool for pathway analysis and visualization. *Bioinformatics,* 26**,** 2342-4.

YAMAKADO, M., TANAKA, T., NAGAO, K., IMAIZUMI, A., KOMATSU, M., DAIMON, T., MIYANO, H., TANI, M., TODA, A., YAMAMOTO, H., HORIMOTO, K. & ISHIZAKA, Y. 2017. Plasma amino acid profile associated with fatty liver disease and co-occurrence of metabolic risk factors. *Sci Rep,* 7**,** 14485.

YASUTAKE, K., NAKAMUTA, M., SHIMA, Y., OHYAMA, A., MASUDA, K., HARUTA, N., FUJINO, T., AOYAGI, Y., FUKUIZUMI, K., YOSHIMOTO, T., TAKEMOTO, R., MIYAHARA, T., HARADA, N., HAYATA, F., NAKASHIMA, M. & ENJOJI, M. 2009. Nutritional investigation of non-obese patients with non-alcoholic fatty liver disease: the significance of dietary cholesterol. *Scand J Gastroenterol,* 44**,** 471-7.

YOSHIDA, N., EMOTO, T., YAMASHITA, T., WATANABE, H., HAYASHI, T., TABATA, T., HOSHI, N., HATANO, N., OZAWA, G., SASAKI, N., MIZOGUCHI, T., AMIN, H. Z., HIROTA, Y., OGAWA, W., YAMADA, T. & HIRATA,

K. I. 2018. Bacteroides vulgatus and Bacteroides dorei Reduce Gut Microbial Lipopolysaccharide Production and Inhibit Atherosclerosis. *Circulation,* 138**,** 2486-2498.

YOUNES, R. & BUGIANESI, E. 2019. A spotlight on pathogenesis, interactions and novel therapeutic options in NAFLD. *Nat Rev Gastroenterol Hepatol,* 16**,** 80-82.

YOUNOSSI, Z., STEPANOVA, M., ONG, J. P., JACOBSON, I. M., BUGIANESI, E., DUSEJA, A., EGUCHI, Y., WONG, V. W., NEGRO, F., YILMAZ, Y., ROMERO-GOMEZ, M., GEORGE, J., AHMED, A., WONG, R., YOUNOSSI, I., ZIAYEE, M., AFENDY, A. & GLOBAL NONALCOHOLIC STEATOHEPATITIS, C. 2019a. Nonalcoholic Steatohepatitis Is the Fastest Growing Cause of Hepatocellular Carcinoma in Liver Transplant Candidates. *Clin Gastroenterol Hepatol,* 17**,** 748-755 e3.

YOUNOSSI, Z., TACKE, F., ARRESE, M., CHANDER SHARMA, B., MOSTAFA, I., BUGIANESI, E., WAI-SUN WONG, V., YILMAZ, Y., GEORGE, J., FAN, J. & VOS, M. B. 2019b. Global Perspectives on Nonalcoholic Fatty Liver Disease and Nonalcoholic Steatohepatitis. *Hepatology,* 69**,** 2672-2682.

YOUNOSSI, Z. M. & HENRY, L. 2021. Epidemiology of non-alcoholic fatty liver disease and hepatocellular carcinoma. *JHEP Rep,* 3**,** 100305.

YOUNOSSI, Z. M., ONG, J. P., TAKAHASHI, H., YILMAZ, Y., EGUCHI, Y., EL KASSAS, M., BUTI, M., DIAGO, M., ZHENG, M. H., FAN, J. G., YU, M. L., WAI-SUN WONG, V., ALSWAT, K., CHAN, W. K., MENDEZ-SANCHEZ, N., BURRA, P., BUGIANESI, E., DUSEJA, A. K., GEORGE, J., PAPATHEODORIDIS, G. V., SAEED, H., CASTERA, L., ARRESE, M., KUGELMAS, M., ROMERO-GOMEZ, M., ALQAHTANI, S., ZIAYEE, M., LAM, B., YOUNOSSI, I., RACILA, A., HENRY, L., STEPANOVA, M. & GLOBAL, N. C. 2021. A Global Survey of Physicians Knowledge About Non-alcoholic Fatty Liver Disease. *Clin Gastroenterol Hepatol*.

YOUNOSSI, Z. M., RATZIU, V., LOOMBA, R., RINELLA, M., ANSTEE, Q. M., GOODMAN, Z., BEDOSSA, P., GEIER, A., BECKEBAUM, S., NEWSOME, P. N., SHERIDAN, D., SHEIKH, M. Y., TROTTER, J., KNAPPLE, W., LAWITZ, E., ABDELMALEK, M. F., KOWDLEY, K. V., MONTANO-LOZA, A. J., BOURSIER, J., MATHURIN, P., BUGIANESI, E., MAZZELLA, G., OLVEIRA, A., CORTEZ-PINTO, H., GRAUPERA, I., ORR, D., GLUUD, L. L., DUFOUR, J. F., SHAPIRO, D., CAMPAGNA, J., ZARU, L., MACCONELL, L., SHRINGARPURE, R., HARRISON, S., SANYAL, A. J. & INVESTIGATORS, R. S. 2019c. Obeticholic acid for the treatment of non-alcoholic steatohepatitis: interim analysis from a multicentre, randomised, placebo-controlled phase 3 trial. *Lancet,* 394**,** 2184-2196.

YOUNOSSI, Z. M., TAMPI, R., PRIYADARSHINI, M., NADER, F., YOUNOSSI, I. M. & RACILA, A. 2019d. Burden of Illness and Economic Model for Patients With Nonalcoholic Steatohepatitis in the United States. *Hepatology,* 69**,** 564-572.

YU, C., JIA, G., DENG, Q., ZHAO, H., CHEN, X., LIU, G. & WANG, K. 2016. The Effects of Glucagon-like Peptide-2 on the Tight Junction and Barrier Function in IPEC-J2 Cells through Phosphatidylinositol 3-kinase-Protein Kinase B-Mammalian Target of Rapamycin Signaling Pathway. *Asian-Australas J Anim Sci,* 29**,** 731-8.

YUILLE, S., REICHARDT, N., PANDA, S., DUNBAR, H. & MULDER, I. E. 2018. Human gut bacteria as potent class I histone deacetylase inhibitors in vitro through production of butyric acid and valeric acid. *PLoS One,* 13**,** e0201073.

ZELBER-SAGI, S., IVANCOVSKY-WAJCMAN, D., FLISS ISAKOV, N., WEBB, M., ORENSTEIN, D., SHIBOLET, O. & KARIV, R. 2018. High red and processed meat consumption is associated with non-alcoholic fatty liver disease and insulin resistance. *J Hepatol,* 68**,** 1239-1246.

ZHOU, Y., ORESIC, M., LEIVONEN, M., GOPALACHARYULU, P., HYYSALO, J., AROLA, J., VERRIJKEN, A., FRANCQUE, S., VAN GAAL, L., HYOTYLAINEN, T. & YKI-JARVINEN, H. 2016. Noninvasive Detection of Nonalcoholic Steatohepatitis Using Clinical Markers and Circulating Levels of Lipids and Metabolites. *Clin Gastroenterol Hepatol,* 14**,** 1463-1472 e6.

ZHU, L., BAKER, S. S., GILL, C., LIU, W., ALKHOURI, R., BAKER, R. D. & GILL, S. R. 2013. Characterization of gut microbiomes in nonalcoholic steatohepatitis (NASH) patients: a connection between endogenous alcohol and NASH. *Hepatology,* 57**,** 601-9.

ZMORA, N., BASHIARDES, S., LEVY, M. & ELINAV, E. 2017. The Role of the Immune System in Metabolic Health and Disease. *Cell Metab,* 25**,** 506-521.